UNIVERSITY OF BIRMINGHAM

THE IMPACTS OF TEMPERATURE AND THE URBAN HEAT ISLAND ON MORTALITY IN THE WEST MIDLANDS AND GREATER LONDON

by

FANG ZHANG

A thesis submitted to the University of Birmingham
for the degree of DOCTOR OF PHILOSOPHY

School of Geography, Earth and Environmental Sciences
University of Birmingham
October 2014

Abstract

Although the direct impact of temperature (heat/cold) on human health has been studied extensively, the impact of the urban heat island (UHI) on mortality has received relatively little attention. This PhD thesis assesses the impacts of temperature and UHI on mortality to distinguish the differential responses between urban and rural residents in the West Midlands and Greater London.

On the basis of comparison between MIDAS air temperature and MODIS remotely-sensed land surface temperature, air UHI intensity (aUHII) and surface UHI intensity (sUHII) are calculated as the temperature difference between the paired urban-rural meteorological stations (Edgbaston-Shawbury in the West Midlands; LWC-Rothamsted in Greater London), and subsequently compared in relation to Lamb Weather Types (LWTs) during cloudless anticyclonic nights. The results identify the UHI 'hotspots' and stronger night-time UHI in summer; London possesses stronger aUHII-sUHII correlation (r~0.7, p<0.01) due to its overall 'urban' characteristics.

Mortality data requested from London and West Midlands Public Health Observatory are used to calculate the mortality rate as the number of deaths per 100,000 population. U-shaped temperature-mortality relationships examined using fractional polynomial regression model demonstrate that the decreased cold-related winter mortality may outweigh the increased heat-related summer mortality for the West Midlands, whereas the increase in heat-related mortality is more significant for Greater London, particularly among the vulnerable very elderly 75+ people.

This research has identified for the first time the quantitative relationships between aUHII and mortality. Overall increasing trends imply the increased impact of urban heating on mortality. Although the mortality rate of the West Midlands is consistently higher, the elevated UHI has a stronger impact on London's 75+ rural people. Each 1°C increase in the aUHII will cause an extra 33 and 77 elderly deaths in summer per year for inner West Midlands and outer London, respectively. The stratification of aUHII and mortality rate by LWT demonstrates that the influence of synoptic conditions is significant on aUHII but insignificant on mortality.

These research findings could form the basis for a better understanding of temperature, and UHI-related impacts on human health that will aid policy development to maximise health benefits and minimise the negative consequences. As the frequency and intensity of heatwaves are likely to increase in the future as a consequence of climate change, the health of vulnerable populations with respect to heat and the UHI need to be particularly monitored. To mitigate the UHI effect, more UHI-health warning systems need to be implemented, helping urban planners to make long-term targeted decisions and design cooler green cities. Further research could consider the impacts of temperature and the UHI on gender- and cause-specific mortality (e.g. cardiovascular and respiratory diseases as the main causes of illness and mortality during a heatwave) with adjustments of air quality.

Acknowledgements

I would like to sincerely thank my supervisors, Dr. Xiaoming Cai and Prof. John Thornes for their valuable supervision and support throughout my PhD research. I am particularly grateful to Xiaoming's patience and concerns at every stage of my research, and to John who provided a lot of internal and external opportunities to develop my research.

I am grateful to Paul Fisher for sharing his dissertation knowledge, also to Charlie Tomlinson for guiding me the ArcGIS technical methodology.

Thanks to George Fowajuh and Tony Dickinson from the West Midland Public Health Observatory (WMPHO), for extracting and preparing the complicated mortality data for the West Midlands. Acknowledgement is also given to the Office for National Statistics (ONS) for providing the detailed mortality data for Greater London.

I am also grateful to Rhodri J. Walters and the editor of Oxbridge Editing for copy editing for conventions of the language, spelling and grammar.

Finally, I would like to thank my parents who live far away in China, and my husband Colin Wang, for their continuous support and encouragement. Their loves make me always look forward to obtaining a satisfied outcome with energy.

Table of Contents

List of Figures

List of Tables

List of Abbreviations

aUHI	Air urban heat island
aUHII	Air urban heat island intensity
DMR	Daily mortality rate
FP	Fractional Polynomial
IPCC	Intergovernmental Panel on Climate Change
LST	Land surface temperature
MIDAS	Met Office Integrated Data Archive System
MODIS	Moderate Resolution Imaging Spectroradiometer
MSOA	Middle layer super output area
sUHI	Surface urban heat island
sUHII	Surface urban heat island intensity
T_{air}	Air temperature
$T_{air/max}$	Maximum air temperature
$T_{air/min}$	Minimum air temperature
T_{mm}	Minimum mortality temperature (heatwave threshold temperature)
UHI	Urban heat island
UHII	Urban heat island intensity
WMPHO	West Midlands Public Health Observatory
LWC	London Weather Centre
LWT	Lamb Weather Type
JJA	June, July and August
MGET	Marine Geospatial Ecology Tools
LP DAAC	Land Processes Distributed Active Archive Centre
ONS	Office for National Statistics

Chapter 1 Introduction

1.1 Research background

Climate change is a highly challenging issue that is likely to have a range of significant impacts on human health. These effects arise from both the direct effects of climate change such as increased temperature, changes in weather patterns and the frequency of extreme weather events, as well as from indirect effects such as changes in air quality, availability of food and water, and deleterious impacts on ecosystems. It is expected that these changes may result in increased morbidity and mortality associated with respiratory and circulatory diseases, as well as heart disease (IPCC, 2014).

The IPCC (2007) Working Group I (WGI) predicted the change in average global temperature by the end of the 21st century (2090-2099) relative to the 1990 baseline (1980-1999). The best estimates for the six SRES scenarios (B1, A1T, B2, A1B, A2, and A1F1) vary between 1.8°C and 4.0°C (where the most likely range is 1.1°C-6.4°C). The three international global temperature datasets maintained by the HadCRUT4 (UK Met Office Hadley Centre and University of East Anglia Climatic Research Unit), NOAA NCDC (National Climatic Data Centre), and NASA GISS (Goddard Institute of Space Studies), have produced that the maximum global average temperature anomaly for 2010 was 0.56°C, 0.53°C and 0.58°C relative to the long-term (1961-1990) average, respectively (MetOffice, 2014a). The latest (IPCC, 2013) WGI used a new set of scenarios; the Representative Concentration Pathways (RCPs) for climate change

modelling. By the end of the 21st century, the increase in global surface temperature relative to the 1850-1900 baseline is likely to exceed 1.5°C-2°C, with high confidence for RCP 4.5 (likely range 1.1°C-2.6°C), RCP 6.0 (likely range 1.4°C-3.1°C) and RCP 8.5 (likely range 2.6°C-4.8°C). On this basis, it is highly likely that global and regional warming will continue.

As highlighted by Rizwan et al. (2008), the UHI effect is a significant 21st century problem, and in recent years, the associated public health problems have become a serious concern. The Met Office reported that over 75% of the British population is classed as urban in the UK (MetOffice, 2011a). During the 20th century, the urban population of England has increased from 77% to 89% (Hicks and Allen, 1999). With rapid urbanisation and climate change, increased temperature is likely to trigger further issues relating to health and wellbeing, particularly among vulnerable elderly populations living in urban areas. Although in winter UHI effects can be beneficial, in summer they produce mostly adverse impacts on human health. For example, the remarkable 2003 European heatwave event caused a dramatic increase in excess deaths (Kosatsky, 2005). The majority of these excess deaths occurred in cities due to the combined effects of heatwave and urban heat island (UHI) (Tan et al., 2010). As a result, many studies have since been performed to assess urban climate and develop urban designs that mitigate the impact of the UHI effect.

Although most urban cities (not all cities though) experience additional warming relative to their surrounding rural areas, it still remains somewhat controversial whether the UHI has any relationship with global warming. In some instances, the maximum urban-rural

temperature difference is several times higher than the increase in temperature recorded by thermometers. On the other hand, the UHI as a local effect, there is no evidence that it biases the trends in homogenised temperature record. Global warming may not lead to a rise in the intensity of UHI, which may remain constant even in an overall warmer globe (Alcoforado and Andrade, 2008, Oke, 1997). Even on some occasions, the UHI intensity may decrease during global warming, as a result of the increase in vertical instability conditions and the consequent urban heat dissipation (Brázdil and Budíková, 1999). The future UHI trends will depend upon the synoptic weather conditions (e.g. anticyclonic, light wind and cloudless) (Morris and Simmonds, 2000, Oke, 1987). It is thought more generally that the impact of UHI on global warming should be negligible due to the small input of additional heat, as urban areas only cover <1% of the global land surface. In fact, urban cities have an indirect impact on global warming contributing ~85% of the anthropogenic greenhouse gases and ozone (Oke, 1997).

The European JRC PESETA (Projection of Economic impacts of climate change in Sectors of the European Union based on bottom-up Analysis)human health study analysed the summer and winter temperature-related mortality in Europe (Watkiss et al., 2009). The results predicted a significant increase in summer heat-related mortality and a reduction in cold-related mortality (warmer winters) by the 2080s. Reduction in cold-related mortality is projected to be greater than increase in heat-related mortality (Donaldson et al., 2001). Considering the economic costs (including resource, opportunities and disutility costs), the reduced winter mortality has greater benefits than the increased summer mortality. As an example, due to the increased heat-related

mortality, air conditioning demand accounting for ~15% of the U.S. energy usage has increased 10% in the last 40 years (Rosenfeld et al., 1998). Keating and Handmer (2013) calculated the costs of climate change impacts i.e. heatwave mortality, which would cause extra 6,214 deaths equivalent to a cost of $6.4 billion ($218 million per year by 2050) in Melbourne. Realistically, a decrease in energy demand directly leads to cost efficiency. However, the knowledge for estimating the health-related impacts and potential economic costs of adaption are relatively limited. There are uncertainties over whether the increased summer mortality can be balanced by the decreased winter mortality. In Chapter 5, the temperature-mortality relationship will be examined to investigate how the urban and rural mortality rate is affected by high/low temperatures.

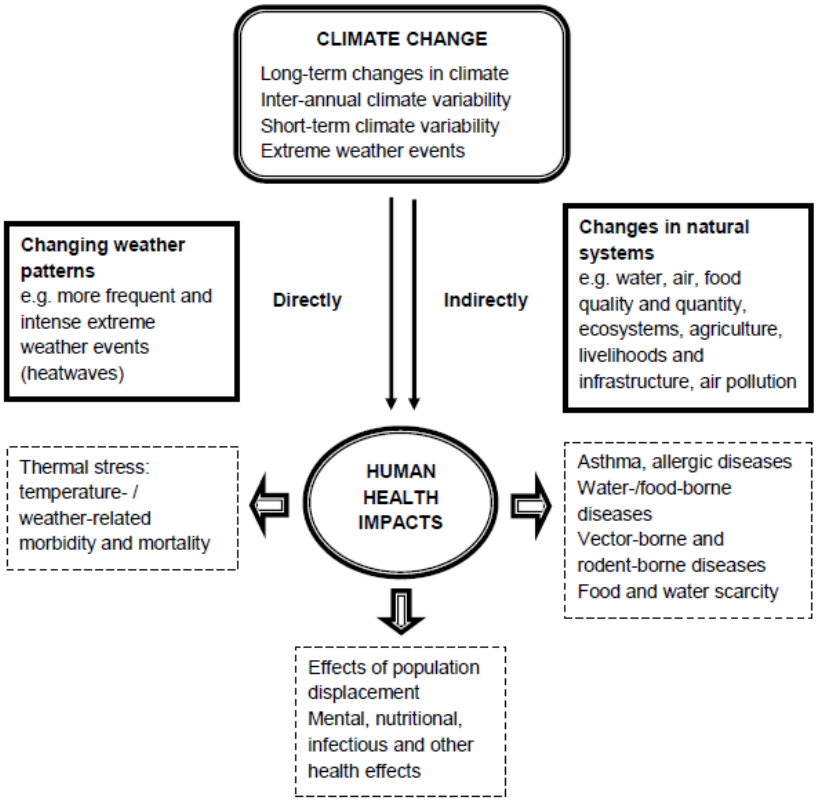

Figure 1.1: Diagram showingimpacts of climate change on human health, adapted from IPCC (2013) and IPCC (2014).

Figure 1.1, adapted from the IPCC WGI/WGII reports (IPCC, 2013, 2014), shows the direct and indirect consequences of climate change on human health. The section on human population health in IPCC (2014) WGII AR5 confirms the impact of heat on human health, particularly for elderly people and those susceptible to developing illness. The heat-related mortality (Baccini et al., 2011, Huang et al., 2011) and cold-related mortality (Analitis et al., 2008) have already been studied extensively. For most European countries, cold-related mortality is greater than heat-related mortality. As a result of climate change, the increased minimum temperature may have beneficial effects in reducing the winter mortality. However, adverse effects resulting from increasingly frequent extreme heatwaves may still outweigh the reduction in cold days (Ebi and Mills, 2013). A severe August heatwave in 2003 caused over 2,000 excess deaths (16% increase) in England and Wales; another marked 2006 heatwave caused 680 excess deaths (4% increase) during 16-28 July. In the 2008-2009 winter, there were 36,450 excess deaths translating to 24% more deaths in comparison to non-winter period (Brown et al., 2010). With a particular focus on all-cause mortality which could be directly affected by heat exposure, the impacts on morbidity such as heart and respiratory diseases mostly occur in winter (Thornes et al., 2014), are not discussed in detail in this thesis but will be considered for in depth analyses for future research.

1.2 Aims and objectives

The aim of this thesis is to investigate the UHI characteristics and the likely impacts of changing temperature and the UHI effect on all-cause mortality for the West Midlands and Greater London which are the only two landlocked regions of the UK. The West Midlands has very high negative climate change impact on mortality and morbidity resulting from an increase in summer deaths due to heatwave warming (WMPHO, 2010). People living in Greater London are at higher risk of heat/cold effect than other UK regions (Hajat et al., 2014, Vardoulakis et al., 2014).

The main objectives are as follows:

1. Assess the temporal and spatial characteristics of UHIs associated with Lamb weather types to confirm the significance of anticyclonic conditions on the UHI intensity (UHII), and identify how ground-based air UHI intensity (aUHII) relates to satellite-derived surface UHI intensity (sUHII) under cloudless anticyclonic conditions.
2. Examine the relationship between temperature and mortality rate using a relatively new and flexible fractional polynomial regression model to determine whether the increased heat-related mortality and the decreased cold-related mortality are balanced.
3. Quantify the differential responses of mortality rate to the aUHII between urban and rural residents in the West Midlands and Greater London, as well as the stratification of aUHII and mortality rate conditioned by the Lamb weather types.

According to the aims and objectives, the following hypotheses are addressed:

1. Due to frequent spells of heatwaves and warmer winters, the heat effect on mortality is expected to outweigh the cold effect on mortality, although cold-related mortality accounts for more deaths than heat-related mortality (Hajat et al., 2014).
2. Heatwaves lead to short-term increased mortality, and the UHI effect may exacerbate heatwaves and urban mortality risk. The impact of the UHI on mortality in Greater London is expected to be stronger than that in the West Midlands. The elderly population is more vulnerable to heat stress and the UHI effect.

1.3 Thesis outline

- **Chapter 1** is an introduction outlining current research background, and the aims and objective of this thesis.
- **Chapter 2** provides a literature review covering primarily the temperature (heat and cold) and mortality (Section 2.2), the UHIs and their impact on human health (Section 2.3). Research gaps (Section 2.4) are identified based on previous research findings.
- **Chapter 3** describes the study areas (Section 3.1), the data acquisition and pre-processing (Sections 3.2-3.6) including MODIS data, MIDAS data, Lamb Weather

Types (i.e. Jenkinson's objective Lamb daily synoptic indices), population estimates and mortality data.

- **Chapter 4** assesses the urban climates in Birmingham and London (Section 4.5.1), ground-based air UHI (Section 4.5.2) and satellite-derived surface UHI (Section 4.5.3) associated with Lamb weather types. A comparison of the air and surface temperatures and intensities of UHIs during cloudless anticyclonic nights is performed (Section 4.5.4).
- **Chapter 5** examines the relationships between temperature and mortality rate (<75 and 75+) using STATA's fractional polynomial regression model in the West Midlands and Greater London. There is a particular focus on the 2003 heatwave (June, July and August) to examine the short-term impact of temperature on mortality, along with the UKCP09 heatwave projection up to the 2080s.
- **Chapter 6** investigate the impacts of air UHI on heat-related mortality (under 75, 75 and over) using daily mortality rate and the positive UHII as the indicator of urban heating for the West Midlands and Greater London, respectively. The aUHI and mortality data are stratified by LWT to see how they vary under different weather conditions.
- **Chapter 7** discusses a critical evaluation of the key components of the thesis, including uncertainty estimates for data and methodology, insight to the strengths and limitations of surprising findings.
- **Chapter 8** concludes the research findings with a comparison between the West Midlands and Greater London, and suggests future research opportunities.

Chapter 2 Literature reviews

2.1 Introduction

The latest IPCC report concluded that climate change has contributed to a significant increase in global mean temperature (IPCC, 2013), and the intensity and frequency of heatwaves are likely to increase the risk of heat-related mortality (death) and morbidity (illness), particularly among vulnerable elderly populations in urban cities. Heat-related mortality as a severe health consequence generally arises from summer heatwaves. People with serious pre-existing illness such as cardiovascular and respiratory diseases might exacerbate the heat-related mortality risk (Basu and Samet, 2002). However, the susceptibility of heat-related morbidity depends on various risk factors such as physiological changes, socioeconomic status, medical conditions, air conditioning, and ageing. Heat-related morbidity may be confined to mild conditions e.g. heat cramps and heat exhaustion, or it may lead to fatal conditions e.g. heatstroke that require close attention to reduce the further mortality risk. Due to the broad categories of morbidity and scarce evidence of direct impact on the UHI, no further analyses of temperature (or UHI)-related morbidity will be discussed in detail in this thesis. Climate change also contributes to negative human-health consequences including precipitation changes resulting in flooding and droughts, and reduced air quality. In addition, positive effects of climate change include the reduction in cold-related mortality and morbidity due to fewer cold extreme events and reduced capacity of vectors to transmit diseases. But the

negative effects are projected to outweigh the positive effects over the 21st century (IPCC, 2014).

The typical relationships between temperature and mortality derived using a variety of methods are reviewed in Section 2.2.1. To determine the summer health impact of extreme heatwaves and the UHI effect, summer heat-related mortality is reviewed in Section 2.2.2 and analyses are presented in Chapter 6. Cold-related mortality is also reviewed in Section 2.2.3. The UHI characteristics, measurement methods and heat island impacts are reviewed in Section 2.3. Two types of UHI (air and surface UHI) are introduced. In particular, remotely sensed surface UHI derived from satellite data is discussed. Several commonly used methods are presented. The use of data obtained from the Moderate Resolution Imaging Spectroradiometer (MODIS)/Aqua instrument is justified. The UHIs in Birmingham and Greater London are then studied in detail. Finally, in Section 2.4, research gaps are identified based on a review of the past and current literatures.

2.2 Temperature and mortality

2.2.1 Temperature-mortality relationships

The relationship between temperature and mortality (T-M relationship) has been widely investigated. Time-series regression models have often been used to assess heat impacts on health (Basu et al., 2005, Curriero et al., 2002, Keatinge et al., 2000). Time-series regression is a simple method that is suitable for examining short-term effects over time. Available methods for time-series regression include linear models (Hatzakis et al., 1986), log-linear models (Baccini et al., 2008), Poisson regression models and Generalised Additive Models (GAMs). Peng et al. (2011) analysed the association between heatwaves and mortality in Chicago using Poisson regression models, which are generally used in the case of parametric nonlinear confounding factor adjustments (Dominici et al., 2002). Many studies have adopted GAMs (Doyon et al., 2008) to estimate heat-related mortality. Almeida et al. (2010) used GAMs adjusted for day of the week and season to model the relationship between apparent temperature and daily mortality in Portugal, with mortality risk increasing with temperature. One of the main advantages associated with GAMs is that they provide a high degree of flexibility in the choice of non-linear function. GAMs can fit smooth non-linear relationships and allow for serial corrections (Jbilou and Adlouni, 2012). As with Poisson regression models, GAMs are more suitable in the presence of confounding factors that need to be adjusted using two or more non-parametric smooth functions (Dominici et al., 2002). Case-crossover approach (also called 'conditional logistic regression') was used by Basu et al. (2005) to examine the association between temperature and elderly cardiovascular mortality in 20

US cities. Case-crossover is a case-control design especially useful for estimating short-term and acute effects. The comparison of time series and case-crossover methods for air pollution and hospital admissions (Fung et al., 2003) concluded that the best risk estimates using time-series methods are more precise than those provided using the case-crossover method. Dessai (2002) examined non-linear regression of an aggregate dose-response relationship between daily excess mortality and temperature by applying an empirical-statistical model. Other methods such as the Box-Jenkins (Box et al., 2008) and ARIMA Models (García-herrera et al., 2005) have been used for temperature-mortality studies but are not as popular as those using time-series regression models. Neural networks as prediction models based on non-linear models, with a higher forecasting accuracy compared with the multiple linear regression model (Gao et al., 2012), have been used to predict the mortality in patients with strokes (Celik et al., 2014) and suspected sepsis (Jaimes et al., 2005).

Despite the advantages of the models discussed above, Royston and Altman (1997) disputed their suitability for epidemiological studies due to the requirement for complex mathematical expressions to describe curves that are difficult to interpret, where an unknown degree of smoothness may result in bias or artefacts. The parametric method of fractional polynomial (FP) regression offers considerable flexibility as an idealised method to analyse smooth, non-linear and complicated curves using fewer parameters than conventional polynomials. Weinberg (1995) and Royston et al. (1999) both suggested that FPs are more suitable for epidemiological studies where modelling of continuous variables is required.

A U-Shaped (or V-Shaped) relationship between temperature and mortality has been observed in previous studies (Kunst et al., 1993). Due to the regional differential responses to heat, higher latitude regions normally have a lower threshold temperature (also called 'minimum mortality temperature', T_{mm}) than in lower latitude regions. The T_{mm} value was found to be 19.6°C for London and 17.7°C for the West Midlands (Hajat et al., 2014). The WMPHO (2010) examined the relationship between daily all-cause mortality and mean temperature in the West Midlands during 2001-2008. The mortality varies with temperature, with a T_{mm} of 17.1°C above which the mortality rapidly increases with temperature, and below which the mortality gradually decreases with temperature. In addition, WMPHO (2010) reported the decreased mortality from milder winters seems to outweigh the increase in mortality from hotter summers. People living in cold regions are more susceptible to high temperatures and those living in warm regions are more susceptible to low temperatures. Smoyer et al. (2000) found that urban populations are likely to be more vulnerable to heat, and vulnerability is increasing with population ageing.

Baccini et al. (2008) analysed the heat effects on mortality in 15 European cities (Figure 2.1). For each city, a Generalised Estimating Equation (GEE) model was used assuming the mortality variable was Poisson distributed. The city-specific epidemiological study found V-shaped (or J-shaped) relationships between daily maximum temperature and log-scaled mortality rate, indicating an excessive risk for temperature exposures above a threshold. Stronger T-M relationships were associated with respiratory diseases, particularly for elderly populations. In an analysis of the London curve (Figure 2.1), the

threshold was 23.9°C (95% CI: 22.6°C to 25.1°C), with a percent change of 1.54 (95% CI: 1.01–2.58) in mortality associated with a 1°C increase in maximum temperature above the age-specific threshold. By comparison, Athens, Milan and Rome possess the top 3 highest threshold temperatures of 32.7°C, 31.8°C and 30.3°C, respectively. Threshold temperature was city-dependent among the 15 cities, varying by geographical location. In general, higher thresholds are observed in populations with higher summer temperatures (southern, lower latitudes or closer to equator) potentially due to acclimatisation and adaptation of local residents to prevailing weather (Gao et al., 2015, Kravchenko et al., 2013), and associated with higher population density (Hajat and Kosatky, 2010). Moreover, populations relied on long-term air-conditioned environment at home or in public areas and vehicles may also affect the physiologic acclimatisation to heat even from lower latitudinal cities (Kravchenko et al., 2013).

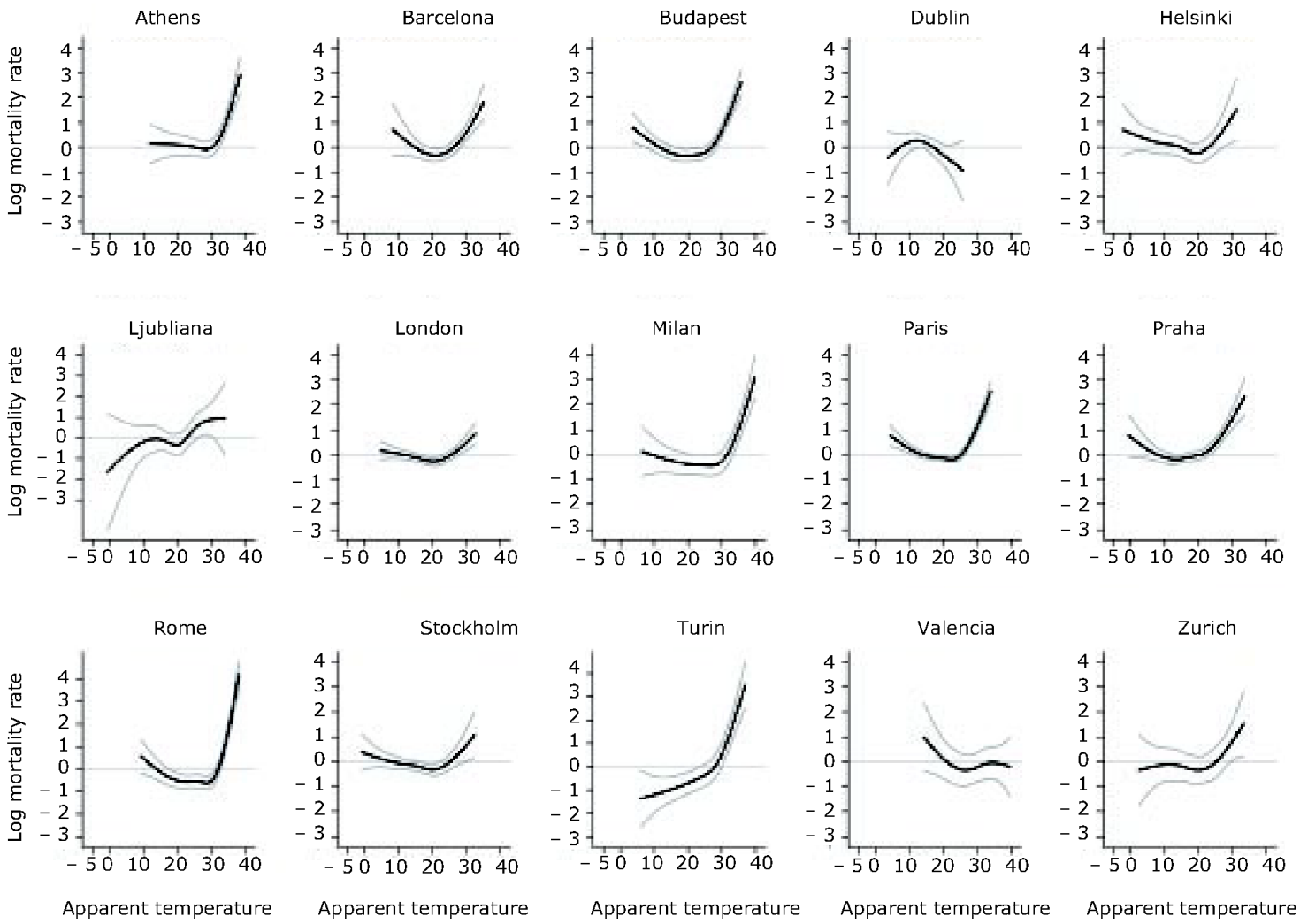

Figure 2.1: Adjusted relationship between apparent temperature (lag 0-3) and log mortality rate including 95% confidence intervals in 15 European cities (Baccini et al., 2008).

2.2.2 Heat-related mortality

The increase in summer mortality due to increased warming (WMPHO, 2010), with increased deaths due to respiratory and cardiovascular disease, is likely to be one of the most significant consequences of climate change. This thesis examines all-cause mortality which is a common indicator used to investigate heat-related mortality. Heatwaves are intermittent events with complex triggers and impacts. It has therefore been somewhat difficult to reach a consensus on how a heatwave should be defined and an adequate definition has only recently been introduced. The World Meteorological Organisation (WMO) proposed that a heatwave be declared when daytime maximum temperature ($T_{air/max}$) exceeds the baseline 1961-1990 average $T_{air/max}$ by 5°C for more than five consecutive days (Frich et al., 2002). Other definitions include defining a heat wave as a period of three or more consecutive days where $T_{air/max}$ exceeds the 95th percentile of summer $T_{air/max}$ (Gosling et al., 2009), or as five consecutive days when $T_{air/max}$is above the 97th percentile of summer $T_{air/max}$ (Hajat et al., 2006). The UK Met Office defined a heatwave in the West Midlands as a period of at least two consecutive days where thresholds of $T_{air/max}$ and night-time minimum temperature ($T_{air/min}$) are exceeded. Robinson (2001) introduced a more subjective definition of a heatwave as an extended period of unusually high heat stress which may cause adverse health problems for the affected population. The heatwave threshold temperature, above which there could be significant effects on health if reached, is different in other regions because of the differing sensitivity of people to heat (Gosling et al., 2009), and in this respect the definition by Robinson (2001) has more practical value.

The Met Office Heat-Health Watch provides regional heatwave threshold temperatures (Figure 2.2) of 30°C ($T_{air/max}$) and 15°C ($T_{air/min}$) for the West Midlands, and similarly for North West England, East Midlands, East of England, South West England and Wales. London has the highest threshold $T_{air/max}$ of 32°C and $T_{air/min}$ of 18°C, but the thresholds for North East England, Yorkshire and the Humber are lower at 28°C and 15°C, 29°C and 15°C, respectively. Following London, South East England has a threshold of 31°C ($T_{air/max}$) and 16°C ($T_{air/min}$). It was noted by the UK Met Office that 'these temperatures could have significant health effects if reached on at least two consecutive days and the intervening night'.

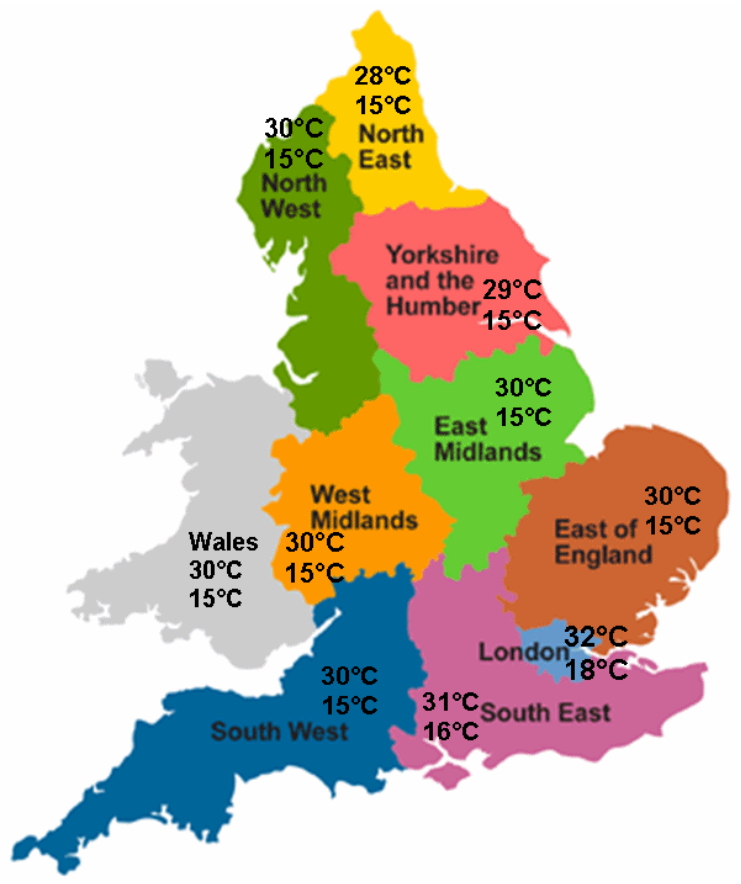

Figure 2.2: Regional distributions of the thresholds ($T_{air/max}$ and $T_{air/min}$) for heatwave definition (MetOffice, 2014b).

A variety of studies on heat-related mortality have been carried out previously, for example, in Europe (Burkart et al., 2011, Koppe et al., 2004), Asia (Pan et al., 1995), and North America (Davis et al., 2003), although there is still no systematic definition of heat-related mortality which can be used during a heatwave (Basu and Samet, 2002). Most studies on temperature-mortality relationships did not use the raw mortality data. Short-term acute mortality increases caused by heatwaves have been isolated by associating temperature with excess mortality to give an indication of the mortality attributable to temperature. In general, excess mortality was calculated by subtracting the baseline (or 'expected') mortality from the observed mortality.

Table 2.1 lists well-known heatwave events, the heat-related mortality that can be attributed to the heatwave, and the method used tocalculate the baseline mortality. Indeed, different methods have their associated advantages and disadvantages. Gosling et al. (2009) summarised several of the most popular methods. One such method is to compute the daily mortality compared with the fixed daily mean mortality for each month in previous years (Dessai, 2002). This method is useful when data in preceding years are available. Other methods compare the daily mortality with a 31- or 30-day moving average for the same year (Dessai, 2002, 2003, Rooney et al., 1998), which is useful when long-term data are not available. The disadvantage of this method is that the inclusion of heatwave days in the moving average introduces a bias into the baseline and complicates the comparison between different extreme events. The computation of the baseline mortality largely depends on the chosen baseline (Dessai, 2002). Gosling et al. (2007) calculated the excess mortality above a baseline mortality rate to provide

lower mortality estimates, rather than using the mortality rate directly (Gosling et al., 2009). Whitman et al. (1997) used three different regression analyses to calculate different estimates of baseline mortality for the Chicago 1995 heatwave. Dessai (2003) demonstrated that future mortality predictions would be more sensitive to uncertainties in climate change, anthropogenic effects and human impacts, although the mortality estimates are sensitive to the chosen method. Furthermore, uncertainties also arise due to the method of classification of mortality in the time series. The choice of definition is important, for instance whether it is based on the recommendations of the World Health Organisation (WHO) or some other definition. Some studies use all-cause mortality (Gosling et al., 2007, Pattenden et al., 2003) including accidents. Others studies use all causes with the exception of external causes such as accidents (Hajat et al., 2002), while others use non-accidental deaths only (Kassomenos et al., 2007).

Table 2.1: Examples of heatwave events, heat-related mortality and calculation of baseline mortality, modified from Gosling et al. (2009).

Heatwave	Attributable mortality	Calculation of baseline mortality	Reference
24 June - 8 July, 1976 Birmingham, UK	Daily mortality increased by 10% during heatwave, mainly affecting among women aged 70-79	Predicted daily mortality	Ellis et al. (1980)
21-31 July, 1987 Athens, Greece	2690 heat-related hospital admissions;926 mortality; excess mortality >2000	Time series regression, adjusted	Katsouyanni et al. (1988)
1995 England and Wales Greater London	619 (8.9% increase, ↑) in England and Wales 136 (16.1%↑) in London	31-day moving average for that period in all-age groups	Rooney et al. (1998)
1995 Chicago	1072 (11%) 838 (35%) for 65+ years	Subtract July 1994 day of week average from daily mortality in July 1995	Semenza et al. (1999)
1-20 August, 2003 France	14,800 (60%↑); women (70%↑), men (40%↑)	Mean of 1-19 August 1999-2002 mortality	Pirard et al. (2005)
2003 Spain	43,212 (8%↑); 75+ years (15%↑ for 75-84; 29%↑ for 85+)	Poisson regression model to historical mortality series 1980-2002, adjusted	Simon et al. (2005)
2003 Netherlands	31 July-13 August 500 June-Sep. 1400-2200	Compared with mortality rates in 1 or more previous years	Garssen et al. (2005)
1 June-31 August, 2003 Rome/Milan/Turin/Bologna, Italy	944 (19%↑) in Rome 559(23%↑) in Milan 577 (33%↑)in Turin 175 (14%↑) in Bologna	Mean daily mortality from a reference period, 1995-2002 for Milan, Roma Bologna; 1998-2002 for Turin	Michelozzi et al. (2005)
2003 Portugal	2,399 (58%↑); women (79%↑), men (41%↑)	averaged period proportional mortality ratio (APPMR)	Trigo et al. (2009)
4-13 August, 2003 England and Wales, UK	2,139 (16%↑)	Average mortality in the same period 1998-2002	Johnson et al. (2005)
2009 Perth, Australia	Daily mortality (8.9%↑) Hospital admissions (10%↓)	31-day moving average; group days into 1-2°C interval of daily $T_{air/max}/T_{air/min}$	Williams et al. (2012)

For example, the 2003 European heatwave increased summer temperatures and temperature variability, causing approximately 35,000 excess heatwave-related deaths (Kosatsky, 2005). These excess deaths mostly affected elderly people (Kovats and Jendritzky, 2006) as their bodies cannot adjust to heat stress as well as the bodies of young healthy people. Studies showed that most of the heatwave-induced mortality occurred in cities (Basara et al., 2010, Laaidi et al., 2012). In England and Wales, Johnson et al. (2005) found an estimated 2,139 excess deaths (16% increase) during the 2003 heatwave period (Figure 2.3). There were 2-day lag times observed between the peak in daily mortality on 11 August and the peak in the CET (Central England Temperature) on 9 August. In particular, elderly people aged 75+ in London had the largest excess mortality increase of 59% based on the expected mortality calculated from the average mortality during 1998-2002. Lag times for the heat-mortality relationships normally vary in the range of 0 to 3 days following a heatwave. Most heat impacts were immediate (lag 0) suggesting the excess risk during heatwaves, can be explained by extreme daytime temperature and by a lack of the relief by night-time minimum temperature. Peak mortality lagged behind the corresponding peak temperature (lag 1-3) demonstrate that heat-related mortality is an acute event requiring timely intervention (Basu and Samet, 2002).

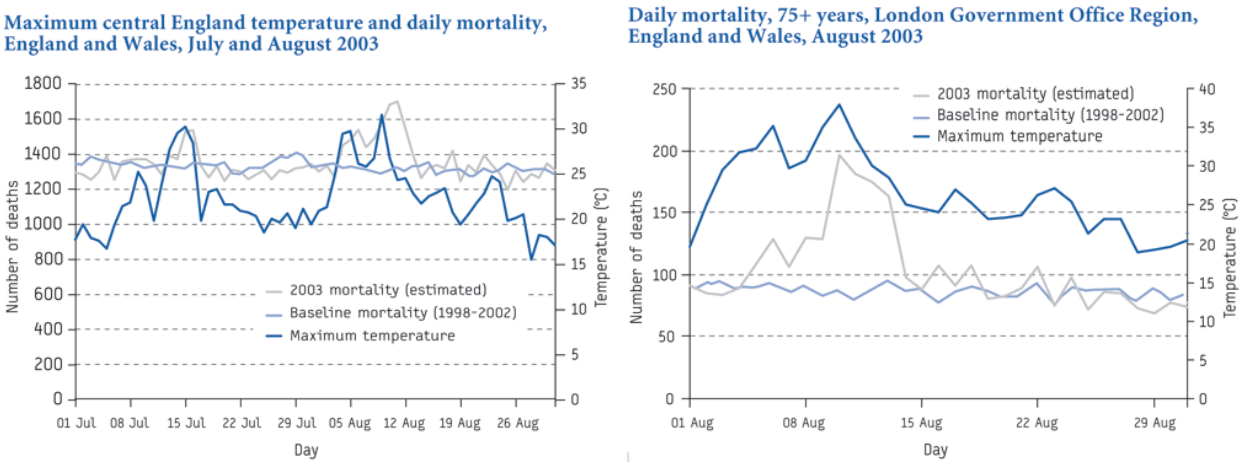

Figure 2.3: Maximum Central England temperature (CET) and daily mortality in England and Wales for July and August 2003; London's daily mortality 75+ years and maximum CET for August 2003 (Johnson et al., 2005).

It has been studied by Qian et al. (2008) that air quality has potential synergistic effect with temperature on mortality. In particular, heatwaves are associated with poor air quality (ozone and $PM_{2.5/10}$) mainly caused by anthropogenic and industrial emissions (IPCC, 2013), leading to significant excess heat-related mortality (Stedman, 2004). Reducing air pollutant concentrations have shown to lessen the effect of climate change on public health (Cifuentes et al., 2001). In fact, confounding factors such as socio-economic factor are related to mortality increase and the exposure to air pollutants, but they are unmeasured and difficult to account for (Marra and Radice, 2011).

2.2.3 Cold-related mortality

Significant causes of cold-related mortality are cerebrovascular, respiratory and ischaemic heart diseases (TheEurowinterGroup, 1997), which normally occur in winter cold weather. The Heath Profile 2010 reported that early mortality rates due to heart disease and stroke, caused mainly by circulatory diseases in both the West Midlands and London,remain worse than the England average (APHO, 2010a, b). The ASC (Adaption Sub-Committee) progress report 2014 pointed out that cold-related mortality is the largest contributor to weather-related mortality in England.

The epidemiological risk assessment performed by Hajat et al. (2014) highlighted the similarity of heat- and cold-related mortality risks. However, there were a larger number of days below the cold-related T_{mm} than above the heat-related T_{mm}. During the study years 2001-2009, the estimate of total heat-related mortality were 1,974, whereas the estimate of total cold-related mortality was as high as 41,408 in all regions of the UK. Brown et al. (2010) analysed the relationship between temperature and mortality in summer and winter during 1993-2007 in England and Wales, and found wide variations in winter mortality. Winter mortality increases as the weather becomes colder, although it also occurs on mild days. The results showed that the maximum mortality occurred in the months with the lowest temperature: December (1,687), January (1,795) and February (1,605). Conversely, daily mortality was lowest between May and October, but the mean daily temperatures were highest between June and August. The summer mortality was around 300-400 less than the winter mortality.

As shown in Figure 2.4A, Hajat et al. (2014) used the Relative Risk (RR) of mortality per 1°C increase (or decrease) above (or below) the pre-defined threshold, which can be identified by a linear-threshold model for the heat effect and chosen as an assumed value for the cold effect. An RR above 1 indicates an increased mortality risk in comparison with the annual mean. In the UK, the heat-related mortality risk (Figure 2.4A) is strongest in London (19.6°C), followed by the East Midlands (18.5°C). The RR for the West Midlands is weaker than for London, but still presents a high heat-related mortality risk (RR=1.02 per 1°C increase above 93rd centile). Unlike the large differences in heat-related RR, the cold-related mortality risk (Figure 2.4B) is very similar in the various UK regions. London still has the largest cold effect (13.2°C), followed by the South West (12.1°C) and Wales (11.9°C). However, the West Midlands region does not have a significant cold-related mortality risk, as indicated by an RR (per 1°C decrease below 60th centile) below the overall value of 1.02.

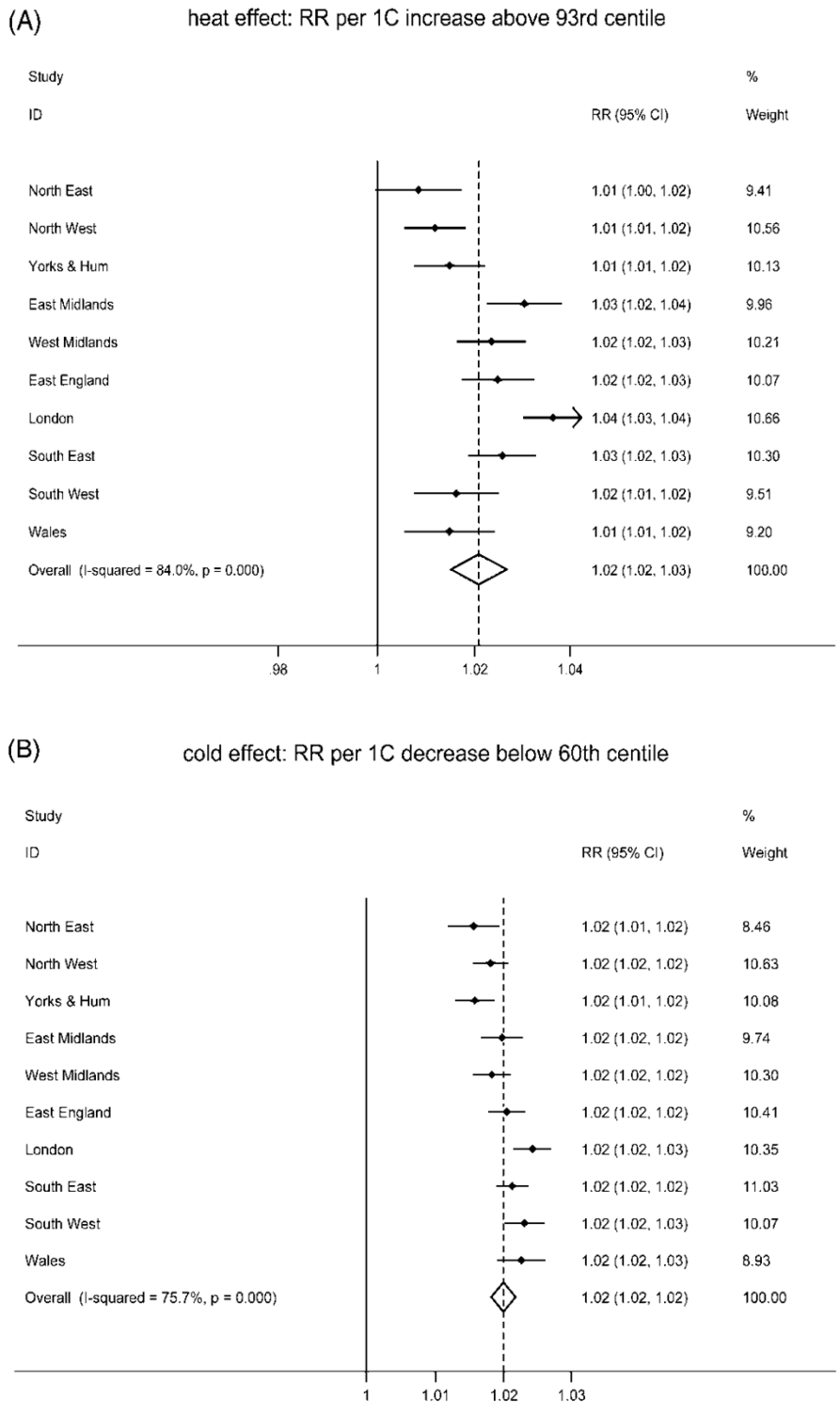

Figure 2.4: The UK region-specific relative risk of (A) heat-related mortality, (B) cold-related mortality for every 1°C increase in daily mean temperature (Hajat et al., 2014).

As illustrated in Figure 2.5, Hajat et al. (2014) projected the UK's heat-related and cold-related mortality expected in the 2080s. Assuming the population size and age structure remain constant, heat-related mortality could increase by 46% (2,882), 169% (5,310) and 329% (8,468) by the 2020s, 2050s and 2080s respectively; cold-related mortality could decrease by 9% (37,681), 26% (30,642) and 40% (24,845) by the 2020s, 2050s and 2080s respectively. These projections (climate only) exclude the confounded population and ageing factors, and the additional heatwave effect which was only significant in London. If the London region were to experience a similar heatwave effect, the projected heat-related mortality would increase by 64%, 70% and 78% by the 2020s, 2050s and 2080s, respectively (Hajat et al., 2014). Further taking into account population growth, the overall heat-related mortality is projected to decrease by 66% (3,281), 257% (7,040) and 535% (12,538) per year by the 2020s, 2050s and 2080s, while the overall cold-related mortality is projected to decrease by 3.5% (42,842), 2.4% (40,397) and 11.8% (36,506) per year by the 2020s, 2050s and 2080s, respectively (ASC (2014) and supporting data table). In the case of the UK, taking into account changes in population size and composition as the key factors in the elevated future heat-related mortality, but in the absence of population adaption, heat-related mortality could increase by ~257% and cold-related mortality could reduce by 2%. However, the additional heatwave effect involved in heat effect projection may not apply to all regions, indeed only in London where heatwave contributes to heat significantly (Hajat et al., 2014). Heat and cold weather may also have adverse impact on morbidity, but not as consistently as with mortality (Hajat et al., 2010).

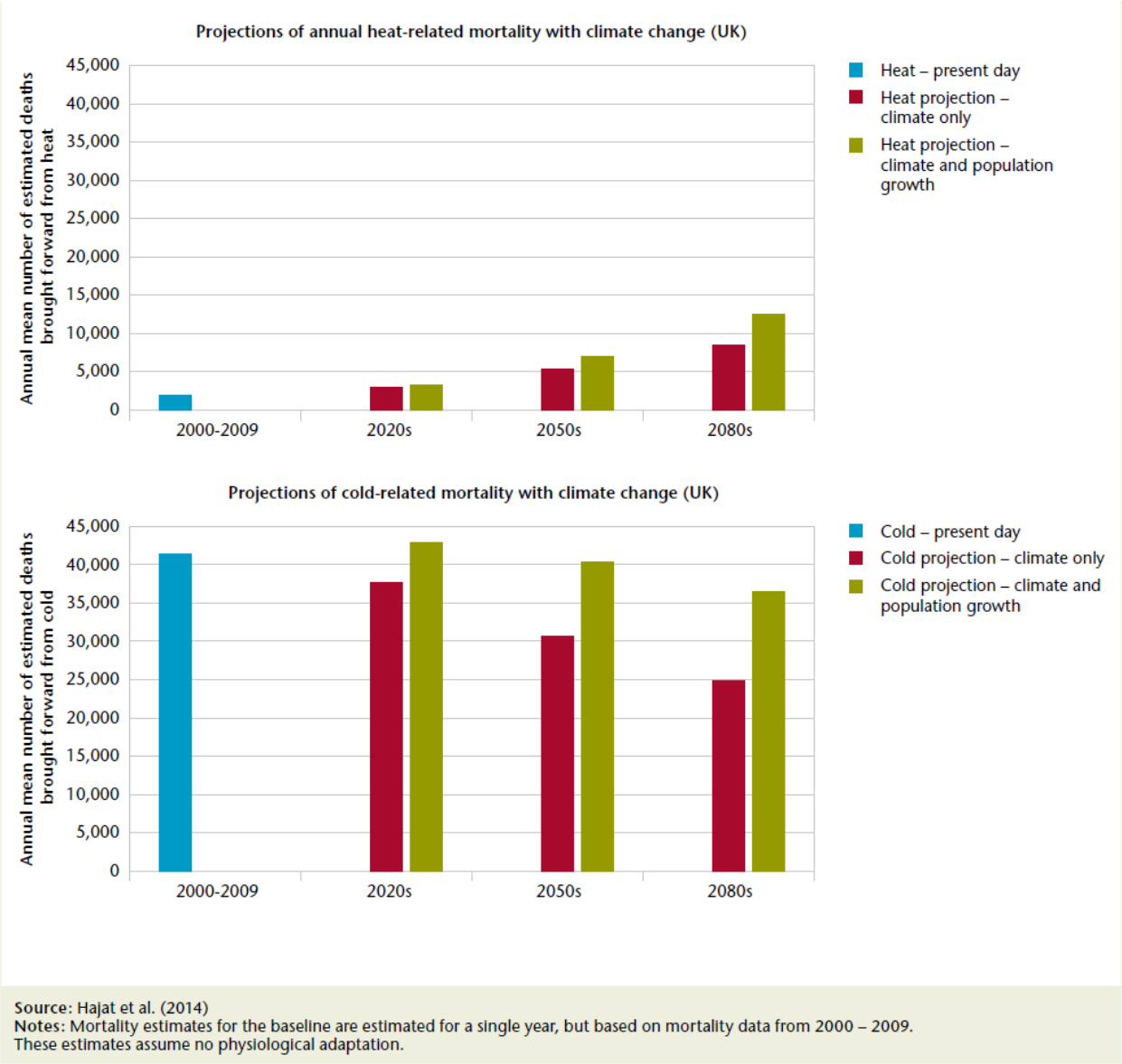

Source: Hajat et al. (2014)
Notes: Mortality estimates for the baseline are estimated for a single year, but based on mortality data from 2000 – 2009. These estimates assume no physiological adaptation.

Figure 2.5: Future projections of annual heat- and cold-related mortality with climate change in the UK. (Sources: ASC (2014); Hajat et al. (2014)).

2.3 Urban heat islands

2.3.1 Background on the UHIs

Along with the fast-growing urbanised urban populations and urban infrastructure, densely built-up cities retain heat due to increased radiation absorption from roofs and buildings during the daytime, but is then not radiated away fully at night. This causes elevated urban temperatures to be 5-6°C higher than the surrounding rural temperatures. This phenomenon is referred to as the UHI effect, which is prominent on summer nights in calm weather conditions (Oke, 1982, 1987).

Key factors contributing to the formation of UHIs include the additional heat, vegetation cover and urban surface properties (Akbari et al., 2008).

- Anthropogenic heat emissions released from air conditioning, transportation and industrial processes;
- Reduced urban vegetation and evapotranspiration;
- Urban construction materials with low albedo, such as roofing and paving, reflect less but absorb more solar radiation;
- Urban canyons (narrow streets lined by tall buildings) obstruct heat released from urban infrastructure;
- Other factors, such as weather (anticyclonic conditions with clear skies and light winds maximise solar absorption and minimise heat release) and geographic location (distance from central area).

Figure 2.6 (upper) is a typical UHI diagram modified from Voogt (2002), illustrating variations in air temperature (T_{air}) and land surface temperature (LST) related to different land-use types during the day and night. Surface UHI (sUHI) is present during the day and at night, but air UHI (aUHI) tends to be very weak during the day. Figure 2.6 (lower) was adapted from Akbari et al. (2008) and modified from Oke (1982), to illustrate the temporal variation in urban/rural and heat island intensity over 24 hours under clear and calm conditions, where surface cooling is associated with radiation exchange. The intensity of aUHI increases after sunset and reaches its peak after 3-4 hours, and then decreases gradually.

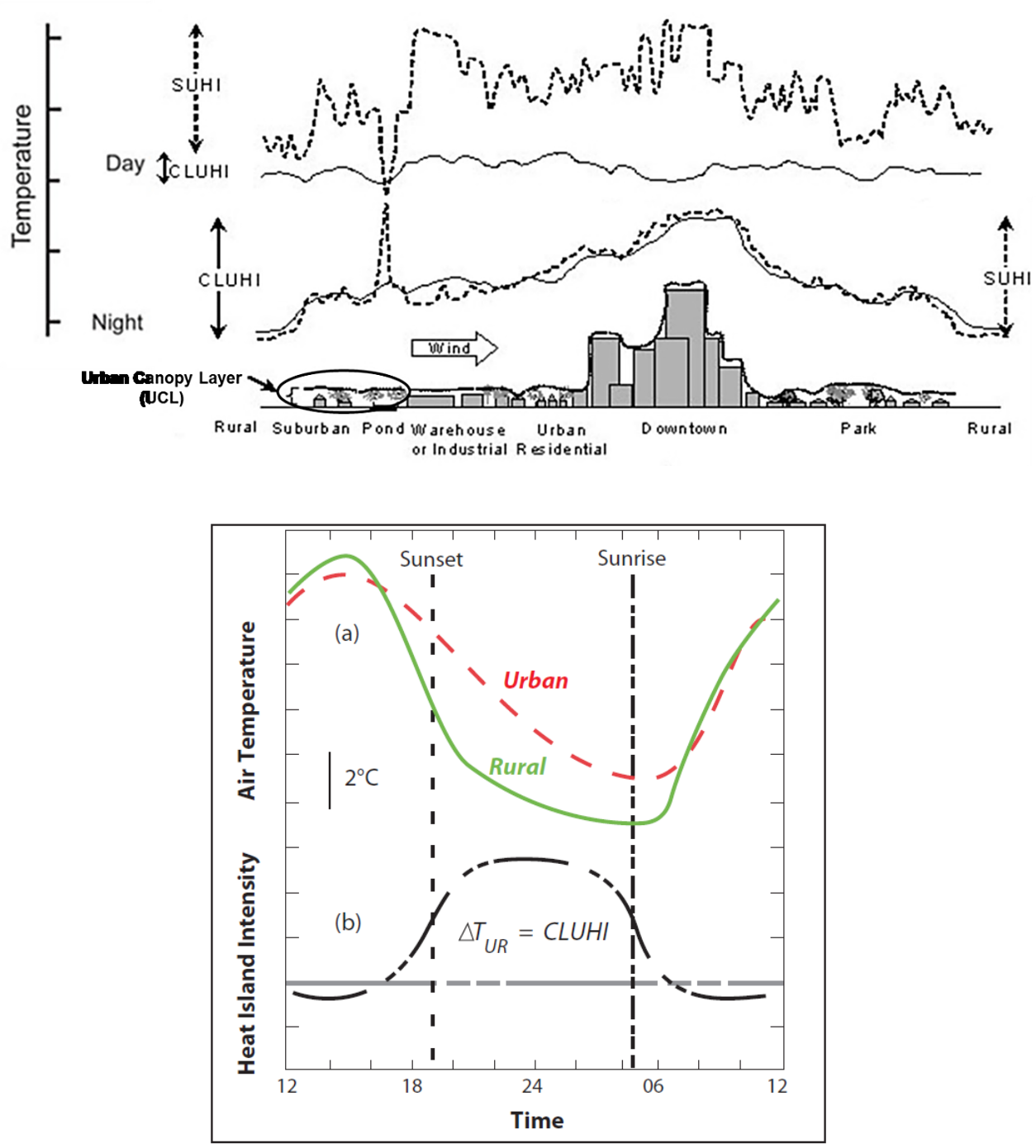

Figure 2.6: (upper) Variation of air temperature (solid line) and land surface temperature (dashed line) over different land-use types during the day and at night, modified from Voogt (2002); (lower) temporal variation of urban/rural air temperature and heat island intensity over 24 hours, Akbari et al. (2008) modified from Oke (1982).

2.3.2 Methods for measuring the UHIs

As described by Voogt (2002), the three main types of UHI include canopy layer UHI ($_{CL}$UHI), boundary layer UHI ($_{BL}$UHI), and sUHI. The urban canopy layer lies between urban surfaces and the tops of buildings and trees. The urban boundary layer is above the canopy layer ~1 km. The surface temperature generally refers to the 'skin' temperature (or LST).

Direct measurement

Most UHIs are derived from T_{air} measured directly by weather monitoring stations within the canopy layer (Voogt, 2002), where temperature sensors are generally installed at a standard screen-level height. Both $_{CL}$UHI and $_{BL}$UHI can be directly derived from T_{air}, and thus are regarded as the T_{air}-related aUHI. As $_{BL}$UHI can be measured by fixed and aircraft-mounted temperature sensors, as well as by remote sensing systems, its characteristics are more complicated. In this thesis, the $_{BL}$UHI is not used, and the aUHI is chosen to represent the $_{CL}$UHI.

Indirect (remote sensing) measurement

The sUHI can be quantified using LST derived from satellite measurements. The radiance reflected by the surface in various wavelength bands is measured by the satellite instrument and is used to estimate temperature. The temperature measurement is indirect in the sense that the temperature is not measured directly by the instrument but has to be estimated from the radiance. Satellite products are therefore more

susceptible to error than a direct measurement of T_{air}. In addition, the LST is sensitive to surface characteristics and has greater spatial and temporal variations than T_{air}.

Tomlinson et al. (2011) reviewed the various satellite remote sensing techniques for the LST measurements. Table 2.2 lists a comparative overview of ongoing major satellite remote sensing products and their applications. The Advanced Very High Resolution Radiometer (AVHRR) (Roth et al., 1989) has a spatial resolution of ~1.1 km (AVHRR, http://noaasis.noaa.gov/NOAASIS/ml/avhrr.html) and MODIS (Wan et al., 2004) has a spatial resolution of 1 km in the thermal infrared bands. There have been very few thermal infrared studies using Landsat-5 Thematic Mapper (TM) (Liu and Zhang, 2011) and Landsat-7 Enhanced Thematic Mapper Plus (ETM+) (120 m for TM and 60 m for ETM+) at very high spatial resolution due to limited temporal coverage (every 16 days) and contamination by cloud (Landsat, http://landsat.gsfc.nasa.gov/). The Advanced Spaceborne Thermal emission and Reflection Radiometer (ASTER) on board the Terra satellite has high spatial resolution (90 m) and daily temporal coverage, but data need to be requested only for commercial purpose and fees applied (ASTER, http://asterweb.jpl.nasa.gov/) and historical data are limited. In recent years, the MODIS instrument operating on the National Aeronautics and Space Administration (NASA)'s Aqua and Terra satellites has been widely used for LST measurements and sUHI studies (Hung et al., 2006). Both satellites can view the entire globe every 1-2 days. Data is acquired in 36 spectral bands at three spatial resolutions: 250 m (Band 1-2), 500 m (Band 3-7) and 1000 m (Band 8-36) (MODIS, http://modis.gsfc.nasa.gov/). In addition, not all bands are available at the three spatial resolutions. The MODIS LST at 5 km

resolution is retrieved in bands 20, 22, 23, 29 and 31-33. For clear-sky pixels, the LST is retrieved in bands 31 and 32 at 1 km resolution (Wan et al., 2004) using the generalized split-window algorithm (Wan and Dozier, 1996). For a given time and location, different satellite images capturing different spatial views of urban LST are generated using the MODIS Aqua and Terra sensors based on their different orbits.

Both methods of measuring UHIs have advantages and disadvantages, and they are related but rarely combined. By contrast, LST is used for estimating the diverse spatial distribution of sUHI. Satellite LST data are derived over pixels. However, this is an indirect measurement from radiance emitted by the land surface, which depends for example on the associated emissivity. Schwarz et al. (2012) combined both satellite-derived LST and ground-based T_{air} for quantifying the UHI in Leipzig, Germany. A strong relationship was found, and the LST data more reliably identified Leipzig's UHI in densely built-up areas than in less populated areas. Tomlinson et al. (2012b) compared summer temperature data for Birmingham, and the results showed that night-time T_{air} obtained from 28 stations is consistently higher than the LST, although station-specific variations exist. In Chapter 4 of this thesis, both methods are adopted to quantify the aUHI and the sUHI for Birmingham and London in relation to Lamb weather types (LWTs). The relationship of T_{air} and LST, and in particular the relationship between aUHII (aUHI intensity) and sUHII (sUHI intensity), are compared during cloudless anticyclonic nights. In Chapter 6, the relationships between aUHII and mortality rate are examined using T_{air} only.

Table 2.2: An overview of ongoing major satellite remote sensing products and applications, adapted from Wikipedia (2014) and Tomlinson et al. (2011).

Data Product	Spatial Resolution	Temporal Resolution	Acquisition (local time)	Strength	Weakness	Launched	Data access
Landsat 7 ETM+	15m, 30m, 60 m	Every 16 days	~10:00h	Free access; very high spatial resolution	Low temporal resolution	April 15, 1999	NASA/USGS: http://landsat.gsfc.nasa.gov http://landsat.usgs.gov/
Landsat 8	15m, 30m, 60m, 100m				Data from 2013	February 11, 2013	
ASTER Terra	15m 30m 90m	Daily	Terra: ~10:30h	High spatial/temporal resolutions	Terra satellite only;Request only for commercial purposes	December 18, 1999	NASA, Government of Japan https://asterweb.jpl.nasa.gov/data.asp LP DAAC: https://lpdaac.usgs.gov/dataset_discovery/aster/aster_products_table
AVHRR/3 (NOAA-15)	~1.1 km	Twice daily: entire planet	07:30h 19:30h	Free; high temporal resolution; long historical record	Lack of night-time images	May 13, 1998	NOAA/USGS: http://edc2.usgs.gov/1KM/avhrr_sensor.php
MODIS Terra Aqua	250m 500m ~1 km	Twice daily	Terra: ~10:30h ~22:30h Aqua: ~13:30h ~01:30h	Free; high spatial/temporal resolutions	-	Terra: December 18, 1999; Aqua: May 4, 2002	NASA: http://modis.gsfc.nasa.gov/data/ LP DAAC: https://lpdaac.usgs.gov/dataset_discovery/modis/modis_products_table
SPOT Satellite pour l'Observation de la Terre	1.5m, 2.5m, 5m, 10m, 20m	1–3 days	Daily revisits to any point on the globe	Very high spatial resolution; high temporal resolution	Data needs to be purchased	SPOT1 in 1986; SPOT6 in 2012	EADS Astrium SPOT 1-5 and 6/7: http://www.geo-airbusds.com/
GOES Geostationary Operational Environmental Satellite	1 km, 4 km, 8 km	Geostationary	At various intervals; up to 8 per hour	Free; geostationary satellite	Low spatial resolution	First Mission 1978	NOAA: http://www.goes.noaa.gov/ NASA: http://goes.gsfc.nasa.gov/
SEVIRI Spinning Enhanced Visible and Infrared Imager	Nadir geometric resolution up to 1 km	Geostationary	Every 15 mins	Very high temporal resolution	constant area, but not global	Meteosat-8 in 2005	https://wdc.dlr.de/sensors/seviri/

Birmingham's UHI

Previous studies for Birmingham's UHI include Unwin (1980) and Johnson (1985). Both studies used the urban Edgbaston station and rural Elmdon station to calculate the heating/cooling rates. There was an overall UHI of 0.27 K, daytime urban cooling of 0.49 K and night-time urban heating of 1.02 K during 1965-1974. By season, the largest night-time UHI occurred in autumn (1.34 K) and spring (1.11 K). The daytime UHI had its maximum absolute value in summer with an urban cooling of 0.59 K. The strongest night-time UHI (2.26 K) occurred under anticyclonic conditions. However, night-time UHI was weakest under cyclonic conditions (Unwin, 1980). By comparison, Johnson (1985) considered the traverse route of 20 km between Birmingham city centre and a rural village. Hourly temperatures were measured at 1.4 m above a car roof using a psychrometer at 27 points during eight days in July 1982. Over the eight sample days, the UHI reached a maximum of 4.7 K after sunset. Similar to Unwin (1980), the largest UHI occurred under calm, clear conditions, and conversely was suppressed by increased wind and cloud.

More recently, Birmingham's Urban Climate Change and Neighbourhood Estimates of Environmental Risk (BUCCANEER Project, 2011) modelled Birmingham's UHI using weather station data and the JULES (Joint UK Land Environment Simulation) model on the UKCP09 Weather Generator. Both MODIS LST and T_{air} from Edgbaston (urban) and Winterbourne (rural) were used. Over 2010, the annual averaged UHI was 0.37°C (night-time UHI was 0.89°C), and the maximum modelled UHI was 5.24°C. During the 2006 heatwave (18 July 2006, 01:00 h), Birmingham's UHI reached as high as 4.35°C

(Figure 2.7). Another recent NERC-funded project 'HiTemp', undertaken by the Birmingham Urban Climate Laboratory (BUCL, 2011), aims to examine the UHI in Birmingham, where the densest network of air temperature sensors is located, to identify possible adaptions to counteract UHI effects on health and wellbeing.

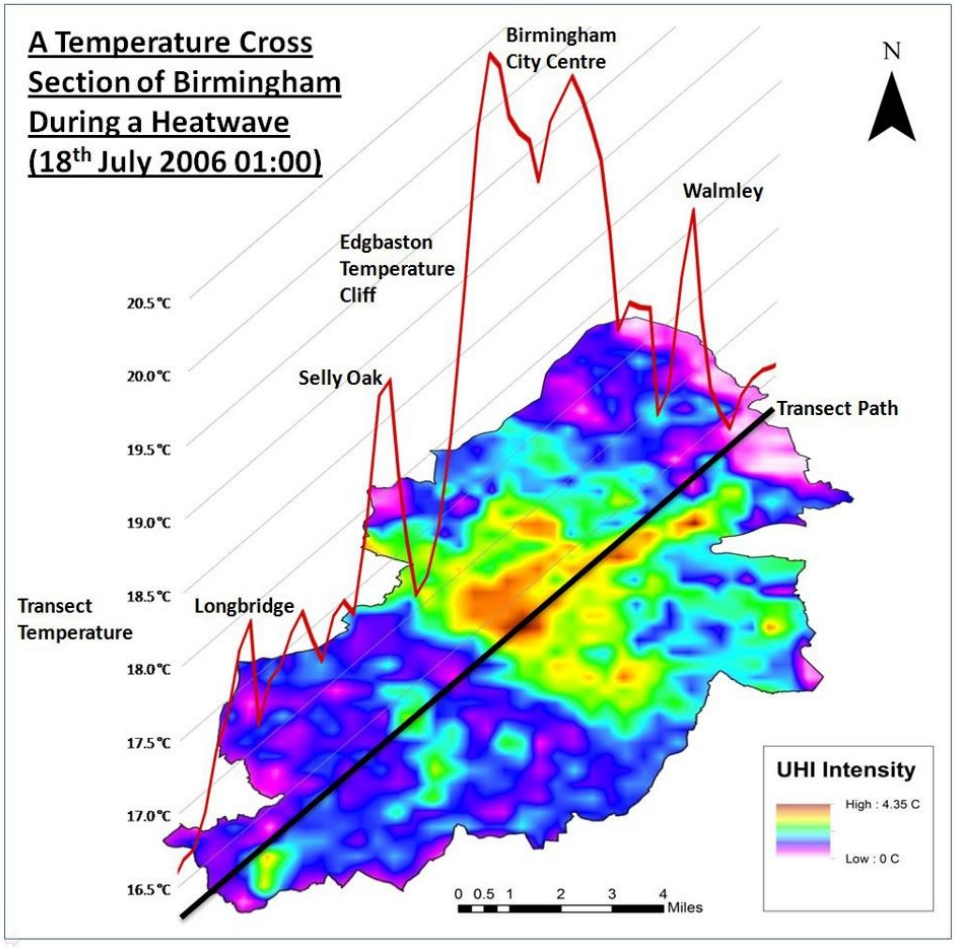

Figure 2.7: A temperature cross-section and spatial distribution of Birmingham's sUHI during a heatwave (18 July 2006, 01:00 h) (BUCL, 2011).

Tomlinson et al. (2012a) also examined the summer night-time sUHI in Birmingham using MODIS/Aqua LST data for different Pasquill-Gifford stability classes (Pasquill and

Smith, 1983): D (neutral), E (slightly stable), F (moderately stable) and G (extremely stable), as shown in Figure 2.8. The stability classes were classified based on wind speed and cloud cover at the Coleshill station. The results showed that the strongest sUHI occurred for the extremely stable class G (sUHII>3°C), and the weakest sUHI occurred for the neutral class D (sUHII>1.5°C). This finding confirms the selection of stable anticyclonic conditions for comparisons of T_{air} and LST, aUHII and sUHII.

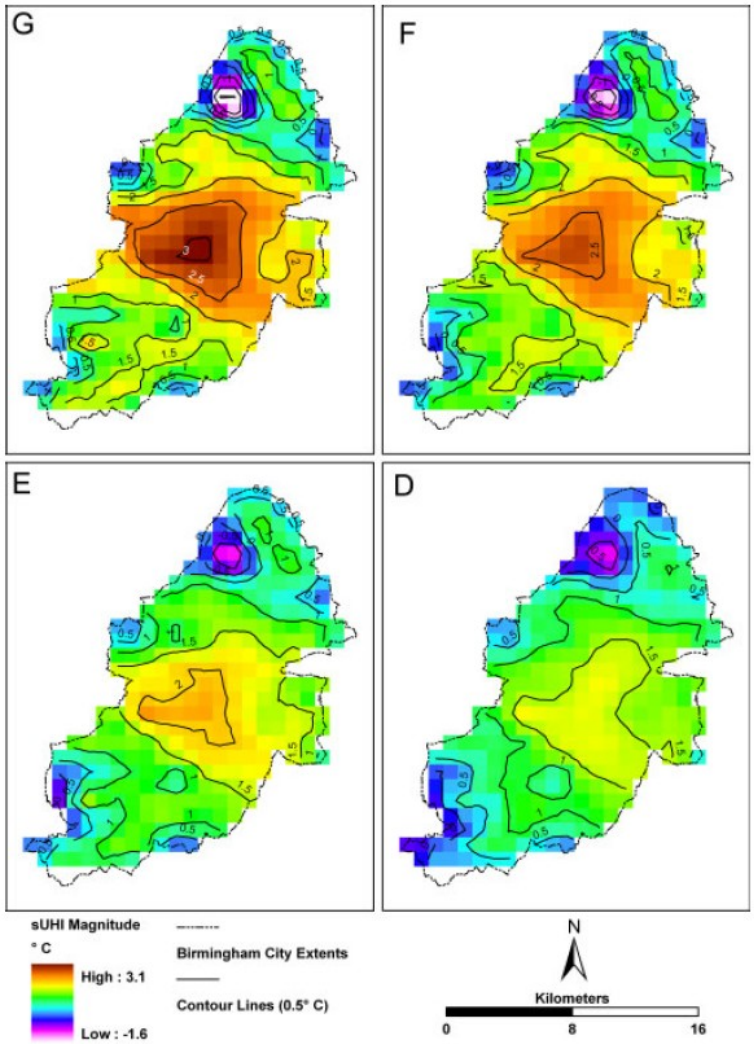

Figure 2.8: Birmingham's sUHI across Pasquill-Gifford stability classes D, E, F, and G (Tomlinson et al., 2012a).

London's UHI

The International Association for Urban Climate (IAUC) republished *'The Climate of London'* by Howard (1833), who first identified the effect of urban areas on local climate. Howard compared his temperature observations from 4 stations (3 rural stations outside London: Plaistow, Tottenham and Stratford and one urban station within London: Royal Society) with those recorded at Somerset House, located by the Royal Society. He concluded that urban temperatures are elevated by artificially generated heat from urban structures, populations and fuel consumption. He conducted a 10-year (1797-1806 in London, 1807-1816 in the country) analysis of daily maximum and minimum temperatures, and found that the night temperature was 3.7° (Fahrenheit) warmer in London than in the surrounding countryside.

Long-term trends in London's aUHI have been examined extensively. Lee (1992) analysed the temperature differences between St. James's Park and Wisley for the period 1962-1989. Results showed marked seasonal variations in London's UHI, which were particularly strong in summer (mean difference of 1.24°C) but weaker in winter (mean difference of 0.83°C). The daytime UHI was considerably weaker than the night-time UHI. Long-term trends showed an increase in night-time UHII but a decrease in daytime UHI intensity. Jones and Lister (2009) found the difference in UHI using different stations for the urban background. For St. James's Park, the UHI for $T_{air/max}$, $T_{air/min}$ and $T_{air/mean}$ was 0.6°C, 1.6°C and 1.1°C, respectively. For LWC, the UHI was stronger: 0.9°C, 2.8°C and 1.8°C, respectively. London's UHI has been analysed more extensively in relation to LWTs (Wilby et al., 2011). Long-term trends in the night-time

UHI during 1959-2009 showed increases in all seasons except winter (DJF). Similarly to the findings by Unwin (1980), London's strongest UHI also occurs under anticyclonic conditions and is weakest under cyclonic or westerly conditions. Wilby (2003) projected London's future UHI using the Met Office HadCM3 climate model. Unfortunately, the UKCP09 projections are not able to predict the future UHI due to the missing contribution from urban surfaces in regional climate models (Wilby et al., 2009).

Holderness et al. (2013) analysed 81 cloudless AVHRR images obtained during summer for the period 1996-2006 to demonstrate London's spatial temperature dynamics. London T_{air} data collected from the LWC, St James's Park, Heathrow and Northolt weather stations were also used to show the temporal temperature variations and generate the UHII metric. Results highlighted the spatial variations in London's UHI. In particular, on the heatwave day 8 August 2003, London's estimated LST reached a high temperature of 34°C and a low temperature of 23°C. London's sUHII was as low as -1.5°C to 0.5°C, and as high as 6°C to 8.8°C in densely built-up areas. The most distinct cold spot is located at Richmond Park in the West End of River Thames. While London's central growth continues, regeneration work is spreading to the surrounding areas, such as Croydon where shows a typical hot spot (Figure 2.9) because it has become one of London's largest property investment boroughs (McFall, 2014).The lack of green spaces due to the increasing buildings could be the main cause of the elevated temperature.

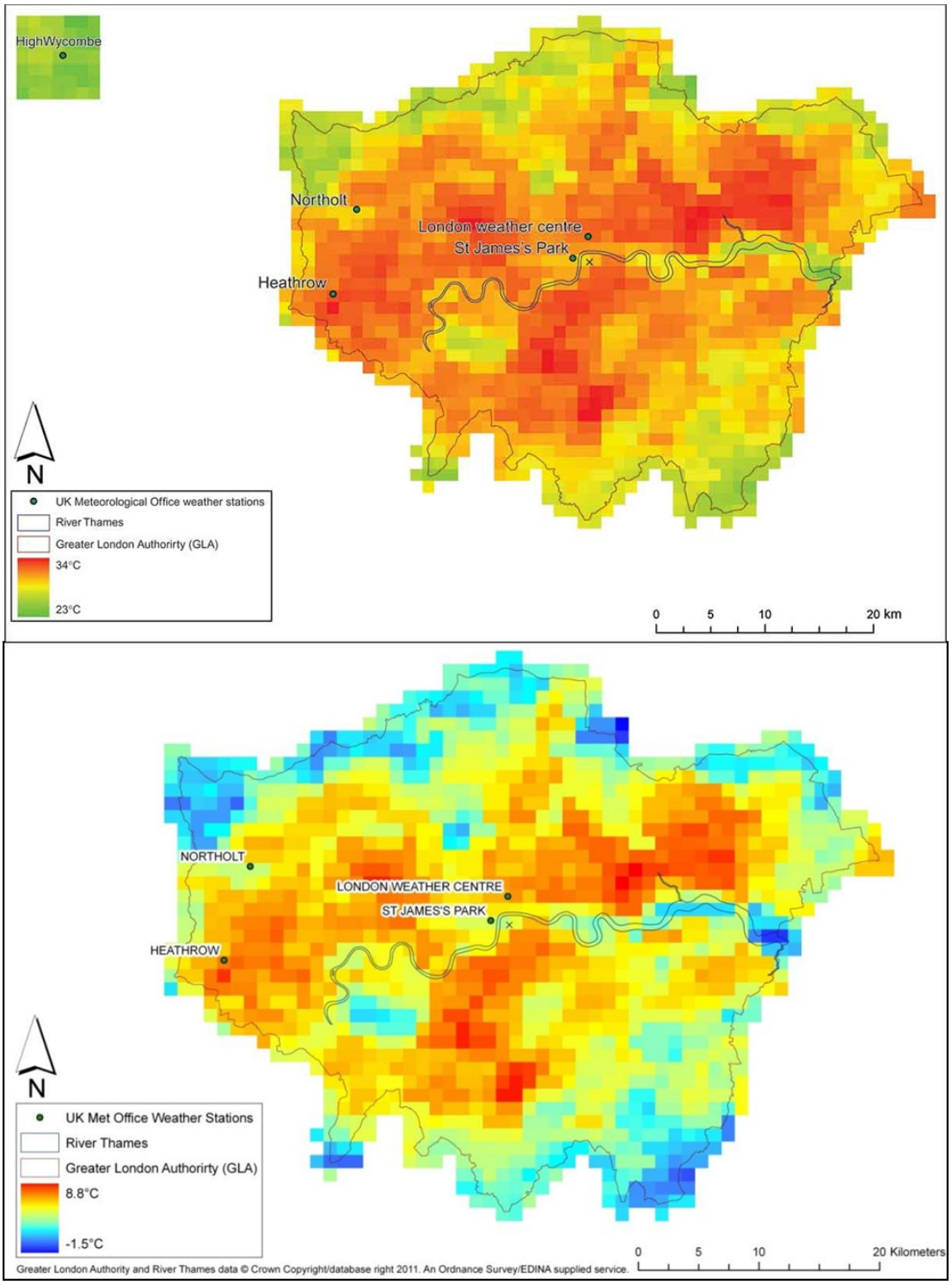

Figure 2.9: Spatial distribution of London's estimated surface temperature and the sUHII from AVHRR data on 8 August 2003 at 14:04 GMT (Holderness et al., 2013).

2.3.3 Heat island Impacts

Health risk

Elevated urban temperature caused by the UHI effect has a wide range of impacts on cities, including heat-related mortality and morbidity, energy consumption, air pollution, and many other aspects related to human health and wellbeing. Some health-related UHI consequences are beneficial, such as reduced winter mortality due to anthropogenic heat and less ice and snow on roads (Akbari et al., 2008). However, the impacts of UHI in warmer cities are mostly adverse to urban health, as it can cause additional heat stress. Studies found that the lack of night-time relief in $T_{air/min}$ is more significant than high daytime $T_{air/max}$ (Kalkstein, 1991). The increased daytime warming and reduced night-time cooling can potentially raise the risk of heat-related mortality and illness. With excessive increases in temperature, the associated increase in human body temperature exacerbates pre-existing health problems such as fever, heart diseases and severe heat stroke, potentially resulting in death in the worst cases. Children and elderly people are most vulnerable, especially during extremely hot days. The intensification of heatwaves in cities caused by UHI was highlighted in August 2003 and July 2006 when London's temperatures were 6-9°C higher than those in southern rural areas, causing nearly 600 excess deaths (GLA, 2006). Wong et al. (2013) reviewed the global UHIs, and found that many have been linked to increased mortality risk in particular as a result of the elevated urban temperatures during heatwaves. During a heatwave event, there is commonly an intense short-term increase in mortality, in which the elderly population suffers a higher mortality rate. In a review of the 2003 heatwave in

France (Dousset et al., 2011), an average excess mortality rate of 40% was recorded, with Paris reaching a +141% increase (4867 heat-related deaths) . After 11-13 August 2003 at the peak of heatwave, an overall decrease in mortality following the heatwave was observed until returning to mortality baseline, and in the following weeks no mortality deficit occurred, this is the so-called 'harvesting effect'. However, there appeared to be a mortality deficit of 20,000 deaths in the country in 2004, as a result of the harvesting effect of the 2003 heatwave (Fouillet et al., 2008). Over the heatwave period, there was a doubling of the elderly mortality risk associated with a 0.5°C increase in night-time temperature. The existence of UHIs has been documented for a large number of global cities. Notably, the largest effect was recorded in Tokyo with an increase of 12°C. Increased mortality rates in London have been linked to increased temperatures even during non-heatwave periods. A study of Montreal's UHI characteristics demonstrated a higher mortality in the heat island area (28% increase) with an average temperature of 26°C compared to the cold island areas (13% increase) with an average temperature of 20°C (Smargiassi et al., 2009).

Future mitigation

A recent report by ARUP (2014) found London's health risk among vulnerable people who at high heat risk in densely built-up areas. The UHI effect is one of the main causes for increasing urban heat risk. Urban temperatures can be potentially reduced by 2-8°C if wider green spaces and infrastructure are implemented, suggesting that green spaces should be in size of at least 0.5 hectares to achieve cooling benefits (Doick and Hutchings, 2013). The aim of urban planning is to promote urban growth associated with

income growth and spatial growth/sprawl. However, urban infrastructure also leads to environmental problems such as poor air and water quality, reduced vegetation cover, thermal stress and energy demand increase (Kahn, 2006). Actions to mitigate the UHI effects at a local scale should be taken include integration of green infrastructure (e.g. 'cool roofs', 'green roofs' and 'cool pavements'), since green spaces (Zupancic et al., 2015) can be beneficial for providing cooling effects and improving air quality and maintaining an 'utopia' sustainable urban communities (Mills, 2006). As an example, London's green infrastructure e.g. 'i-Tree Eco assessment', can provide flood protection, shade and biodiversity etc. (GLA, 2014).

2.4 Research gaps

According to the literature review, some topics have so far received little or no attention and require further study and research in the future. The following research gaps have been identified:

1. The intensities of aUHI and sUHI are correlated with weather patterns, such as pressure and wind speed. In depth studies are needed to stratify the UHIs by the LWTs, along with a comparison between T_{air}-related aUHI and LST-related sUHI during cloudless anticyclonic nights.

It may be worthwhile to combine these topics in a future research study, on the basis of previous UHI studies for Birmingham and London. The UHI has been properly studied in

association with LWTs (Wilby et al., 2011) (Morris and Simmonds, 2000)but the mortality has been rarely linked to the weather conditions. Measurements of T_{air} and LST have been compared by Tomlinson et al. (2012b) for 28 stations across Birmingham, and by Mildrexler et al. (2011) for WMO stations on a global scale. However, comparisons of aUHI and sUHI have so far not been tackled in previous studies.

2. The T-M relationships for the West Midlands and Greater London using a more flexible and straightforward method, and an FP regression model in STATA (Data Analysis and Statistical Software), based upon previous research on health effects of climate change in the West Midlands (WMPHO, 2010).

Previous studies have applied time-series regression models (e.g. GAMs) to the T-M relationships (details in Section 2.2.1). These models commonly need complex mathematical equations or adjustments for confounding factors. In this thesis, the detection of T_{mm} for a non-linear T-M curve is more straightforward using an FP regression model. The least predicted mortality can be found easily from the FP output, and the corresponding T_{mm} can be deduced immediately. In addition, a short-term heatwave episode analysis for 2003 was conducted. The latest IPCC (2014) WGII pointed out that studies on the health impacts of climate change have received a lot of attention, but urban and rural areas have not been properly distinguished. This thesis aims to investigate the health impacts for the urban area and rural area separately.

3. The relationship between aUHII and mortality rate for the West Midlands and Greater London, using bin-average analyses in each 0.5°C aUHII interval allowing a reduction in observation biases.

In recent years, the importance of the impact of UHI has been explored extensively. In particular, heatwaves and the number of hot days can be exacerbated by the UHI effect (Tan et al., 2010), and resulting in anincreased mortality risk due to heat exposure. However, it remains an outstanding question how the UHI directly relates to mortality. It should be noted that the origin of the urban-rural temperature difference is the result of an anomalously high urban temperature or an anomalously low rural temperature. In this respect, the aUHI for the West Midlands and Greater London should be based on variations in T_{air} during the selected study period. Unlike the direct impact of heatwave on mortality, the relationship between aUHII and mortality has not been investigated using strong evidence. All the available previous studies relate to the effects of temperature (in particular the heatwave) on human health using traditional methods, as described in Section 2.2. However, the relationship between aUHI and health (mortality) has not been investigated in depth. In this thesis, the aUHI-related mortality will be analysed using the summer temperature data. The bin-average analyses are then used to bin the aUHI data into categories.

Chapter 3 Study areas, data collection and pre-processing

This chapter provides background information about the chosen study areas (the West Midlands and Greater London), and describes the data used throughout this thesis. In Chapter 4, two types of temperature datasets: MODIS satellite observation data and the Met Office Integrated Data Archive System (MIDAS) observation data, are used to quantify the urban climate and the spatial/temporal UHIs of the West Midlands and Greater London. There are several procedures for obtaining and processing the MODIS data to derive the required LSTs. Details are discussed in Section 3.2. The MIDAS data were collected separately and processed for each weather station. Some duplicate and missing values were removed, and the MIDAS data were checked and arranged in individual files for further analysis. Details of the MIDAS data processing are discussed in Section 3.3. The MIDAS T_{air} data were used to calculate the intensity of aUHI used in Chapters 5-6. In Chapter 4, the LWTs were used to analyse the variation in aUHI and sUHI. Data preparation was conducted to extract the corresponding days for each LWT. Details are described in Section 3.4. Daily mortality data for the West Midlands and Greater London were requested from public health observatories in the UK. In conjunction with the regional population data in Section 3.5, mortality data were used to calculate the mortality rates used in Chapters 5-6. Details about the use of the mortality data are discussed in Section 3.6.

3.1 Study areas

The regional assessment in this thesis includes the relationship between temperature and DMR (Chapter 5), and the relationship between aUHII and DMR (Chapter 6) for the outer and inner band of the West Midlands and Greater London, respectively. An important concept is the urban-rural boundary, which separates the urban built-up areas (inner band) and the surrounding rural areas (outer band). It is first necessary to identify proper urban-rural boundaries to select representative weather stations before further analyses.

Urban-rural categories vary widely. In 2007, there were around 30 different classifications used across the UK (Scott et al., 2007). The ONS (Office for National Statistics) urban-rural definition for the Middle Layer Super Output Area (MSOA) in England is shown in Appendix 1. The classifications are mainly based on land-use types and population size. In the UK, settlements with a population of more than 10,000 are considered to be urban areas. However, settlements with a population of 3,500 to 10,000 can be categorised differently (Pateman, 2011). In general, urban areas have more business and residential buildings, higher population densities and more developments (e.g. buildings, parks and roads). The rural areas include large open spaces and small settlements, and are far away from the central areas. In other words, the rural areas can be defined as the inverse or residual of the urban areas (IPCC, 2014, Lerner and Eakin, 2011). Indeed, the urban-rural boundaries between the inner band and the outer band are not absolutely fixed. In this thesis, the urban characteristics can be identified from the satellite images (1 km^2 pixel) for the urban weather stations at

Edgbaston and LWC; the rural characteristics can be identified from the satellite images for the rural weather stations at Shawbury and Rothamsted (details see Section 3.1.1 and Section 3.12).

The UHII is calculated (Section 4.4) by subtracting the rural temperature from the urban temperature. This is probably the most important but sensitive procedure, because the calculated UHII varies sensitively with the paired combination of temperature. If any urban temperature (or rural temperature) were to be substituted with the temperature measurement from an alternative weather station, the calculated value would change appreciably. Therefore, the urban and rural weather stations for the West Midlands and Greater London were very carefully selected. The UK Met Office aims to select ideal weather stations (e.g. level ground without trees and buildings etc.) that represent observations from a wider area surrounding the station, which are unduly affected by local effects such as shading, warming or wind effects caused by trees, buildings or topography (MetOffice, 2011b). Indeed, it is impossible to find a perfect weather station.

In this thesis, the selection of urban and rural weather stations is mainly based on their locations (Table 3.1) and surrounding environments for the West Midlands and Greater London. There are multiple reasons for selecting these weather stations. Firstly, the selected stations should satisfy the data availability used throughout the thesis, for example, the MIDAS/MODIS data, and the mortality and population data. Secondly, the urban and rural stations should be the best available representation of the urban and rural characteristics. That is, an urban station should be located in a central area, densely populated, and largely surrounded by buildings; a rural station is better located

in an open space with fewer buildings but more vegetation coverage. Thirdly, the distance between the urban station and the rural station should not be too close, so that the temperature difference is representative of the urban-rural difference.

The effect of differences in elevation on the UHI calculation have been discussed by Jones and Lister (2009), and Peterson and Owen (2005). In this study, the 88 m elevation difference between the Edgbaston and Shawbury weather stations, and the 85 m elevation difference between the London Weather Centre and Rothamsted weather stations, were not compensated. Based on the atmospheric lapse rate of 6.4°C/km of elevation above the ground level, the offset in temperature due to the difference in elevation is expected to be small and will be mentioned in the text where relevant. Elevation details for the selected weather stations can be found in Table 3.1.

Table 3.1: Information on local weather stations in the West Midlands and Greater London.

Weather Station	BADC Station ID	Latitude (WGS 84)	Longitude (WGS 84)	Elevation (m)	Station type	Station Start Date	Station End Date
West Midlands							
Edgbaston	587	52.4755	-1.93518	160	Urban	01/01/1893	Oct. 2012
Coleshill	19187	52.4801	-1.69072	96	Sub-urban	01/09/1997	Current
Shawbury	643	52.7947	-2.66465	72	Rural	01/01/1944	Current
Greater London							
London Weather Centre (LWC)	19144	51.5215	-0.11249	43	Roof top	01/01/1929	01/02/2010
Rothamsted	471	51.8067	-0.36017	128	Rural	01/01/1872	Current

3.1.1 West Midlands

The West Midlands is located in western central England, and comprises the UK's second most populous city (Birmingham) and a county which includes seven metropolitan boroughs (Birmingham, Coventry, Wolverhampton, Dudley, Sandwell, Solihull and Walsall). It covers 13,004 km^2 with a population of 5,602,000. The city of Birmingham covers 268 km^2 with a population of 1,073,000 (ONS, 2011).

In order to hierarchically associate the regional temperature (or UHI intensity) with mortality, two bands (outer andinner band, Figure 3.1a) with increasing population densities from outer to inner band were adopted to represent exclusive datasets. As shown in Appendix 1, Birmingham is considered to be urban, and the Metropolitan County (MC) is classed as urban and less sparse town and fringe. The remaining areas in the West Midlands are mostly village, hamlet and isolated dwellings. Unfortunately, the urban-rural boundary for the West Midlands is vague and debatable. According to the ONS Beginners Guide to UK Geography - Metropolitan Counties and Districts, the West Midlands MC is defined as one of the most heavily urbanised regions in England. In this thesis, the boundary separating the inner and outer band was self-defined. The inner band of the West Midlands is the MC, including the UKs second most populous urban city outside London, i.e. Birmingham. The outer band of the West Midlands is defined as the regional difference between the West Midlands Government Office Region (GOR) and the MC, including 7 metropolitan boroughs and 24 local authorities (Figure 3.1a).

To represent the spatial distribution of sUHII in MSOA scale, the West Midlands MSOA shapefile extracted from the 'English Middle Layer Super Output Areas 2001' was

downloaded from the EDINA UKBORDERS, UK Data Service. The West Midlands MSOA includes a total of 34 local authorities (735 local names), which were compiled by WM Health GIS Service (WMHGIS).

For the West Midlands, the urban and rural weather stations were selected from the 'Met Office MIDAS Stations' system from 129 available stations. The Edgbaston station and the Shawbury station were selected to represent the urban area and the rural area of the West Midlands, respectively. In Figure 3.1(b), the Edgbaston station (52.4755°N, -1.93518°W) is located in Birmingham's central redevelopment area, approximately 2 km to the west of the city centre at an elevation of 160 m. In Figure 3.1(c), the Shawbury station (52.7947°N, -2.66465°W) in Shropshire is located approximately 65 km to northwest of Edgbaston at an elevation of 72 m. Because the West Midlands region has various land-use types and the urban area is limited, the rural station located within the West Midlands GOR is a good choice. Xoserve (2013) indicated that the Edgbaston station was closed until the end of October 2012. However, the closure of Edgbaston station does not affect the study period of 2001-2009. Furthermore, it is considered the most suitable urban weather station in comparison to other potential stations, such as the sub-urban Coleshill station which is located ~4.5 km from Birmingham's eastern edge (Figure 3.1a). In this thesis, the Coleshill station was only used for obtaining the cloud cover data that are not available at the Edgbaston and Shawbury stations. It will be mentioned where appropriate.

(a)

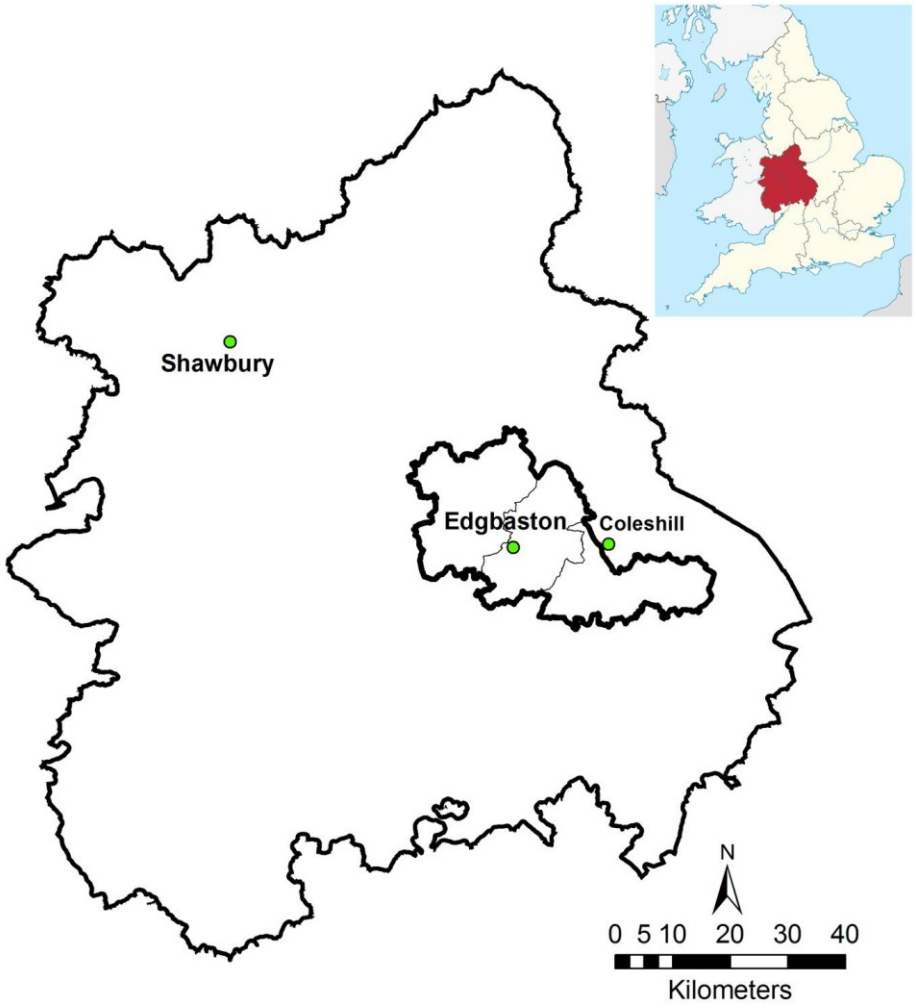

Local Authorities:

Outer band (GOR-MC) includes: Bridgnorth, Bromsgrove, Cannock chase, East Staffordshire, Lichfield, Malvern Hills, Newcastle-under-Lyme, North Shropshire, North Warwickshire, Nuneaton and Bedworth, Oswestry, Redditch, Rugby, Shrewsbury and Atcham, South Shropshire, South Staffordshire, Stafford, Staffordshire Moorlands, Stratford-on-Avon, Tamworth, Warwick, Worcester, Wychavon, and Wyre Forest.

Inner band (MC) includes: Birmingham, Coventry, Dudley, Sandwell, Solihull, Walsall, and Wolverhampton.

(b)

(c)

Figure 3.1: (a) Map of the West Midlands showing the outer-inner band distinction and local authorities; Google Earth views of the local weather stations across the West Midlands at (b) Edgbaston and (c) Shawbury.

3.1.2 Greater London

Greater London is located in southeast England and includes the capital city of London and 32 London boroughs (Wikipedia, 2015). It covers an area of 1,572 km^2 with a population of 8,174,000 (ONS, 2011). Similarly to the West Midlands, the shapefiles for the Greater London MSOA extracted from the 'English Middle Layer Super Output Areas 2001' were downloaded from EDINA UKBORDERS, including a total of 33 local authorities (Figure 3.2a).

Although the entire Greater London area is classed as less sparse urban with a population of more than 10,000 (Appendix 1), the outer and inner London areas have been officially defined. Figure 3.2(a) shows the inner band of Greater London including the city of London and 12 London boroughs, and the outer band of Greater London including 20 London boroughs. For Greater London, the urban and rural weather stations were selected from the 'Met Office MIDAS Stations' system from 397 available stations. According to the rationale for the selection of weather stations on page 60, the London Weather Centre (LWC) and the Rothamsted weather stations (Figure 3.2b and Figure 3.2c) were selected to represent urban and rural areas, respectively. The sensor picture shown in Figure 3.2(c) was obtained from the UK Environmental Change Network (ECN). These two stations were selected based on their locations and data availability. The LWC is located on the roof top in a developed area of London, has been classified as an urban station. It moved from Clerkenwell Road at an elevation of 77 m in 1992 to its current location at an elevation of 43 m. According to the dry adiabatic lapse rate, the change is just under 1°C centigrade per 100 m elevation, and therefore the effect of location change should have only a minor impact (~0.2°C) leading to slightly

higher temperatures. Although the LWC was closed in February 2010, its closure does not affect the London study period 2001-2009. The LWC station is likely not an ideal choice as a typical urban weather station since it has rooftop effect. Indeed, good stations in London are very limited. The LWC could be a better choice compared to other popularly used stations, such as St James's Park (Wilby et al., 2011), which is not located in a central developed area and is known to be cooler due to the vegetation coverage. Some rural weather stations were used in previous studies such as Wisley (~32 km from LWC) (Lee, 1992), Rothamsted (Wilby et al., 2011), Kew (~13 km from central London) and Heathrow (~26 km from central London). Rothamsted (in Hertfordshire) is the second Hadley CET station, approximately 43 km to the north-west of LWC, and was selected as a rural station, although it is not located within the Greater London region. As shown in Appendix 1, the urban-rural local authority classification in England does not show rural local authorities for Greater London. It is worth noting that the local authority types are defined by population (e.g. large urban areas have populations of 250,000 to 750,000). Due to London's overall urban characteristics, it is better to select a rural station outside the London region. In terms of the possible rural stations, Rothamsted is furthest away from central London and is expected to be a better choice to quantify the urban-rural temperature difference.

(a)

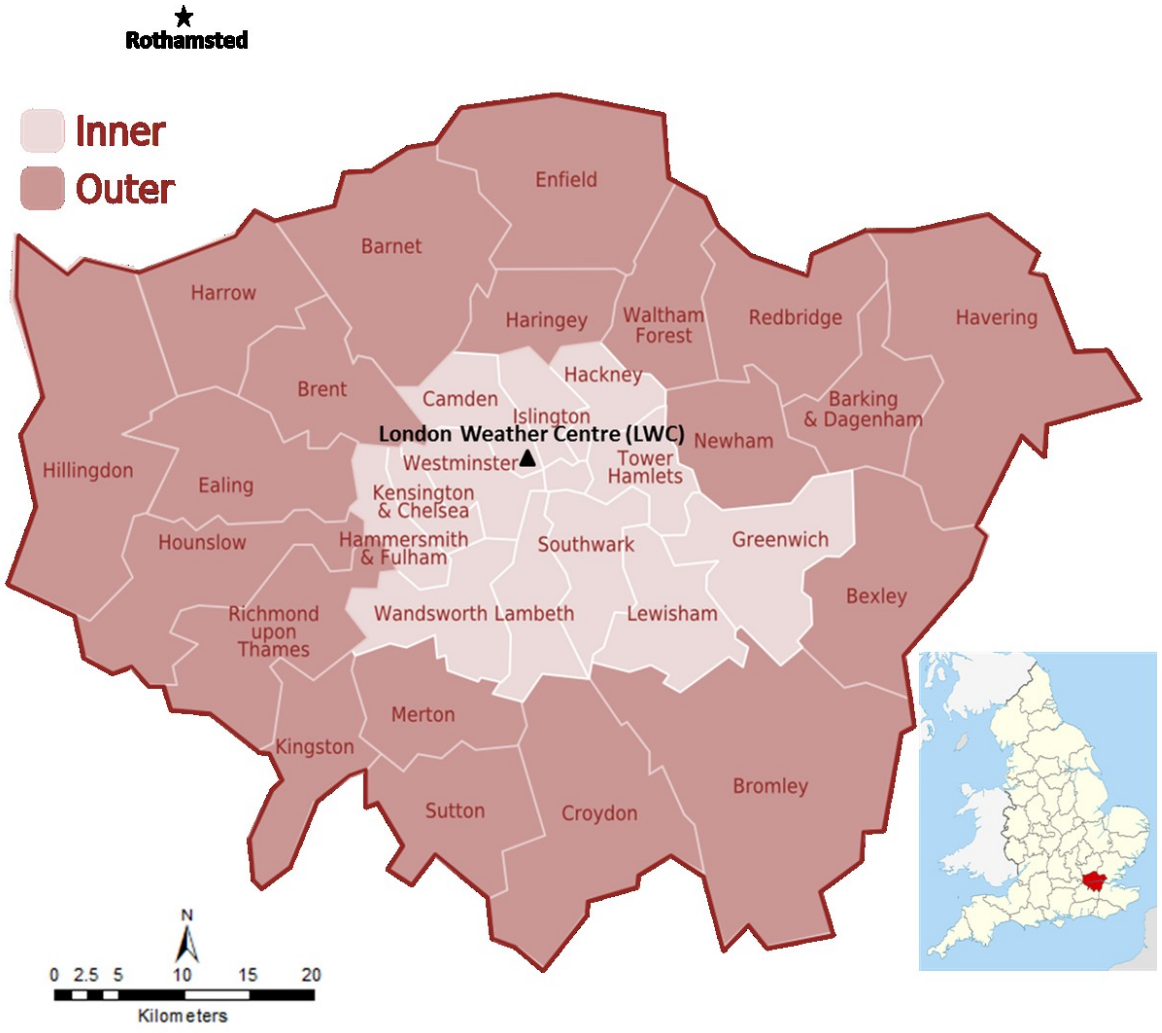

Local Authorities:

Outer band includes: Barking and Dagenham, Barnet, Bexley, Brent, Bromley, Croydon, Ealing, Enfield, Haringey, Harrow, Havering, Hillingdon, Hounslow, Kingston upon Thames, Merton, Newham, Redbridge, Richmond upon Thames, Sutton, Waltham Forest.

Inner band includes: City of London; Camden, Greenwich, Hackney, Hammersmith and Fulham, Islington, Kensington and Chelsea, Lambeth, Lewisham, Southwark, Tower Hamlets, Wandsworth, Westminster.

(b)

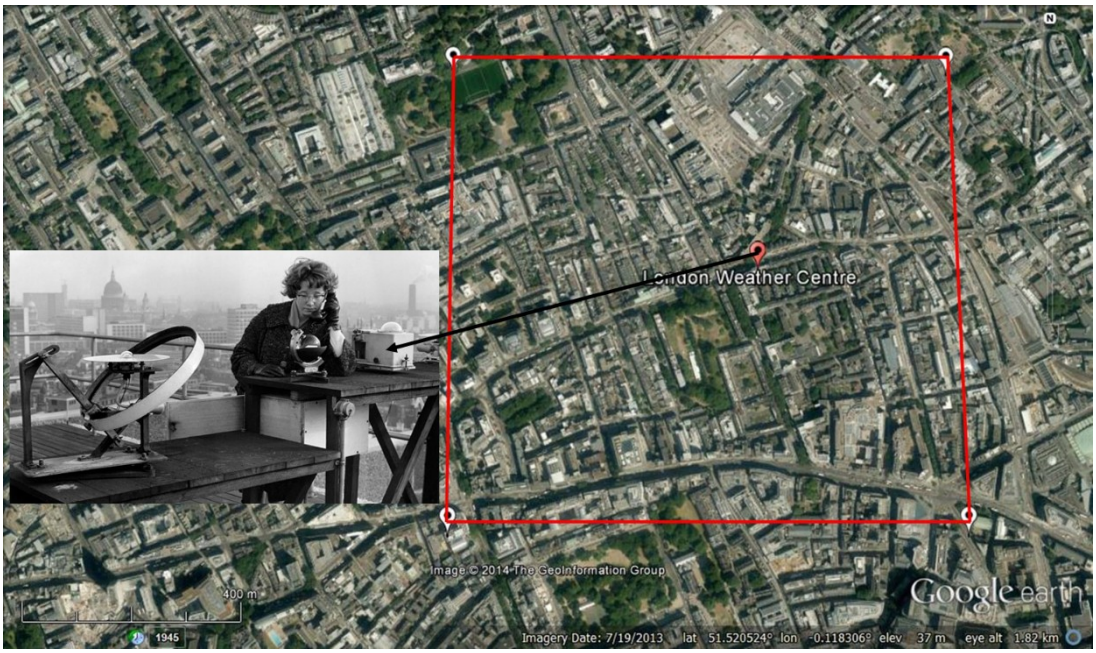

(c)

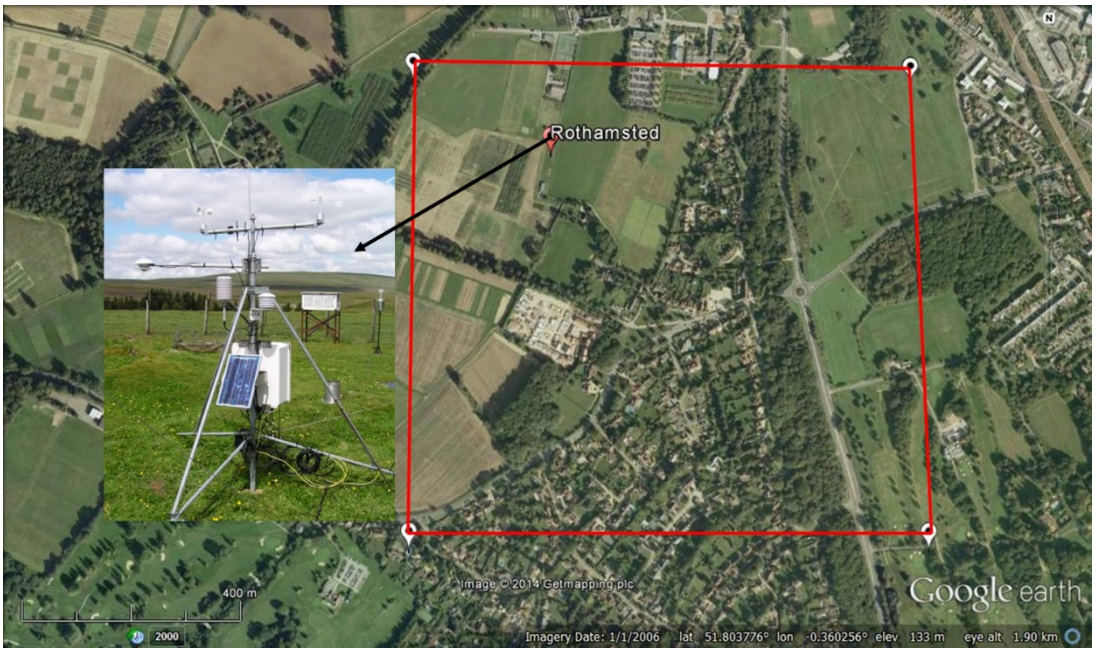

Figure 3.2: (a) Map of Greater London showing the outer-inner band distinction and local authorities (modified from Wikitravel (2009); Google Earth views of local weather stations at (b) LWC and (c) Rothamsted.

3.2 MODIS data

3.2.1 MODIS overview

As discussed in Section 2.3.2, the UHI can be determined using satellite remote sensing measurements. Compared with other widely used datasets for the study of urban surface characteristics (including the Landsat TM and ETM+, MODIS, ASTER and AVHRR), the MODIS sensor was chosen due to its better temporal resolution, global coverage, clear-sky observations and accurate calibration in the thermal infrared bands (Wan et al., 2004). It has a broad viewing swath of 2,330 km and detects the entire Earth's surfaces in 36 spectral bands every 1 to 2 days. MODIS provides 44 standard data products, for the land, ocean and atmosphere. The data has a variety of applications in mapping global land surface characteristics including LST and emissivity, surface reflectance, vegetation indices and so on. Three spatial resolutions are available: 250 m, 500 m and 1,000 m. The Land Processes Distributed Active Archive Centre (LP DAAC) also provides a higher level resolution product at 5,600 m. Data from the MODIS instrument is provided at daily, 8-day, 16-day, month, quarterly and yearly temporal resolution (MODIS Overview, 2014). Although the Landsat ETM+ can acquire measurements at finer spatial resolution, the repeat cycle for imaging the same geo-location is 16 days. By comparison, MODIS has a repeat cycle of 1-2 days.

The MODIS sensor flies aboard both the Terra and Aqua satellite platforms, which form part of the Earth Observing System (EOS). The EOS-Terra satellite was launched on 18 December 1999 (Terra, 2014), the EOS-Aqua satellite was launched on 4 May 2002 (Aqua, 2014). The MODIS/Aqua acquisition time is around 13:30 UTC (local time) in ascending (daytime) mode and 01:30 UTC in descending (night-time) mode. The

MODIS/Terra acquisition time is around 22:30 UTC in ascending mode and 10:30 UTC in descending mode (Wan et al., 2004). For this study, 1 km spatial resolution and daily temporal resolution is required. Therefore, two MODIS products were considered: MYD11A1 (MODIS/Aqua Land Surface Temperature and Emissivity Daily L3 Global 1 km Grid SIN) and MOD11A1 (MODIS/Terra Land Surface Temperature and Emissivity Daily L3 Global 1 km Grid SIN). Level-3 processing provides the gridded variables for each pixel at a given spatial and temporal resolution. The MODIS/Aqua product MYD11A1 was selected for further analysis, as the local acquisition time in Birmingham and London is at approximately 01:30 UTC. As determined by comparing the noise equivalent temperature (i.e. a way to state Aqua/Terra instrument noise level of thermal fluctuations in the sensors) of the datasets, the MODIS/Aqua data is of better quality than the MODIS/Terra data in most thermal infrared bands (Wan et al., 2004). Furthermore, only the night-time LSTs derived from MODIS/Aqua data were processed to analyse the spatial patterns of sUHI. As there is less cloud cover and weaker winds at night, the Earth's surface can be considered to be mostly homogeneous and isothermal. Settled weather conditions are ideal conditions for UHI research. During the daytime, measurements are limited by solar radiation and vegetation shadows. Due to the presence of vegetation, the measured surface temperatures are lower under shadows than those measured directly in the sunlight (Wan and Dozier, 1996, Wang et al., 2008).

3.2.2 MODIS product - MYD11A1 and data collection

The chosen MODIS/Aqua product, MYD11A1, was obtained using a generalised split-window LST algorithm (Wan and Dozier, 1996). It includes 12 Scientific Data Sets (SDS) comprising daytime and night-time observations (LSTs, quality control, observation time, viewing zenith angle, and clear-sky coverage). Tile-based gridded values of LSTs are provided as well as surface emissivity for land cover types at a ~1 km (precisely at 0.928 km) spatial resolution. The LST data are derived from radiance emitted by the land surfaces (i.e. canopy in areas covered with vegetation, or soil surface in open areas), which is detected by the MODIS sensor. The interference of cloud may cause confusion for the measurement of LST, as suggested by Wan et al. (2004) that the LST can only be derived in clear-sky conditions, because thermal infrared radiation can be absorbed by clouds. In this thesis, it is important to get rid of any measurements that might have cloud in them before inverting the radiance measurements to deduce the LST.

The data access tool for obtaining MODIS data is the NASA LP DAAC Data Pool. The MYD11A1.005 data directories are readily accessible for HTTP download at http://e4ftl01.cr.usgs.gov/MOLA/MYD11A1.005/. MODIS/Aqua LST data are available from 8 July 2002 up to the present day. Only the Hierarchical Data Format (HDF) files were downloaded. The MODIS product MYD11A1 is projected onto a sinusoidal grid. The MODIS sinusoidal grid tiling system (Figure 3.3) was obtained from the NASA Distributed Active Archive Centre (DAAC) at NSIDC. The tile identifier h17v03 was selected to acquire the data across Birmingham. The tile identifiers h17v03 and h18v03 were selected to acquire data across London.

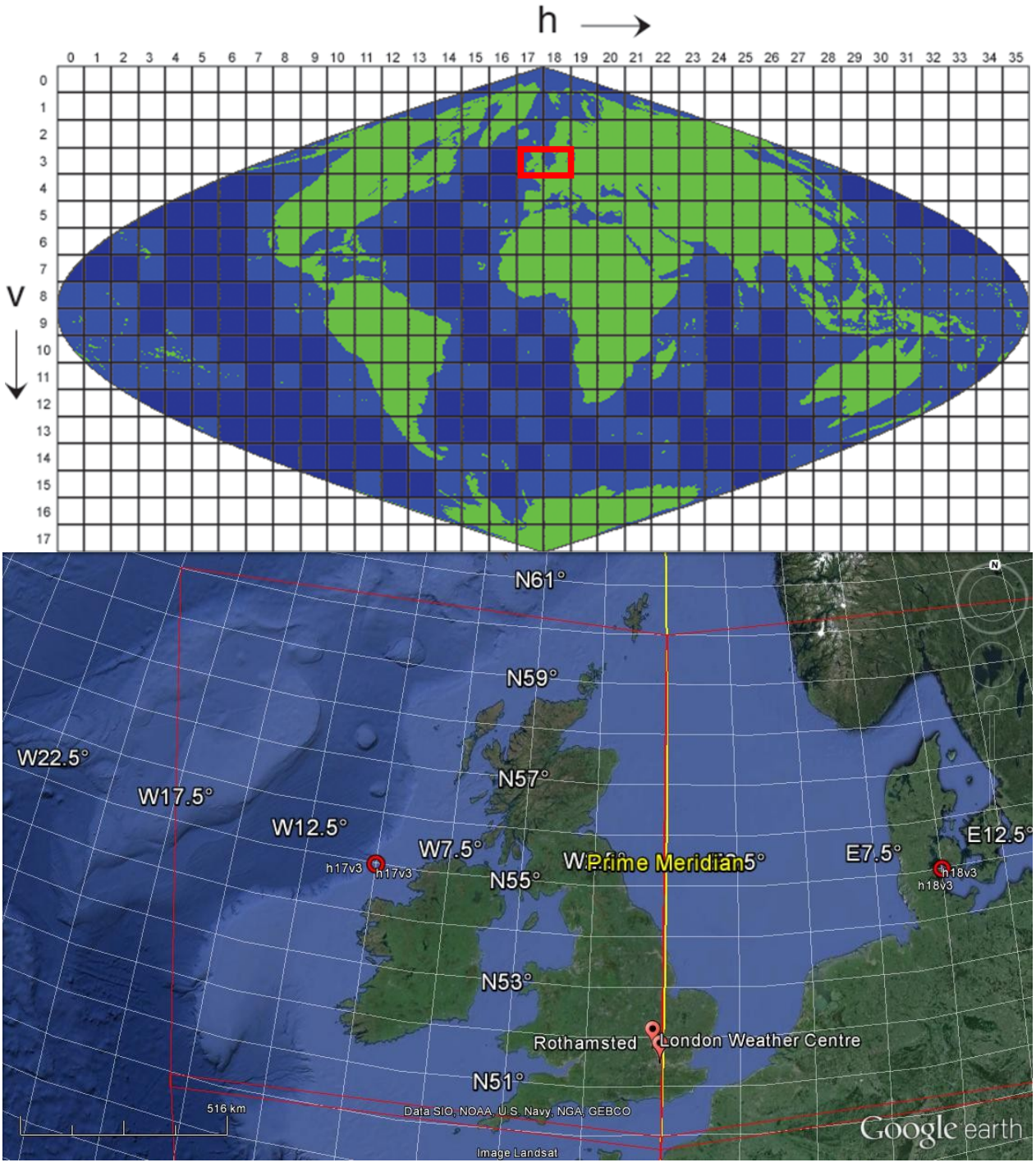

Figure 3.3: MODIS sinusoidal grid tiling system (h17v03 and h18v03 highlighted in red box).

3.2.3 Pre-processing MODIS data

The obtained MODIS data in HDF format are not able to directly map as spatial patterns, therefore, specific conversion tools are needed to work with the embedded geographic coordinate information in the data file. For the purpose of processing the MODIS HDF-EOS data in the sinusoidal projection, NASA DAAC has introduced several popular tools to manipulate the MODIS data. MODIS Reprojection Tool (MRT) is a software tool to reproject the gridded MODIS Level-2G, Level-3 and Level-4 land products, and convert them to GeoTIFFs; MODIS Conversion Toolkit (MCTK) is a plugin for Environment for Visualizing Images (ENVI) that can import and convert the MODIS product to a projected and geo-referencing output coordinates.

In this thesis, the downloaded MODIS LST data in HDF with a sinusoidal grid projection were converted to ArcGIS raster format (i.e. ArcInfo Binary Grid) using the Marine Geospatial Ecology Tools (MGET) (Roberts et al., 2010) toolbox, which can be easily installed in ArcGIS as a geo-processing toolkit, for mapping the spatial patterns of LST and sUHI. The main reasons for selecting MGET as the MODIS data processing tool are: (1) it includes all the necessary functions with over 300 tools, e.g. read and view MODIS HDF data; convert to ArcGIS raster format directly. Although the procedures (Figure 3.4) are somewhat complicated, step-by-step ArcGIS tutorials (Roberts, 2011) simplify the procedure; the technical installation instructions are available at the MGET official website (http://mgel.env.duke.edu/mget). (2) it works perfectly as an interface in ArcGIS provided with detailed tutorials, and can be written in R, MATLAB, and C++, and also fits statistical model such as GAM; (3) it has been utilised successfully by (Tomlinson et al. (2012a)) for determining Birmingham's sUHI characteristics.

After installing MGET, it can be accessed from the ArcToolbox window in ArcGIS applications such as ArcMap and ArcCatalog. The 'Convert SDS in HDF to ArcGIS Raster' tool from the MGET toolbox was used to process the MODIS/Aqua night-time LST data. Once the night-time MODIS LST images were converted to ArcInfo Binary Grid format, the spatial patterns were mapped using ArcMap by combining the raster outputs with the Birmingham and London MSOA shapefiles. The instruction flow diagram is shown in Figure 3.4.

The step-by-step instructions to process the MODIS data using the MGET tool are given as below.

1. Open MGET's '**Conversion**' tool, select '**to ArcGIS Raster**', and select '**From HDF SDS**', and select '**Convert SDS in HDF to ArcGIS Raster**'.
2. Import the downloaded HDF file and create an ArcGIS raster. The SDS name should be specified as '**LST_Night_1km**' i.e. night-time LST at 1 km spatial resolution. The X and Y coordinates of lower-left corner are calculated using the following formulas, which are provided in the MGET official website:
    - **Tile width or height** = Earth width / 36 = (20015109.354 + 20015109.354) / 36 = 1111950.5196666666 m
    - **Cell size** = tile width / cells = 1111950.5196666666 / 1200 = 926.625433055556 m
    - **X coordinate of lower-left corner** = -20015109.354 + horizontal tile number * tile width
    - **Y coordinate of lower-left corner** = -10007554.677 + (17 - vertical tile number) * tile height

For the tile identifier h17v03, X coordinate of lower-left corner is -1111950.51966666 m, Y coordinate of lower-left corner is 5559752.59833333 m.

For the tile identifier h18v03, X coordinate of lower-left corner is –0.00000012 m, Y coordinate of lower-left corner is 6671703.1179999 m. Cell size is 926.625433055556 for both tile identifiers.

3. Define the '**Post-conversion processing**'.
4. Under '**Spatial Reference Properties**', select to create new projected and geographic coordinate systems.
5. Create a new projected coordinate system called '**MODIS_V5_Sinusoidal**', select projection name as '**Sinusoidal**'.
6. Select to create a new geographic coordinate system.
7. Define the new geographic coordinate system as '**MODIS_V5_Sphere**', and both semi-major axis and semi-minor axis are defined as of **6371007.181**(i.e. sphere of the MODIS sinusoidal projection). The angular unit is set as '**Degree'**, and the Prime Meridian is '**Greenwich**'.

Finally, the map algebra expression needs to be set as '**float(inputRaster) * 0.02 – 273.15**' to express the LST data in unit of Celsius (°C).

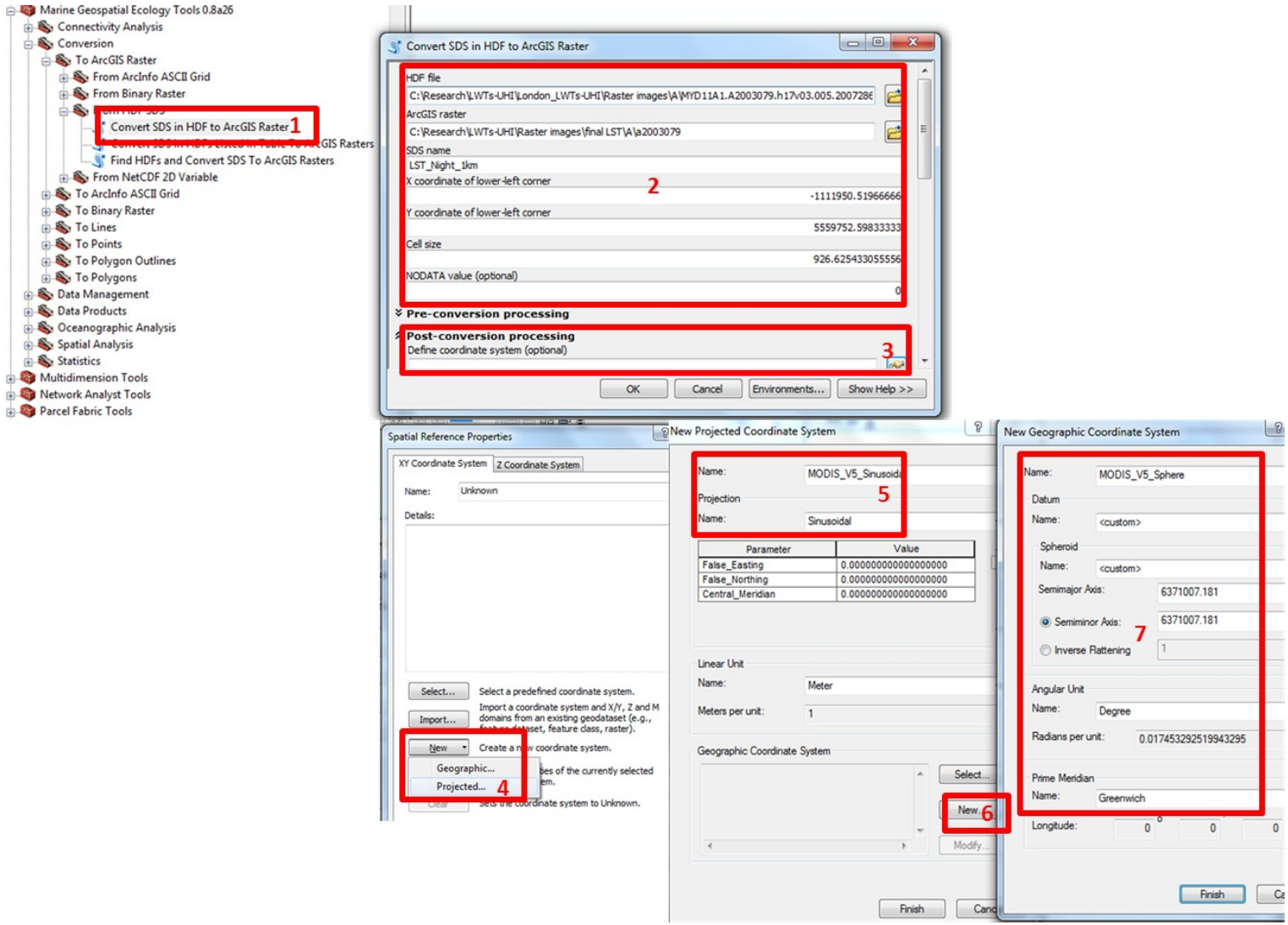

Figure 3.4: Converting MODIS SDS in HDF to ArcGIS raster using the MGET toolbox in ArcMap's ArcToolbox.

3.3 MIDAS data

The UK Met Office Integrated Data Archive System (MIDAS) Land Surface Stations data were requested from the British Atmospheric Data Centre (BADC) by submitting BADC Dataset/Service registration (Appendix 2). Among all the available types of weather data, this thesis uses the UK Daily Temperature (TD) and UK Hourly Weather (WH), i.e. daily T_{air}, hourly T_{air} and cloud cover data (BADC, 2011). These data in ASCII format are comprised of $T_{air/max}$, $T_{air/min}$, hourly T_{air}, wind speed and direction, mean sea level air pressure (MSLP) and cloud cover.

The obtained raw daily TD and hourly WH datasets include a number of duplicate, null or erroneous values. There are various observation hour counts (12-hour or 24-hour), domain names, version numbers and data types (CLBD or DCNN). In order to simplify the datasets, very careful extraction and elimination are needed. After processing the MIDAS daily/hourly T_{air} and cloud cover data, the extracted data files were ready to be used. Detailed data extraction procedures are listed as below.

First of all, extract the chosen weather stations in the West Midlands and Greater London (Table 3.1) using the BADC station number ('*src_id*'), i.e. Edgbaston (587), Coleshill (19187), Shawbury (643), LWC (19144), and Rothamsted (471).

For daily TD data (https://badc.nerc.ac.uk/data/ukmo-midas/TD_Table.html)

- If '*ob_end_time*' = 09:00 and '*ob_hour_count*'= 12, it means that the data were measured during the night-time (21:00 to 09:00) and, are used as daily $T_{air/min}$.

- If "*ob_end_time*' = 21:00 and '*ob_hour_count*' = 12, it means that the data were measured during the daytime (09:00 to 21:00) and, are used as daily $T_{air/max}$.
- Values indicating as '*ob_hour_count*' = 24 (i.e. 09:00-09:00) were removed from the dataset, unless there are no available data with '*ob_hour_count*' = 12.
- The climatological station number ('*id_type'* = DCNN) was used in priority, the WHO number ('*id_type'* = WMO) is an alternative option when DCNN is not available.
- Data with TD file column headers of '*src_id*', '*max_air_temp*' and '*min_air_temp*' were extracted for this thesis.
- Remove duplicate and null values, make sure only one row of daily data for each weather station.

For hourly WH data (https://badc.nerc.ac.uk/data/ukmo-midas/WH_Table.html)

- Only the values with observation version number ('*version_num*') '1' were used, because these have been quality checked by the Met Office.
- Extract available climatological station numbers (including DCNN, WHO, or ICAO-id).
- Extract SYNOPs or METARs measurement for each hour.
- Data with WH file column headers of '*src_id*' (BADC station number), '*air_temperature*' (hourly air temperature) and '*cld_ttl_amt_id*' (total cloud amount, unit of oktas) were extracted for this thesis.
- Remove duplicate and null values, make sure only one row of hourly data for each weather station.

3.4 Lamb weather types

Lamb (1972) originally classified daily synoptic weather conditions based on the variations in surface pressure patterns over the British Isles (50-60°N, 2°E-10°W). The following classifications of LWTs are included in the analysis: eight directional types (South-easterly [SE], Southerly [S], Northerly [N], Westerly [W], South-westerly [SW], North-westerly [NW], Easterly [E] and North-easterly [NE]), two non-directional types (Anticyclonic [A], Cyclonic [C]), and one Unclassified [U] type which represents days with weak or chaotic circulation patterns (Hulme and Barrow, 1997).

Jenkinson and Collinson (1977) applied an objective LWTs scheme using daily grid-point MSLP data, to classify daily circulation patterns into twenty-seven categories. Apart from the original LWTs recognised by Lamb (1972) and non-existent days (-9), the remaining types were classified into [A]/[C] hybrid types including anticyclonic-related ANE, AE, ASE, AS, ASW, AW, ANW and AN, and cyclonic-related CNE, CE, CSE, CS, CSW, CW, CNW and CN.

Jenkinson's objective daily synoptic indices (Figure 3.5) were downloaded from the Climatic Research Unit, University of East Anglia (http://www.cru.uea.ac.uk/). Jenkinson's objective Lamb daily synoptic index is provided as a .txt file. Data are stored by year (rows), month (12 rows for each year), and day (columns). The original data format is shown using numbers (Figure 3.5). In order to clearly classify the data into LWTs, the eleven LWTs and hybrid types were re-organised into individual files in chronological order for each LWT. Considering the availability of data of Jenkinson's objective daily synoptic indices until 31 July 2007 and the data availability of the MODIS

LST from 8 July 2002, the data analysis was performed over the period from 8 July 2002 to 31 July 2007 (N=1850 days). During the study period, the days associated with the original eleven LWTs account for approximately 73.6% of the total days. The remaining [A]/[C] hybrid types account for 26.4% of the total days. Similarly to Unwin (1980), due to the relatively lower proportion of hybrid types, this thesis mainly focuses on the eleven LWTs. The hybrid types are only mentioned where appropriate.

0	Anti-cyclonic			20	Cyclonic
1	ANE	11	NE	21	CNE
2	AE	12	E	22	CE
3	ASE	13	SE	23	CSE
4	AS	14	S	24	CS
5	ASW	15	SW	25	CSW
6	AW	16	W	26	CW
7	ANW	17	NW	27	CNW
8	AN	18	N	28	CN
	-1 Unclassifiable			-9 No data	

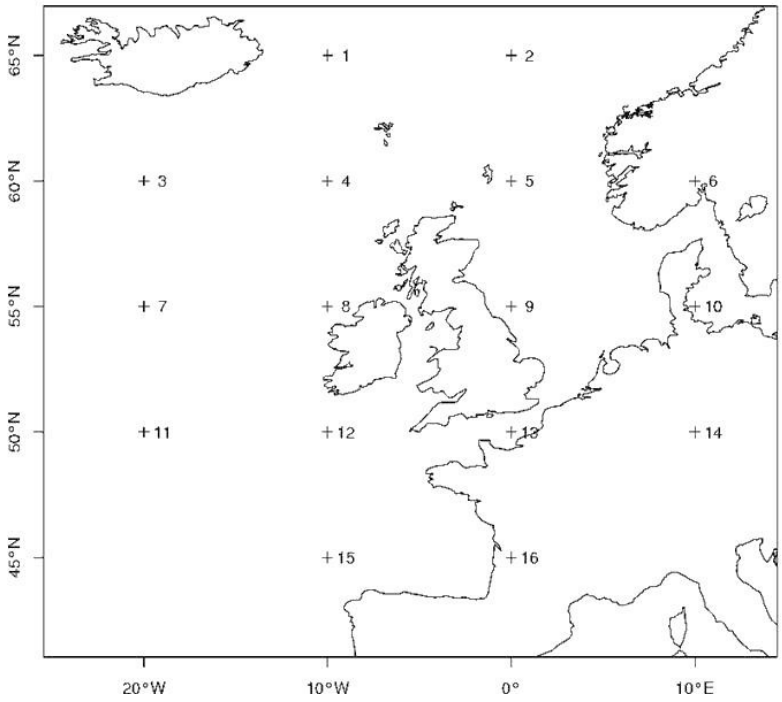

Figure 3.5: Jenkinson and Collinson's extended classification based on the original LWTs, indicating number coding of LWTs and hybrid types.

There have been some UHI studies undertaken in relation to synoptic weather types, such as that by Unwin (1980) for Birmingham, showing that the mean night-time aUHII peaked at 1.34 K in autumn (10 September to 19 November) during 1965-1974. Anticyclonic circulation was associated with a maximum mean night-time aUHII of 2.26 K, and cyclonic circulation was associated with a minimum mean night-time aUHII of 0.49 K. Morris and Simmonds (2000) examined the relationship between the UHI intensity and anomalous synoptic conditions in Melbourne, Australia. These studies suggested that anticyclonic conditions favour the development of the aUHI (and by inference the surface urban heat island, sUHI). In addition, it should be noted that the frequency of LWTs vary with location, for example, London is dominated more by anticyclonic, easterly and southerly weather types than Birmingham due to its relatively continental location (O'Hare et al., 2005).

3.5 Population data

Population data for the West Midlands and Greater London were obtained from the Office for National Statistics (ONS). A population estimates analysis tool was used to extract the required population estimates. This tool is an excel-based spreadsheet produced by the ONS, providing easy-operating options to extract population estimates by area (broad and local), specific age group, gender, etc.

Figure 3.6 illustrates the population growth for the West Midlands and Greater London from 2001 to 2009 (data series attached in Appendix 3). It can be found that all-age and <75 populations have very similar growth patterns, but have not changed significantly over the 9 years (West Midlands 2.8% increase, Greater London 5.6% increase). Since the life expectancy has increased, populations at older ages may increase (i.e. healthy aging) on the basis of the guaranteed quality of life. The 75+ population for the West Midlands has progressively increased by 9.3%, however, the 75+ population for Greater London has a turning point in 2004 leading to an overall decrease of 2.4%. The sudden reduction in London's 75+ populations is supposed due to the large amount of vulnerable elderly deaths suffered from preceding 2003 heatwave events, population compensations take time to reinstate back to normal level.

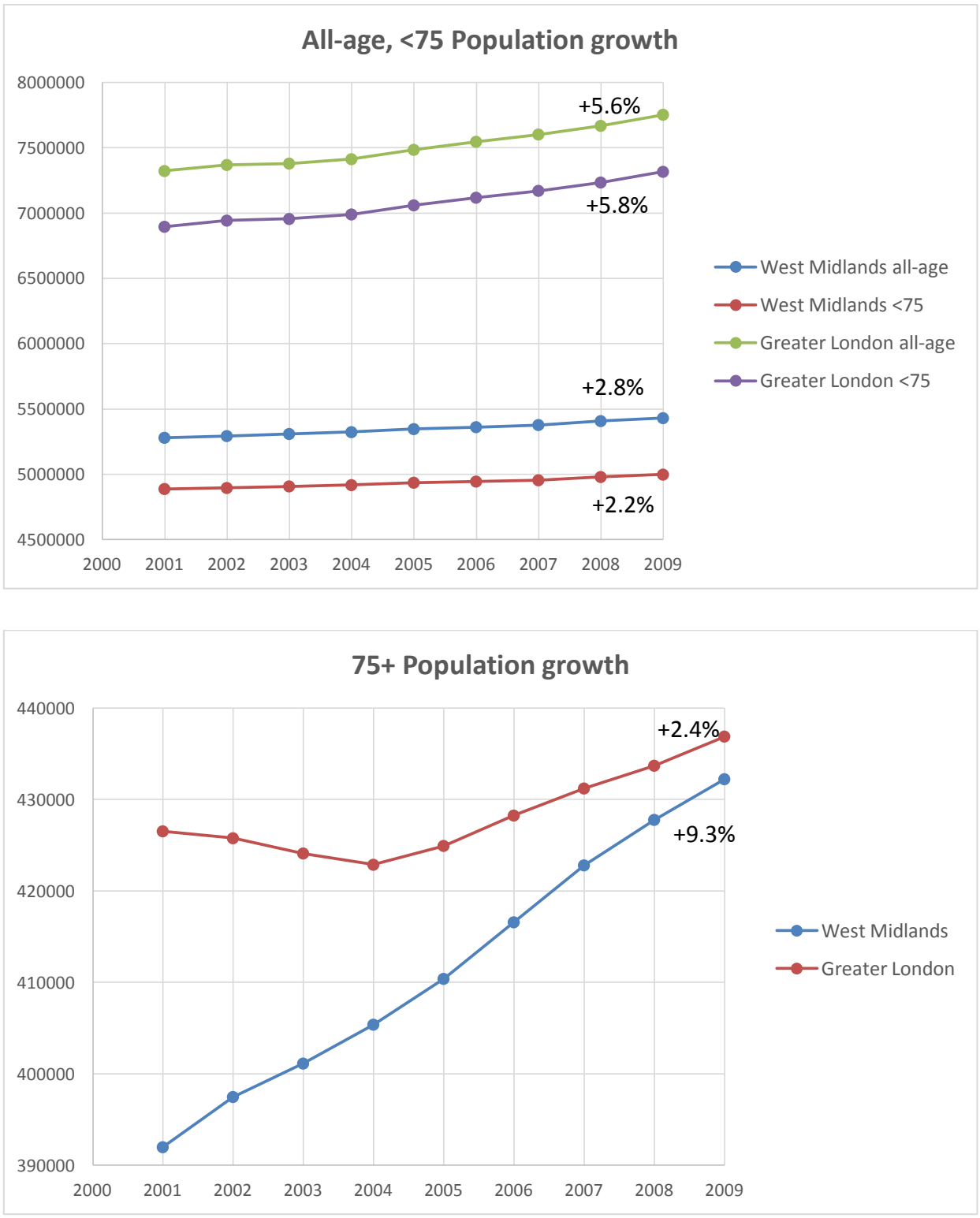

Figure 3.6: Population growth (all-age, <75 and 75+) from 2001 to 2009.

Geographical bands and mid-2009 population estimates and densities for the West Midlands and Greater London are listed in Table 3.2. The total mid-2009 population estimates of the West Midlands GOR are 5,431,079. The all-age population estimates are 2,792,400 in the outer band and 2,638,700 in the inner band. The inner band of the West Midlands (MC) is one of the most densely urbanised counties in the UK. Its population density reaches 2,925 per km^2. It is over 12 times higher than that in the outer band (231 per km^2), although the population in the outer band is higher than in the inner band by 153,700. For 75+ elderly people, the mid-2009 population estimates were 302,500 in the outer band and 129,700 in the inner band. The ONS reports that there was a decrease in the population aged 65-84 during 2001-2009, but a 14.5% increase in those aged over 85. According to the ONS 2008 mid-year population estimates, the West Midlands Regional Observatory (WMRO) reported more people aged over 40 living in rural areas, particularly in the 60-69 age group. The West Midlands has an increasing young population aged 20-29 living in the urban area. All-age population estimates are 4,933,046 in outer London and 2,820,509 in inner London. The 75+ elderly population estimates are 308,100 in outer London and 128,600 in inner London. By contrast with the West Midlands, the Greater London area is much smaller (1,572 km^2) but having a huge population of 7,753,555. Surprisingly, the inner London (including the city of London and 12 London boroughs) has a large population density of 8,842 per/km. The outer London (including 20 London boroughs) has approximately doubled the estimated population, but population density is much less. By 2011, the population density in inner London exceeded 10,000 per km^2, while the population density in outer London decreased from 3,937 to 3,900 (from mid-2009 to 2011).

Table 3.2: Geographical areas, age-specific population estimates (mid-2009) and population density (per km^2) in the West Midlands and Greater London.

Geographical area	Area (km^2)	**All-age**		**Under 75**		**75 and over**	
		Total	Pop. Density	Total	Pop. Density	Total	Pop. Density
West Midlands	13,004	5,431,100	418	4,998,900	384	432,200	33
Inner band	902	2,638,700	2,925	2,441,300	2,707	197,400	219
Outer band	12,102	2,792,400	231	2,557,600	211	234,800	19
Greater London	1572	7,753,555	4,932	7,316,855	4,654	436,700	278
Inner band	319	2,820,509	8,842	2,691,909	8,439	128,600	403
Outer band	1,253	4,933,046	3,937	4,624,946	3,691	308,100	246

3.6 Mortality data

This section introduces the sources of mortality data and age-specific variations for the West Midlands and Greater London over the study periods 2001-2009. Detailed figures are listed in Appendix 3.

3.6.1 West Midlands

Daily mortality data for the West Midlands were requested from the West Midlands Public Health Observatory (WMPHO). Key data source is the National Statistics Public Health Mortality File, as supplied for use in the PHOs National Statistics mid-year population estimates. Mortality data within the West Midlands GOR, the MC and Birmingham during 2001-2009 were extracted and prepared by the WMPHO technical staff, Tony Dickinson, by sub-dividing into age groups of all-age, under 75 (<75), 75 and over (75+), sex (female and male) and disease (all causes, circulatory, respiratory and other causes) for each geographical area. Due to data protection issues, cells with mortality counts under 3, including 0 in a defined geographical area are marked by an asterix *. In this thesis, these values are labelled as blank. For the West Midlands GOR, Figure 3.7 (a) shows the annual total all-cause mortality for different age groups (all-age, <75 and 75+) during 2001-2009. The 75+ elderly populations contribute to the majority of total mortality compared with those aged <75. Over the 9-year period, there were a total of 474,442 all-age deaths, 307,157 deaths aged 75+, and 167,285 deaths aged <75. All-cause mortality was found to decrease over time for each age group (all-age by -12.2%, 75+ by -6.2%, and <75 by -24.2%).

(a)

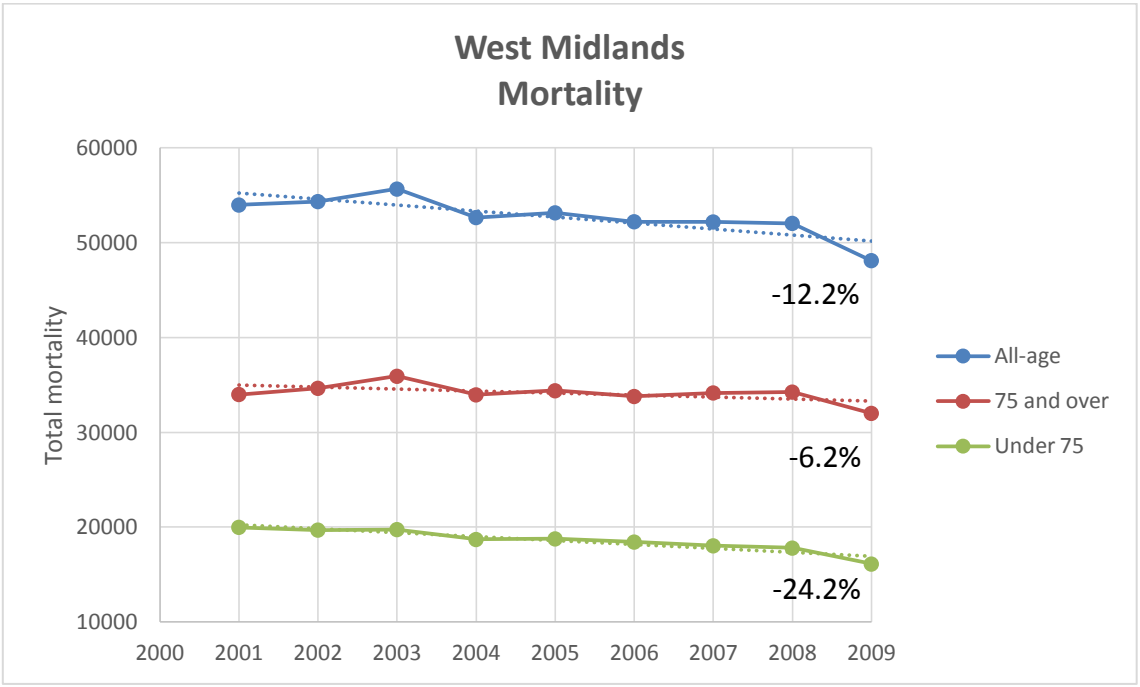

(b)

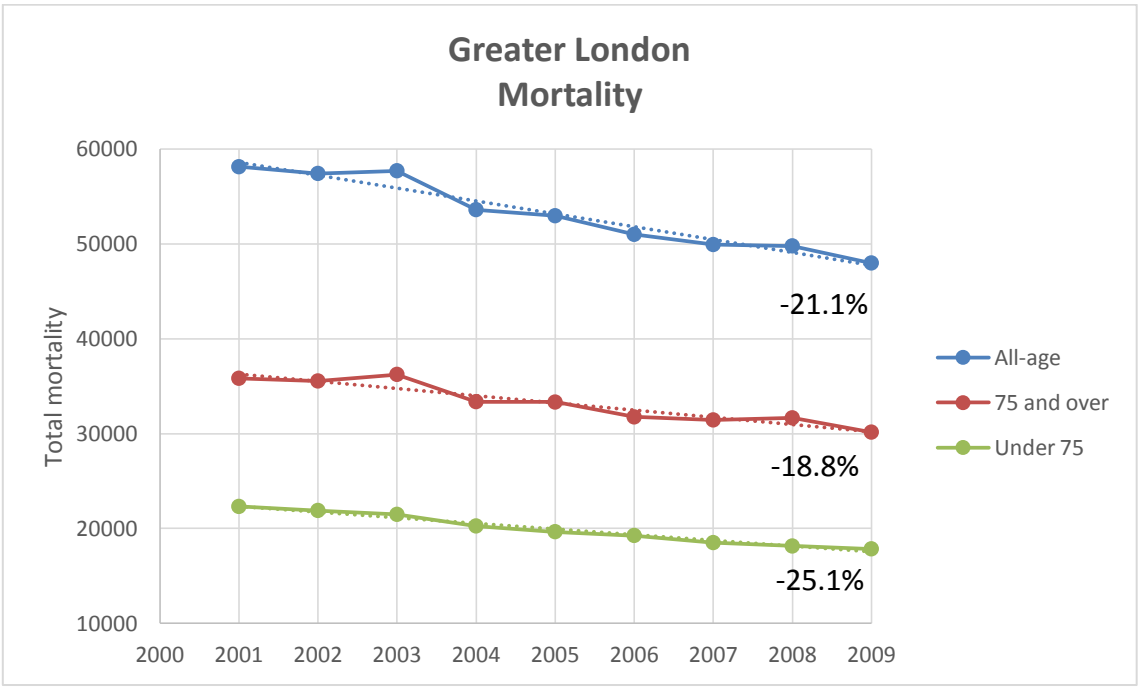

Figure 3.7: Total all-cause mortality by year in age groups: all-age, 75 and over, and under 75 in (a) the West Midlands and (b) Greater London.

3.6.2 Greater London

The raw mortality data for Greater London were requested from the ONS. These data were listed in MS Excel as mortality for each month and day for the years 2001-2009 and were broken down according to the variables of MSOA (Middle Layer Super Output Areas), sex, age, and underlying cause of mortality. Cause-specific mortality was coded using the 10th revision of the International Classification of Diseases (ICD-10) defined as cardiovascular disease (ICD-10 codes: I00-I99), respiratory disease (ICD-10 codes: J00-J99), other-cause mortality, and all-cause mortality. In order to sort the data by variable clearly, the raw data were saved separately into individual files (by age, sex, disease, time series, and MSOA) and re-analysed specifically. For Greater London, Figure 3.7(b) shows the annual total all-cause mortality for different age groups during 2001-2009. As in the case of the West Midlands, the 75+ elderly group contributes the majority of total mortality. Over the 9-year period, there were a total of 478,711 all-age deaths, 299,360 deaths aged 75+, and 179,351 deaths aged <75. The decrease in all-cause mortality over time was -21.1% (all-age), -18.8% (75+), and -25.1% (<75). In particular, the decreased mortality trends for all-age and 75+ populations are approximately 2-3 times greater than the West Midlands.

The progressive reduction in all-cause mortality has been related to a certain reduction in annual pollutant concentrations, such as PM2.5 (Miller, 2010). The trends are likely to be affected by factors like social, environmental and health-care etc. (Carson et al., 2006).

3.6.3 Mortality rates

In this thesis, the mid-2009 population estimates are sub-divided by age group (all-age, <75 and 75+). Population estimates for each year are applied to correspond with mortality data for the calculation of mortality rate. As in this thesis an age-specific assessment is conducted, the daily mortality rate (DMR) is calculated directly by dividing daily mortality by population from daily mortality data. Figure 3.8 shows the trends of annual mean DMR per 100,000 population for the West Midlands and Greater London. No matter how the mortality and population change over time during 2001-2009, the DMR for very elderly people aged 75+ is particularly outstanding in comparison of all-age and <75 DMRs as shown in Figure 3.8 (a) and Figure 3.8 (b). To look into the regional variations, the <72 and 75+ DMRs for the West Midlands and Greater London were further compared in Figure 3.8 (c) and Figure 3.8 (d), which shows similar variations, but the mean values of DMR for the West Midlands are found to be consistently higher than those in Greater London.

Although the ONS provides the mortality rate data, these data are age-standardised, eliminating the effects of age structure using the 2013 European standard population (ESP). As shown in Figure 3.6 and Figure 3.8, all-age and <75 age groups show very similar trends in population and mortality rate, this thesis examines the detailed impacts of temperature and UHI on mortality risk using a broad <75 age group to compare with very elderly people aged 75+ years, although infants and children are also sensitive to heat effects (Danks et al., 1962).

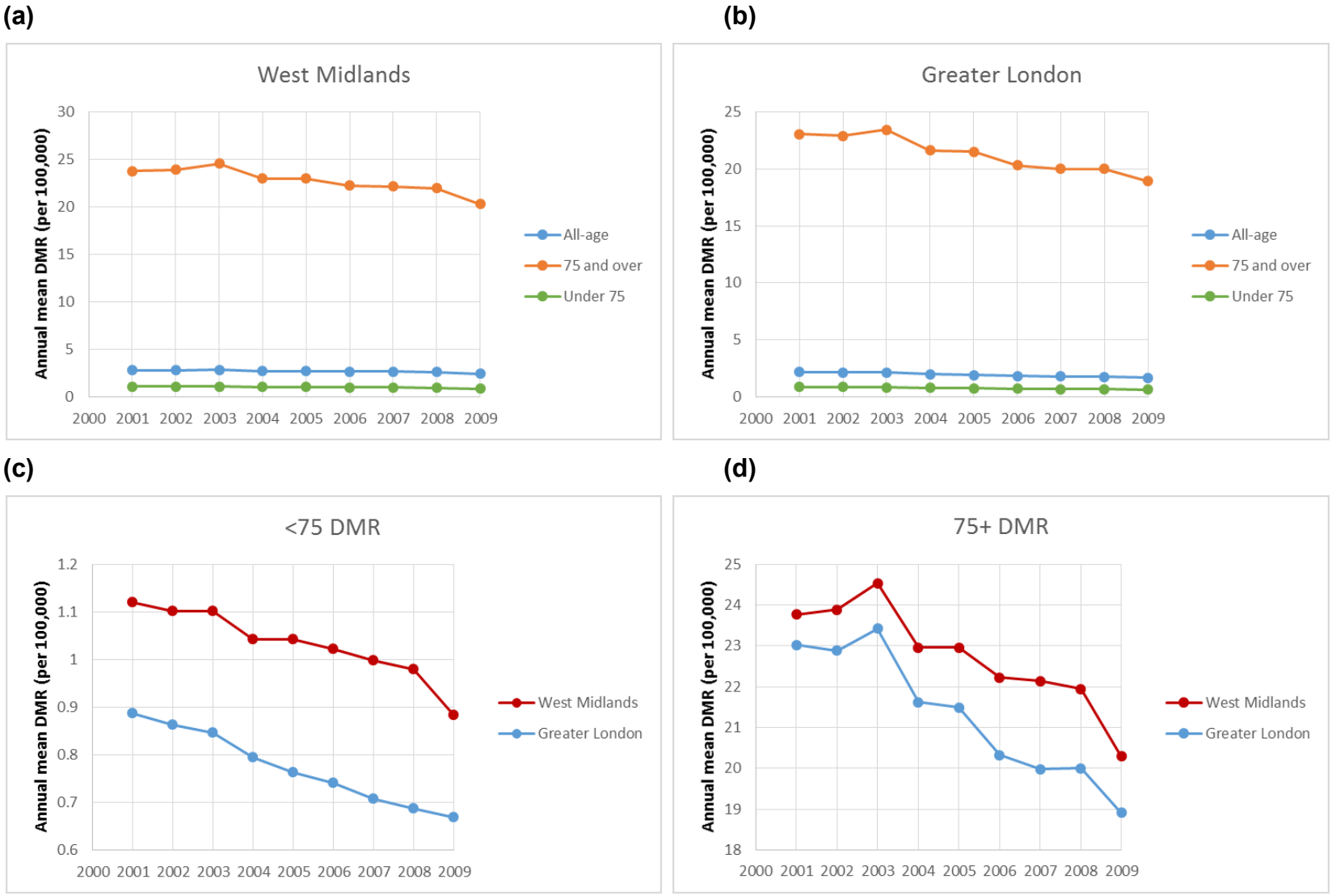

Figure 3.8: Age-specific annual mean DMRs (per 100,000 population) for the West Midlands and Greater London, 2001-2009.

Chapter 4 Urban climates, urban heat islands associated with Lamb weather types

4.1 Overview

Satellite-derived MODIS LST has been compared extensively in the literature with ground-based MIDAS T_{air}. However, the relationship between aUHI and sUHI has received little attention. Studying this relationship will allow a generic methodology to be developed for the derivation of spatial patterns of aUHI from satellite measurements. This chapter investigates urban climates in the West Midlands and Greater London, and the characteristics of aUHI and sUHI associated with LWTs. The assessment builds upon synoptic methods used to examine aUHI in Unwin (1980), and methods to map the night-time sUHI using MODIS/Aqua satellite images in Tomlinson et al. (2012a). The LWTs have been introduced due to the well-known impact of this parameter on the night-time UHI effect (Unwin, 1980, Wilby et al., 2011). The relationships between T_{air} and LST, aUHI and sUHI have mainly been investigated for cloudless nights, which predominate under anticyclonic conditions.

4.2 Study areas and data

The study areas in this thesis are the West Midlands and Greater London, as described in Section 3.1. Figure 3.1(b) and Figure 3.1(c) shows the Google Earth views of the MODIS 1 km^2 pixels (red box) covering the urban Edgbaston and rural Shawbury weather stations. The tile identifier h17v03 was chosen to acquire data across the West Midlands. As shown in Figure 3.1(b), the Edgbaston station is mainly surrounded by densely built-up areas, consisting of buildings, vegetation and a small part of Edgbaston reservoir. By contrast, the Shawbury station (Figure 3.1c) is surrounded by a large proportion of grassland (or arable land) with a few clusters of low-density built-up areas. The Royal Air Force (RAF) Shawbury Defence Helicopter Flying School is located next to the weather station at Shawbury. The surrounding environment between Edgbaston and Shawbury emphasises the difference in land-use between urban and rural areas, which results in the urban-rural temperature difference. Figure 3.2 shows the Google Earth view of the environment surrounding the LWC and Rothamsted weather stations in Greater London overlaid with the outline of the co-located MODIS 1 km^2 pixel. Data acquired from the tile identifiers h17v03 and h18v03 were added to the ArcGIS layers to allow mapping of the spatial patterns of LST and sUHI. Figure 3.2(b) shows that the LWC weather station is largely surrounded by buildings and gardens. Gray's Inn Gardens is located very close to the LWC station. St. George's Gardens and Brunswick Square Gardens are also located within the MODIS 1 km^2 pixel. Figure 3.2(c) shows that the area surrounding Rothamsted is mostly comprised of open grassland, trees, and very few low-density built-up areas.

A brief description of the data used in this chapter is now provided. Jenkinson's objective daily synoptic indices obtained from the Climatic Research Unit, University of East Anglia, are used to represent the LWTs. The downloaded data spans 1 January 1880 to 31 July 2007. This chapter mostly uses eleven original LWTs (Lamb, 1972): [SE], [S], [N], [W], [SW], [NW], [E], [NE], [A], [C], [U], and an additional [A]/[C] hybrid type. The reader is referred to Section 3.4 for a full description of the data collection and pre-processing.

High-quality night-time satellite images were derived using the MODIS/Aqua product MYD11A1. As shown in Figure 3.3, daily HDF files for both tile identifiers h17v03 and h18v03 were downloaded from the LP DAAC Data Pool. Please see Section 3.2 for details about obtaining and pre-processing the MODIS data. The MODIS/Aqua data available for download spans 8 July 2002 up to the present. For consistency with the LWTs, the study period is defined as from 8 July 2002 until 31 July 2007.

For the West Midlands, ground-based MIDAS meteorological data comprised of hourly T_{air} at the Edgbaston and Shawbury weather stations, and cloud cover data at the Coleshill weather station, were chosen for analysis. The location and good data availability of the sub-urban Coleshill station made it a suitable choice for the collection of cloud cover data. Cloud cover data were not available from the urban Edgbaston station. It was decided that the rural Shawbury station was located too far away from the central area and was therefore not representative of the cloud conditions. The Coleshill station is located between the urban and rural stations.

For Greater London, ground-based MIDAS meteorological data are comprised of hourly T_{air} at the LWC and Rothamsted weather stations. Cloud cover data was obtained from the LWC station. The MIDAS data were also extracted between 8 July 2002 and 31 July 2007. This is consistent with the availability of MODIS LST data and Jenkinson's objective daily synoptic indices. The MIDAS T_{air} is measured at screen height. For the urban stations of Edgbaston and LWC, T_{air} is measured within the urban canopy layer. Daily $T_{air/max}$ and $T_{air/min}$ were derived from the hourly T_{air}. Hence, the measurement time of $T_{air/max}$ (or $T_{air/min}$) may vary somewhat from day to day. Further details about MIDAS data are included in Section 3.3.

In comparisons of T_{air} against LST presented Section 4.5.4, the values of meteorological variables acquired at 01:00 UTC and 02:00 UTC were averaged. This allows the ground-based measurements to be temporally co-located with the satellite images acquired at ~01:30 UTC, assuming that the meteorological variables vary linearly with time during 01:00-02:00 UTC. Detailed information about the exact timing of the MODIS/Aqua image acquisition and the MIDAS Tair measurement can be found in Appendix 5.

Correspondence was ensured between the extracted Jenkinson's objective daily synoptic indices (including eleven original LWTs and one [A]/[C] hybrid type) and the MIDAS data. The LWT-specific MIDAS data were then saved into separate files in a suitable form for further analysis. Only night-time cloudless MODIS data between 8 July 2002 and 31 July 2007 were selected for the comparison of aUHI and sUHI under anticyclonic conditions. In this case, nights associated with values of 0-okata MIDAS cloud cover were extracted individually.

4.3 MODIS satellite image selection

For the LWT-specific UHI analyses, the MODIS satellite images were selected according to the following criteria:

1. Complete pixel coverage of night-time LST across Birmingham and London;
2. Clear-sky conditions i.e. 0-okta cloud cover;
3. Night-time aUHII above 5°C, representing a pronounced urban-rural temperature difference;
4. No unrealistic extremely high/low LST values.

For Birmingham, a total of 77 night-time images satisfied these criteria. Among the 77 nights, 48 nights belong to LWT [A] type, 2 nights to [C], 9 nights to [SW], 2 nights to [W], 4 nights to [NW], 3 nights to [S], 2 nights to [N], 3 nights to [SE], 2 nights to [U], 1 night to [E] , 1 night to [NE], and 10 nights to [A]/[C] hybrids (details see Table 4.3).

For London, a total of 97 night-time images satisfied these criteria. Among the 97 nights, 39 nights belonged to the LWT [A]-type, 2 nights to [C], 5 nights to [SW], 6 nights to [W], 6 nights to [NW], 4 nights to [S], 5 nights to [N], 4 nights to [SE], 2 nights to [U], 1 night to [E], and 23 nights to [A]/[C] hybrids (Table 4.5).

4.4 Calculation of the UHI intensity

The aUHII is defined as the T_{air} difference between the urban station (Edgbaston for the West Midlands; LWC for Greater London) and the rural station (Shawbury for the West Midlands; Rothamsted for Greater London).

The sUHII is defined as the LST difference computed by subtracting the LST value retrieved for the 1 km^2 pixel covering the referenced rural stations (Shawbury and Rothamsted) from the 2-D LST values (i.e. LST in each regional 1 km^2 pixel). Unlike the aUHII calculation, the sUHII calculation is more complicated, as it is based on the spatial distribution of LST. In this chapter, the spatial patterns of LST for each LWT were obtained using the MODIS LST images for the corresponding LWT averaged using the ArcMap Spatial Analyst Tools (Map Algebra → Raster Calculator). After averaging the LST images for each LWT, the sUHII was calculated using ArcMap tools (Zonal Statistics → Spatial Analyst) using the LST values at the urban and rural stations.

4.5 Results and discussion

4.5.1 Urban climates

Urban climate refers to the atmospheric conditions (such as temperature and cloud cover) which distinguish between urban and rural areas. To analyse the climate of the West Midlands, daily temperature data during summer months (JJA) at the Edgbaston and Shawbury stations from 2001 to 2009 were used, with a particular focus on unusually high temperatures. In the case of London, daily temperature data during JJA at the LWC and Rothamsted stations from 2001 to 2009 were used. Trends in aUHII during summer were also assessed for the study period. According to the heatwave threshold temperatures defined by the UK Met Office, the days with temperatures above 30°C ($T_{air/max}$) and 15°C ($T_{air/min}$) for the West Midlands can be regarded as extreme hot days. For London, the thresholds are higher, with $T_{air/max}$ of 32°C and $T_{air/min}$ of 18°C. Table 4.1 lists the extreme hot days identified at the urban Edgbaston station (2001-2009) in the West Midlands and the urban LWC station (2001-2009) in Greater London. According to the region-specific thresholds, there were 6 extreme hot days in the West Midlands over 10 years, and 11 extreme hot days in Greater London over 9 years. Especially hot days occurred on 9 August 2003 ($T_{air/max}$ of 33.2°C at Edgbaston and 36°C at LWC) and 19 July 2006($T_{air/max}$ of 33.5°C at Edgbaston and 34.5°C at LWC). Greater London experienced more hot days in excess of the heatwave threshold than the West Midlands. Furthermore, London's urban warming was particularly strong during the 2003 heatwave.

Table 4.1: Extremely hot days identified from the Edgbaston station and the LWC station, 2001-2009.

Date	Edgbaston $T_{air/max}$	Edgbaston $T_{air/min}$
15/07/2003	30.8	15.1
09/08/2003	**33.2**	**17.7**
17/07/2006	30.5	16
18/07/2006	30.9	18.5
19/07/2006	**33.5**	**17.1**
25/07/2006	30.1	17.8

Date	LWC $T_{air/max}$	LWC $T_{air/min}$
29/07/2002	32.2	19.9
06/08/2003	35.7	21.1
09/08/2003	**36**	**20.9**
10/08/2003	37.6	23.7
11/08/2003	34.6	19.7
19/06/2005	33.1	18.1
12/06/2006	32.4	21.2
02/07/2006	32.1	19.5
19/07/2006	**34.5**	**18.7**
21/07/2006	32.1	19.8
26/07/2006	33.6	22.1

West Midlands

Figure 4.1 shows the annual variations in mean T_{air}, and mean aUHII at Edgbaston and Shawbury during JJA 2001-2009. The highest summer T_{air} was observed in the 2003 and 2006 heatwave years. The T_{air} value at the urban Edgbaston station is consistently higher than that observed at the rural Shawbury station, although daytime $T_{air/max}$ at both stations are similar. There is a larger difference in night-time $T_{air/min}$ between Edgbaston and Shawbury, resulting in a higher night-time aUHII. Night-time aUHII computed using $T_{air/min}$ was strongest in 2003 and 2006, reaching a peak of 6.6°C on 13 July 2003. Daytime aUHII computed using $T_{air/max}$ was particularly strong in 2003, and peaked at 4.6°C on 6 August 2003. More specifically, on 19 July 2006, the $T_{air/max}$ for the urban Edgbaston and rural Shawbury peaked at 33.5°C and 32.8°C, respectively. The second hottest day was on 9 August 2003, and was associated with $T_{air/max}$ values of 33.2°C at Edgbaston and 32°C at Shawbury.

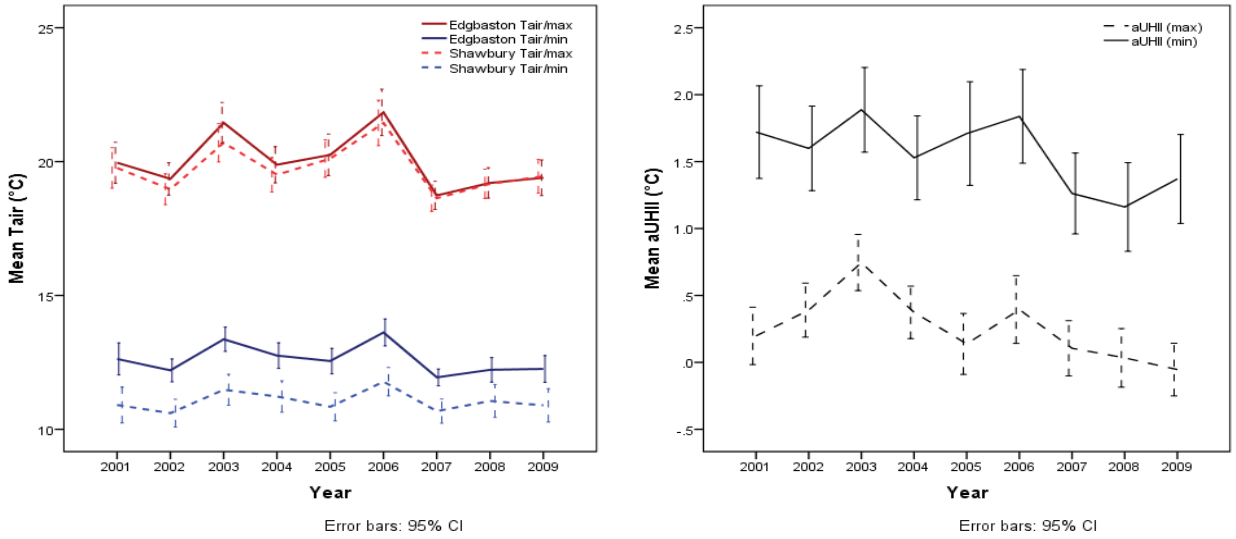

Figure 4.1: Annual variations of mean T_{air} at Edgbaston and Shawbury; and mean aUHII (Edgbaston-Shawbury), JJA 2001-2009.

The hourly variations of T_{air} at Edgbaston and Shawbury, and the corresponding aUHII over 24 hours for the extremely hot day occurring on 9 August 2003 are shown in Figure 4.2. The reverse pattern between T_{air} and aUHII from 07:00 UTC to 21:00 UTC was observed. During the daytime, T_{air} increased after sunrise reaching its peak in the afternoon. Conversely, the aUHII remained low during the daytime but increased rapidly after sunset, peaking around midnight at 23:00 UTC.

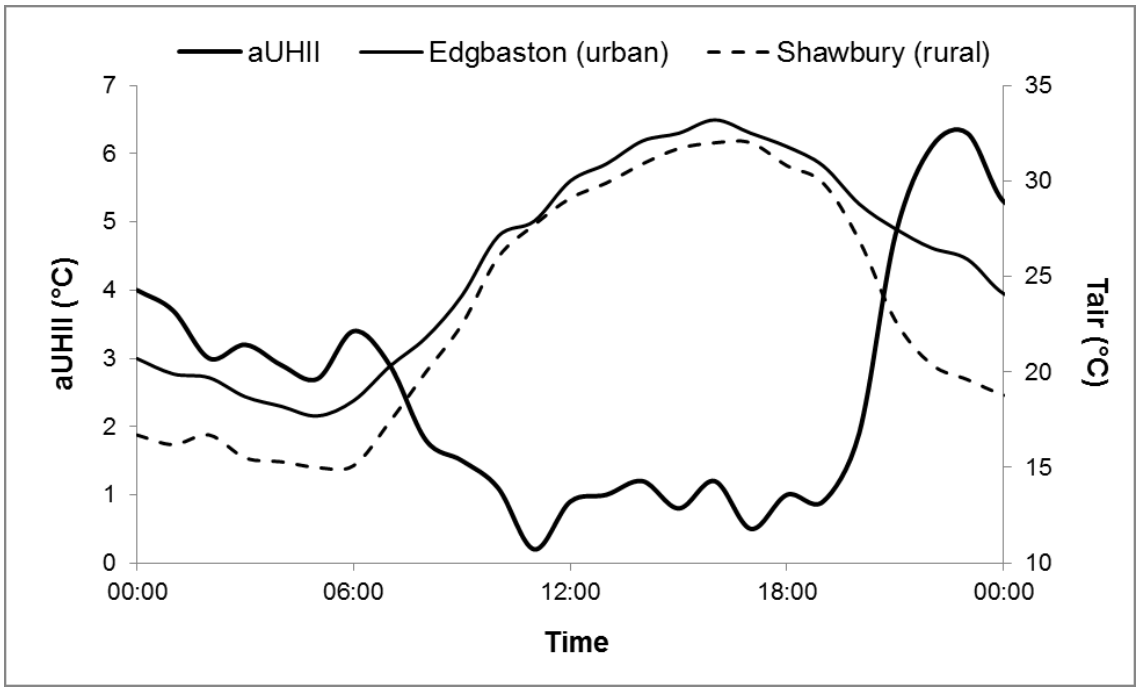

Figure 4.2: Hourly variations in urban and rural T_{air} and the aUHII (Edgbaston-Shawbury) over 24 hours, 9 August 2003.

The spatial patterns of MODIS/Aqua LST across the West Midlands and Birmingham are shown in Figure 4.3. A warming signal is visible in the metropolitan county, particularly in the city of Birmingham. The surrounding areas outside the metropolitan county (i.e. the outer band of the West Midlands) do not show patterns associated with significant warming. The urban Edgbaston station located inside Birmingham records a distinctly higher temperature than the rural Shawbury station located in the surrounding area. Birmingham displays a typical central warming, with the highest night-time LST of 18.3°C observed on 9 August 2003.

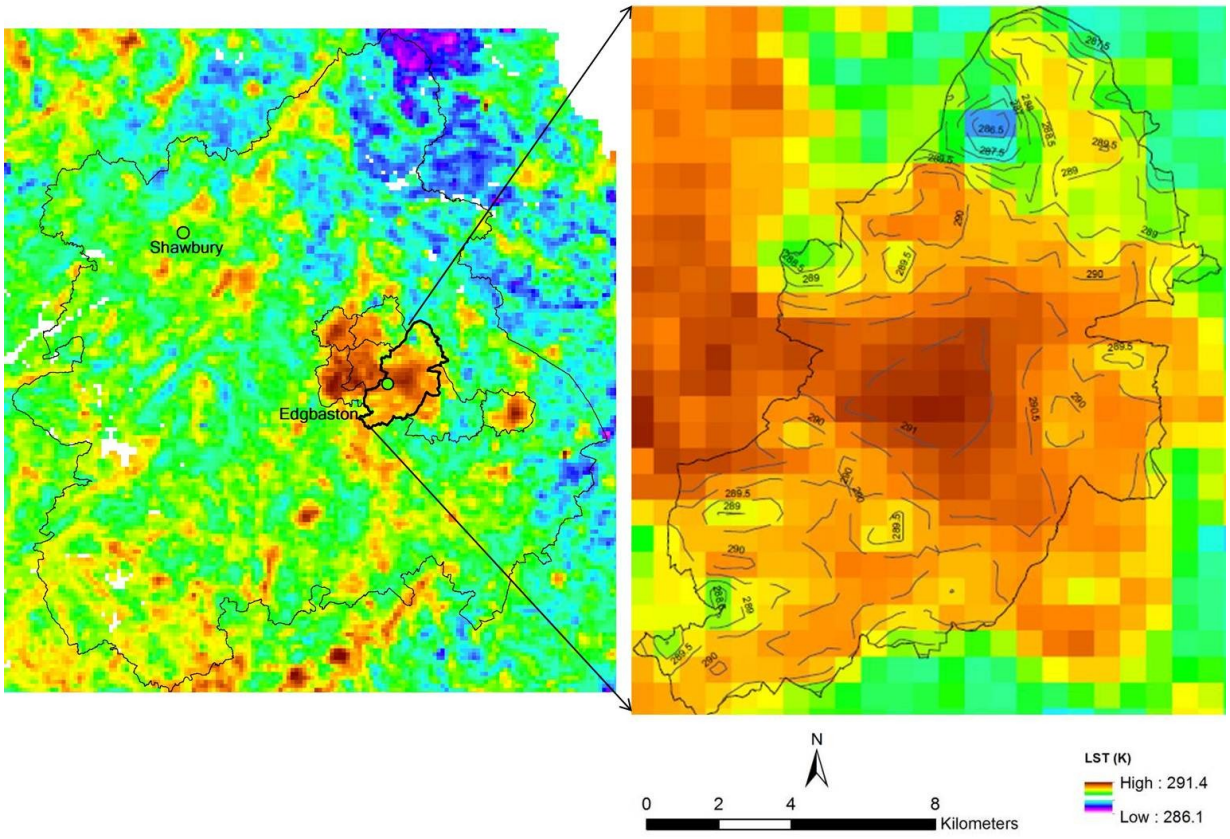

Figure 4.3: Spatial patterns of MODIS/Aqua LSTs in the West Midlands (left) and Birmingham (right), 9 August 2003 01:30 UTC.

Greater London

Figure 4.4 shows the annual variations in mean T_{air} at the urban LWC and rural Rothamsted stations, and the calculated aUHII during JJA 2001-2009. As for the West Midlands, 2003 and 2006 were the hottest years. T_{air} at the LWC station is consistently higher than that recorded at Rothamsted. There are significant differences in daytime and night-time T_{air} at both stations. Larger night-time T_{air} difference results in larger night-time aUHII. The hottest day was recorded on 10 August 2003 (37.6°C at LWC, 36°C at Rothamsted), followed by 9 August 2003 (36°C at LWC, 34.1°C at Rothamsted), and 19 July 2006 (34.5°C at LWC, 33.8°C at Rothamsted). The night-time aUHII was strongest in 2003 by a considerable margin. Surprisingly, London's daytime aUHII was lowest in the typical 2003 and 2006 heatwave years. The low daytime mean aUHII is caused by negative aUHII values in the range of -0.1°C and -0.8°C. On those days, overall T_{air} in inner London was lower than that in outer London (so-called 'urban cool islands'). This situation may have occurred due to larger coverage green spaces in central areas. However, at there is not enough evidence to ascertain the exact mechanism.

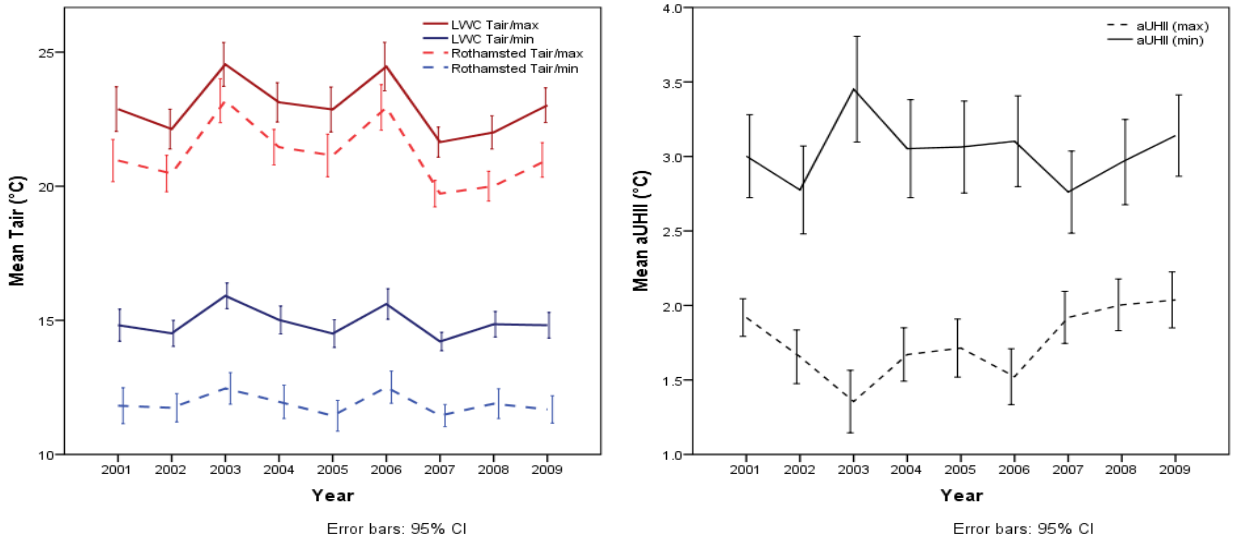

Figure 4.4: Annual variations of mean T_{air} at LWC and Rothamsted, and mean aUHII (LWC-Rothamsted), JJA 2001-2009.

On the characteristic hot day of 9 August 2003, the hourly variations in T_{air} at LWC and Rothamsted and the calculated aUHII over 24 are hours are shown in Figure 4.5. During the daytime, T_{air} increased from the early morning reaching a peak between 14:00 UTC and 17:00 UTC. The aUHII was lowest at 10:00 UTC and increases gradually. Whereas the aUHI in London peaked at 7.1°C in the early morning (01:00-02:00 UTC) when matches the MODIS acquisition time, the aUHI in the West Midlands peaked at 6.3°C just before mid-night (~23:00 UTC).

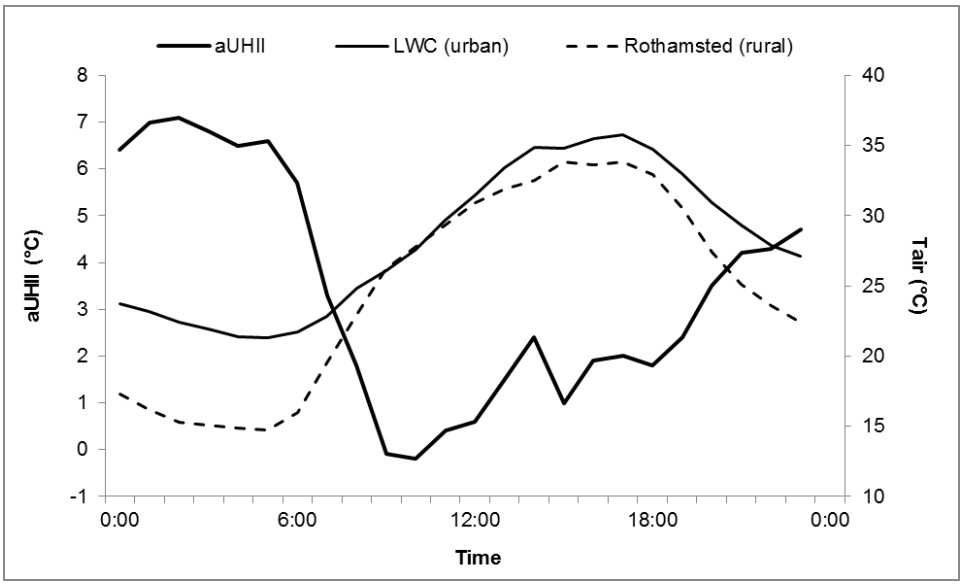

Figure 4.5: Hourly variations in urban and rural T_{air} and aUHII (LWC-Rothamsted) over 24 hours, 9 August 2003.

Figure 4.6 shows the spatial patterns of MODIS/Aqua LSTs on 9 August 2003 in Greater London. A notable sUHI pattern is observed, with a peak LST of 22.1°C detected around the central part of the city gradually decreasing towards the surrounding areas. The lowest LST of ~12.9°C was detected around the London boundaries. The coldest areas were found in north-west London, which has large areas of woodland and vegetation. In particular, Northolt contains large open spaces and parks as well as a Jet Centre surrounded by very few buildings. Large areas comprising golf courses and sports centre playing fields also contribute to the lower temperatures. It is interesting that there is an elongated warming band along the River Thames (blue line in Figure 4.6) towards the eastern boundary outside of the central warm area. ARUP supported the London Development Agency (LDA) to plan and design a heat network in the Thames Gateway where has ~1.45 million residents. Thames Gateway development, including sea

defences by building barrier and housing land on flood plains and other economic activities e.g. investment in transportation (GLA, 2014), potentially resulting in pressure to population growth and Gateway regional warming. This area comprises a series of reservoirs including the King George's, William Girling, Banbury, Lockwood, High/Low Maynard and Warwick Reservoirs. The water supply infrastructure from these reservoirs provides fresh water to London, which may contribute to the warmer surroundings. Another warming point is found south-west of London at Heathrow: the world's busiest airport.

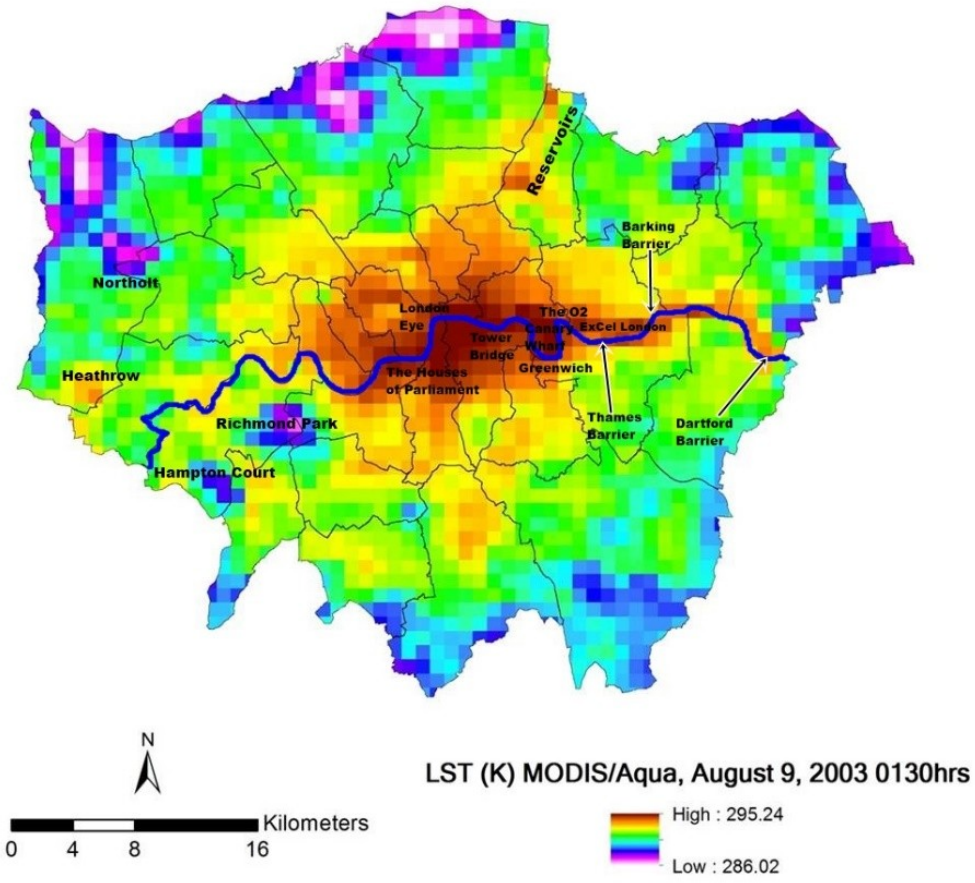

Figure 4.6: Spatial patterns of MODIS/Aqua LSTs in Greater London, 9 August 2003 01:30 UTC.

During the study period, the summer mean temperature in Greater London was about 1-3°C warmer than for the West Midlands. The West Midlands had a maximum night-time aUHII of 6.6°C. In Greater London, the maximum night-time aUHII was larger reaching 8.1°C. The spatial patterns of LST in the West Midlands highlight significant sUHI in the metropolitan county, particularly in the city of Birmingham. On a typical heatwave day, 9 August 2003, Birmingham's LST reached its peak at 18.3°C in central areas, and London's LST reached its peak at 22.1°C around the city of London. Using the Shawbury pixel and the Rothamsted pixel as the rural background, the peak night-time sUHII was 3.8°C in Birmingham and 8.7°C in London. The LST along the River Thames was particularly high towards London's eastern boundary.

4.5.2 Ground-based aUHI

A threshold value for a heat-island event was chosen for daily $T_{air/min}$. Following the method in Unwin (1980), the heat island threshold is the first value in excess of one standard deviation above zero. For the West Midlands, days with night-time aUHII in excess of 1.5°C are regarded as UHI events. For Greater London, the threshold is higher at 3.5°C. A value of 5°C was chosen as a threshold for extreme UHI events for both regions. Night-time aUHII was grouped by LWT and an Analysis of Variance (ANOVA) was conducted.

West Midlands

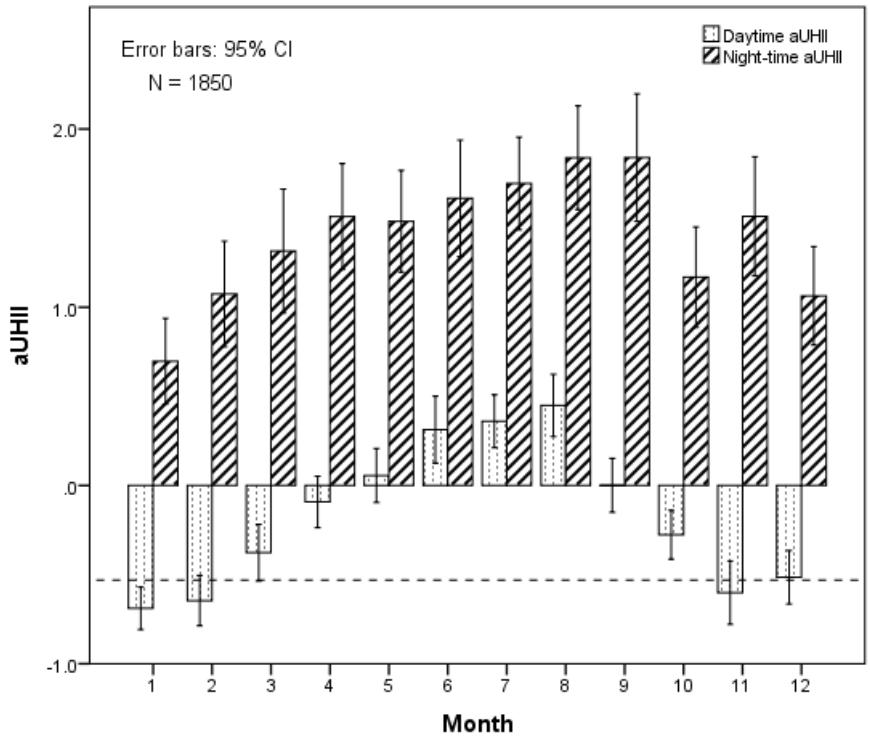

Figure 4.7: Monthly mean daytime and night-time aUHII at urban Edgbaston station and rural Shawbury station, between 8 July 2002 and 31 July 2007 (dashed line at -0.53°C indicates the level of aUHII=0°C if a temperature lapse rate of 6°C/km was considered).

Figure 4.7 shows the monthly variations of aUHII from 8 July 2002 to 31 July 2007 (N = 1850) at the urban Edgbaston and rural Shawbury station. Error bars refer to the 95% Confidence Interval (CI) based on standard error estimates computed for the aUHII means. The results show consistently stronger night-time aUHII than daytime aUHII for all seasons (spring: MAM; summer: JJA; autumn: SON; winter: DJF). In the period from May to August, the daytime aUHII remains positive. Statistical analysis of the daytime aUHII provides an annual mean value of -0.2°C. The negative values of daytime aUHII from October to April (or November, January and February, if the elevation correction is made) imply an urban cold island which can likely be attributed to urban shading. The weak (or absent) daytime aUHI is not be discussed further concentrating instead on the heat-island effect.

Systematic difference in temperature between two stations caused by factors other than land-use may affect the interpretation of results (Peterson and Owen, 2005). For example, systematic differences in temperature measurements between stations are expected to arise from differences in elevation, such that stations at a higher elevation are expected to be cooler in general when considering the climatological temperature lapse rate. For a lapse rate 6°C km^{-1}, the aUHII would be 0.53°C higher given the respective elevations of the Edgbaston (160 m) and Shawbury stations (72 m). In other words, the UHII calculated from the direct temperature measurements at the two stations underestimates the true UHII. An offset of -0.53°C can be applied to the horizontal line representing 'aUHII=0' in Figure 4.7 (as indicated by the dashed line) to

account for differences in station elevation. Correspondingly, all aUHII values should be increased by 0.53°C.

Table 4.2 lists the seasonal mean values and standard deviations of night-time aUHII, and the number of heat island events (night-time aUHII > 1.5°C), together with extreme heat island (night-time aUHII >5°C) events over the 1850 nights. The mean maximum night-time aUHII in summer is 1.7°C and the mean minimum in winter is 0.8°C. The aUHI is therefore most prominent for summer nights but weakest in winter. This is because heat absorbed during the daytime is highest in summer but lowest in winter.

During the study period, 39.8% (N = 737) of the sample days were heat island events and 3.0% (N = 58) were extreme heat island events. Heat island events most commonly occurred in summer (47.7%), followed by autumn (43.5%) and spring (39.3%), and least commonly occurred in winter (28.2%). Extreme heat island events mainly occurred in spring (3.9%) and summer (3.7%).

Table 4.2: Seasonal mean night-time aUHII and (extreme) heat island events for the West Midlands, 8 July 2002 to 31 July 2007.

Season	Night-time aUHII (Std. deviation)	A. No. nights	B. No. of aUHI nights>1.5°C (% of column A)	C. No. extreme aUHI nights>5.0°C (% of column A)
Spring (MAM)	1.4 (1.80)	460	181 (39.3%)	18 (3.9%)
Summer (JJA)	1.7 (1.63)	484	231 (47.7%)	18 (3.7%)
Autumn (SON)	1.5 (1.82)	455	198 (43.5%)	14 (3.1%)
Winter (DJF)	0.8 (1.61)	451	127 (28.2%)	8 (1.8%)
Total	1.4 (1.91)	1850	737 (39.8%)	58 (3.0%)

Table 4.3: Summary of night-time aUHII, number of nights and (extreme) heat island events for the West Midlands in relation to LWTs, 8 July 2002 to 31 July 2007.

Lamb weather types	Night-time aUHII				A. No. nights (% of 1850 nights)	B. No. aUHI nights >1.5°C (% of column A)	C. No. extreme aUHI nights >5.0°C (% of column A)	D. Cloudless (0-okta)
	Min	Max	Mean	Std. Deviation				
Anticyclonic [A]	-8.5	7.0	2.5	2.11	391 (21.1%)	255 (65.2%)	47 (12%)	48
Cyclonic [C]	-1.7	7.3	0.9	1.52	217 (11.7%)	57 (26.3%)	5 (2.3%)	2
South-westerly [SW]	-2.0	6.7	1.1	1.80	173 (9.4%)	58 (33.5%)	5 (2.9%)	9
Westerly [W]	-3.3	5.3	1.0	1.66	160 (8.7%)	55 (34.4%)	2 (1.3%)	2
North-westerly [NW)	-1.7	5.4	1.2	1.40	107 (5.8%)	36 (33.6%)	1 (0.9%)	4
Southerly [S)	-7.2	7.2	1.1	2.08	104 (5.6%)	32 (30.8%)	4 (3.8%)	3
Northerly [N]	-1.3	4.9	0.9	1.41	74 (4.0%)	21 (28.4%)	-	2
South-easterly [SE]	-0.9	5.2	0.9	1.67	54 (2.9%)	14 (25.9%)	1 (1.9%)	3
Unclassified [U)	-0.9	6.2	2.2	1.93	30 (1.6%)	16 (53.3%)	3 (10%)	2
North-easterly [NE]	-2.0	4.9	0.7	1.65	25 (1.4%)	5 (20.0%)	-	1
Easterly [E)	-1.4	4.5	0.6	1.53	25 (1.4%)	5 (20.0%)	-	1
[A]/[C] hybrids	-11.2	6.5	1.3	1.86	490 (26.4%)	200 (40.8%)	10 (2.0%)	10

Unwin (1980) analysed the aUHI of Birmingham using Edgbaston as an urban station and Elmdon as a rural station, and classified the data into LWTs for the period 1965-1974. In this study, similar analyses were conducted for the West Midlands and Greater London using the MIDAS data in Section 3.3 and the LWTs data in Section 3.4.

The threshold for a heat island event in the West Midlands is definedas a night-time minimum aUHII >1.5°C. An extreme heat island event is defined as a night-time minimum aUHII >5°C. Table 4.3 summarises the night-time aUHII, the occurrence of LWTs and total number of nights of (extreme) heat island events for each LWT in the West Midlands (Edgbaston-Shawbury) from 8 July 2002 to 31 July 2007. Over the study period, [A], [C], [SW] and [W] types have been recognised as the most commonly occurring LWTs for aUHI, occurring in 21.1%, 11.7%, 9.4% and 8.7% of cases, respectively. The results are consistent with the findings of O'Hare et al. (2005) who found that the top three most frequent weather types [A], [W] and [C] account for approximately 50% of total days over the British Isles. Unlike in Unwin (1980), the [W] (22.3%) and [A] (18.4%) types were the top two most frequently occurring LWTs during 1965-1974. For the study period 2002-2007, type [A] occurred with the highest frequency (21.1%) and type [W] occurred on just 8.7% of occasions. Unwin (1980) also found that type [C] was associated with the least night-time UHI effect (0.49 K), results presented in this thesis show that type [C] was associated with a mean aUHII of 0.9°C, which is higher than for the [N], [NE] and [E] types. The 9.4% frequency for [SW] is more than double the frequency of 3.9% recorded in Unwin (1980). The dominant type [A] was associated with a mean night-time aUHII of 2.5°C, and comprised the largest proportion

(65.2%) of UHI events and 12.0% of extreme UHI events for all LWTs, with a maximum aUHII of 7°C. The two least commonly observed types, [NE] and [E], were associated with mean night-time aUHII of 0.7°C and 0.6°C, respectively. Although type [U] occurred with low frequency, its mean night-time aUHII reached 2.2°C. During the 30 type [U] nights, with approximately 60% (17 nights) occurring in summer. For many other LWTs, type [C] was positively skewed with a peak at aUHII=0°C suggesting no heat island effect. The results of the one-way ANOVA analysis confirm that the eleven LWTs explain a significant fraction of the variance in aUHII ($p < 0.01$). The excluded hybrid LWTs are statistically insignificant ($p > 0.05$).

Greater London

Figure 4.8 represents the monthly variations of aUHII from 8 July 2002 to 31 July 2007 (N = 1850) at the urban LWC and rural Rothamsted stations. Error bars refer to the 95% CI based on standard error estimates associated with the aUHII means. The results show consistently stronger night-time aUHII than daytime aUHII for all seasons. Heat islands effects in London are prominent. Even daytime aUHII values are positive and over 1°C. Annual mean daytime aUHII is ~1.6°C, and night-time aUHII is ~2.9°C. Unlike the results for the West Midlands, no negative aUHII was found in London.

The lapse rate in temperature due to differences in elevation may alter the interpretation of results to some extent. Assuming a climatological lapse rate in temperature of 6°C km^{-1}, the aUHII would be 0.51°C lower due to the relative elevation of the LWC (43 m) and Rothamsted stations (128 m). This implies that the UHII calculated from the direct temperature measurements at the two stations overestimates the true UHII. An offset of +0.51°C may be applied to the horizontal line representing aUHII = 0°C in Figure 4.8 (as indicated by the dashed line). Correspondingly, all aUHII values should be decreased by 0.51°C.

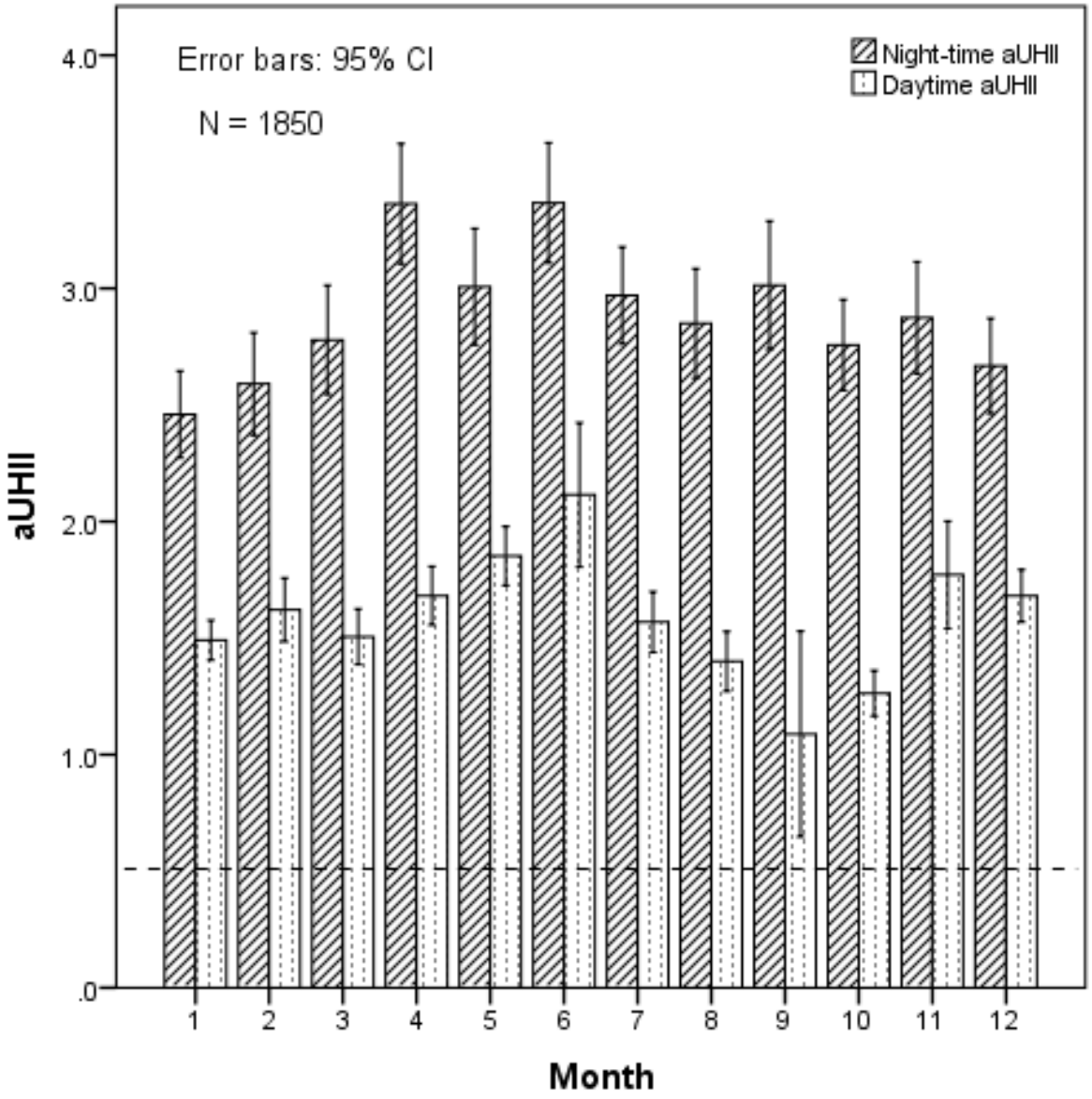

Figure 4.8: Monthly mean daytime and night-time aUHII at urban LWC station and rural Rothamsted station, between 8 July 2002 and 31 July 2007 (the dashed line at +0.51°C indicates the level of aUHII = 0°C if a temperature lapse rate of 6°C/km was considered).

Table 4.4 lists the seasonal mean night-time aUHII, and the number of heat island events (night-time aUHII > 3.5°C) together with extreme heat island events (night-time aUHII > 5°C) over the 1850 nights. The aUHI is most prominent on summer nights (3.1°C) but weakest in winter (2.6°C). During the study period (8 July 2002 to 31 July 2007), 28.2% (N = 522) of the sample days were heat island events and 11.3% (N = 209) extreme heat island events. Heat island events in London most commonly occurred in spring (34.1%), followed by summer (32.6%) and autumn (26.8%), and least commonly occurred in winter (18.8%). Extreme heat island events in London mainly occurred in spring (14.1%) and summer (12.6%).

Table 4.4: Seasonal mean night-time aUHII and (extreme) heat island events for Greater London, 8 July 2002 to 31 July 2007.

Season	Night-time aUHII (Std. deviation)	A. No. nights	B. No. aUHI nights>1.5°C (% of column A)	C. No. extreme aUHI nights>5.0°C (% of column A)
Spring (MAM)	3.0 (1.56)	460	157 (34.1%)	65 (14.1%)
Summer (JJA)	3.1 (1.51)	484	158 (32.6%)	61 (12.6%)
Autumn (SON)	2.9 (1.48)	455	122 (26.8%)	55 (12.1%)
Winter (DJF)	2.6 (1.26)	451	85 (18.8%)	28 (6.2%)
Total	2.9 (1.47)	1850	522 (28.2%)	209 (11.3%)

Table 4.5: Summary of night-time aUHII, number of nights (%) and (extreme) heat island events for Greater London in relation to LWTs, 8 July 2002 to 31 July 2007.

Lamb weather types	Night-time aUHII				A. No. nights (% of 1850 nights)	B. No. aUHI nights >3.5°C (% of column A)	C. No. extreme aUHI nights >5.0°C (% of column A)	D. Cloudless (0-okta)
	Min	Max	Mean	Std. Deviation				
Anticyclonic [A]	-0.6	7.7	3.2	1.60	391 (21.1%)	154 (39.4%)	63 (16.1%)	39
Cyclonic [C)	0.1	6.8	2.4	1.11	217 (11.7%)	25 (11.5%)	8 (3.7%)	2
South-westerly [SW]	0.7	6.9	3.3	1.67	173 (9.4%)	68 (39.3%)	34 (19.7%)	5
Westerly [W)	0.6	7.3	2.8	1.39	160 (8.7%)	41 (25.6%)	14 (8.8%)	6
North-westerly [NW)	0.8	6.6	2.4	1.12	107 (5.8%)	16 (15.0%)	3 (2.8%)	6
Southerly [S)	1.2	7.0	3.2	1.53	104 (5.6%)	39 (37.5%)	15 (14.4%)	4
Northerly [N]	0.6	8.1	2.3	1.19	74 (4.0%)	6 (8.1%)	3 (4.1%)	5
South-easterly [SE]	1.3	6.5	2.9	1.17	54 (2.9%)	13 (24.1%)	3 (5.6%)	4
Unclassified [U)	1.0	7.2	3.4	1.44	30 (1.6%)	11 (36.7%)	5 (16.7%)	2
North-easterly [NE]	1.1	6.0	2.3	1.51	25 (1.4%)	4 (16.0%)	2 (8%)	1
Easterly [E)	1.0	6.6	2.7	1.55	25 (1.4%)	6 (24%)	3 (12%)	0
[A]/[C] hybrids	-1.6	7.2	2.9	1.44	490 (26.4%)	139 (28.4%)	53 (10.8%)	23

For Greater London, a heat island event is defined as a night-time minimum aUHII >3.5°C (Section 4.3), and an extreme heat island event is defined as a night-time minimum aUHII >5°C. Table 4.5 summaries the night-time aUHII, the occurrence of LWTs and total number of nights of (extreme) heat island events for each LWT in Greater London (LWC-Rothamsted) from 8 July 2002 to 31 July 2007. Over the study period, types [A], [C], [SW] and [W] have been recognised as the most commonly occurring LWTs occurring during UHI events, accounting for 21.1%, 11.7%, 9.4% and 8.7% of cases, respectively. The dominant type [A] was associated with a mean night-time aUHII of 3.2°C, and accounts for the largest proportion, 39.4%, of UHI events and 16.1% of extreme UHI events among all LWTs, with a large aUHII of 7.7°C. Surprisingly, [N] type generated the most extreme night-time aUHI events (8.1°C) on 31 August 2003, even higher than significant 7.7°C under [A] type on 10 August 2003. The expected extreme value could be caused by dramatic reduction in night-time $T_{air/min}$ at Rothamsted and relatively gentle reduction in $T_{air/min}$ at LWC on that day, details see Section 5.3.2 where detailed heatwave analysis was conducted. Under the consideration of that too fewer nights to be averaged for [N] type, more attention will be focused on [A] type which associated with 48 nights. The two least dominant types, [NE] and [E], were associated with mean night-time aUHII of 2.3°C and 2.7°C, respectively. Although [U] type occurred with low frequency, the mean night-time aUHII reached a maximum of 3.4°C; even higher than for [A] type. The results of the one-way ANOVA analysis confirm that the eleven LWTs explain the majority of the variance in aUHI (p <0.01). The excluded hybrid LWTs are statistically insignificant (p >0.05).

4.5.3 Satellite-derived sUHI

Birmingham

Figure 4.9 shows the averaged spatial patterns of sUHII for Birmingham calculated from MODIS/Aqua night-time LST for each LWT. The urban warming in Birmingham relative to the surrounding rural areas is apparent. The number in the lower-right corner of each image indicates the number of nights to be averaged. A concentric pattern is found in Birmingham central areas with the sUHII decreasing towards sub-urban or rural areas, particularly when influenced by [A], [SW] and [S] types. An urban warming in Birmingham of up to 4.16°C has been detected under the influence of [A] type. This is the averaged maximum sUHII value over 48 [A] nights. Heat islands associated with [SE], [C] and [U] types can also be discerned but with relatively low confidence. Results highlight the significance of type [A] as dominating Birmingham's sUHI patterns. Unfortunately, for some LWTs (e.g. [C], [W], [N], [U], [NE] and [E]), only a small number of nights satisfied the experimental criteria and thus interpretation of the results should be made with caution due to the small sample size.

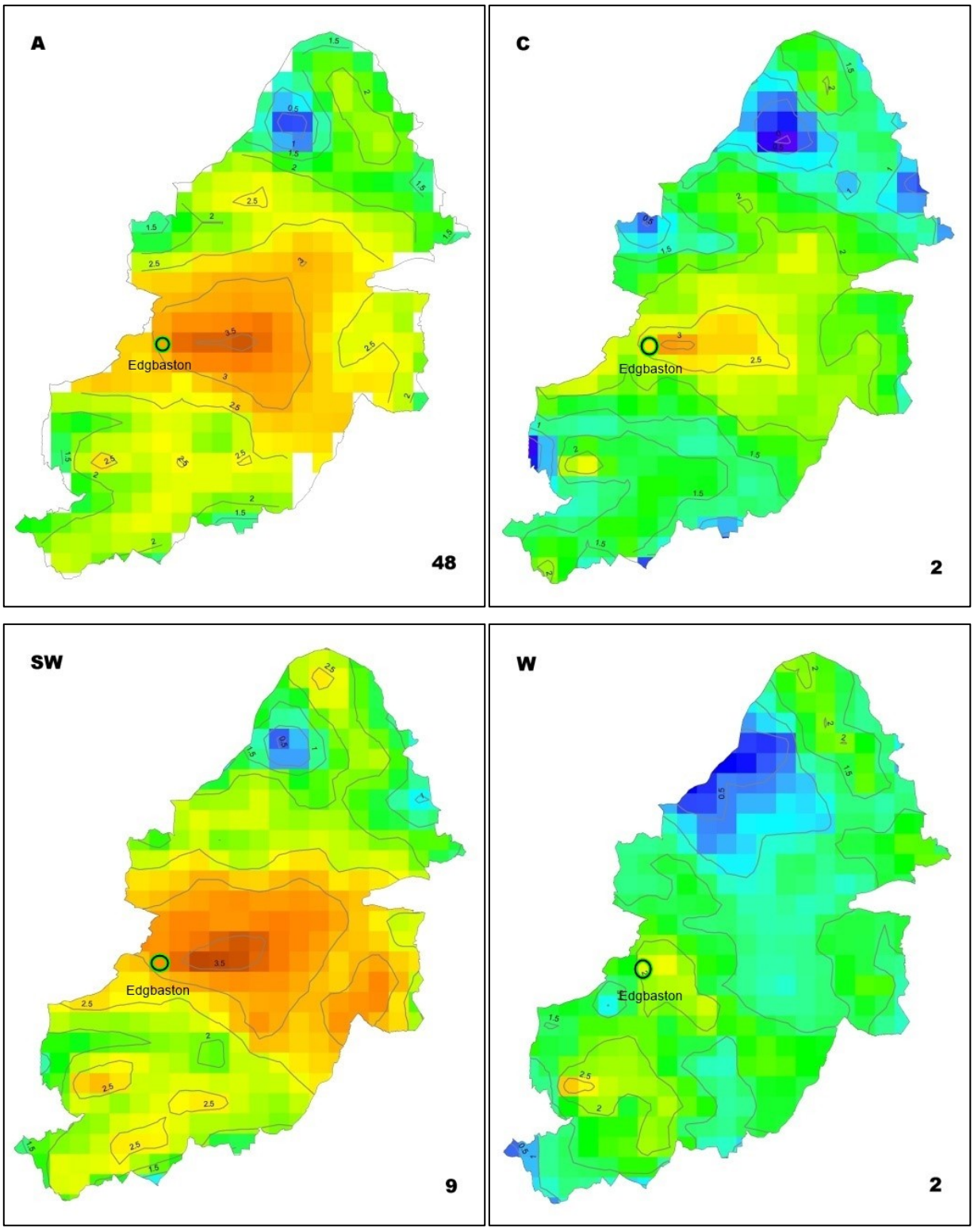
A
Edgbaston
48
C
Edgbaston
2
SW
Edgbaston
9
W
Edgbaston
2

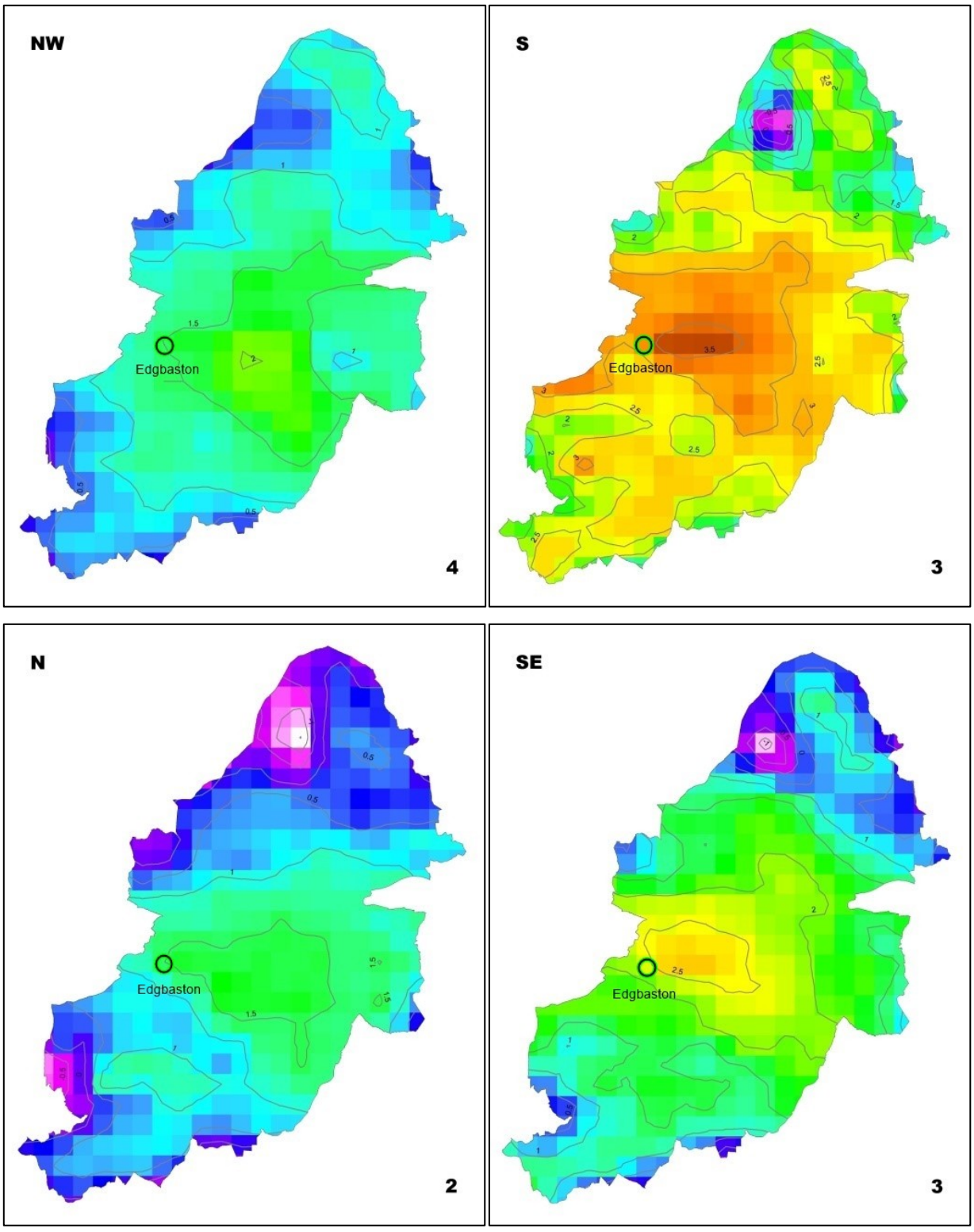
NW
Edgbaston
4
S
Edgbaston
3
N
Edgbaston
2
SE
Edgbaston
3

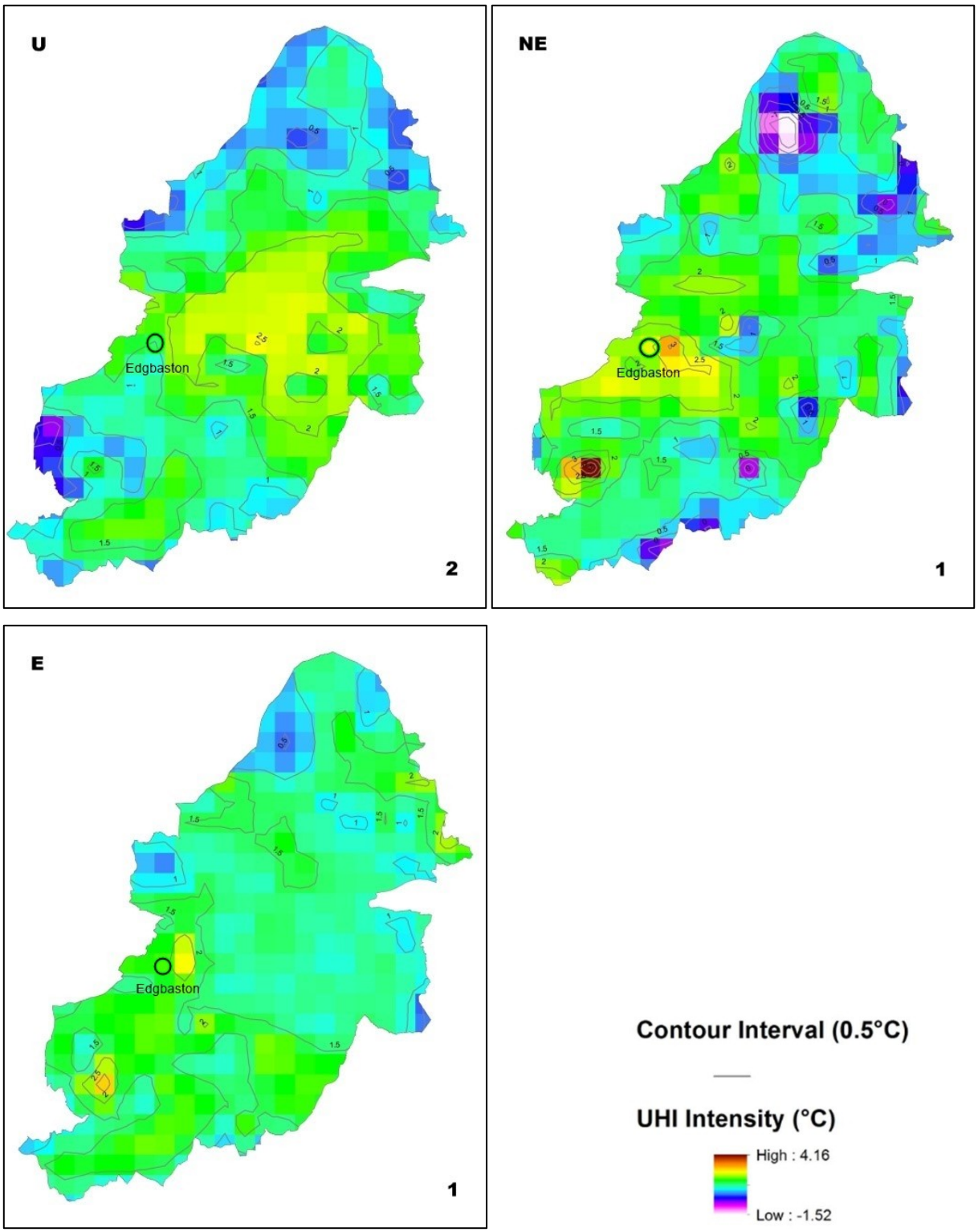

Figure 4.9: Satellite-derived sUHII for Birmingham calculated from the MODIS/Aqua night-time LST for eleven LWTs (number in the lower-right corner of each image is the number of days to be averaged).

London

Figure 4.10 shows the averaged spatial patterns of sUHII in London calculated using MODIS/Aqua night-time LST for each LWT. The urban warming of London relative to the surrounding rural areas is evident. The number in the lower-right corner of each image is the number of nights to be averaged. A 'concentric pattern' is found in central London areas with sUHII decreasing towards the surrounding areas, particularly when influenced by [A], [SW], [S] and [U] types. An urban warming in London of up to 7.34°C has been detected under the influence of [A] type. It should be noted that this is the average value over 39 cloudless nights calculated using the LWC cloud cover data. Heat islands associated with [C], [W], [NW], [SE] and [E] types can also be discerned but with relatively low confidence. These results highlight the significance of [A] type in dominating London's sUHI. Only a small number of nights satisfied the experimental criteria for the selection of MODIS satellite imagery for the less significant LWTs (e.g. [C], [S], [SE], [U] and [E]).

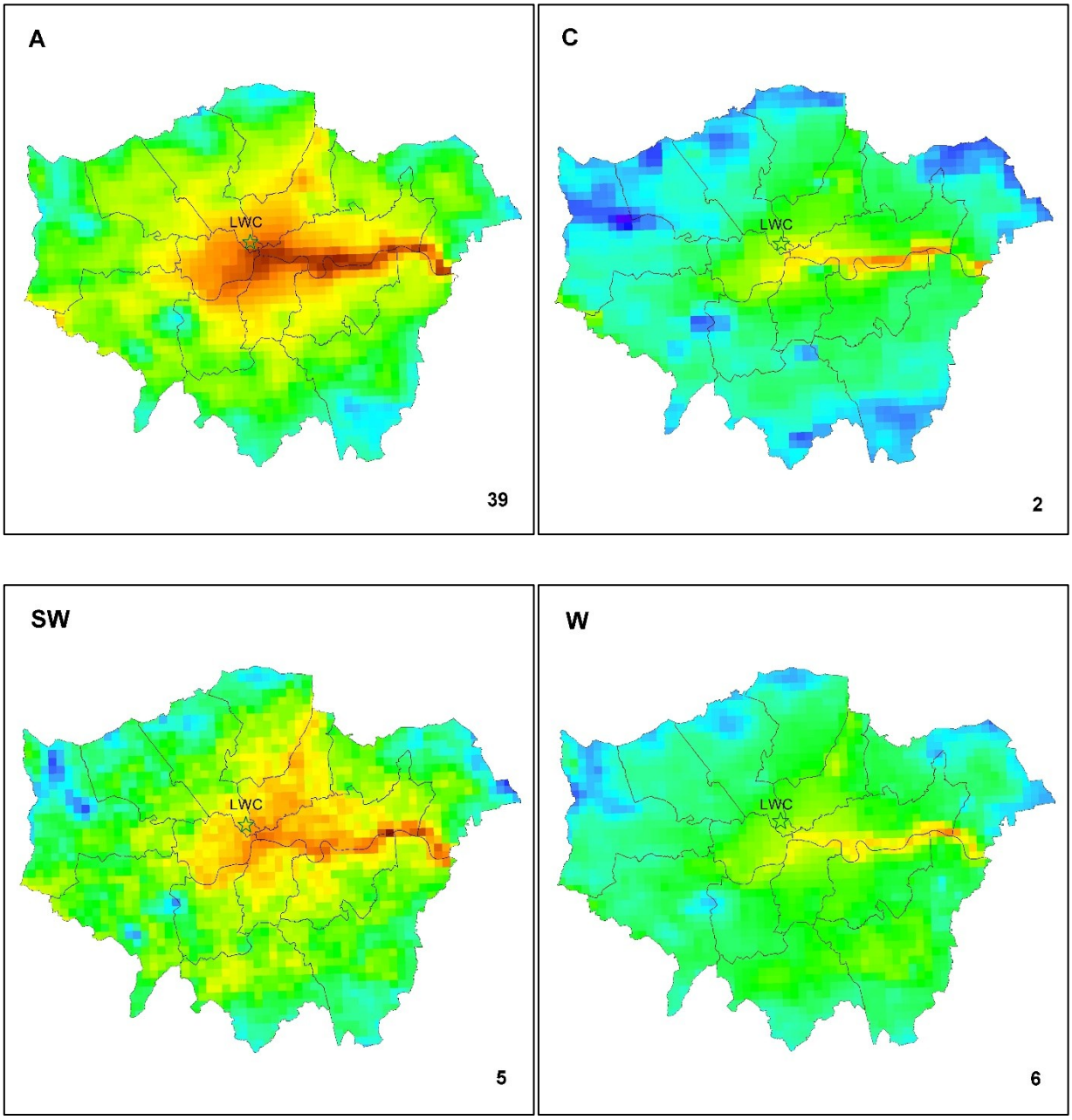
A
LWC
39
C
LWC
2
SW
LWC
5
W
LWC
6

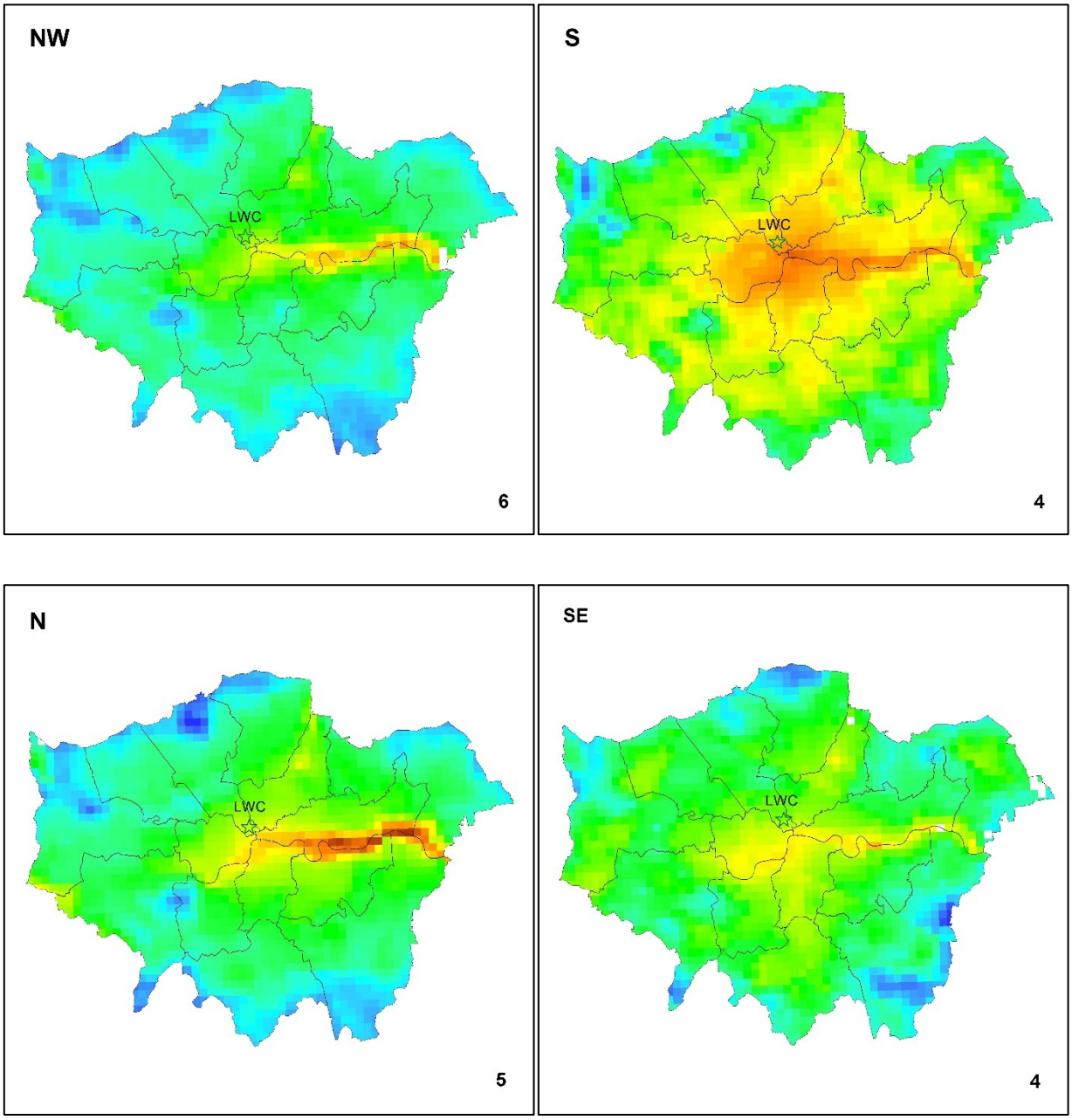
NW
LWC
6
S
LWC
4
N
LWC
5
SE
LWC
4

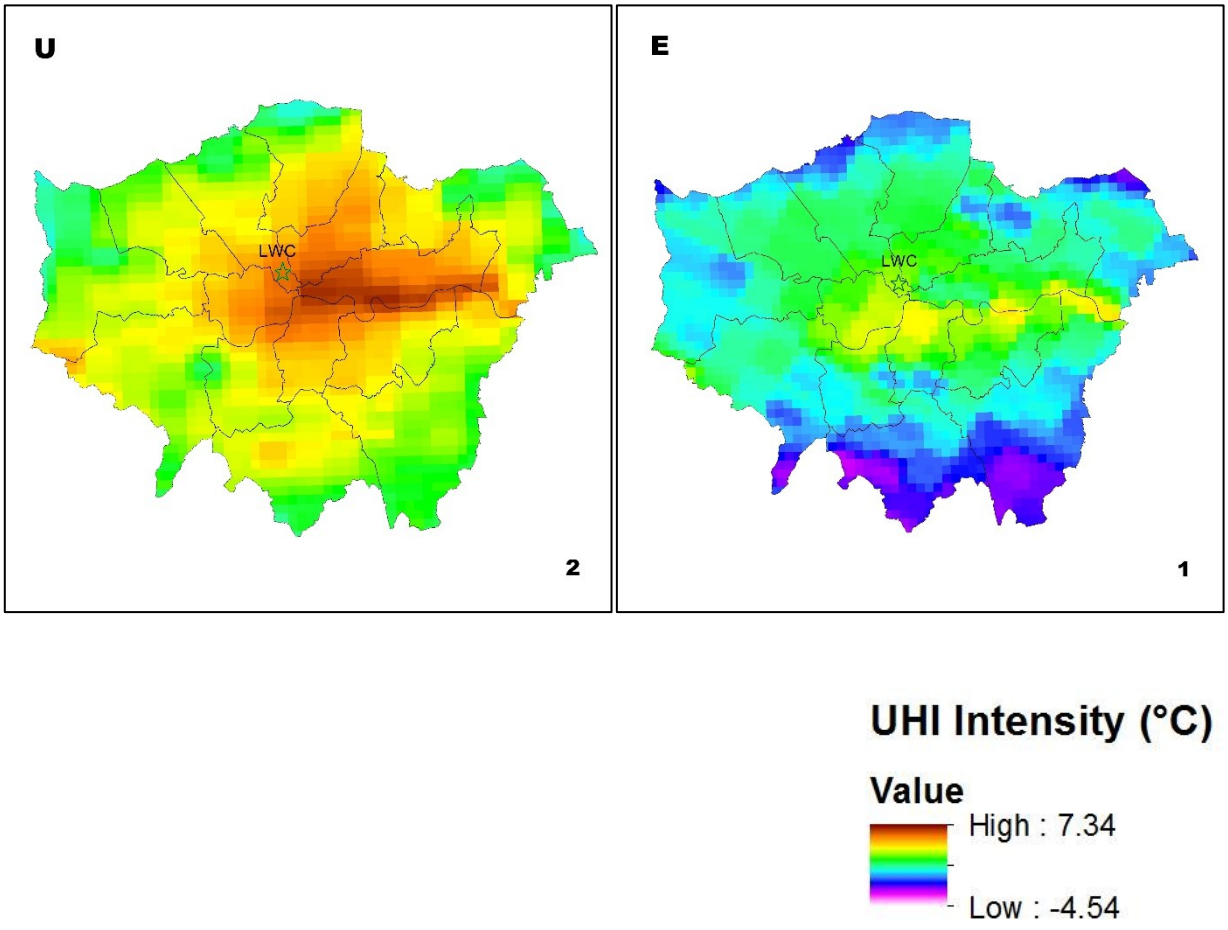

Figure 4.10: London's satellite-derived sUHII calculated from the MODIS/Aqua night-time LST for ten LWTs (number in the lower-right corner of each image is the number of days to be averaged).

4.5.4 Relationships between T_{air}-related aUHI and LST-related sUHI in cloudless anticyclonic conditions

Interpretation of the comparison between T_{air} and LST should be made cautiously as T_{air} is measured directly from a single-point weather station whereas the LST is measured indirectly using satellite remote sensing at the 1 km^2 pixel spatial resolution. In principle, the LST reading of a pixel can be interpreted as an aggregated temperature within that pixel of all upward-facing surfaces visible to the satellite sensor (e.g. roads, roofs, tree tops and vegetation cover). For the urban stations of Edgbaston and LWC shown in Figure 3.1(b) and Figure 3.2(b), T_{air} is measured inside the urban canopy layer, whereas the LST obtained from the MODIS/Aqua sensor may have been influenced by rapidly cooled exposed surfaces, such as park areas, tree tops and water bodies (especially larger water bodies such as the reservoir or lake areas). In this section, the night-time T_{air} and LST are analysed for 48 cloudless anticyclonic nights at the Edgbaston and Shawbury stations, and 39 cloudless anticyclonic nights at the LWC and Rothamsted stations.

West Midlands

In Figure 4.11, the averaged night-time T_{air} and LST for each month are plotted together with the averaged aUHII and sUHII from the Edgbaston and Shawbury weather stations. The bars indicate the number of cloudless anticyclonic nights in each month. The spring season (MAM) has the highest number of cloudless anticyclonic nights, whilst the autumn/winter season (October-January) has the lowest number. The highest sUHII (5.9°C) occurred on 2 September 2002 and the highest aUHII (6.8°C) occurred on 11 April 2007 (peaks not shown in the plot). Figure 4.11 also shows that, although T_{air} and LST follow the normal seasonal pattern, the aUHII and sUHII do not vary significantly across seasons. By excluding those months with only one or two nights (January, August, October-December), a difference in sUHII is found between the summer months (June and July) and spring months (MAM) (i.e. a positive sUHII value in summer, negative in spring). This difference is not as significant for aUHII. The mean aUHII for all 48 nights is 3.4°C, which is slightly higher than the mean sUHII by 0.4°C.

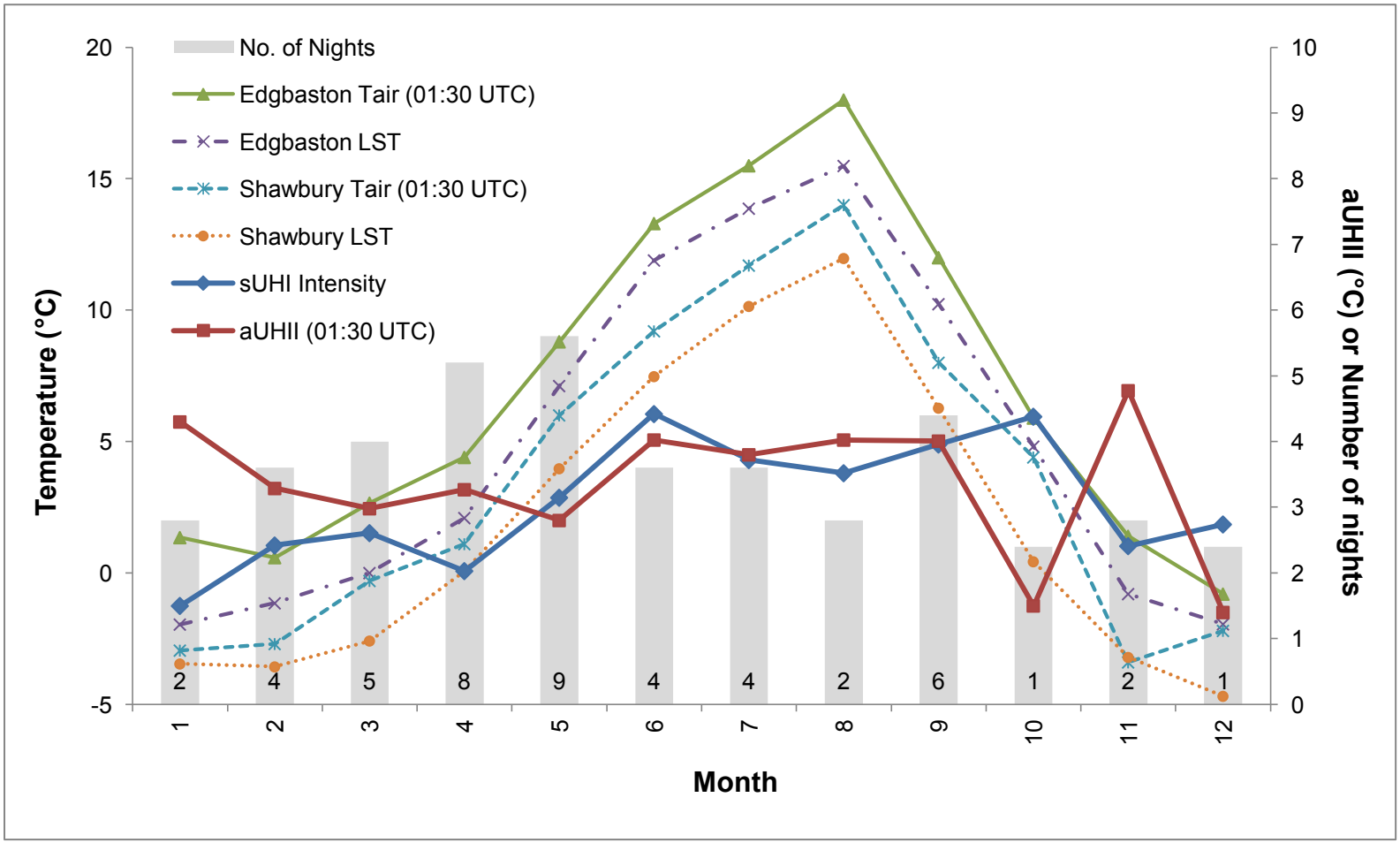

Figure 4.11: Monthly mean T_{air} (01:30 UTC) and LST, aUHII (01:30 UTC) and sUHII at the Edgbaston and Shawbury stations for the 48 cloudless anticyclonic nights (including the number of nights for each month).

Greater London

Figure 4.12 shows the averaged night-time T_{air} and LST together with the monthly averaged aUHII and sUHII at the LWC and Rothamsted weather stations. The highest number of cloudless anticyclonic nights occurred in March, followed by August and September. There was no satisfactory data in January and November. Excluding those months with less than two nights (January, February, June and November), the sUHII is consistently higher than the aUHII, but seasonal variations in aUHII and sUHII are rather weak. The mean aUHII for all 39 nights is 4.5°C, which is lower by 1°C than the mean sUHII of 5.5°C. The highest sUHII (8.2°C) occurred on a typical heatwave day, 10 August 2003. The highest aUHII (7.2°C) occurred on 6 July 2004 (single-day peaks not shown in the plot). For both weather stations, the values of T_{air} were consistently higher than the LST, with the exception of the LWC station in June. For the urban station, this may be attributed to the fact that LST is influenced by cold exposed surfaces within the pixel. For the rural station, however, night-time temperature inversion due to radiative cooling at the surface might explain the warmer T_{air} compared to LST. Comparing by station, both T_{air} and LST at urban stations are significantly higher than the values recorded rural stations.

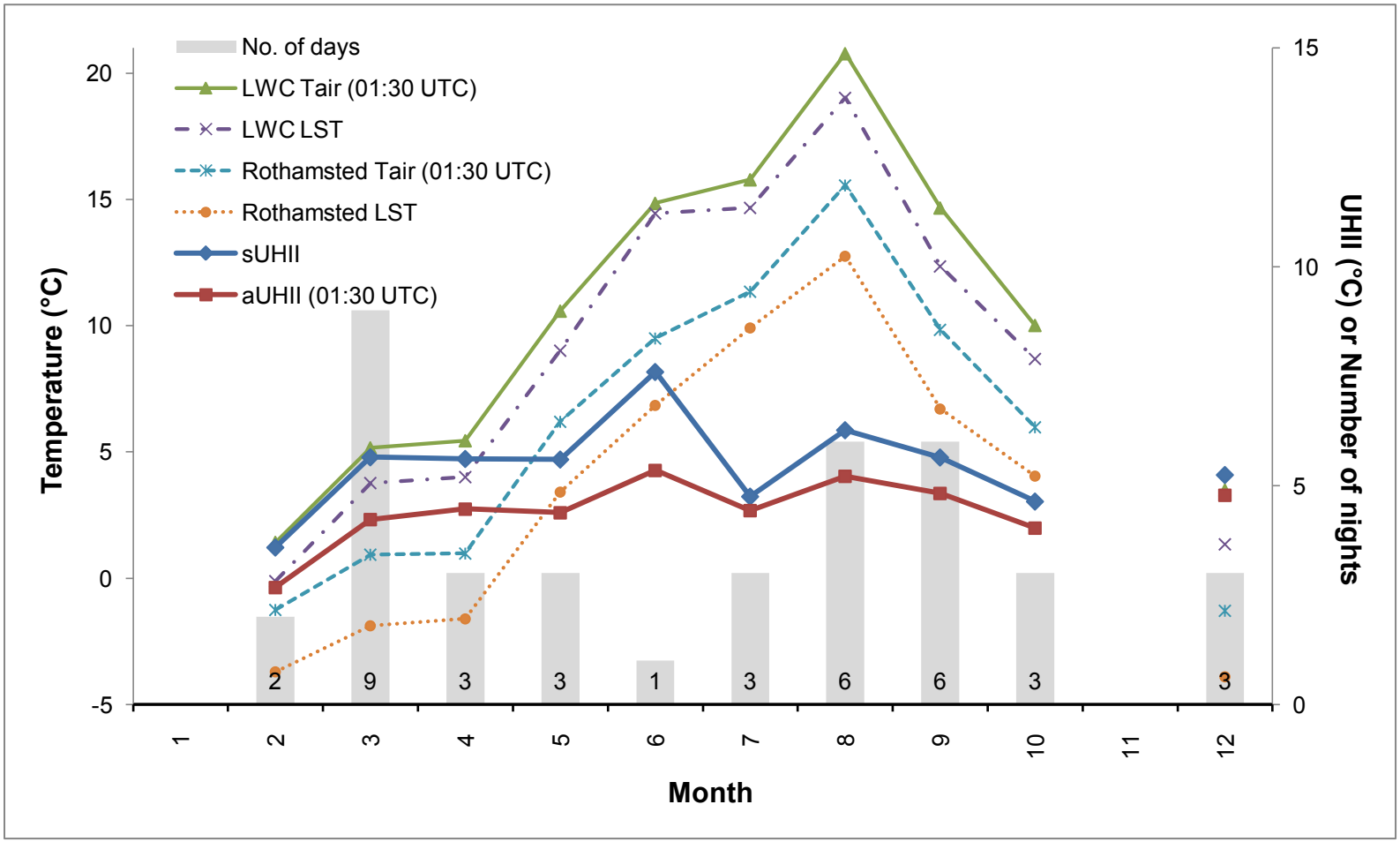

Figure 4.12: Monthly mean T_{air} (01:30 UTC) and LST, aUHII (01:30 UTC) and sUHII at the LWC and Rothamsted stations for the 39 cloudless anticyclonic nights (including the number of nights for each month).

Correlations of T_{air} and LST, aUHI and sUHI

Figure 4.13 (a) and (b) illustrate the correlations between T_{air} and LST for all 48 nights for the Edgbaston and Shawbury stations. The intercept at LST = 0°C can be interpreted as the difference between T_{air} and LST when the regression line has a slope equal to unity. This difference is ~2.2°C for the Edgbaston station and ~1.6°C for the Shawbury station. The slope of the regression line for Shawbury is indeed about 1, suggesting that the lower LST (mean LST = 2.6°C; mean T_{air} = 4.2°C) due to radiative cooling is independent of season. On the other hand, the slope of the regression line for Edgbaston is 0.96, suggesting that the difference between T_{air} and LST is weakly seasonally dependent, and reduces from 2.2°C at LST = 0°C, to 1.6°C at LST = 15°C, to 1.4°C at LST = 20°C. The mean T_{air} of 7.6°C and mean LST of 5.6°C in Edgbaston are consistently higher than those in Shawbury. For each station, night-time T_{air} and LST are strongly correlated at the 0.01 significance level (r >0.98 for Edgbaston, r >0.97 for Shawbury, p <0.01).

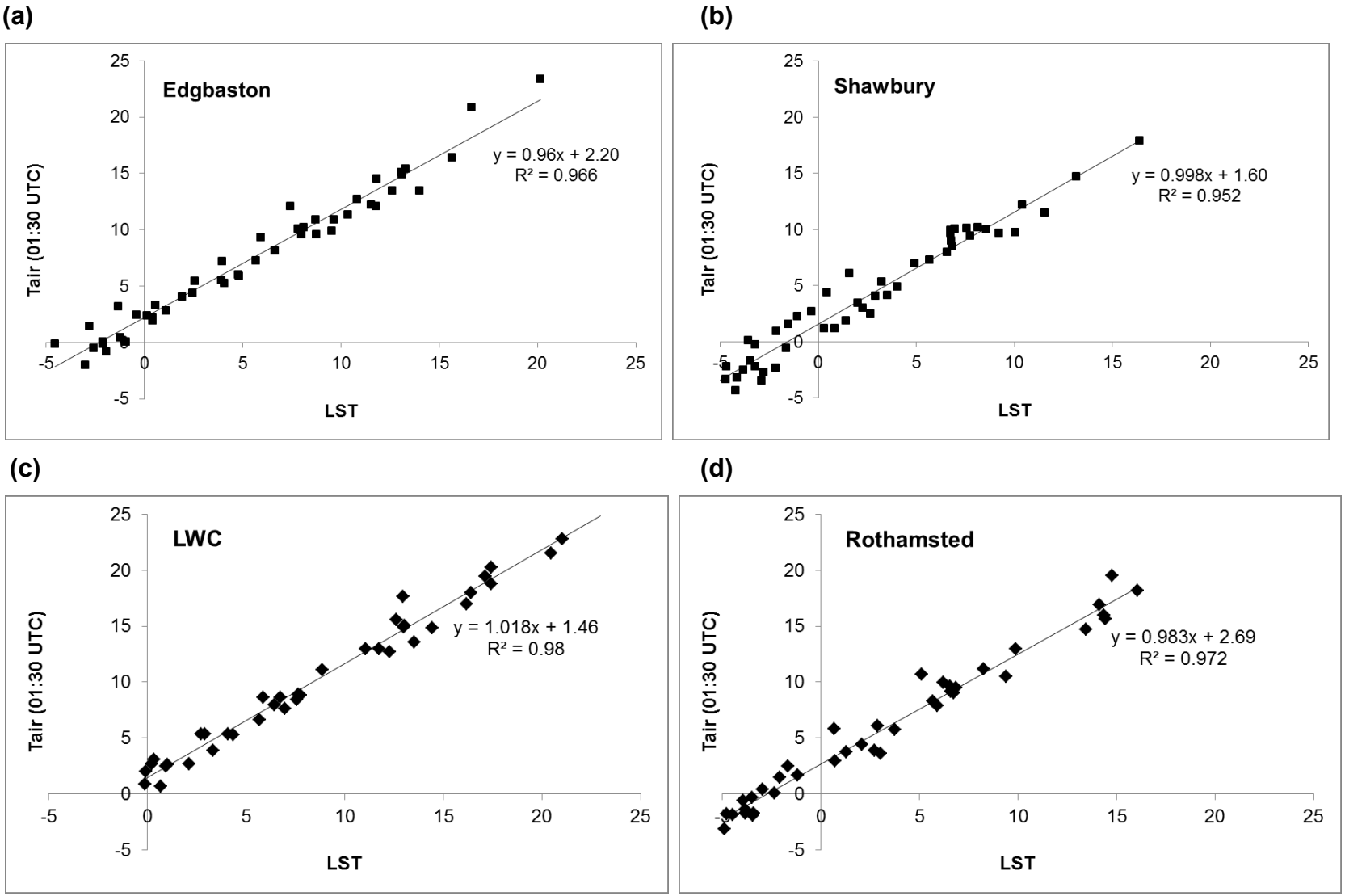

Figure 4.13: Relationships between T_{air} (01:30 UTC) and night-time LST at (a) Edgbaston and (b) Shawbury in 39 cloudless anticyclonic nights; (c) LWC and (d) Rothamsted in 39 cloudless anticyclonic nights.

Figure 4.13 (c) and (d) demonstrate the correlation between T_{air} and LST for all 39 nights for the LWC Rothamsted stations. The intercepts at LST = 0°C can be interpreted as the difference between T_{air} and LST when the regression line has a slope equal to unity. This difference is ~1.5°C for the LWC station and ~2.7°C for the Rothamsted station. The slope of the regression line for LWC is indeed about 1, suggesting that the lower LST (mean LST = 9.0°C; mean T_{air} = 10.6°C) due to radiative cooling is independent of season. On the other hand, the slope of the regression line for Rothamsted is ~0.98, suggesting that the difference between T_{air} and LST is weakly seasonally dependent, and reduces from 2.7°C at LST = 0°C, to 2.4°C at LST = 15°C, and finally to 2.3°C at LST = 20°C. The mean T_{air} of 6.1°C and mean LST of 3.5°C in Rothamsted are significantly lower than those at the LWC station. For each station, night-time Tair and LST are strongly correlated at the 0.01 significance level (r = 0.99 for LWC, r >0.98 for Rothamsted, p<0.01).

(a)

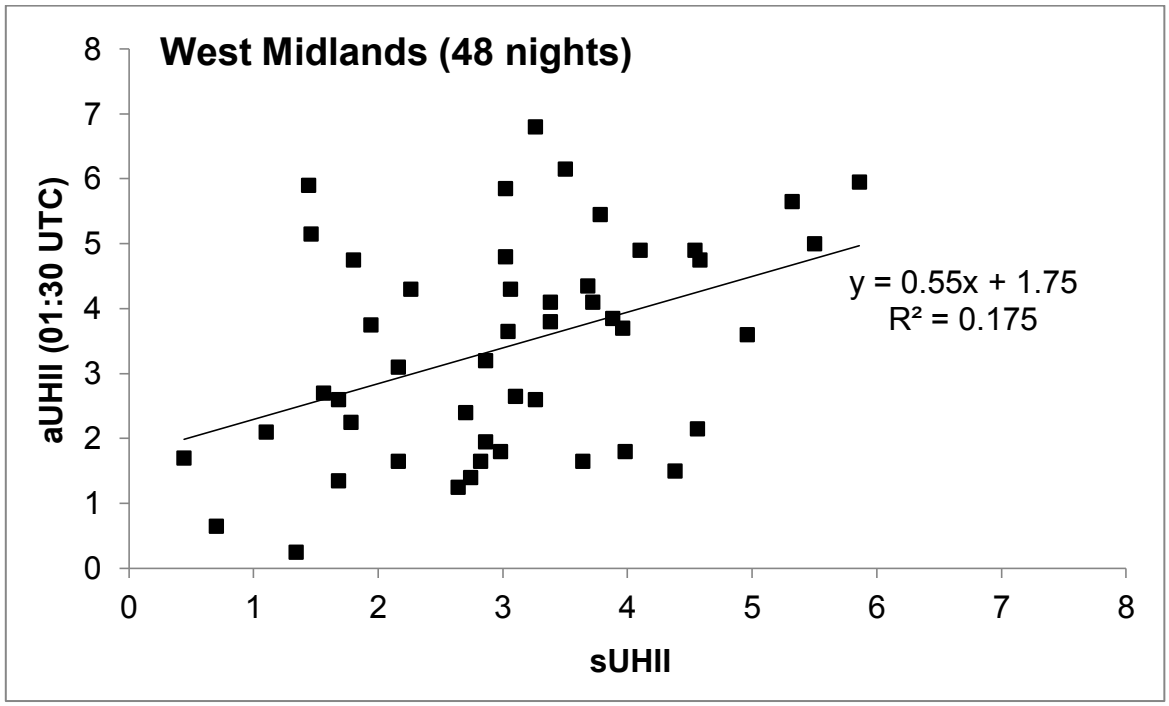

(b)

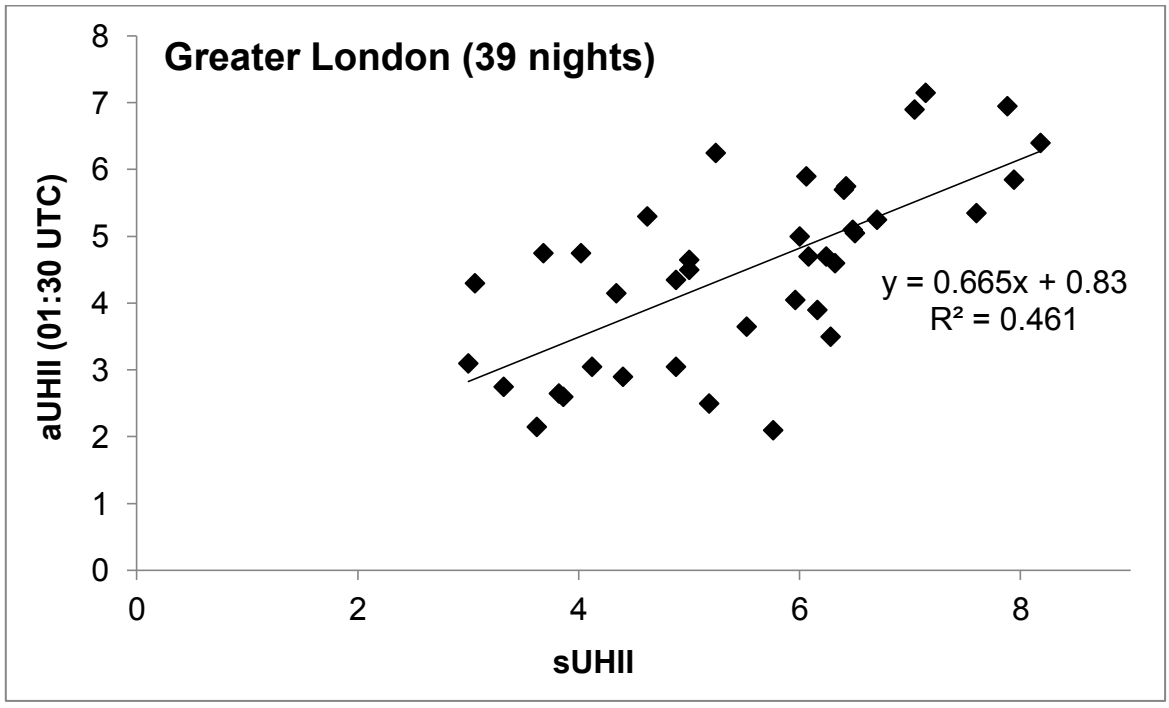

Figure 4.14: Relationships between aUHII (01:30 UTC) and sUHII for (a) the West Midlands (48 nights); (b) Greater London (39 nights).

Figure 4.14 (a) and Figure 4.14 (b) shows the scatterplots of aUHII (01:30 UTC) and night-time sUHII for 48 cloudless anticyclonic nights in the West Midlands, and 39 cloudless anticyclonic nights in Greater London respectively, together with the associated linear regression lines. Detailed information of T_{air} and LST at the urban and rural stations and the calculated aUHII and sUHII for the West Midlands (48 nights) and Greater London (39 nights) are listed in Appendix 4. The aUHII was calculated from the average T_{air} recorded at 01:00 UTC and 02:00 UTC, to match the MODIS acquisition time of ~01:30 UTC. Correlations for both regions are statistically significant (p <0.01).

For the West Midlands, aUHII and sUHII are correlated with Pearson correlation coefficient r >*0.4* and account for ~18% of the variance in aUHII. For Greater London, the correlation is stronger (r >0.67) and accounts for ~46% of the variance in aUHII. The aUHII-sUHII relationship for Greater London shows more scatter than the West Midlands, and the values of aUHII and sUHII are larger overall. The value of sUHII in London varies in the range 3-8°C. This may be caused by the large difference in surface land-use characteristics (Figure 3.2). Central urban areas in London are surrounded by extensive densely built-up areas in contrast to the large open spaces covered by vegetation in rural Rothamsted. In the West Midlands, the values of aUHII are slightly higher than the values of sUHII. Within the 1 km^2 Edgbaston pixel, the presence of large areas of vegetation and the reservoir may cause a reduction in the urban LST.

The linear relationship between aUHII and sUHII can also be explained by the simple analytical model described in Box 4.1. This model is derived taking into account several reasonable assumptions. The model is expressed by Equation (8):

$$\mathrm{aUHII} = \frac{1}{\alpha} \cdot \mathrm{sUHII}$$

which implies that aUHII and sUHII are linearly related with a slope of $\frac{1}{\alpha}$, where $\alpha = \Delta f^{(b)}$is the difference in 'built-up' area fraction between the urban pixel and the rural pixel. Referring to Figure 3.1 and Figure 3.2, $\Delta f^{(b)}$ is positive due to greater coverage by the urban 'built-up' land-use type for the Edgbaston and LWC pixels than for the Shawbury and Rothamsted pixels. Although this model explains the linear relationship between aUHII and sUHII, the magnitude of the slope is larger than that in Figure 4.14(a) and Figure 4.14(b). This mismatch is attributed to simplifications underlying the model. One example is the inaccuracy of Equation (6) in Box 4.1. In general, under cloudless conditions, $\mathrm{T}_{\mathrm{air}(r)} > \mathrm{T}^{(o)}$, due to radiative cooling of the surface layers and the resulting temperature inversion (as discussed earlier). This assumption replaces $\mathrm{T}^{(o)}$ (a lower value) in Equation (4) by $\mathrm{T}_{\mathrm{air}(r)}$ (a larger value) and results in a smaller temperature difference $(\mathrm{T}^{(b)} - \mathrm{T}^{(o)})$. The coefficient α in Equation (7) is therefore larger and consequently the slope given by $\frac{1}{\alpha}$ is smaller.

As discussed earlier, the relationship between T_{air} and LST has been investigated in depth. This thesis has provided further insight into the relationship between aUHII and sUHII, particularly in the case of settled anticyclonic conditions. The results presented in this thesis may serve as a basis for future work deriving spatial patterns of aUHI using satellite-derived thermal images under certain conditions (e.g. cloudless nights).

Box 4.1: A simple analytical model demonstrating a linear aUHII–sUHII relationship with a slope of the difference of 'build-up' area fraction between the urban pixel and the rural pixel.

Assumption 1: It is assumed that the ground surface of a pixel of the satellite imagery consists of two land-use types: 'built-up' (buildings, streets, etc.) and 'other' (parks, open ground etc.). It is also assumed that the satellite-derived land surface temperature of a pixel is the weighted average of two temperatures, one for the 'built-up' surfaces, $\mathrm{T}^{(b)}$, and the other for the 'others' surfaces, $\mathrm{T}^{(o)}$:

$$\mathrm{LST} = f^{(b)}\mathrm{T}^{(b)} + (1 - f^{(b)})\mathrm{T}^{(o)} \quad (1)$$

where $f^{(b)}$ is the area fraction of the pixel taken by the 'built-up' land-use type, the superscript $^{(b)}$ denotes 'built-up', and the superscript $^{(o)}$ denotes 'other'. For an urban pixel (e.g. the pixel for the urban Edgbaston and LWC stations shown in Figure 3.1(b) and Figure 3.2(b), equation(1) becomes

$$\mathrm{LST}_{(u)} = f^{(b)}_{(u)}\mathrm{T}^{(b)} + (1 - f^{(b)}_{(u)})\mathrm{T}^{(o)} \quad (2)$$

For a rural pixel (e.g. the pixel for the rural Shawbury and Rothamsted stations shown in in Figure 3.1(c) and Figure 3.2(c), equation(1) becomes

$$\mathrm{LST}_{(r)} = f^{(b)}_{(r)}\mathrm{T}^{(b)} + (1 - f^{(b)}_{(r)})\mathrm{T}^{(o)} \quad (3)$$

where the subscript $_{(u)}$ denotes an 'urban pixel' and the subscript $_{(r)}$ denotes a 'rural pixel'. It is noted that $f^{(b)}_{(r)}$ can be zero if a rural pixel contains no built-up land-use type (i.e. covered entirely by an open ground). Using the definition of $\mathrm{sUHII} = \mathrm{LST}_{(u)} - \mathrm{LST}_{(r)}$, the subtraction of equation (3) from equation (2) yields

$$\mathrm{sUHII} = \alpha \cdot (\mathrm{T}^{(b)} - \mathrm{T}^{(o)}) \quad (4)$$

where, $\alpha = \Delta f^{(b)} = f^{(b)}_{(u)} - f^{(b)}_{(r)}$, interpreted as the difference of 'built-up' area fraction between the urban pixel and the rural pixel.

Assumption 2: It is further assumed that at night, the air temperature measured at an urban weather station, $\mathrm{T}_{\mathrm{air}(u)}$, is in equilibrium with the surface temperature of the 'built-up' land-use type, $\mathrm{T}^{(b)}$, i.e.,

$$\mathrm{T}_{\mathrm{air}(u)} = \mathrm{T}^{(b)} \quad (5)$$

and that air temperature measured at a rural weather station, $\mathrm{T}_{\mathrm{air}(r)}$, is in equilibrium with the surface temperature of the 'other' land-use type, $\mathrm{T}^{(o)}$, i.e.,

$$\mathrm{T}_{\mathrm{air}(r)} = \mathrm{T}^{(o)} \quad (6)$$

Recalling the definition of $\mathrm{aUHII} = \mathrm{T}_{\mathrm{air}(u)} - \mathrm{T}_{\mathrm{air}(r)}$, substitution of equation (5) and equation (6) into substitution (4) yields,

$$\mathrm{sUHII} = \alpha \cdot \mathrm{aUHII} \quad (7)$$

This equation demonstrates that sUHII and aUHII has a linear relationship with a slope of $\Delta f^{(b)}$. Inorder to match the relationships in Figure 4.14(a) and Figure 4.14(b), equation (7) can be rearranged as:

$$\mathrm{aUHII} = \frac{1}{\alpha} \cdot \mathrm{sUHII} \quad (8)$$

4.6 Conclusions

This chapter investigated urban climates in the West Midlands (JJA 2001-2009) and Greater London (JJA 2001-2009). Ground-based aUHI and satellite-derived sUHI were presented, and the relationship between aUHII and sUHII (derived from ground-based T_{air} at local weather stations and satellite-derived LST) in relation to LWTs was investigated over the period 8 July 2002 and 31 July 2007, with a particular focus on cloudless anticyclonic nights.

Overall, London was found to be much warmer than Birmingham. According to the UK Met Office heatwave thresholds: 30°C for $T_{air/max}$ and 15°C for $T_{air/min}$ for the West Midlands, and 32°C for $T_{air/max}$ and 18°C for $T_{air/min}$ for Greater London. There were 6 extreme hot days in the West Midlands and 11 extreme hot days in Greater London. Annual variations in aUHII highlight the consistently high peaks for both daytime and night-time aUHII in 2003 in the West Midlands. For Greater London, night-time aUHII reached its peak in 2003, but daytime aUHII displayed an inverse low peak in 2003. The mechanism underlying the presence of an inverse low peak during this heatwave is still uncertain. On a typical heatwave day, 9 August 2003, night-time aUHII for the West Midlands peaked at 6.3°C at 23:00 UTC, and night-time aUHII for Greater London peaked at 7.1°C at 02:00 UTC. Birmingham's central sUHII peaked at 3.8°C and London's central sUHII was much higher, peaking at 8.7°C.

Over the study period 2002-2007, the night-time aUHI in summer was strongest out of the four seasons, associated with an aUHII (Edgbaston-Shawbury) of 1.7°C and an aUHII (LWC-Rothamsted) of 3.1°C. London's summer mean aUHII was nearly double

that of the West Midlands. The most frequently occurring LWT, [A] (391 nights, 21.1% of 1850 nights), gave the strongest mean (or maximum) night-time aUHII of 2.5°C (or 7°C) and the largest proportion of night-time heat island events (255 nights, 65.2% of 391 nights) in the West Midlands. For Greater London, the LWT of [A] gave a mean (or maximum) night-time aUHII of 3.2°C (or 7.7°C) and the largest proportion of night-time heat island events (154 nights, 39.4% of 391 nights). Indeed, the strongest mean night-time aUHII of 3.4°C was associated with the [U] type, followed by the [SW] type, associated with mean night-time aUHII of 3.3°C. Extreme heat island events with night-time aUHII > 5°C were also associated with the [SW] type (34 nights, 19.7% of 173 nights) and [U] type (5 nights, 16.7% of 30 nights). Overall, the night-time aUHII dominated by the [A] type was still strong enough to affect London's night-time aUHII.

Mean sUHII and aUHII for the West Midlands over the 48 cloudless anticyclonic nights were 3.0°C and 3.4°C, respectively. Mean sUHII and mean aUHII for Greater London over the 39 nights were 5.5°C and 4.5°C, respectively. The scatterplots for night-time aUHII and sUHII demonstrated a linear aUHII-sUHII relationship. London's regression line displayed a stronger correlation, $r > 0.67$ ($p < 0.01$), compared with the West Midlands regression line ($r > 0.4$, $p < 0.01$). A simple analytical model was developed that links the slope of the aUHII-sUHII relationship to the difference in built-up area fraction between the urban pixel and the rural pixel. The model partly accounts for the physical basis underlying the relationship. The stronger aUHII-sUHII correlation in London can be explained by the smaller difference in built-up area fraction between the urban and rural pixels. Because the entire Greater London area is considered to be

urban, the urban-rural fractional difference should be smaller. Unlike for land-use types in the West Midland, where the urban and rural areas are more distinguishable, the urban-rural difference in built-up area fraction should be larger in Greater London.

The MIDAS T_{air} averaged at 01:30 UTC was used corresponding with the acquisition time of MODIS/Aqua satellite images at ~01:30 UTC (Section 4.5.4). The true time at which $T_{air/min}$ (or $T_{air/max}$) occurred may have varied from day to day. The precise times of acquisition for the MODIS/Aqua imagery and MIDAS measurements for the West Midlands are provided in Appendix 3.

Chapter 5 Temperature-mortality relationships and heatwave episode analyses

5.1 Introduction

This chapter contains two sections. The first section deals with long-term temperature-mortality (T-M) relationships, and the second section presents short-term analyses of the 2003 heatwave event. The aim is to quantify the differential responses of mortality rate on temperature between urban and rural residents in the West Midlands and Greater London. Analyses of age-specific (<75 and 75+) all-cause mortality illustrate how people in different age groups are affected by temperature.

The T-M relationship has been studied extensively using different methods by researchers worldwide (see Section 2.2.1 for a detailed review). Some traditional methods for analysing the T-M relationship include non-parametric (local-influence) methods, such as the popular GAMs (Hastie and Tibshirani, 1990) which was previously mentioned on page 24. Such methods offer significant advantages but have not been implemented in the STATA statistics package. Conversely, the use of fractional polynomial (FP) as the model function can be implemented in any GAMs or general statistical package. The best fit curves can be plotted using 3rd-order or 4th-order polynomial regression in MS Excel 2007. However, as stated above, polynomials may not be the best choice to model the curve of heat-related mortality. The most comprehensive implementation is obtained using the *fracpoly* and *mfp* commands in

statistical software such as STATA. The *fracplot* command can immediately plot the datasets with 95% CI, the best-fit line, and the predicted and partial residuals of imported data. The *fracpred* and *browse* commands are also very useful. Unlike in most previous studies using epidemiological methods for modelling the T-M relationship, this chapter uses a relatively new technique, which is more flexible and better fitted to the non-linear T-M curves; an FP regression model associated with the statistical software STATA 11. The FP regression model function was first described in detail by Royston and Altman (1994). The FP regression model is a parametric method (non-local influence) that can easily obtain the predicted values i.e. threshold T_{mm}. Royston and Altman (1994) demonstrated the advantages of FP which provides a better fit and greater flexibility than is possible using conventional polynomials, especially when modelling non-linear and complicated relationships. Conventional polynomials are limited to a range of curve shapes. For example, quadratic (2^{nd} order polynomials) were found to be less flexible and cannot be used to model relationships such as asymptotic regions (McCullagh and Nelder, 1989). High-order polynomials may provide a poor fit to extreme values, and are susceptible to producing oscillations and edge effects (Royston and Altman, 1994). Methods using FPs offer all the advantages of conventional polynomials, and eliminate most of their disadvantages.

Threshold temperature, T_{mm}, is the representative threshold temperature above which mortality increases rapidly, and below which mortality generally decreases gradually with temperature. However, several variables may have a significant impact such as cause of mortality (Huynen et al., 2001), seasonality (Davis et al., 2003) and location (WMPHO,

2010). This chapter defines the specific T_{mm} for each geographical band and age group (<75 and 75+) to see how T_{mm} varies with temperature, location and age. Because both extreme high and low temperatures have adverse impacts on health, $T_{air/max}$ and $T_{air/min}$, rather than $T_{air/mean}$, were each associated separately with the mortality rate. In Chapter 4, a significant signal associated with extreme temperatures was identified particularly during the 2003 heatwave event. Considering the well-known impacts of heatwave on mortality, analyses of this notable episode were conducted during the months corresponding to the intense heatwave; July and August 2003. Harvesting and lag effects between high mortality and temperature are assessed. In the end, projections of future heatwaves are modelled using the UKCP09 up to the 2020s, 2050s and 2080s.

5.2 Data and methodology

5.2.1 Data

Referring to Section 3.1.1 (West Midlands) and Section 3.1.2 (Greater London) for a full description of the study areas, include the geographical inner and outer bands representing urban and rural areas, respectively.

Daily $T_{air/max}$ and $T_{air/min}$ were used separately to analyse the T-M relationships. For the West Midlands, the MIDAS temperature data at the Edgbaston station were associated with the inner band, and the MIDAS temperature data at the Shawbury station were associated with the outer band. For Greater London, the MIDAS temperature data at the LWC station were used to represent the inner band, and the MIDAS temperature data at

the Rothamsted station were used to represent the outer band. Further details about the MIDAS data collection and pre-processing can be found in Section 3.3.

The mortality data request and pre-processing were described in Section 3.6. This chapter uses all-cause daily mortality data in the age groups of <75 and 75+ in the West Midlands and Greater London. To analyse the T-M relationship, the DMR rather than the raw mortality data is used to represent mortality. The DMR is defined as the daily mortality scaled to the size of population. In this chapter, the DMR was calculated separately for each band corresponding to the relevant mortality and population data (Section 3.5), in units of per 100,000 population. The DMR depends on the regional population, age-specific mortality and the age distribution across the study area. Through age-/population- standardisations, the DMR can better distinguish mortality for regions with differing population and age distributions.

5.2.2 Methodology

T-M relationships

To examine the T-M relationship using the FP regression model using the statistical software STATA 11, the datasets were initially saved as .csv (Excel comma separated values) files. The comma-delimited data was then imported into STATA. Following the method described in Fisher (2009), elaborate methodology instructions are shown as a flow diagram in Figure 5.1, and the major commands (Royston and Altman, 1995) used for running the FR regression model in STATA 11 are listed as below.

1. **fracpoly regress *y x*, degree(2)**

where *y* is the title for the mortality data, *x* is the title for the temperature data, and degree(2) is the default degree of FP model to be fit.

2. **fracplot** - to plot the data and fit, with 95% Confidence Intervals, from most recently fit FP model.
3. **fracpred predicted** - to create new variable containing prediction, the fitted index or deviance residuals for the whole model.
4. **browse**

A new file will be created. Sorting the '*predicted*' column, the predicted mortality data will be listed into ascending order, so the first value in the corresponding temperature column means the T_{mm}, at which least deaths occur (WMPHO, 2010).

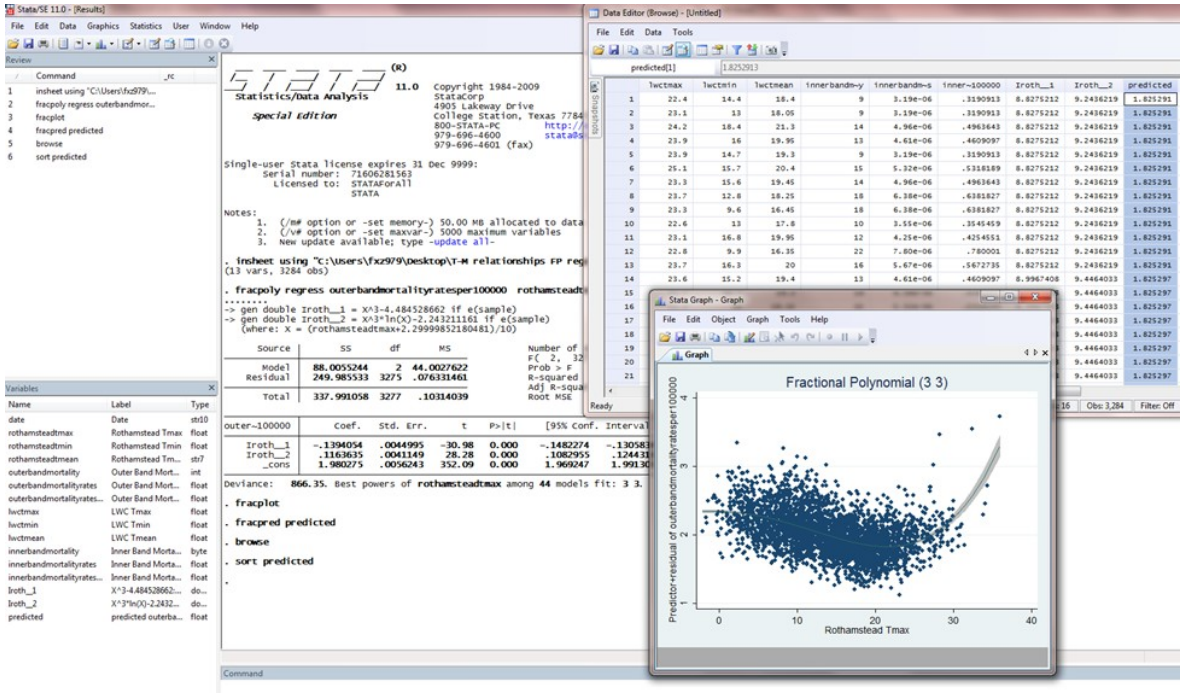

Figure 5.1: Flow diagram of running the FP regression model in STATA 11.

Future projections of heatwaves using UKCP09

The UK Climate Projections (UKCP09) can be used to generate synthetic time-series of weather variables at 5 km resolution that are consistent with the underlying 25 km resolution climate projections. A range of extremes (e.g. heatwave) can be produced using the Weather Generator (WG). The Threshold Detector (TD) applied to the WG output can be used to define the threshold temperatures during a heatwave (http://ukclimateprojections.metoffice.gov.uk/). The UKCP09 has been used by the WMPHO (2010) to predict the health effects of climate change in the West Midlands, demonstrating that decreased winter mortality seems to outweigh the increased summer mortality. Over the 21st century, summer and winter temperatures are likely to increase and heatwaves are likely to become more frequent.

5.3 Results and discussion

5.3.1 T-M Relationships

Figure 5.2 and Figure 5.3 illustrate the predicted all-cause DMR (per 100,000 population) for the populations aged <75 and 75+ years against temperatures. The best-fit FP curves are shown together with the 95% CI for each band. In these plots, the solid vertical reference lines indicate T_{mm} for the predicted relationship between DMR and $T_{air/max}$ (or $T_{air/min}$). The dashed lines indicate the $T_{air/mean}$ computed as the long-term average of $T_{air/max}$ and $T_{air/min}$.

Royston and Altman (1997) defined the degree of an FP model, *m,* as the number of terms in powers of *X* (predicted variable):

For degree $m = 1$, $Y = b_0 + b_1X^{-1}$

For degree $m = 2$, $Y = b_0 + b_1X^{-1} + b_2X^2$

Royston and Altman (1997) suggested that a good fit to non-noisy data can be generated with a 2nd degree ($m = 2$) FP model. According to the statistical output from STATA 11 (see Appendix 6), the best-fit FP model with degree $m = 2$ and power $p = (3, 3)$ among 44 FP models (including 8 repeated powers) corresponds to the regression function:

$$Y = b_0 + b_1X^3 + b_2X^3\ln X$$

The values of b_0, b_1 and b_2 can be ascertained directly from the STATA output (If $p = 0$, X^0 is taken as $\ln X$).

Royston and Altman (1995) provided the full definition of a FP regression model is

$$\phi_m(X;\boldsymbol{\beta};\mathbf{p}) = \beta_0 H_0(X) + \beta_1 H_1(X) + \cdots + \beta_m H_m(X)$$

where $H_0(X) = 1$, $p_0 = 0$ and for $j = 1, \ldots, m$,

$$H_j(X) = \begin{cases} X^{(p_j)}, & \text{if } p_j \neq p_{j-1}; \\ H_{j-1}(X)\ln X, & \text{if } p_j = p_{j-1}. \end{cases}$$

The best advantage of using FP regression model is that there is no need to manually build up complex formulae, using specific commends to run the model can achieve the output straightaway. Detailed information can be found in Appendix 6.

(a)

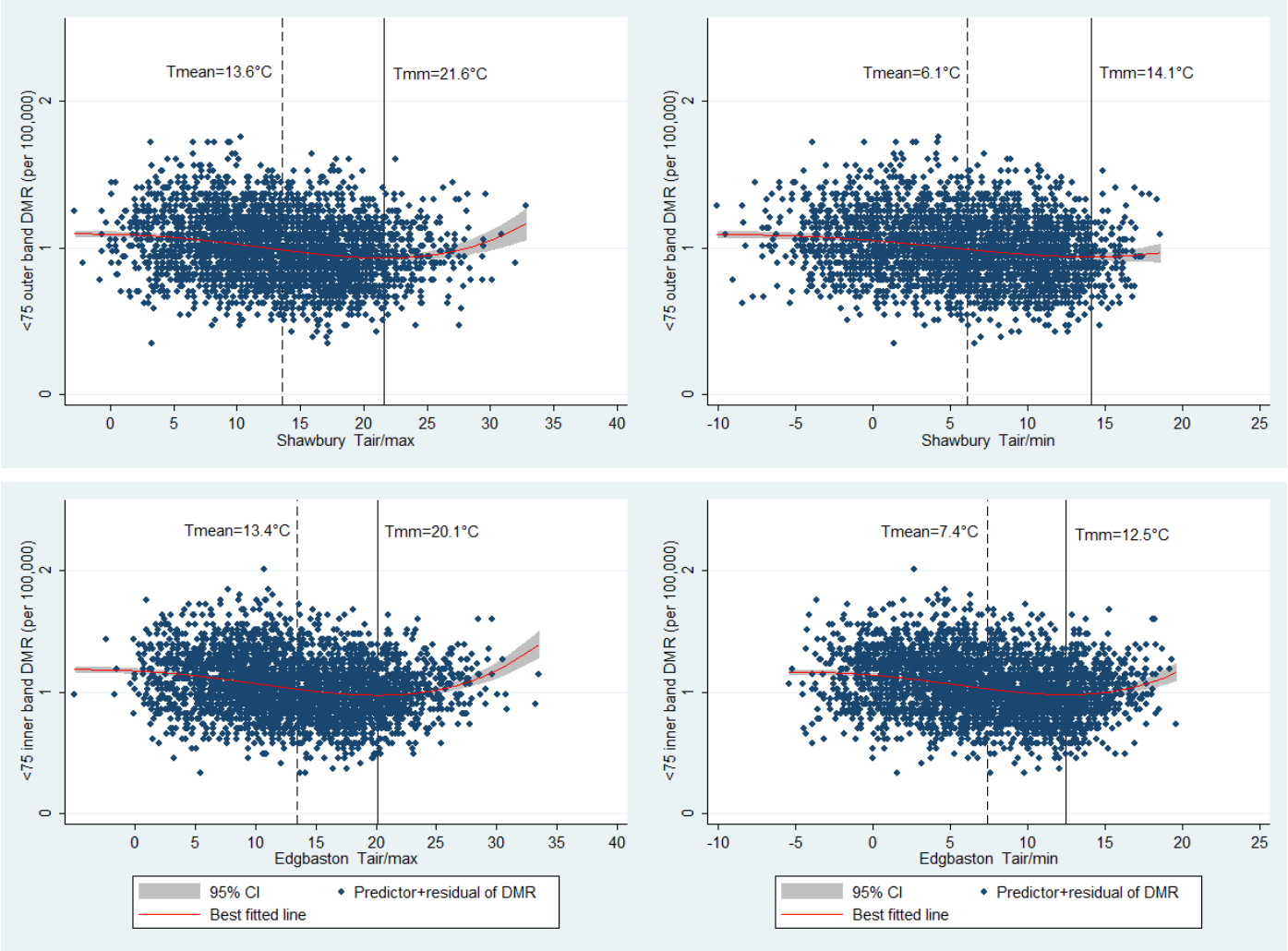
Tmean=13.6°C
Tmm=21.6°C
<75 outer band DMR (per 100,000)
Shawbury Tair/max
Tmean=6.1°C
Tmm=14.1°C
Shawbury Tair/min
Tmean=13.4°C
Tmm=20.1°C
<75 inner band DMR (per 100,000)
Edgbaston Tair/max
Tmean=7.4°C
Tmm=12.5°C
Edgbaston Tair/min
95% CI
Predictor+residual of DMR
Best fitted line

(b)

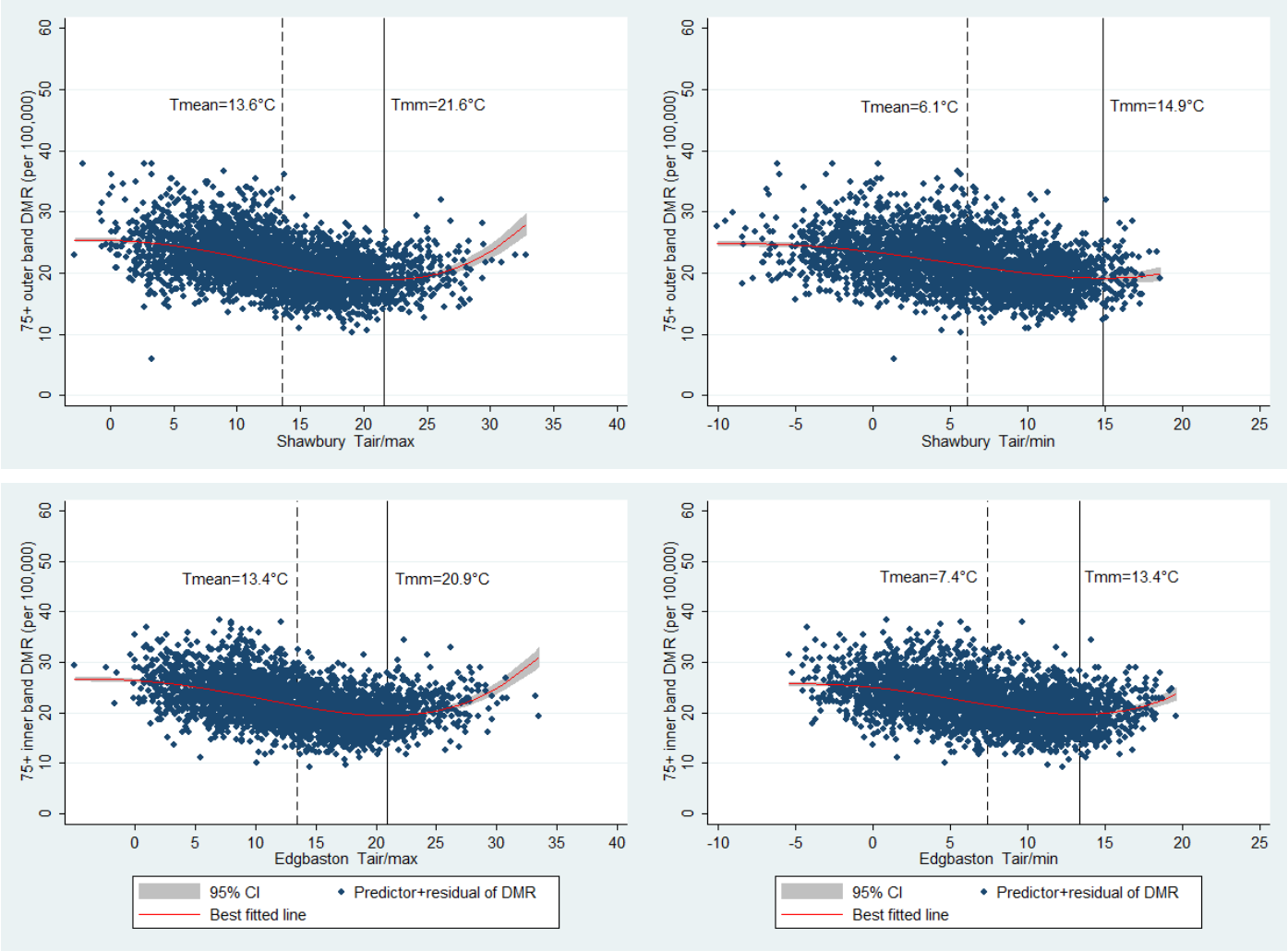

Figure 5.2: Relationships between temperatures and (a) <75 DMR (b) 75+ DMR in outer band and inner band of the West Midlands, 2001-2009

(a)

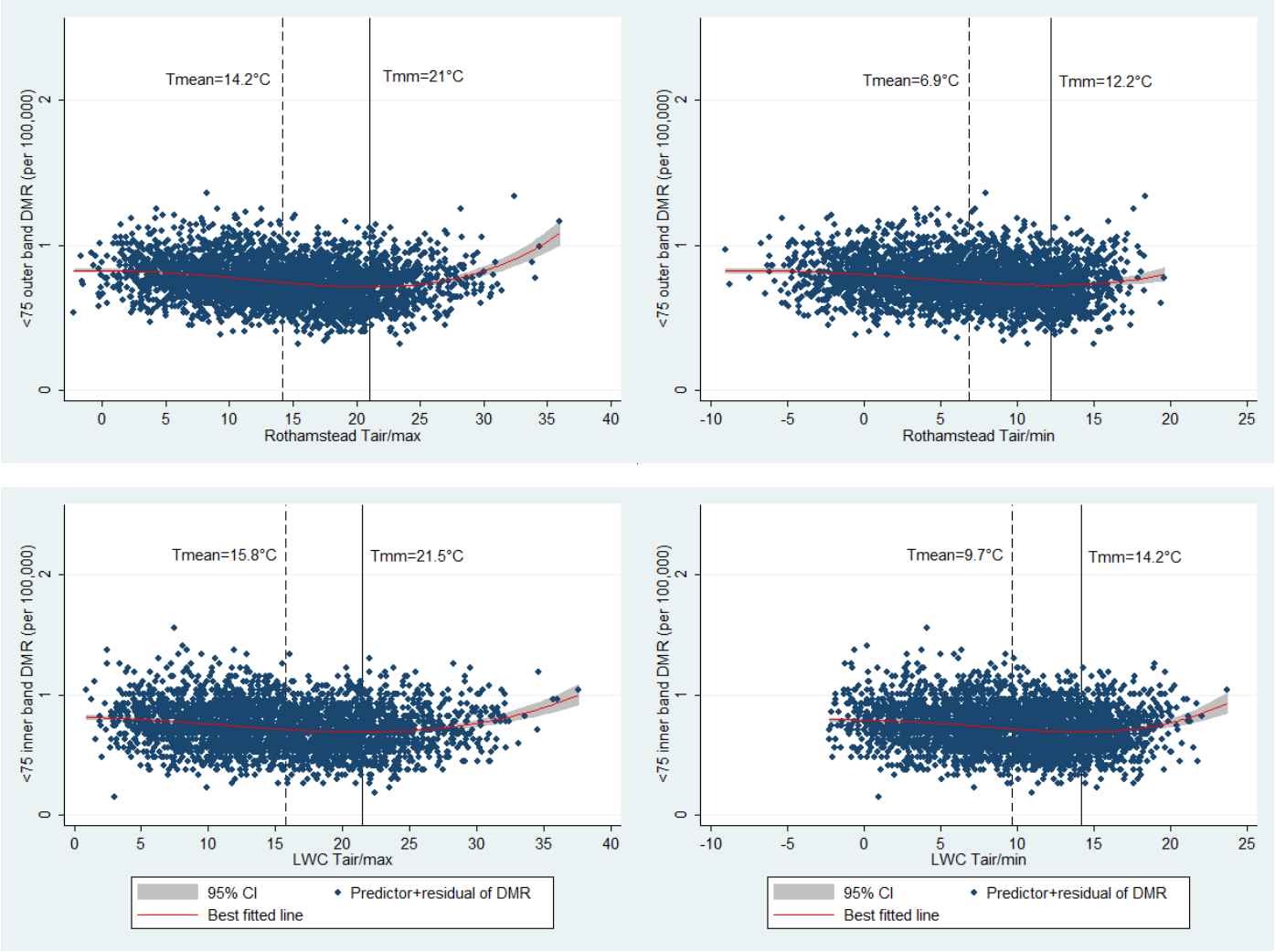
Tmean=14.2°C
Tmm=21°C
<75 outer band DMR (per 100,000)
Rothamstead Tair/max
Tmean=6.9°C
Tmm=12.2°C
<75 outer band DMR (per 100,000)
Rothamstead Tair/min
Tmean=15.8°C
Tmm=21.5°C
<75 inner band DMR (per 100,000)
LWC Tair/max
Tmean=9.7°C
Tmm=14.2°C
<75 inner band DMR (per 100,000)
LWC Tair/min
95% CI
Predictor+residual of DMR
Best fitted line
95% CI
Predictor+residual of DMR
Best fitted line

(b)

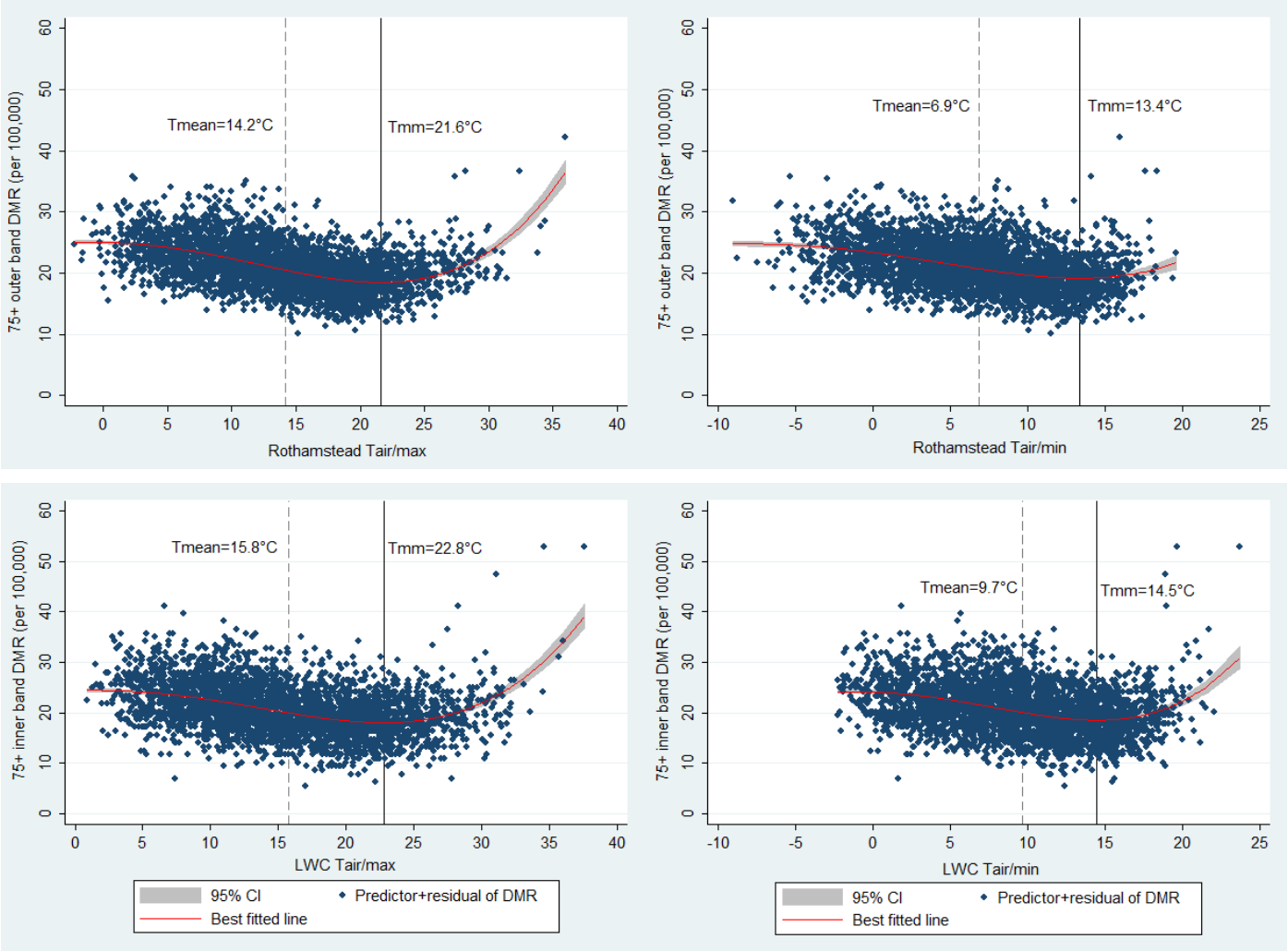

Figure 5.3: Relationships between temperatures and (a) <75 DMR (b) 75+ DMR in outer band and inner band of Greater London, 2001-2009.

West Midlands

Running the FP regression model in STATA, Figure 5.2 (a) illustrates the predictor and residual of DMRs (per 100,000 population) for the <75 populations against temperature for the West Midlands during 2001-2009. The best-fit FP curves are indicated along with the 95% CI for each band. Results for elderly people aged 75+ are shown in Figure 5.2 (b). Edgbaston $T_{air/max}$ and Edgbaston $T_{air/min}$ are associated with the inner band DMRs, and Shawbury $T_{air/max}$ and Shawbury $T_{air/min}$ are associated with the outer band DMRs.

For the <75 populations shown in Figure 5.2 (a), the mean DMR was found to be slightly lower for the inner band (DMR of 1.00 per 100,000 population) than for the outer band (DMR of 1.04/100,000). The non-linear U-shaped relationships between DMRs and $T_{air/max}$ shown in the left panels suggest higher DMRs at lower temperatures (most likely in winter), and the DMRs grow rapidly with increasing temperature after reaching the T_{mm} (most likely in summer). The right panels show that the FP curves for $T_{air/min}$ are relatively flat without a rapid increase above T_{mm}, particularly for the outer band. Curves in Figure 5.2 (b) are as for those shown in Figure 5.2(a), but for the elderly population aged 75+. In general, there is a much higher mean DMR for the elderly population than for the <75 populations. A mean DMR of 21.3/100,000 for the outer band and a mean DMR of 21.91/100,000 for the inner band are found among the elderly populations, approximately 20 times greater than that for the <75 populations. On the hottest day (Edgbaston $T_{air/max}$ = 33.5°C, Shawbury $T_{air/max}$ = 32.8°C), the inner band DMR was 19.3/100,000 and the outer band DMR was 23/100,000. The results indicate that the

significantly higher mortality risk from heat stress for 75+ elderly population than those aged <75 years.

Greater London

Figure 5.3 (a) and (b) illustrate the relationship for DMRs against $T_{air/max}$ and $T_{air/min}$, measured at the LWC and Rothamsted stations for Greater London (2001-2009) for the <75 and 75+ elderly populations, respectively. The LWC $T_{air/max}$ and LWC $T_{air/min}$ are associated with the inner band DMR, and Rothamsted $T_{air/max}$ and $T_{air/min}$ are associated with the outer band DMR. Using the same DMR scale as for the West Midlands, the values of DMR in these relationships become smaller and less scattered. When zooming in using the proper DMR scale, they tend to have more distinct U-shaped curves, compared with the flatter broad U-shaped curves for the West Midlands (Figure 5.2).

For the <75 populations (Figure 5.3a), distinct U-shaped curves are found for DMRs (per 100,000 population) against Rothamsted $T_{air/max}$ (T_{mm}=21°C) in the outer band of Greater London, and DMR against LWC $T_{air/max}$ (T_{mm}=21.5°C) in the inner band. These two curves have distinct T_{mm} turning points and increasing tails above the T_{mm}. the mean DMR for the outer band (0.76/100,000) is found to be similar to that for the inner band (0.73/100,000). For the 75+ elderly population (Figure 5.3b), mean DMR for the outer band is 20.28 per 100,000 population. Mean DMR is slightly lower for the inner band (19.14/100,000). Although the outer band elderly populations are more than doubled than those living in inner band (outer band 308,100; inner band 128,600). The similarity in DMR is mainly caused by the high number of vulnerable elderly populations living in the surrounding outer band.

Extreme DMR outliers

From the curves shown in Figure 5.2 and Figure 5.3, it may be noted that there are DMR data points scattered at lower and higher temperatures. These outliers (extreme high or low values) could lead to lower reliability of the results, and could potentially affect the overall trend of the T-M curves.

In the West Midlands, the DMR data become scattered in the lower and higher temperature zones, particularly when temperatures fall below T_{mean} and above T_{mm}. Indeed, both cold and heat stress could be dominant factors behind the high DMRs. For the 75+ populations, the cold stress appears to have a stronger effect on mortality than heat stress. It could be that these DMR outliers are due to elderly people in the West Midlands experiencing a higher degree of vulnerability to a cold (or mild) climate than to a hot climate. In addition, DMR data for the <75 populations have a wider spread than data for the 75+ populations. In Greater London, the DMR data are less scattered in comparison to the DMRs for the West Midlands.

Interestingly, the 75+ elderly DMRs (Figure 5.3b) are particularly scattered with individual outliers under hot climatic conditions when temperatures rise above T_{mm}. This could imply a relatively higher mortality risk for elderly people living in Greater London. More specifically, outliers for Greater London occurred during the typical heatwave days of 10-13 August 2003. Although several winter DMR outliers are also observed, the summer DMR outliers with temperatures above T_{mm} appear to be more significant in Greater London.

It can be concluded that the decrease in winter mortality may outweigh the increase in summer mortality in the West Midlands. The results agree with the conclusion by the WMPHO (2010). In contrast, the outstanding DMRs in Greater London mostly occurred in summer during a heatwave event. The rapid increases in DMRs under hot climatic conditions could be explained mainly by the additional heat stress, together with other causes (e.g. respiratory and cardiovascular disease) in relation to poor air quality, and this significantly outweighs the decrease in DMRs observed under cold and mild climatic conditions.

T_{mm} (minimum mortality temperature)

Using the command of *fracpred* in FP regression model in STATA, the predicted and residual DMRs were created. By sorting the predicted DMRs into ascending order, the T_{mm} was derived corresponding to the lowest predicted DMR.

The variation in T_{mm} by region, temperature and age group are shown in Figure 5.4. Above $T_{mm,}$ the heat-related mortality increases rapidly. Greater London shows the largest inner band T_{mm} values for 75+ populations with a $T_{air/max}$ of 22.8°C. The T_{mm} for the inner band $T_{air/max}$ in the West Midlands is ~2°C lower than Greater London. It is interesting that the largest outer band T_{mm} for 75+ populations with a Shawbury $T_{air/min}$ 14.9°C occurred in the West Midlands. One possible explanation is that people (in particular elderly people) living in rural areas of the West Midlands can withstand lower temperatures than people living in rural areas around Greater London. As with the lower T_{mm} values for the inner band $T_{air/max}$, the West Midlands has lower T_{mm} for the inner

band $T_{air/min}$ as well. By age, the values of T_{mm} for each region are generally 0.6°C-1.3°C larger for the 75+ populations than for the <75 populations. Overall, the inner band T_{mm} values for Greater London are higher than for the West Midlands. Due to the warmer climate in southern regions, people living in central areas of Greater London can withstand higher temperatures than those living in the central West Midlands, which leads to a larger T_{mm} and lower mortality.

Figure 5.4: Age-specific variations of the T_{mm} for $T_{air/max}$ and $T_{air/min}$ in the outer and inner bands of the West Midlands and Greater London.

5.3.2 Heatwave episode analyses

The age-specific DMRs (<75 and 75+) can be related to temperatures during July and August 2003 for the outer and inner bands of the West Midlands and Greater London.

West Midlands

The first of the three strongest heatwave periods that occurred across the West Midlands occurred in July and the second occurred in August (Figure 5.5). During the most severe heatwave period (4-10 August 2003), a total mortality of 570 and 488 were recorded in the outer and inner bands of the West Midlands, respectively. Over the same time period, about 58-66% of mortality occurred among elderly people aged 75+, with a total mortality in the outer and inner band of 375 and 285 respectively.

For the <75 populations, the correlations between temperatures and DMRs are not as notable as those for the 75+ populations (Figure 5.5 (c) and (d)). On 15 July 2003, a peak Shawbury $T_{air/max}$ (29.5°C) was observed and the outer band experienced an immediate same-day peak in DMR of 24/100,000 (corresponding to 58 deaths) and a further increasing DMR of 25/100,000 (corresponding to 59 deaths) the day after. For the inner band on 15 July, a peak in the Edgbaston $T_{air/max}$ (30.8°C) and a peak in inner band DMR (~27/100,000, corresponding to 53 deaths) were positively correlated and occurred on same day. The peak in outer band DMR (27.3/100,000) on 10 August demonstrated a positive correlation with the highest Shawbury $T_{air/max}$ of 32°C on 9 August 2003.

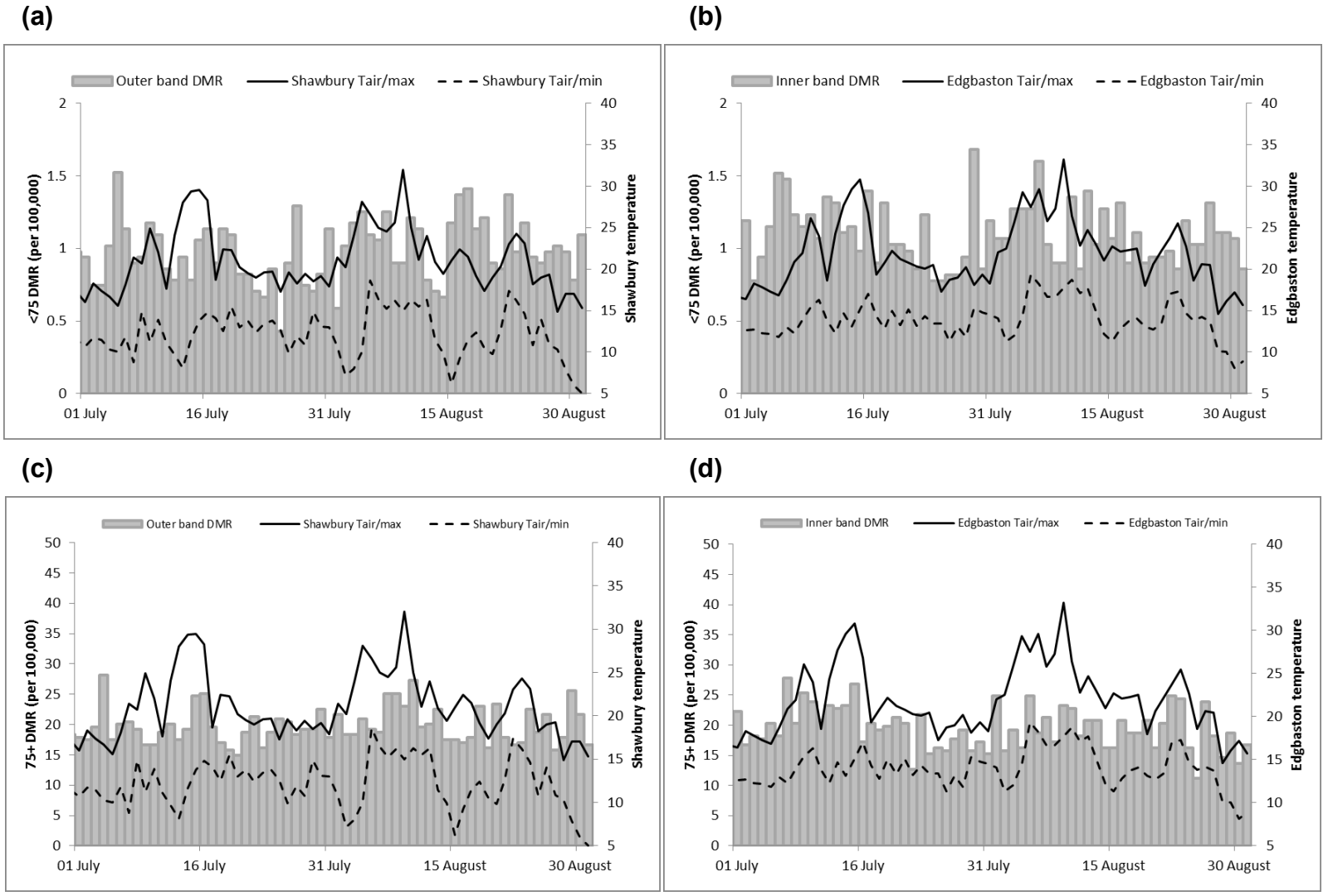

Figure 5.5: <75 DMRs and temperatures in (a) outer band and (b) inner band; 75+ DMRs and temperatures in (c) outer band and (d) inner band for the West Midland, JJA 2003.

Greater London

Compare to the heatwave analyses for the West Midlands, results for Greater London are far more interesting, as shown in Figure 5.6. Even for the broadly aged <75 populations, the 2003 August heatwave event (6-11 August 2003) was much more significant, although there were relatively minor signals of a heatwave in July. All-age mortality for the outer and inner bands of Greater London of 850 and 442 were recorded, respectively. Approximately 65%-70% of mortality occurred among the elderly population aged 75+, with a total mortality of 586 and 286 in the 75+ age group recorded in the outer and inner bands, respectively. In the outer band, a peak in Rothamsted $T_{air/max}$ of 36°C was recorded on 10 August 2003. A peak in <75 DMR of 1.3 was observed on the next day. Similar trends were also observed in the inner band for the <75 population.

More interestingly, there was also a strong correlation between $T_{air/max}$ and DMRs for the 75+ elderly populations. On a typical hot day (10 August 2003), the inner band DMR reached as high as 53, followed by continuously high outer band DMR for an additional 3 days. When $T_{air/max}$ becomes extremely high, the DMR also increases, but declines rapidly once $T_{air/max}$ begins to decrease.

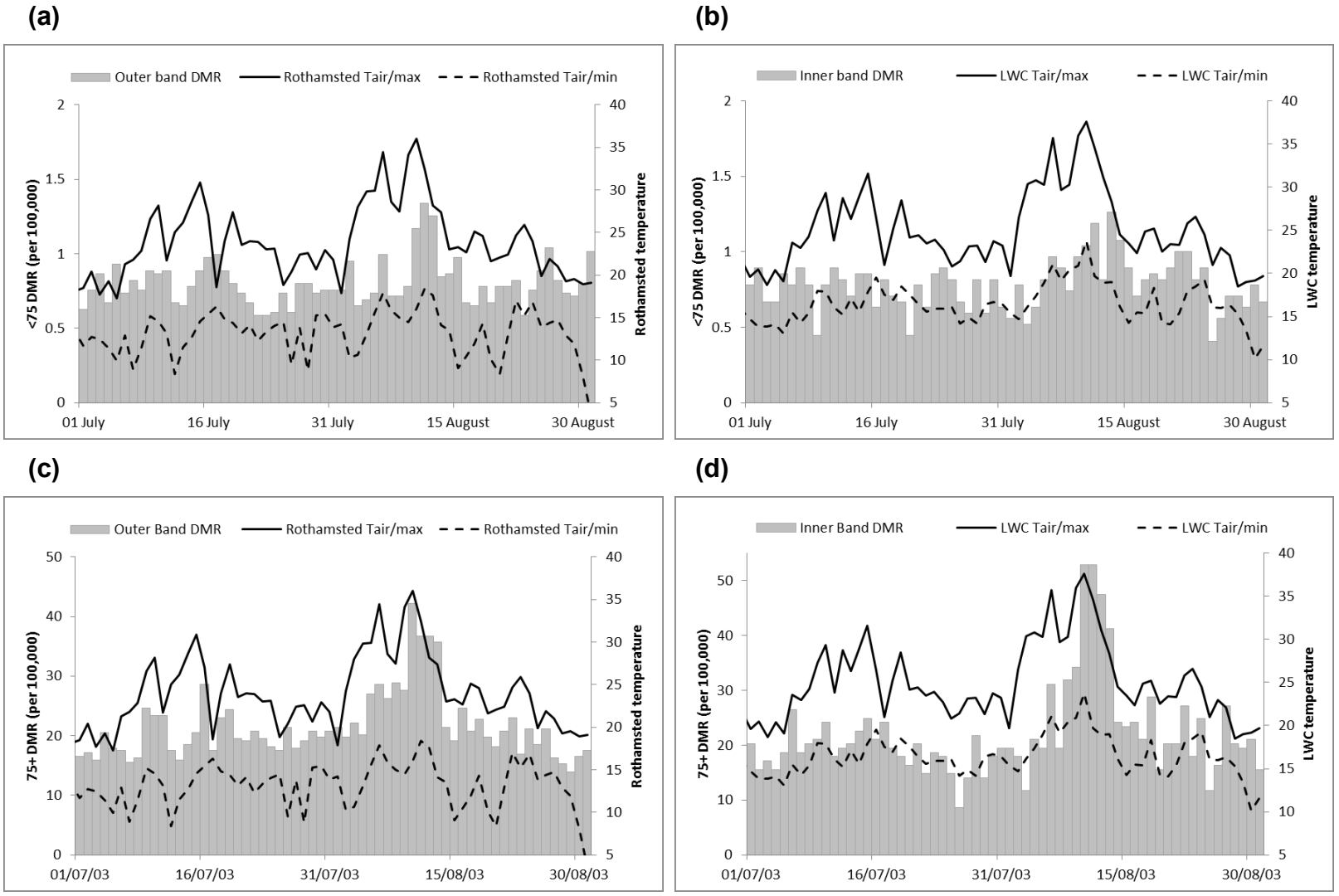

Figure 5.6: <75 DMRs and temperatures in (a) outer band and (b) inner band; 75+ DMRs and temperatures in (c) outer band and (d) inner band for Greater London, JJA 2003.

Harvesting and lag effects

Harvesting effect is typically identified as the missing deaths following a heatwave event. Toulemon and Barbieri (2008) proposed two hypotheses: firstly, the heatwave killed indiscriminately in the overall population; secondly, owing to unobserved heterogeneity, those who died during the heat wave had a poor inherent health status before August 2003. Thus, without the heat wave they would have died sooner than those in the same age and sex group who survived. There has been observed a reduction in DMR during the subsequent days after a heatwave event, as shown in Figure 5.6 (c) and (d) which may be explained as compensatory reduction in mortality suggesting the heatwave has impacts on people whose health is already compromised that they would have died in the short-time (Huynen et al., 2001).

The lag times due to thermal mass for the strongest temperature-mortality correlations range from the same day up to 3 days following a heatwave event (Basu and Samet, 2002). In the West Midlands, peaks in DMRs corresponded to peaks in temperatures with a same-day lag (DMR and $T_{air/max}$ peak on 15 July) and 1-day lag (DMR peak on 10 August, $T_{air/max}$ peak on 9 August). In the outer band of Greater London, the correlations between 75+ DMRs and the Rothamsted $T_{air/max}$ were strongest on the same day (10 August 2003), with a peak in the Rothamsted $T_{air/max}$ of 36°C and a peak in DMR of 42.2 per 100,000 population. For the inner band, the correlations between DMRs and the LWC $T_{air/max}$ were strongest for same-day (or 1-day) lag times. The peak in LWC $T_{air/max}$ of 37.6°C occurred on 10 August, with an <75 DMR peak of 1.2 on 11 August and

another higher peak of 1.3 on 13 August, and 75+ DMR peak of ~53/100,000 on 11-12 August.

Clarke (1972) found that the heat-related DMR during heatwaves is generally higher in urban area than for the surrounding area, due to climate modification dominated by urbanisation. In this chapter, London's results showed that the elderly populations in the inner band could be significantly affected by heatwaves, resulting in a significant increase in mortality. Overall, Greater London is classed as urban, although there is no explicit urban-rural boundary. Therefore, both outer and inner bands displayed very strong correlations between heat-related DMR and temperature. Here, the correlations for the West Midlands were not as strong as those for Greater London. Possible reasons could be the large variations.

5.3.3 Climate change projections of heatwaves

Heatwave projections were produced up to the 2080s using the UKCP09 Climate Change Projections. In this study, the UKCP09 WG was run for each 30-year period (2020s, 2050s and 2080s) under the low, medium and high emission scenarios for Edgbaston (Grid cell ID: 4050290) to provide a projection of future heatwave periods. The WG variable used was heatwave. The TD was applied to the WG outputs afterwards, providing the number of heatwave periods when the heatwave threshold for the West Midlands ($T_{air/max}$ = 30°C and $T_{air/min}$ = 15°C) was exceeded. Table 5.1 is the UKCP09 outputs of projected heatwave periods ($T_{air/max}$ >30°C and $T_{air/min}$ >15°C for at least two consecutive days) corresponding to the 1961-1990 baseline period, showing

the projected summer heatwaves (JJA) in Edgbaston up to the 2080s under low, medium and high emission scenarios.

Table 5.1: UKCP09 WG TD outputs of projected heatwave periods corresponding to the 1961-1990 baseline period.

Time Period Emission Scenario	2020s Low	2050s Low	2080s Low	2020s Medium	2050s Medium	2080s Medium	2020s High	2050s High	2080s High
June	1.6	2.2	2.9	1.6	2.2	4.3	1.4	3.0	5.2
July	0.9	3.1	4.6	0.9	4.2	9.3	0.9	5.1	11.6
August	1.0	2.7	4.1	0.3	3.5	7.9	0.6	3.1	10.7

By the 2080s, a significant increase in the number of heatwaves was projected under medium (a) and high emission scenarios (Figure 5.7b). Edgbaston (Grid Cell ID: 4050290) is likely to experience an average of four heatwaves in June, nine in July and eight in August by the 2080s under the medium emission scenario. A higher occurrence of heatwaves was predicted under the high emission scenario. In this case, there is an average of five heatwaves in June, eleven in July and ten in August by the 2080s. Due to the increased summer temperatures, the UHI may affect the number of heatwave days, potentially raising the heat-related mortality risk. By analysing the number of heatwave days with $T_{air/max}$ exceeding 30°C during JJA 2001-2009, it was found that there were four heatwave days in Shawbury and six heatwave days in Edgbaston. Urban areas suffer more heatwave days than the surrounding rural areas, potentially resulting in an increase in urban mortality due to heat stress. Fisher (2009) estimated

that the balance between winter and summer mortality under the UKCP09 medium emission scenario will change as follows through the twenty first century in the West Midlands:

	2020s	2050s	2080s
Winter mortality	-0.8%	-2.7%	-4.6%
Summer mortality	-0.3%	-0.3%	+0.5%

Overall, mortality decreases by 255 per year by 2020s, 693 by 2050s and 912 by the 2080s as temperatures increase. During summer in the years 2001-2009, one heatwave occurred in June, eight in July and three in August. Of these heatwaves, only one heatwave in the outer band occurred in July and one in August. In the inner band, there were five in July and one in August. The UKCP09 projections for heatwave days demonstrate that Edgbaston, being located in the urban area, is likely to have a total of 19 (38) heatwave days over JJA under the medium (high) emission scenario up to the 2080s.The main limitation of TD is that it can only be used on the WG outputs, and only works under outputs configured with 100 probabilistic samples of 30-year daily time-scale datasets. The TD can provide the number and exceedances of events, but only one event can be recorded each time. Overlaps between events cannot be identified.

(a)

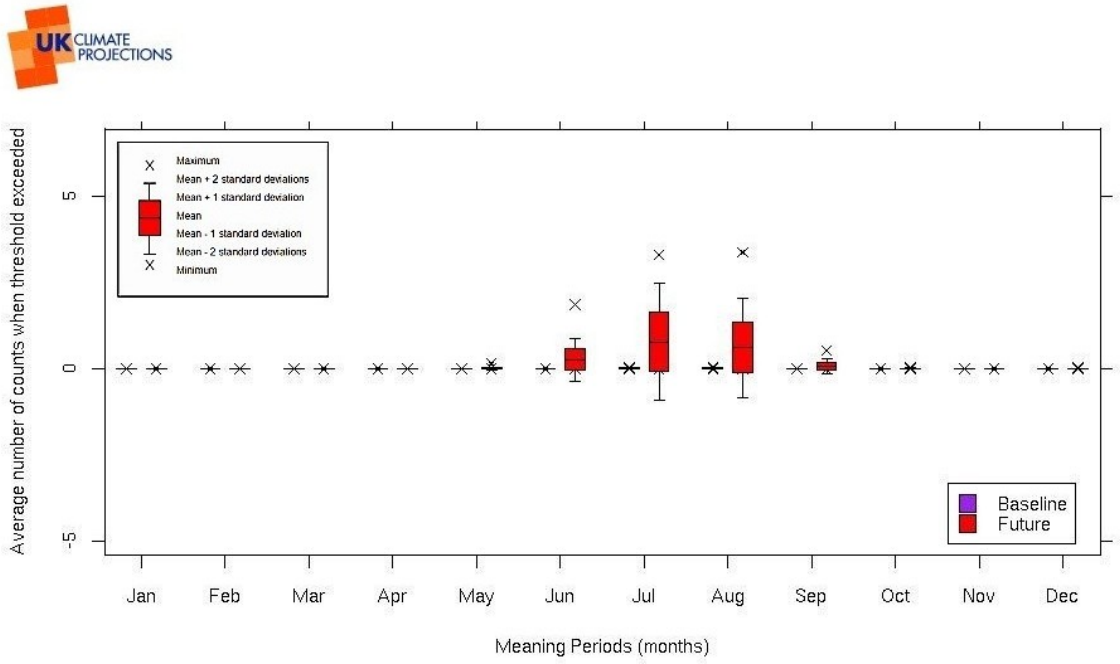

(b)

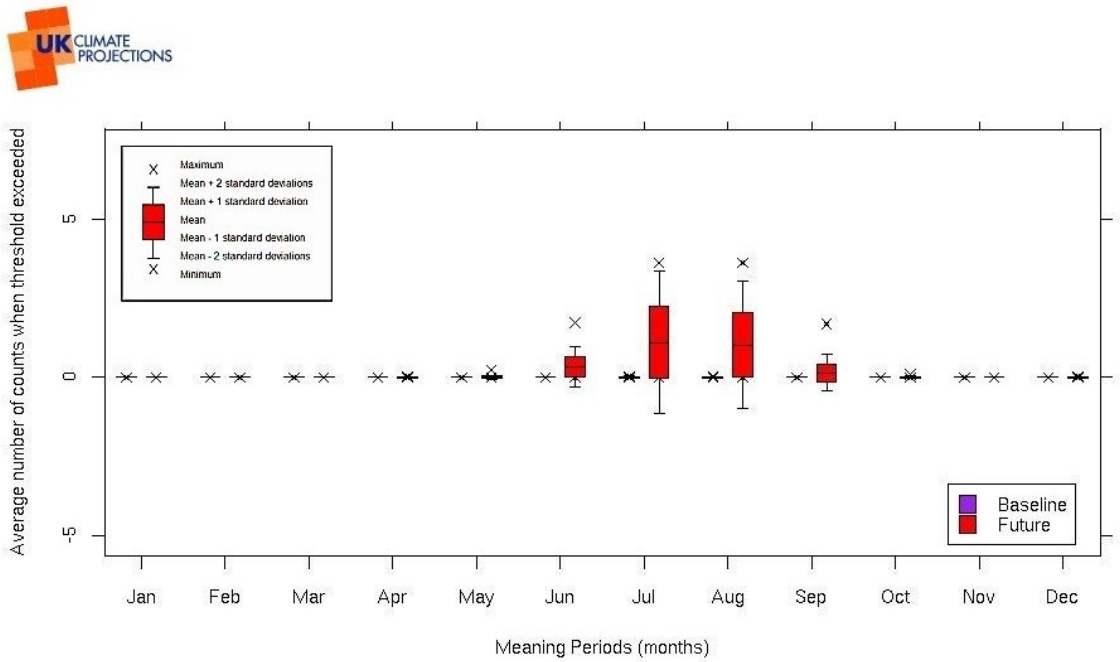

Figure 5.7: Future projections of heatwave periods in the 2080s (2070-2099), under the (a) medium and (b) high emission scenario, for a 5 km grid cell in Edgbaston.

5.4 Conclusions

Using the FP regression model, U-shaped relationships between temperatures and DMRs (<75 and 75+) between 2001 and 2009 were found to be significant for the West Midlands and Greater London, particularly during the typical heatwave months, JJA 2003. The high and low temperature tails of the curves demonstrated the effect on mortality under cold and hot climatic conditions. Outliers and non-random variations could be inspected in residual plots (El-Zein et al., 2004), the DMR outliers identified in Figure 5.2 and Figure 5.3 mostly lay in the above-T_{mm} zone. Although no in depth statistical analyses were conducted for these individual DMR outliers, similar analyses of the mortality and temperature conducted by El-Zein et al. (2004) have proven that neither the coefficients of the below-T_{mm} variable nor the significance of any variables were affected when the outliers were dropped. In this thesis, since these outliers all occurred on typical hot days in 2003, they provide valuable information about the association between high temperature and high mortality, and thus should be retained in the FP model as an indication of the extreme mortality risk.

In the West Midlands, the decreased winter mortality appeared to outweigh the increased summer mortality, although elderly people aged 75+ living in cities are expected to be particularly vulnerable to heat stress. In Greater London, the increased summer mortality was more significant than the decreased winter mortality, particular above the T_{mm}. Several DMR outliers observed under hot climatic conditions were confirmed as arising as a result of heatwave events. The comparison of T_{mm} by region, temperature and age showed the resilience of the Greater London urban residents to

higher temperatures. Rural residents in the West Midlands are better able to withstand lower temperatures.

Both regions experienced the heatwave event of 2003, during 4-10 August in the West Midlands and during 6-11 August in Greater London. Analysis of this particular event confirmed the significance of extreme high temperatures on the significant increase in mortality observed during the heatwave. However, there were differences in heatwave impact between different regions. Associations between $T_{air/max}$ and DMR were strongest with lag times ranging from the same day up to 1-3 days in the West Midlands and Greater London. Significant increases in mortality and temperature were followed by a rapid decrease in mortality several days after the peak, followed by a return to ordinary mortality levels.

To examine whether the T-M relationships are affected by the periods chosen in this study, an analysis for even and odd years during the 2001-2009 period was conducted for the West Midlands. The results (data not shown) indicated that there were no significant effects dependent on the chosen year. Similar patterns and T_{mm} values were found to those computed throughout the 9-year study period. The T-M relationships for Greater London were modelled directly using the available 9-year data (2001-2009) rather than by testing the impact of effects related to specific years within that time period.

Chapter 6 The aUHI and heat-related mortality: West Midlands and Greater London

6.1 Introduction

Most previous studies have focused on the potential impacts of climate change and heatwaves on health, highlighting the relationship between the UHI and land cover/use, but mostly ignoring UHI-related mortality.

The literature review has identified a highly relevant study by which investigates the UHI and its impact on heatwaves and human health in Shanghai. The number of hot days with $T_{air/max}$ exceeding 35°C was associated with 11 urban, suburban and exurban (or rural) stations. Hot days occurred with higher frequency in urban stations and with lower frequency in the surrounding stations. In addition, heatwave duration was closely related to UHI, with the longest duration (i.e. 10+ consecutive hot days) occurring in the urban area. Interestingly, the findings suggest a relationship between the UHII and population-adjusted excess mortality rate (Figure 6.1). This plot indicates a significant correlation between UHII and excess mortality for the 1998 heatwave in particular. Correlation can also be discerned for the 2003 heatwave. This implies that the impact of UHI on mortality can be exacerbated during extreme hot weather. The urban mortality rate reached ~27.3 per 100,000 population, while the mortality rate in the surrounding area was ~7 per 100,000 population.

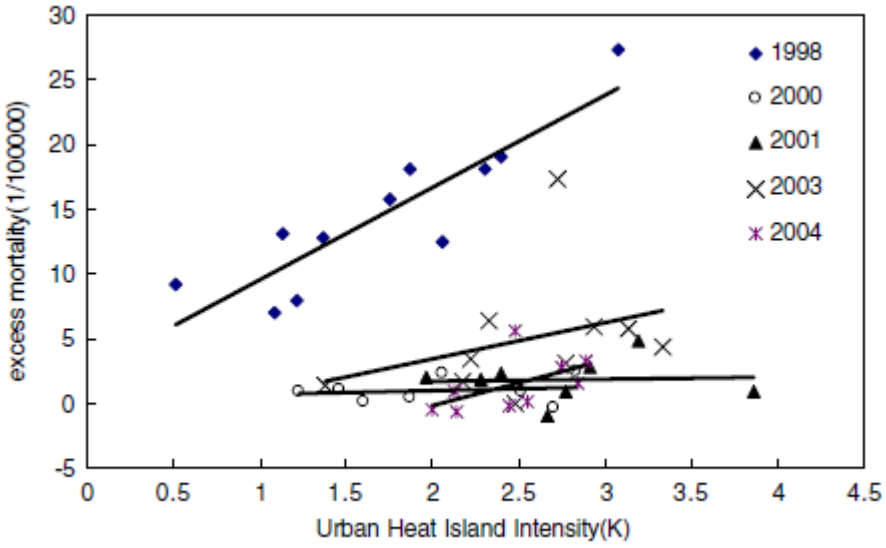

Figure 6.1: Excess mortality rate and the UHII for heatwaves in Shanghai (Tan et al., 2010).

Such findings have encouraged researchers to pay more attentions to the impacts of UHI on heatwaves and health. For this purpose, this chapter aims to quantify the differential responses to the T_{air}-related aUHI on heat-related mortality rate in summer months between the urban and rural residents across the West Midlands and Greater London, respectively.

6.2 Data and methodology

6.2.1 Study areas and data

As described in Sections 3.1.1 and 3.1.2, the West Midlands and Greater London were chosen as the study areas in this chapter. For each region, two bands were selected to represent the exclusive regional datasets. For the West Midlands, the outer band is the geographical difference between the West Midlands GOR and the MC. The Shawbury station is used to represent the rural area. The inner band is the MC including 7 metropolitan boroughs. The Edgbaston station is used to represent the urban area. The outer and inner bands for Greater London are graphically illustrated in Figure 3.2(a). The LWC station and the Rothamsted station represent the urban and rural areas, respectively.

Daily mortality data for the West Midlands GOR, the MC and Birmingham were requested from the WMPHO. As described in Section 3.6.1, the original requested data were broken down by age (0-74 and 75+), sex (female and male) and disease (all-cause, circulatory and respiratory diseases) for each geographical area. Daily mortality data for Greater London were requested from the ONS. As described in Section 3.6.2, the requested raw data were broken down by the MSOA, age, sex and disease (all-cause, cardiovascular and respiratory diseases).

To represent the mortality data scaled by population size, the population was divided by the daily mortality to give the DMR. The corresponding population estimates for each age group and each band are listed in Table 3.2 for the West Midlands and Greater

London, respectively. This chapter uses the mortality data in the <75 and 75+ age groups.

The MIDAS T_{air} (details in Section 3.3) measured at the four weather stations (Edgbaston and Shawbury; LWC and Rothamsted) generally varied in phase. However, the low number of appropriate weather stations in the outer band makes it different to estimate the precise aUHII.

Referring to Section 3.4, Lamb (1972) and Jenkinson and Collinson (1977) provide Lambs daily synoptic indices. Eleven weather types (A, C, SW, W, NW, S, N, SE, U, NE and E weather types) were initially used to associate with night-time aUHII. The LWTs were subsequently used to stratify the relationships between aUHII and DMR during JJA 2001-2009.

6.2.2 Methodology

In this chapter, the relationships between the aUHII and the DMR for the outer band and inner band in the West Midlands and Greater London, as shown in Figure 3.1(a) and Figure 3.2(a), are studied to quantify the impact of aUHI on heat-related mortality. Referring to the calculation of the UHII in Section 4.4, the aUHII used in this chapter is defined as the T_{air} difference between the urban area (the urban weather stations at Edgbaston and LWC) and the rural area (the reference rural weather stations at Shawbury and Rothamsted).

Bin-average analyses in linear regression

Tolman (1998) discussed the effects of observation errors in linear regression and bin-averaged (BA) analyses using wind speeds, and found that a conventional linear regression systematically underestimates the slope of trend line and overestimates the random model errors. As BA analysis is sensitive to observation errors, error correction is recommended. In this chapter, the BA validation analysis was applied to the raw DMR data, to investigate the relationship between aUHI and mortality by averaging the datasets into 0.5°C aUHII intervals. The Paired-Samples T-test and Pearson correlation were also computed to estimate the significance level and correlation.

Corresponding to the incident of the LWTs associated with UHIs (Chapter 4), an additional analysis of the urban heating and DMR stratified by LWT was conducted to unify the interrelationship among the LWTs, UHI and mortality. Firstly, the 11 main LWTs were associated with mean aUHII (positive values only, for summer heat-related mortality) between 2001 and 2009. Secondly, top 5 most frequently occurring LWTs ([A], [C], [SW], [W] and [S]) which also corresponds to high night-time aUHII, were selected for further analyses of LWT-specific UHI-mortality relationship in the West Midlands and Greater London.

6.3 Results and discussion

As the relationship between local temperature and mortality has been extensively investigated in previous studies (Section 2.2), in Chapter 5 of this thesis, the relationship was analysed into outer and inner bands for the West Midlands and Greater London. It has been confirmed that high/low temperatures have direct effects on mortality, but the effect strength depends upon age structure (old people more vulnerable), location and other potential confounding factor (e.g. residents' adaption level to varied weather, socio-economic status etc.). On the basis of temperature-related effects on regional mortality, the following analyses try to look into the potential effects of the additional urban heating on urban and rural populations respectively, and examine if the elevated aUHI leads to increasing mortality rate.

6.3.1 The aUHI and mortality rate (West Midlands, JJA 2001-2009)

Figure 6.2 illustrates the age-specific DMR against aUHII for the outer and inner bands of the West Midlands during JJA, 2001-2009. The slope of the linear regression line is interpreted as DMR per 100,000 population per degree Celsius (°C) of the aUHII (Edgbaston-Shawbury). Overall, examination of the impact of the UHI on heat-related mortality demonstrates an increasing trend in the relationship between all-cause DMR and the aUHII in summer. Although these trends are not statistically significant using Pearson correlation (p>0.05) and the correlations are quite weak, the increasing trends give ideas about the impact of aUHI on DMR, leading to use BA analysis to average bias in each 0.5°C aUHII interval. The increased summer DMR is mainly due to the

increased urban summer temperature. As the aUHII increases, it implies that the mortality rates in warmer urban areas are higher than those in the rural areas. As a whole, the elevated aUHI may have very minor effect on DMR aged <75 years. Digging into the very elderly populations aged 75+, it can be found that the aUHII-induced DMRs are significantly higher than the younger <75 age group. The linear regression slope may indicate the strength of the impact of aUHII on the DMR, the slope is particularly steeper for the 75+ populations living within the inner band.

Figure 6.2 (b) implies that each 1°C increase in aUHII will cause extra daily mortality of 0.3 (~27 deaths per summer). In other words, each 2.8°C increase in aUHII will cause one extra daily death per 100,000 population. On average, the aUHI exacerbates the summer DMRs, particularly for the 75+ very elderly populations living within the inner band, i.e. the West Midlands MC.

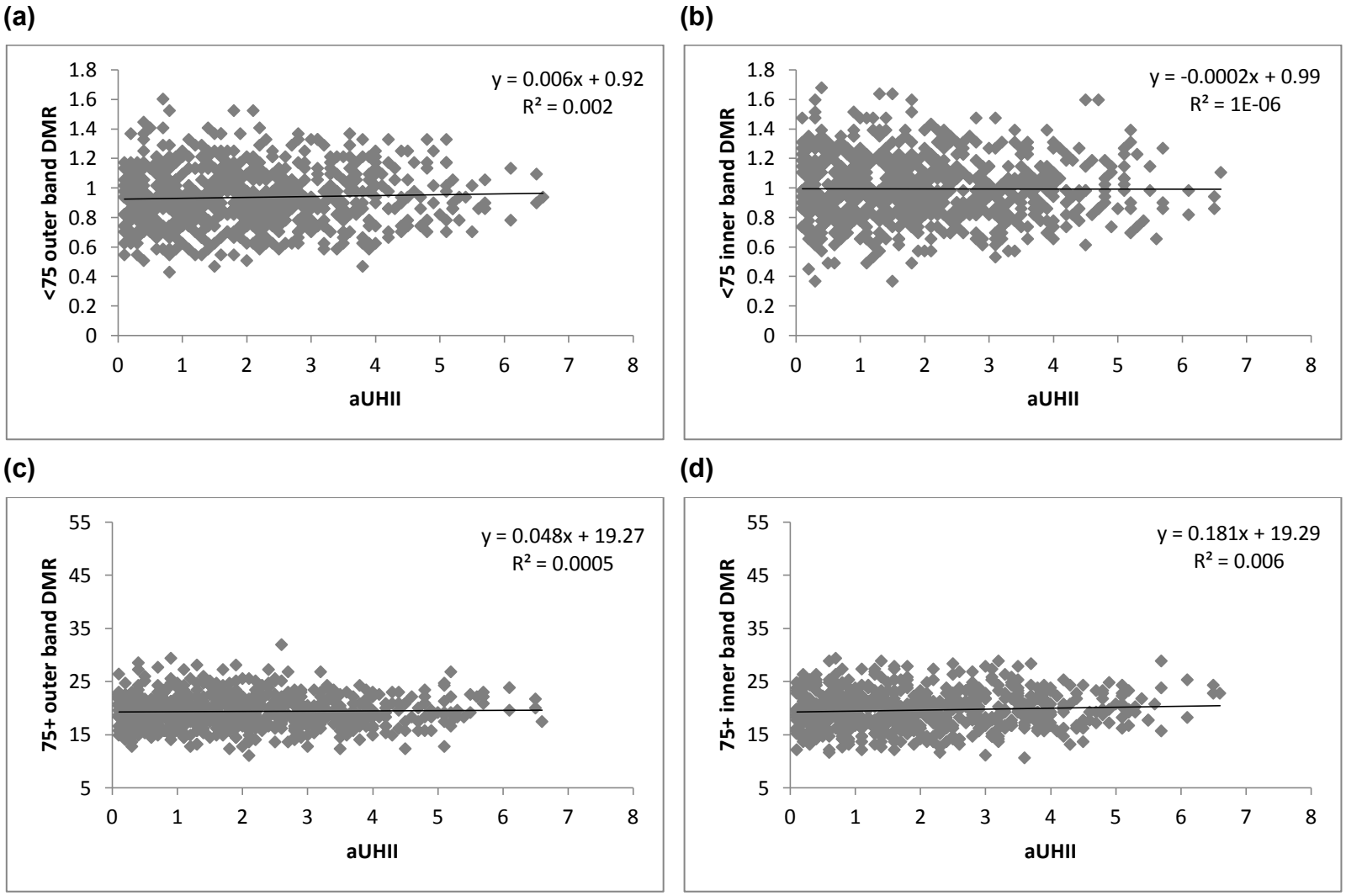

Figure 6.2: Age- and band-specific DMRs (per 100,000 population) and aUHII (Edgbaston-Shawbury) in the West Midlands, JJA 2001-2009.

BA analyses (West Midlands, JJA 2001-2009)

The BA method in linear regression was used to bin the long-term raw observations during JJA 2001-2009 in 0.5°C aUHII interval. Data binning is mainly for bin-averaging the biases and reducing the effect of minor observation errors. A BA analysis requires the choice of a bin width and minimum number of data per bin (Tolman, 1998). According to data circumstances, each BA value includes at least 10 data points in this study.

Figure 6.3 illustrates the bin-averaged relationships between <75 and 75+ DMRs (per 100,000 population) and the aUHII in each 0.5°C interval for the outer band and inner band of the West Midlands. Statistical test confirms that the <75 outer band DMR is significantly correlated with the aUHII at the 0.05 level (p<0.05). Due to the research core of urban heating on mortality, only positive aUHII values were used to analyse the relationship between aUHII and DMR. In the plots, the aUHII labelled as 0.5°C is in fact in the range 0.1-0.5C, and the aUHII labelled as 1C is in the range 0.6°C-1°C. Extreme aUHII values above 5C are averaged entirely and labelled as 5.5°C. The most frequent aUHII was in the range 0.1°C-1°C. Up to the aUHII of 2.5°C, the occurrence covers 67% of the total 666 days.

(a)

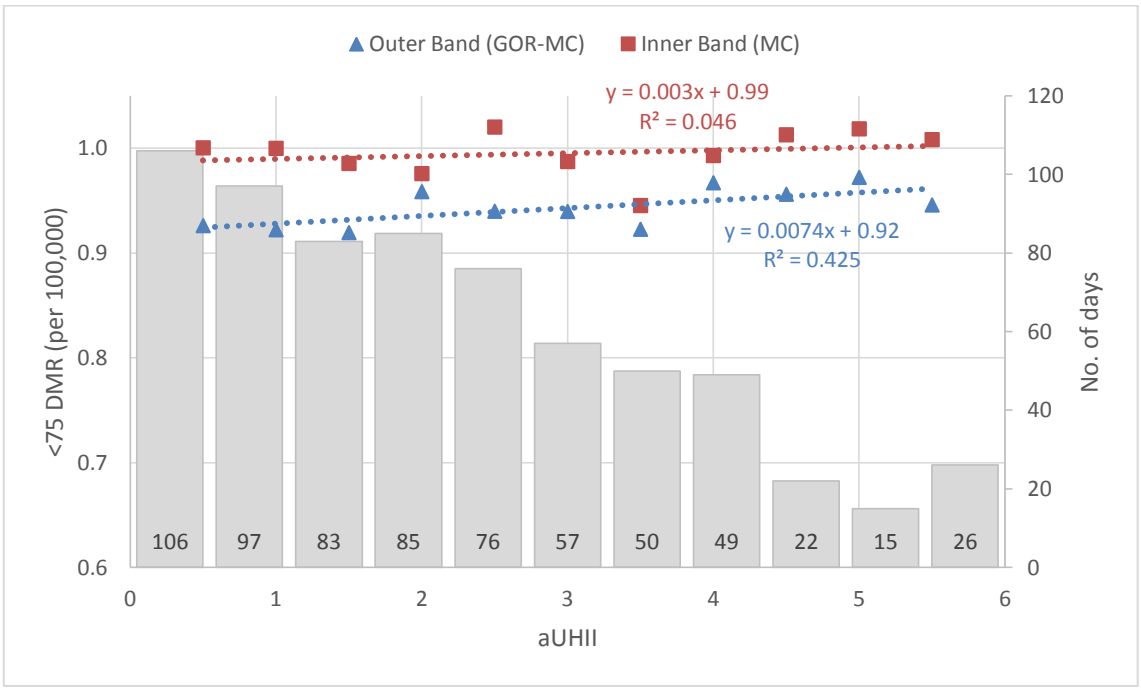

(b)

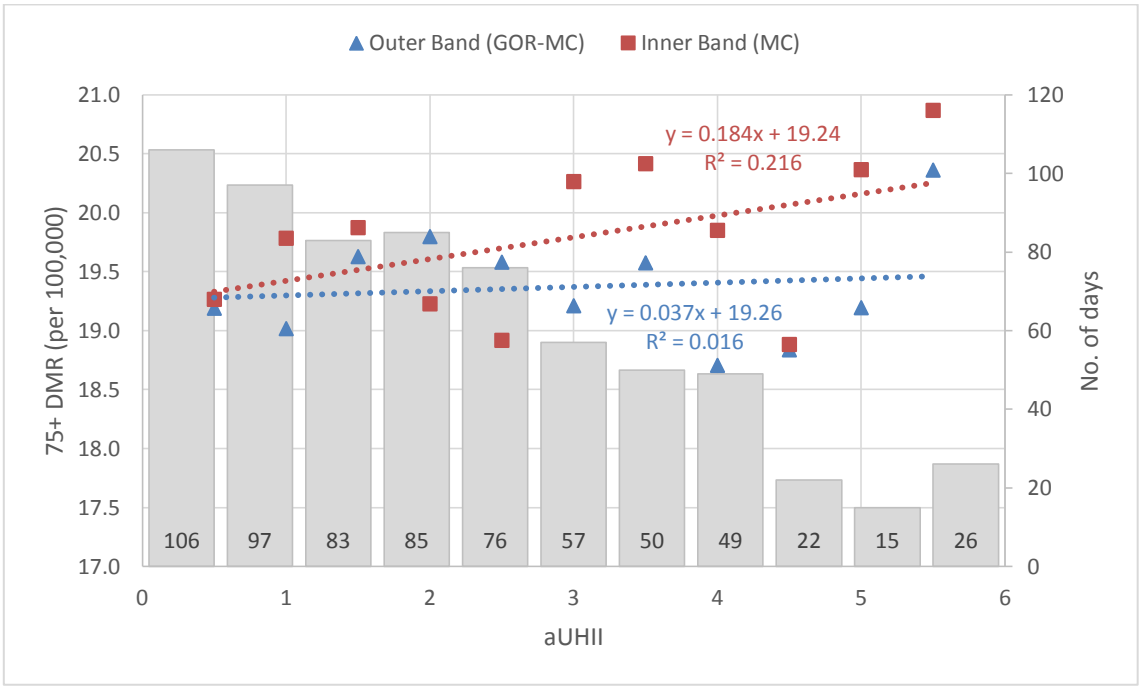

Figure 6.3: Bin-averaged analyses of the relationship between age-specific DMRs and aUHII (Edgbaston-Shawbury) for populations aged (a) <75 and (b) 75+ in the West Midlands, JJA 2001-2009.

As shown in Figure 6.3 (a) and (b), the inner band DMRs are consistently higher than the outer band DMRs, for both younger <75 and older 75+ age groups. The findings agree with the expectation that urban residents may experience higher mortality risk as a result of the elevated aUHI effect. Possible reasons could be the densely built-up areas, air pollutant emissions from anthropogenic and commercial purposes. It is particularly interesting that the inner band DMR for 75+ populations increases sharply with the elevated aUHI effect (Figure 6.3b), implying that each 1°C increase in aUHII will cause an extra daily mortality of ~0.4 (equivalent to 33 extra deaths per summer) in the inner band for the West Midlands. In other words, each ~2.8°C increase in aUHII will cause a unit increase in daily mortality in the West Midlands metropolitan region.

Over the study period of JJA 2001-2009, there were a total of 19,748 daily deaths aged <75 in the outer band, and 19,829 in the inner band. The total 75+ daily mortality was 37,412 in the outer band and 32,085 in the inner band. In view of crude mortality, there was similar mortality distribution among <75 populations, but there was over 5,000 more 75+ daily deaths in the outer band. However, the DMR was calculated on a scale of population estimates, the final higher inner band DMRs could be dominated by the smaller inner band population base (see Table 6.4).

In general, the effect of elevated aUHII on mortality for the age group <75 is minor (Figure 6.3a). However, the extremely strong aUHI effect may cause significant increase in DMRs for very elderly residents living in central area of the West Midlands, particularly when the aUHII exceeds 4.5°C (Figure 6.3b).

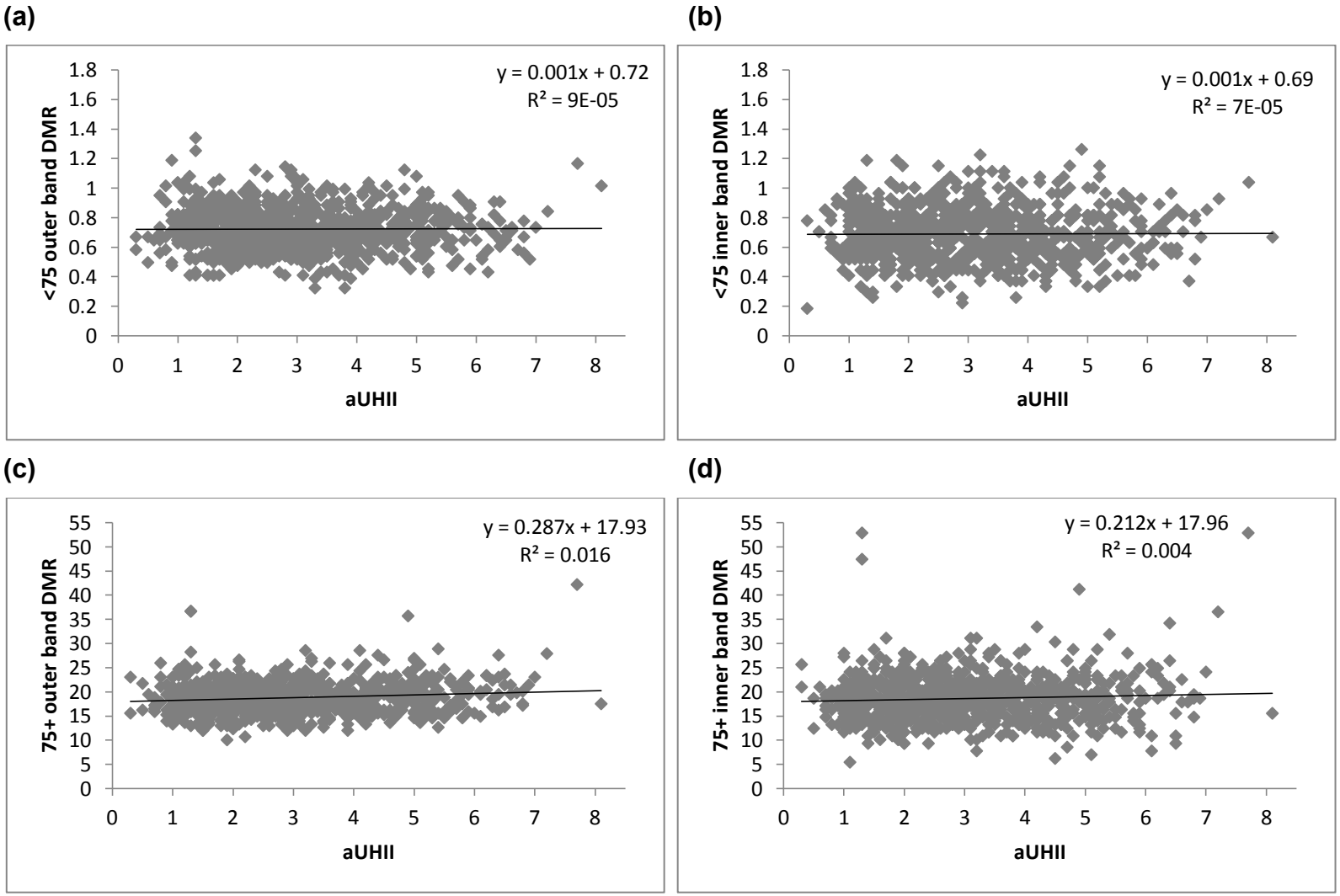

Figure 6.4: Age- and band-specific DMRs (per 100,000 population) and aUHII (LWC-Rothamsted) in Greater London, JJA 2001-2009.

6.3.2 The aUHI and mortality rate (Greater London, JJA 2001-2009)

Figure 6.4 illustrates the age-specific all-cause DMRs against aUHII (LWC-Rothamsted) for the outer and inner bands of Greater London during JJA 2001-2009. The slope of the linear regression line is interpreted as DMR per 100,000 population per °C of the aUHII. Overall, the examination of the aUHI impact on heat-related mortality demonstrates a positive correlation between 75+ DMRs and the aUHII in summer (Figure 6.4 (b) and (d)), except the relationships for <75 age group which indicate very minor effect (Figure 6.4 (a) and (c)).

The DMRs for the populations aged 75+ are much higher compared with those aged <75. As shown in Figure 6.4 (b), each 1°C increase in outer band (with a mid-2009 75+ population of 0.31 million) aUHII will cause an additional daily mortality of ~0.9 (equivalent to 81 deaths each summer), and each 1.1°C increase in aUHII will cause one extra daily death. In the inner band with a mid-2009 75+ population of 0.13 million (Figure 6.4d), each 1°C increase in aUHII will cause an additional daily mortality of ~0.3 (equivalent to 25 deaths each summer), implying that each 3.7°C increase in aUHII will cause one extra daily death. It is therefore expected that increases in aUHII will have a more pronounced effect on rural elderly residents than on urban residents.

BA analyses (Greater London, JJA 2001-2009)

Some particularly unusual biases can be observed among 75+ elderly populations, as shown in Figure 6.4. Some occurred in the zone of lower aUHII and some in the zone of higher aUHII. These outliers might be caused by a single higher daytime urban temperature or a lower rural temperature. Alternatively, they may be due to observation errors. A BA analysis was performed to average the DMR data into bins. For the long-term analyses for Greater London during JJA 2001-2009, the raw DMR data were bin-averaged into each 0.5°C aUHII interval, and each BA value included at least 10 data points. Only positive aUHII values were used to indicate urban heating. The most frequent aUHII range is between 1.6°C and 2.5°C, accounting for 13.3%-14.2% of a total of 828 days.

After bin-averaging, Figure 6.5 illustrates the relationship between the <75 and 75+ DMRs (per 100,000 population) and the aUHII in each 0.5°C interval for the outer and inner band of Greater London. Statistical analysis confirms that the 75+ outer band DMR is significantly correlation with the aUHII at the 0.05 level (p=0.05), with a relatively strong correlation r>0.6.

(a)

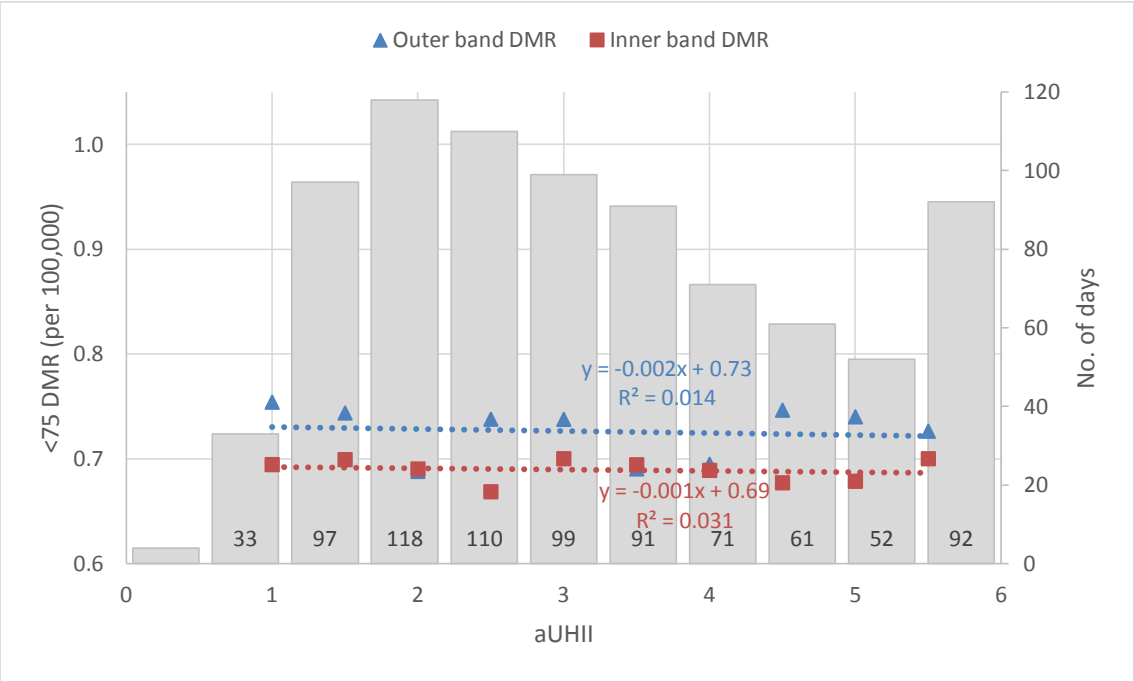

(b)

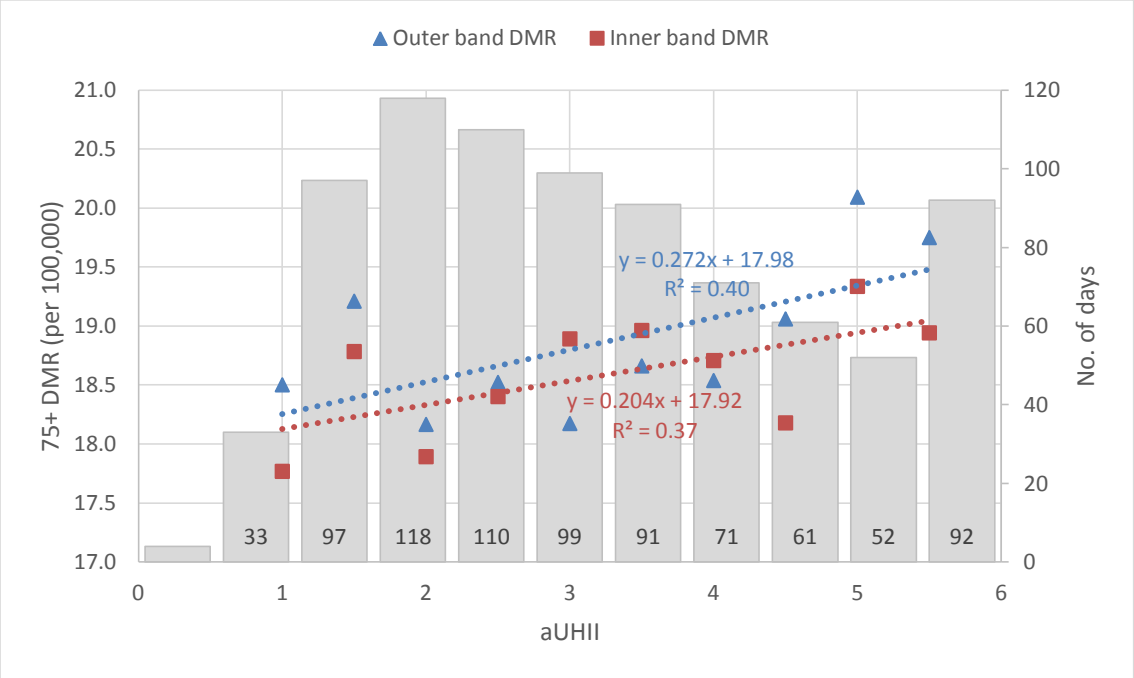

Figure 6.5: Bin-averaged analyses of the relationship between age-specific DMRs and aUHII (LWC-Rothamsted) for populations aged (a) <75 and (b) 75+ in Greater London, JJA 2001-2009.

For the <75 populations, the outer band DMRs are consistently higher than the inner band DMRs (the mean outer band DMR is 0.72/100,000 compared to the mean inner band DMR of 0.69/100,000). Figure 6.5(a) demonstrate the negligible effect of aUHI on DMR for the relatively younger age group <75 years. As shown in Figure 6.5(b) for the 75+ populations, each 1C increase in the outer band aUHII will cause extra daily mortality of ~0.8 (equivalent to 77 deaths each summer), i.e. each 1.2C increase in aUHII will cause one extra daily death. In the inner band, each 1°C increase in aUHII will cause an additional daily mortality of ~0.3 (equivalent to 24 deaths in summer), and each 3.8C increase in aUHII will cause one extra daily death.

Over the 9-year summer months, JJA 2001-2009, there were a total of 27,652 daily deaths aged <75 in the outer band, and 15,360 in the inner band. The total 75+ daily mortality was 47,968 in the outer band and 19,807 in the inner band. The crude mortality distributions dominate the higher outer band DMRs.

These deaths are associated with warmer temperature in the inner band of Greater London. The aUHI-related DMR shows an overall gradually increasing trend. Although the signal relating to the increase is not significantly strong, this research is an initial attempt to determine whether the impact of aUHI on mortality is similar to the impact of temperature on mortality.

6.3.3 Stratification of aUHI and mortality by LWT

Unlike the analyses of LWTs and UHIs in Chapter 4, which associated with both ground-based daytime and night-time aUHII (Section 4.5.2) and satellite-derived sUHII (Section 4.5.3) between 8 July 2002 and 31 July 2007 (study period limited based upon data availability and consistence), in this chapter, the stratification of aUHII and DMR by LWT is conducted, and these three variables of LWTs, DMR and aUHII are attempted to unify all together to examine whether the trends are affected under various synoptic conditions or not. Statistical analyses were performed to confirm if the LWT-specific aUHII and DMR are significantly distributed.

aUHII by LWT, JJA 2001-2009

Figure 6.6 shows the summer and annual night-time aUHII stratified into eleven LWTs during 2001-2009. Only positive aUHII (>0°C) was analysed to indicate the urban heating. Statistical details of LWT-specific aUHII can be found in Table 6.1. In overall, summer aUHI is stronger for most cases, except [C], [N], [S] and [SW] weather types for the West Midlands and except [C], [E] and [SE] for Greater London. Typically, [NE] and [SE] types (from continental Europe, Wilby et al. (2011)) have stronger aUHII in summer.

In the West Midlands, high aUHII values with lower standard errors occurred among [A], [S], [SW] and [W] weather types. In Greater London, top aUHII values with lower standard errors were conditioned by [S], [SW], [A] and [W] types. Although [C] type corresponds to relatively low aUHII, its very high occurrence makes it a non-negligible type. The most frequently occurring [A] and [C] types, accounted for 27% and 20% of total days for the West Midlands; 26% and 21% of total days for Greater

London during JJA 2001-2009. In association with the aUHII, [A] type was linked with relatively higher annual mean aUHII of 2.55°C (West Midlands) and 2.97°C (Greater London). More intense night-time aUHI occurred in summer, accompanying with even higher mean aUHII of 2.65°C (West Midlands) and 3.4°C (Greater London). Conversely, the frequently occurring [C] type was linked with relatively lower annual mean aUHII of 1.45°C (West Midlands) and 2.53°C (Greater London). Unlike the summer stronger [A]-dominated aUHI, in summer, [C]-dominated aUHI was even weaker with an intensity of 1.42°C (West Midlands) and 2.47°C (Greater London). These results agree with Morris and Simmonds (2000)'s findings that anticyclonic circulation is associated with the mean largest UHIs and that cyclonic conditions are associated with small mean UHIs, as well as Wilby et al. (2011)'s findings that more intense night-time heat islands tend to develop in summer, anticyclonic is the most significant weather type and the cyclonic or westerly are the least significant types.

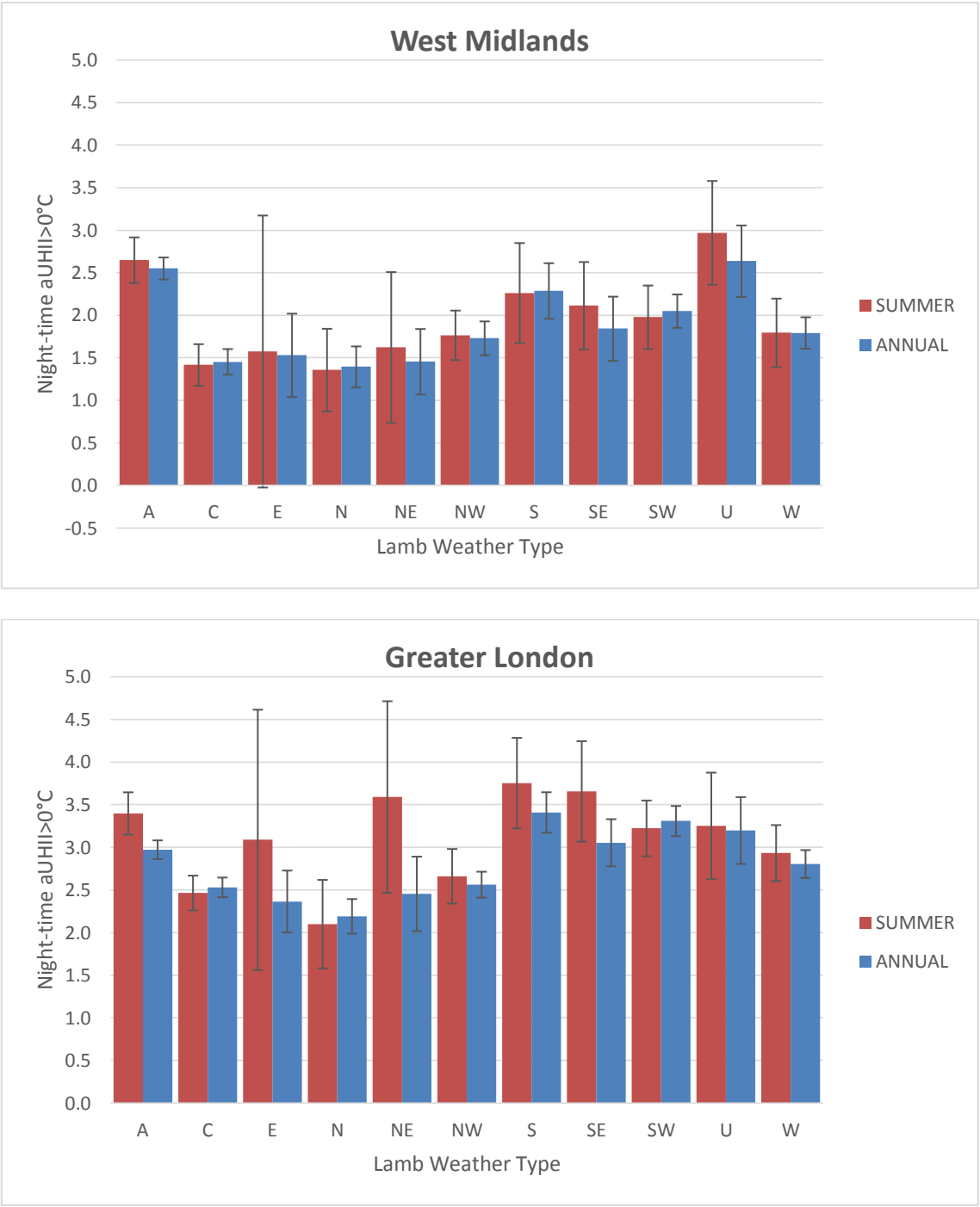

Figure 6.6: Summer and annual night-time aUHII stratified into eleven LWTs for the period 2001-2009 (Error bars denote the 95% CI of mean aUHII).

Table 6.1: Statistical information of summer (JJA) and annual LWT-specific night-time aUHII for the West Midlands and Greater London, 2001-2009.

West Midlands

Annual								
LWTs	**N**	Mean	Std. Error	Maximum	Minimum	95% Confidence Interval for Mean		Std. Deviation
						Upper Bound	Lower Bound	
A	564	2.55	0.066	7.5	0.1	2.680	2.422	1.564
C	300	1.45	0.076	8.5	0.1	1.604	1.304	1.322
E	23	1.53	0.236	3.7	0.1	2.020	1.041	1.133
N	81	1.40	0.121	4.9	0.1	1.635	1.155	1.087
NE	31	1.45	0.189	3.9	0.1	1.840	1.070	1.050
NW	138	1.73	0.101	5.6	0.1	1.929	1.532	1.181
S	102	2.29	0.164	7.2	0.1	2.613	1.961	1.660
SE	49	1.84	0.188	6.7	0.1	2.220	1.466	1.313
SW	210	2.05	0.099	6.6	0.1	2.246	1.854	1.441
U	36	2.64	0.207	5.7	0.5	3.057	2.215	1.243
W	205	1.79	0.094	6.5	0.1	1.978	1.609	1.339
Summer								
LWTs	**N**	Mean	Std. Error	Maximum	Minimum	95% Confidence Interval for Mean		Std. Deviation
						Upper Bound	Lower Bound	
A	133	2.65	0.135	6.5	0.1	2.917	2.381	1.563
C	95	1.42	0.123	5.2	0.1	1.662	1.172	1.202
E	4	1.58	0.502	2.6	0.3	3.173	-0.023	1.005
N	21	1.36	0.233	3.9	0.1	1.843	0.872	1.067
NE	9	1.62	0.384	3.9	0.2	2.509	0.736	1.153
NW	47	1.77	0.145	4.0	0.3	2.057	1.475	0.991
S	27	2.26	0.286	6.6	0.7	2.850	1.676	1.484
SE	21	2.11	0.246	3.9	0.1	2.627	1.602	1.126
SW	55	1.98	0.186	5.1	0.1	2.351	1.605	1.380
U	20	2.97	0.291	5.7	0.8	3.579	2.361	1.302
W	52	1.79	0.201	6.5	0.1	2.197	1.391	1.448

Greater London

Annual								
LWTs	**N**	Mean	Std. Error	Maximum	Minimum	95% Confidence Interval for Mean		Std. Deviation
						Upper Bound	Lower Bound	
A	669	2.97	0.056	7.7	0.3	3.082	2.863	1.446
C	461	2.53	0.059	10.1	0.1	2.646	2.416	1.260
E	49	2.37	0.180	6.6	0.4	2.728	2.003	1.263
N	128	2.19	0.102	8.1	0.1	2.394	1.989	1.159
NE	44	2.45	0.217	7.2	0.7	2.892	2.017	1.438
NW	193	2.56	0.077	6.4	0.7	2.715	2.411	1.070
S	158	3.41	0.120	7.0	0.3	3.647	3.172	1.509
SE	81	3.05	0.139	6.8	0.9	3.331	2.778	1.250
SW	318	3.31	0.090	7.2	0.1	3.485	3.132	1.602
U	48	3.20	0.195	5.9	1.1	3.590	2.806	1.349
W	305	2.80	0.083	9.0	0.2	2.968	2.642	1.450
Summer								
LWTs	**N**	Mean	Std. Error	Maximum	Minimum	95% Confidence Interval for Mean		Std. Deviation
						Upper Bound	Lower Bound	
A	157	3.40	0.126	7.7	0.3	3.646	3.149	1.577
C	132	2.47	0.103	6.5	0.8	2.669	2.262	1.181
E	8	3.09	0.646	6.4	1.0	4.615	1.560	1.827
N	32	2.10	0.254	8.1	0.5	2.619	1.581	1.438
NE	11	3.59	0.504	7.2	1.9	4.714	2.467	1.672
NW	54	2.66	0.159	5.4	0.8	2.981	2.342	1.171
S	32	3.75	0.261	6.1	0.3	4.285	3.222	1.474
SE	23	3.66	0.284	6.8	1.6	4.245	3.068	1.362
SW	70	3.22	0.164	6.1	1.4	3.550	2.896	1.372
U	25	3.25	0.303	5.9	1.1	3.877	2.627	1.514
W	70	2.93	0.165	6.3	0.5	3.262	2.604	1.378

DMRs by LWT, JJA 2001-2009

Deeper into the analyses of LWT-specific mortality data (Figure 6.7), a statistical summary can be found in Table 6.2. The peak in [E]-dominated DMR is observed due to the high minimum DMR value, but should not be considered in priority because of too small sample size of 4. Other LWT-specific DMRs are almost evenly distributed.

Among the <75 populations, the DMRs living in the West Midlands are significantly higher compared with those living in Greater London. However, the 75+ DMRs for both the West Midlands and Greater London are high, but differences between two regions are very minor.

Results do not show distinct LWT-dominated DMR differences between each other. It means the insignificant effect of synoptic conditions on mortality. In overall, the West Midlands <75 DMRs are more influenced under [E]-related weather types, such as [E], [SE] and [NE]. Due to the small sample size (i.e. occurrence) for [E]-related types, in view of statistically significance, [A] type is associated with higher DMRs and [C] type is associated with lower DMR. In Greater London, [W] and [SW] types are also associated with lower 75+ DMRs.

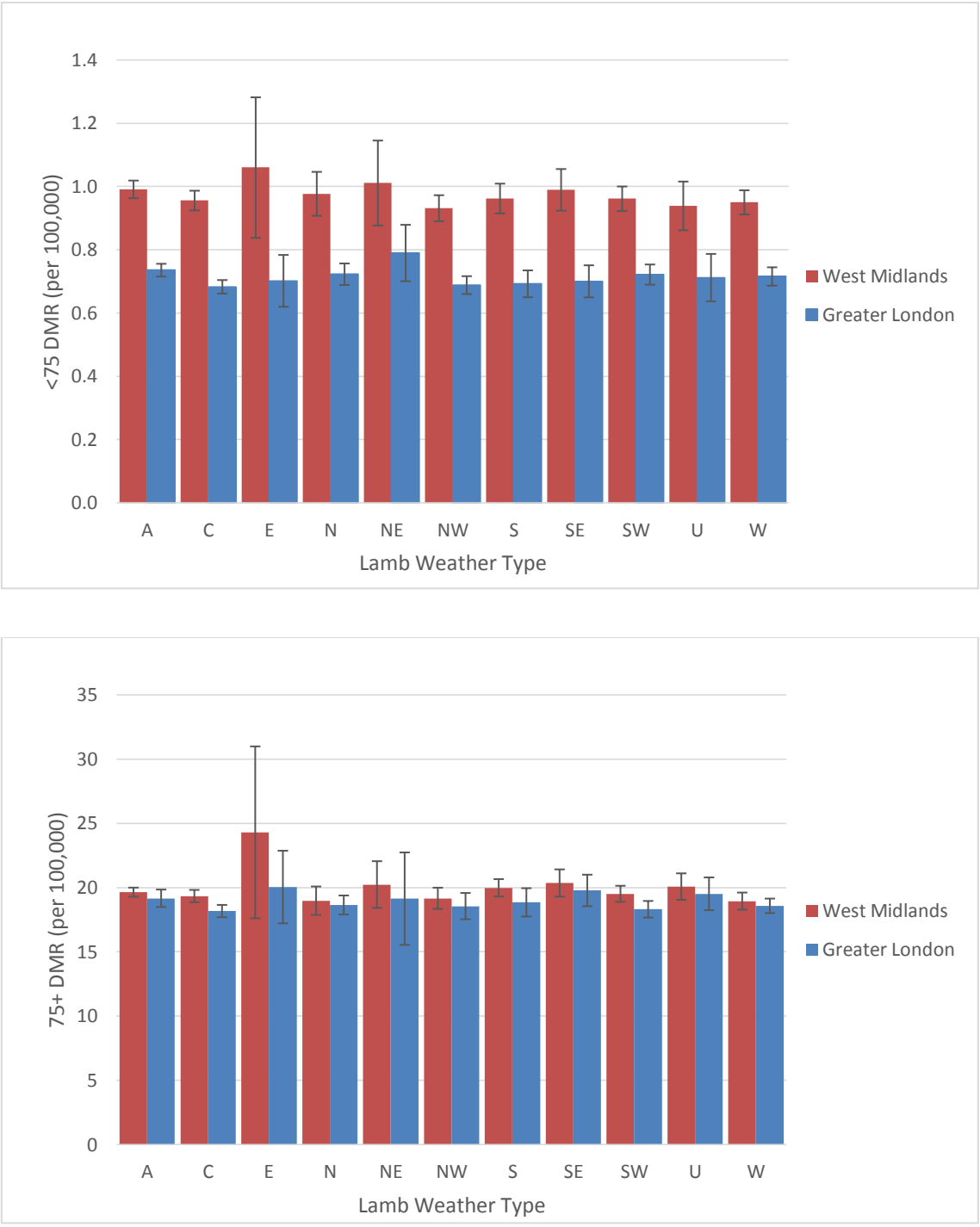

Figure 6.7: Summer DMRs stratified into eleven LWTs for the period JJA 2001-2009 (Error bars denote the 95% CI of mean DMR).

Table 6.2: Statistical information of LWT-specific DMRs (<75 and 75+) for the West Midlands and Greater London, JJA 2001-2009.

West Midlands - summer DMRs								
<75								
LWTs	**N**	Mean	Std. Error	Maximum	Minimum	95% Confidence Interval for Mean		Std. Deviation
						Upper Bound	Lower Bound	
A	133	0.99	0.014	1.5	0.7	1.019	0.964	0.162
C	95	0.96	0.016	1.4	0.6	0.987	0.925	0.153
E	4	1.06	0.070	1.2	0.9	1.282	0.838	0.140
N	21	0.98	0.033	1.3	0.7	1.047	0.908	0.152
NE	9	1.01	0.058	1.2	0.7	1.146	0.877	0.175
NW	47	0.93	0.020	1.2	0.6	0.973	0.891	0.140
S	27	0.96	0.023	1.2	0.7	1.009	0.915	0.119
SE	21	0.99	0.032	1.2	0.7	1.056	0.924	0.145
SW	55	0.96	0.019	1.2	0.6	1.001	0.923	0.144
U	20	0.94	0.037	1.2	0.7	1.016	0.862	0.164
W	52	0.95	0.019	1.2	0.6	0.988	0.912	0.137
75+								
LWTs	**N**	Mean	Std. Error	Maximum	Minimum	95% Confidence Interval for Mean		Std. Deviation
						Upper Bound	Lower Bound	
A	133	19.64	0.179	27.5	15.5	19.992	19.283	2.066
C	95	19.34	0.241	25.0	13.0	19.815	18.856	2.352
E	4	24.29	2.102	29.6	20.6	30.982	17.606	4.203
N	21	18.97	0.530	23.4	14.3	20.079	17.867	2.430
NE	9	20.23	0.788	22.9	16.9	22.049	18.416	2.363
NW	47	19.16	0.411	26.8	14.1	19.987	18.333	2.816
S	27	19.98	0.330	23.4	15.3	20.654	19.297	1.715
SE	21	20.35	0.508	24.1	16.2	21.410	19.290	2.328
SW	55	19.51	0.311	24.5	15.5	20.134	18.889	2.303
U	20	20.07	0.492	24.3	15.7	21.101	19.042	2.200
W	52	18.94	0.331	25.2	14.6	19.607	18.277	2.389

Greater London - summer DMRs								
<75								
LWTs	**N**	Mean	Std. Error	Maximum	Minimum	95% Confidence Interval for Mean		Std. Deviation
						Upper Bound	Lower Bound	
A	157	0.74	0.010	1.3	0.3	0.756	0.716	0.128
C	132	0.68	0.011	1.1	0.4	0.705	0.662	0.124
E	8	0.70	0.035	0.9	0.6	0.784	0.620	0.098
N	32	0.72	0.017	0.9	0.6	0.757	0.689	0.094
NE	11	0.79	0.040	1.0	0.6	0.879	0.701	0.133
NW	54	0.69	0.014	1.0	0.5	0.717	0.660	0.104
S	32	0.69	0.021	1.0	0.4	0.735	0.650	0.118
SE	23	0.70	0.024	1.0	0.5	0.751	0.650	0.117
SW	70	0.72	0.016	1.1	0.5	0.754	0.690	0.134
U	25	0.71	0.036	1.0	0.4	0.787	0.637	0.182
W	70	0.72	0.015	1.1	0.4	0.745	0.687	0.122
75+								
LWTs	**N**	Mean	Std. Error	Maximum	Minimum	95% Confidence Interval for Mean		Std. Deviation
						Upper Bound	Lower Bound	
A	157	19.16	0.344	45.3	12.1	19.841	18.484	4.305
C	132	18.17	0.242	26.3	12.1	18.646	17.688	2.782
E	8	20.04	1.195	25.9	15.8	22.861	17.212	3.379
N	32	18.64	0.362	14.9	14.9	19.381	17.902	2.051
NE	11	19.13	1.614	30.5	10.1	22.727	15.535	5.353
NW	54	18.55	0.510	37.3	13.3	19.575	17.530	3.747
S	32	18.84	0.541	25.9	12.1	19.945	17.738	3.060
SE	23	19.77	0.591	26.3	15.6	20.998	18.548	2.833
SW	70	18.31	0.324	24.3	13.1	18.953	17.659	2.714
U	25	19.51	0.618	26.3	14.0	20.785	18.235	3.088
W	70	18.57	0.282	24.3	12.8	19.136	18.012	2.356

6.3.4 Summary

Interpretations for the relationships between DMR and aUHII in Sections 6.3.1 and 6.3.2, for <75 and 75+ populations in the West Midlands and Greater London, are organised into Table 6.3.

Table 6.3: Implied values of additional daily mortality and summer (JJA) mortality for each 1°C increase in aUHII obtained from Figures 6.2-6.5.

		<75		75+	
		outer band	inner band	outer band	inner band
West Midlands	daily mortality	0.18	0.07	0.09	**0.36**
	summer mortality	17	6	8	**33**
Greater London	daily mortality	-0.09	-0.03	**0.84**	**0.26**
	summer mortality	-9	-2	**77**	**24**

According the data analyses, the increases in aUHII generally lead to additional aUHI-related daily mortality. An exception for London's <75 age group with very slight negative signal, can also be regarded to have tiny or no influence of an increasing aUHI effect on mortality.

It is worth noting that each 1°C increase in aUHII (Edgbaston-Shawbury) will cause an additional daily mortality of 0.36, equivalent to 33 deaths each summer (JJA) for the urban very elderly people aged 75+ in the West Midlands. Each 1°C increase in aUHII (LWC-Rothamsted) has stronger influences on the 75+ very elderly people compared with <75 residents in Greater London, causing extra daily mortality of 0.84 (77 summer deaths) in the outer band and 0.26 (24 summer deaths) in the inner band of Greater London.

As a whole, the increasing aUHI effect provides stronger mortality risk on the very elderly people aged 75+, more significant for the urban 75+ people in the West Midlands and for the rural 75+ people in Greater London. London's outer band mortality risk caused by the increasing aUHII is over triple that of those living in urban areas. The age-specific analyses eliminate the potential impact of age structure. Other potential factors (e.g. air pollution) affecting the DMR variations need to be confirmed as a new research topic by further studies.

Looking into the Table 6.4 showing the mortality and mid-2009 population estimates (for reference use only here, actual DMR calculation used year-to-year corresponding population estimates with mortality data), the higher inner band DMR in the West Midlands is mainly caused by the fewer populations which leads to larger mortality rate per unit of 100,000 population. Although outer London's populations are also

more than inner London, the prominent mortality difference between outer band and inner band plays a stronger role in causing London's higher outer band DMRs.

Table 6.4: Summary of mortality and mid-2009 population estimates for the West Midlands and Greater London, JJA 2001-2009.

West Midlands					
Mortality	<75	75+	**Population**	<75	75+
outer band	19748	37412	outer band	2557600	234800
inner band	19829	32085	inner band	2441300	197400
Greater London					
Mortality	<75	75+	**Population**	<75	75+
outer band	27652	47968	outer band	4624946	308100
inner band	15360	19807	inner band	2691909	128600

Based on the stratification of night-time aUHII by the LWTs during JJA 2001-2009, the analysis of DMRs were also stratified by the LWTs to confirm if the mortality is affected by the variation in synoptic conditions.

ANOVA output (Table 6.5) indicates the significance levels for the aUHII, <75 DMR and 75+ DMR conditioned by the LWTs. All the aUHII for both study areas are significantly conditioned by the LWTs at the 0.01 level (p<0.001). However, the first attempted DMRs conditioned by the LWTs are mostly insignificantly distributed, except the 75+ DMR in the West Midlands.

Table 6.5: Significance levels from the ANOVA output

West Midlands			**Greater London**		
	Annual	**Summer**		**Annual**	**Summer**
aUHII	0.000**	0.000**	aUHII	0.000**	0.000**
<75 DMR	0.280†	0.369†	<75 DMR	0.734†	0.026†
75+ DMR	0.006*	0.001**	75+ DMR	0.094†	0.235†

**. Significant at the 0.01 level

*. Significant at the 0.05 level

†. Insignificant

Results of LWT-specific aUHII indicate that the strongest aUHI develop under [A], [S], [SW] and [W] types, and the weakest under [C] and [N] types. Unfortunately, the first attempt to analyse the LWT-specific DMRs does not illustrate distinct difference between the LWTs. The only outstanding [E]-related 75+ DMR may not be taken into account due to the limitation of its small sample size.

6.4 Conclusions

This chapter focused on the long-term relationships between aUHII and DMR for each outer and inner band of the West Midlands and Greater London. Long-term relationships over the summer months, particularly among the very elderly 75+ people, demonstrated positive increasing correlations except London's <75 age group, although the regression slopes were somewhat weak. The BA analyses allowed some biases to be averaged in each 0.5°C aUHII interval. Different trends imply differing impacts of aUHI effect on mortality between these regions.

During JJA 2001-2009 excluding the days identified as urban cool islands i.e. aUHII≤0, the results demonstrate stronger impact of the increasing aUHI effect on urban mortality rate in the West Midlands. The 75+ urban populations were most vulnerable to the increasing aUHI. By way of contrast, the mortality risk in outer London was higher than that in inner London, and both the urban and rural 75+ residents were entirely at risk as the aUHI effect becomes stronger. In general, the residents aged <75 had very minor impact on the elevated aUHI effect. The results matched expectations that elderly people living in central areas are particularly vulnerable to the elevated heat stress. Excluding the aging effects, other possible factors influencing higher urban DMRs include deprivation, air pollution or certain diseases and pre-illness. Region-specific comparison suggests that London is more significantly affected by the increasing aUHI, in particular the rural residents are at a higher mortality risk. It should be noted that the increasing trends are very sensitive to the number of data points in each aUHII interval. Care has been taken to ensure that the proper statistical analyses were applied to the data and that the effects of outliers, small sample sizes and observation error on the results were minimised as

far as possible. In addition, winter relationships have been analysed but are not presented in this thesis because the thesis focus on heat-related mortality affected by the aUHI. The relationships between mortality rate and aUHI in winter displayed decreased trends, which are exactly reversed compared with the summer relationships. Literature reviews highlighted the high cold-related winter mortality. It is generally thought that the adverse effects on heat-related mortality in summer are most significant, since the winter UHI effect is known to result in some benefits. In the UK, the winter mortality clearly outweighs the summer mortality; but this is different from the situation in other countries. Once wider impacts are taken into account, it is likely that the overall health impact in the UK will be detrimental. However, it is difficult to argue that the direct effects of increased temperature will have a negative impact in the short-medium term. A greater understanding of both the negative and positive impacts will aid policy development that maximises the health benefits and minimises the negative health impacts.

The findings demonstrate how the aUHI affects heat-related mortality. This will become increasingly important as rising temperatures driven by climate change increase the frequency and intensity of heatwaves. Studies on the direct impact of UHI on health have been noticeably limited. These research findings are relatively new attempt and could be used to guide other researchers into similar relationships in other large cities. Further research should be considered to examine the complex UHI-health relationships, since the UHI has dual effects on health (beneficial and adverse). Assessment of cause-specific mortality, such as cardiovascular and respiratory diseases, may increase the understanding of specific health impacts, and offer additional insights not available considering all-cause mortality alone.

Chapter 7 Discussion

The key data sets used throughout this thesis include the MODIS remotely-sensed data, the Met Office MIDAS weather observations, Jenkinson's objective Lamb daily synoptic indices (i.e. LWTs), population estimates and mortality data. All data sources are reliable as they were requested and obtained from official data centres (such as LP DAAC Data Pool, the BADC, the UEA Climatic Research Unit, the ONS and Public Health Observatory), as previously mentioned in Chapter 3. However, some potential uncertainty estimates may exist during data preparation and pre-processing procedures. The following sections discuss the selection of the MODIS data product, processing and potential uncertainties; data partitioning of mortality and population estimates; and the choices of methodology, such as the calculation of mortality rate and fractional polynomial regression model for examining the T-M relationships.

7.1 Justification of MODIS, MGET and pixel geolocation errors

The MODIS/Aqua product MYD11A1 was used to derive the night-time LSTs data for the analyses of spatial sUHI in Birmingham and London. In comparison with alternative thermal products (e.g. Landsat, AVHRR and ASTER etc.), the MODIS product provides a better combination of appropriate temporal and spatial resolutions. Referring to Table 2.2: the overview of ongoing major satellite remote sensing products and applications, Landsat has very high spatial resolution (up to 100 m) but very low temporal resolution (every 16 days); ASTER on board Terra satellite (daytime pass over at ~10:00h) has very high spatial and temporal resolutions (up to

90 m, daily), but data are requested only for commercial purpose and fees applied; the AVHRR product is very similar to the MODIS product, providing moderate spatial resolution (~1.1 km) and very high temporal resolution (twice daily) but there is a lack of night-time satellite images.

Using the MGET tool for processing the original MODIS HDF-EOS data in the sinusoidal projection, potential uncertainties might include the pre-defined projected and geographic coordinate systems. The custom sinusoidal projection is based upon a spheroid axis of 6371007.181m. However, the UK shapefiles are in the 'British National Grid' projected coordinate system and the 'GCS_OSGB_1936' geographic coordinate system. It can be difficult to get other data (such as UK shapefiles) into the MODIS sinusoidal projection, because the MODIS projection does not correspond to an ellipsoid. Roberts (2011) suggested two methods to match the data with different projections: (1) using the ArcGIS gro-processing tool 'Create Custom Geographic Transformation', and (2) by directly loading data into ArcGIS and ignoring the geographic coordinate system warming. In this thesis, the second method was used to associate the converted MODIS raster images with the UK shapefiles (clipped to the West Midlands and Greater London). If necessary, the images were overlapped using the 'Project' tool. It's worth noting that the chosen method may not be exactly accurate due to the uncertainties in the differences between the custom sinusoidal projection (details in Section 3.2.3) and the UK pre-defined coordinate system.

It should be noted that the pixel coordinates for the MODIS product may be affected by precision issues and pixel geolocation errors (Wolfe et al., 2002), which arise during the MODIS satellite image pre-processing procedures and may produce small

alterations in the interpolated values of LST at a given point, since MODIS Level-3 product used in this thesis is reported on a fixed sinusoidal grid. Also, geolocation errors will not change the spatial resolution, as they only cause an offset in where the pixel has been registered at Level-2. The spatial resolution is mainly determined by the instrument IFOV (Instantaneous Field of View). The pixel size is generally precise to the order of 10's of meters. The nominal pixel size is given to 3 significant figures as 0.928 km. However, in this thesis and elsewhere, this nominal pixel resolution is rounded up to 1 km when referring to the spatial resolution of the instrument. Relating to the surroundings of local weather stations covered within the 1 km^2 pixel (Google Earth views shown in Figure 3.1 and Figure 3.2), the LST measurement for the urban Edgbaston weather station (Figure 3.1b) might be affected somewhat by the accuracy of the geolocation. The edge of Edgbaston reservoir is about ~150 m from the Edgbaston station, and the reservoir partially covers the 1 km^2 pixel. Some of the 1 km^2 MODIS pixel contain water bodies, in summer will hence be cooler than the surrounding areas. However, the presence of the reservoir could increase ambient temperature in winter relative to surrounding land. If the location of the pixel is shifted towards the reservoir in different seasons, the LST measurement tends to produce alternation. The absolute location of the pixel will determine what proportion of that pixel is water, and consequently the pixel temperature. Determining upper and lower bounds on the proportion of water contained in the pixel could in principle be modelled. However, it is somewhat complicated due to the necessity of considering both the geolocation error and the interpolation of swath pixels to the geolocation of the sinusoidal grid point used at Level-3. This thesis did not look at the land-use distribution in detail, suggesting only a rough estimate. The geolocation for the Level-

3 product is pre-defined at a given point on Earth and thus there is no uncertainty about where that point is. However, in general when computing the value of LST at the predetermined point, other errors such as how the interpolation procedure is performed, how data are composited and screened will be more important in determining the value of LST at that point than the geolocation error.

7.2 Data partitioning and calculation of mortality rate

The mortality data and population estimates were chosen as the <75 and 75+ age split. As illustrated in Figure 3.6 and Figure 3.7, population estimates in the West Midlands and Greater London increased steadily, but numbers of mortality decreased more sharply. Considering the variations in increase rates of population and decreases rates of mortality for each age group in the West Midlands and Greater London, the DMR was calculated as the daily mortality divided by the corresponding population estimates for each year (Appendix 3). In fact, this is a straightforward method to represent the mortality situation per unit of 100,000 population. Over the study period, these variations potentially cause uncertainties in mortality rates. The 75+ very elderly people, as the most vulnerable community, are associated with the majority of the total all-cause mortality than the <75 people. In this case, no matter how the population estimates change over time, the calculated mortality rates for the very vulnerable elderly people will always be greater than the younger people.

Officially, the ONS uses age-standardised mortality rates. Age-standardised rates are calculated based on the 2013 European Standard Population (ESP) and revised population estimates for 2002-2010 (the 2011 Census). These statistics are

considered to be more precise as they eliminate the effects of age structure, and hence changes in the age-standardised rate are not affected by the changes in the population age. In this thesis, standard ONS age standardisation was not performed due to the limited age groups of broad <75, and 75+ only. Although the age distribution of the 75+ populations may have changed over the study period of 2001-2009 (see Figure 3.6), it is expected to have a minor impact on the overall analyses.

Wolf and McGregor (2013) stated the sensitivity of people to heat, similarly to the UHI, depends upon a range of factors which may affect the adaptability dominated by demographic nature, health status and social service. Age-specific population variations may affect the sensitivity of heat islands, since the area having a large population could potentially produce more anthropogenic heat. The high cooling demand particularly of the vulnerable elderly people in extremely hot areas could affect the city's sustainability.

7.3 Fractional polynomial regression model

The FP regression model was applied to the temperature and mortality data to examine the typical T-M relationships which have been popularly studied (reviews in Section 2.2.1). Unlike other studies, this relatively new method was considered mainly due to its greater flexibility than conventional polynomials and the ability to reveal the 'true' curve shapes (Royston and Altman, 1995). Although the regression model needs complex formulae (see Section 5.3.1) to support, the best fitting curves can be obtained straightaway by running specific commands such as '*fracpoly*', '*fracplot*' and '*fracpred*' rather than setting up formulae manually.

However, parametric methods such as fractional polynomials have disadvantages. The model estimates the predicted and residues of the dependent variable, i.e. the mortality data (DMR) in the T-M relationship (Figure 5.2 and Figure 5.3), and the estimates at a given point may be affected by observations, subsequently causing local bias. Unfortunately, the end effects of using FP regression model at the extreme predictor values may be poor. This disadvantage may weaken the evidence of the impact of unusual extreme hot or cold weather on the mortality rate. Alternatively, the splines and kernel methods used in non-parametric GAMs can overcome such problems (Royston et al., 1999).

7.4 Surprising findings and outliers

Sometimes research findings mismatch with the expectation, such as unexpected patterns, values or outliers. Several typical surprising findings are discussed as below.

In Chapter 4, annual variations of daytime aUHII (LWC-Rothamsted) in Greater London (Figure 4.4) illustrate the lowest peaks over the summer months in typical heatwave years of 2003 and 2006. Similar to the patterns of T_{air}, the night-time aUHII shows the expected highest peak in hot 2003 and 2006 years. For comparison, both daytime and night-time aUHII in the West Midlands (Figure 4.1) show the highest peak as expected. Looking into the details of the data, the lowest peaks are caused by negative aUHII values implicating 'urban cooling' in those years, i.e. the recorded T_{air} is lower at the LWT weather station than the Rothamsted weather station. One possible reason includes the location of LWC station at the rooftop potentially speeding up the wind speed and thus lowering the T_{air}. However, the elevation of the

Rothamsted station is at a height of 128 m compared with LWC's 43 m. As illustrated in Figure 4.8, London's aUHII would be 0.51°C lower due to the elevation difference between Rothamsted and LWC, assuming a temperature lapse rate of 6°C/km. In this case, Rothamsted is expected to be cooler than LWC. The unexpected results could be caused by alternative uncertain reasons. Data indicate that those negative aUHII values were recorded during intense heatwave period, city heat storage could be strong within the urban canopy on very hot days, and the raised rooftop seems the main reason for the reduced T_{air} record. Rothamsted station located in a relatively open area, the recorded T_{air} could be synchronous overall in the rural area. Generally, the intensity of aUHI is significantly dominated by the selection of paired urban-rural weather stations. In particular the LWC weather station may not a perfect urban station as it is located on rooftop, as discussed in Section 3.1.2, it is good enough within the limited choices of alternative stations in central London.

In Chapter 5, the T-M curves modelled using the FP regression demonstrate some scattered outlier at the very hot and very cold ends. As noted above, the findable weakness of FP regression model is the inappropriate end effects at the extreme predictor values. London's 75+ curves as shown in Figure 5.3 (b) show more obvious outlier above the T_{mm} in the hot climate zone. Looking into London's 75+ data, these top four mortality rate outliers were observed on 10-13 August 2003 indicating the significance of extreme temperature on mortality, despite the presence of individual data point may alter the shape of fitting curve in certain aspect. By contrast, there are much less outliers observed for the West Midlands (Figure 5.2), except several occur in the cold climate zone below the T_{mean}. Additionally, the produced T_{mm} varies differently by region and outer/inner band (Figure 5.4). For the $T_{air/max}$ in summer,

inner London possess the highest T_{mm} values at which least mortality occurs, suggesting London central residents' better resistance to heat. Nevertheless, for the $T_{air/min}$ (most likely in winter), the lowest T_{mm} values were recognised among the <75 people in London (12.2°C) and followed by the West Midlands (12.5°C), implicating that younger people may withstand the cold climate better than elderly people. Moreover, the 75+ rural people in the West Midlands have the worst tolerance to cold.

Table 7.1 lists a summary of the mean DMR and T_{mm} values and the corresponding predicted DMR. It can be found that the <75 DMRs between the outer band and the inner band are very similar. For the 75+ DMRs, the West Midlands is found to have higher inner band mean DMR (~21.9 per 100,000), but Greater London is found to have higher outer band mean DMR (~20.3 per 100,000). However, the overall age-age DMR is relatively higher in the outer band of the West Midlands, and this could be caused by aging issue with larger elderly residents living in surrounding areas. If looking into the higher 75+ DMR in the inner band, the causes could be the vulnerability of elderly people to the urban elevated heat, highly built-up living environment and the synergistic effects of air quality. By comparison, all the DMRs are lower for Greater London, and the residents in outer London are overall at higher mortality risk. Referring to Table 3.2, the populations in the outer and inner West Midlands are almost evenly distributed; differently, London's population structure is distributed with a much larger outer population than the inner population, leading to more housing demand, anthropogenic heat release and air pollutants. In the social views, the deprivation, homeless people and relatively weaker local service (e.g. emergency) may also the possible causes of the higher DMR in outer London.

Table 7.1: Summary of the mean DMR, T_{mm} values and the corresponding predicted DMR

Mean DMR

West Midlands			
	All-age	<75	75+
outer band	2.71	1.00	21.39
inner band	2.60	1.04	21.91
Greater London			
	All-age	<75	75+
outer band	2.02	0.76	20.28
inner band	1.63	0.73	19.14

T_{mm} and the corresponding predicted DMR (per 100,000)

West Midlands			
<75		predicted DMR	T_{mm} (°C)
outer band	T_{max}	0.93	21.6
outer band	T_{min}	0.94	14.1
inner band	T_{max}	0.97	20.1
inner band	T_{min}	0.98	12.5
75+			
outer band	T_{max}	18.9	21.6
outer band	T_{min}	19.2	14.9
inner band	T_{max}	19.4	20.9
inner band	T_{min}	19.7	13.4

Greater London			
<75		predicted DMR	T_{mm} (°C)
outer band	T_{max}	0.71	21.0
outer band	T_{min}	0.73	12.2
inner band	T_{max}	0.69	21.5
inner band	T_{min}	0.69	14.2
75+			
outer band	T_{max}	18.5	21.6
outer band	T_{min}	19.2	13.4
inner band	T_{max}	18.0	22.8
inner band	T_{min}	18.5	14.5

In Chapter 6, the comparative relationships between aUHI and mortality in summer reveal the consistent higher DMR in the West Midlands than Greater London, under

the consideration of the variations in mortality and population estimates over time (details in Section 6.3.4 and Table 6.4). Since Greater London suffers warmer weather and larger population density and city infrastructure, the mortality risk is expected to be higher consequently. In fact, the results demonstrate the West Midlands' overall higher summer DMR during 2001-2009, particularly among the <75 people. Specifically by local region, the inner West Midlands has higher DMR and the outer London has higher DMR. The higher than expected DMR in the West Midlands could be led by the higher regional infant mortality rate (with 6.0 deaths per 1,000 live births) in the West Midlands and London having low rates, which has been well confirmed by the ONS and '*Health Profile – West Midlands'* and Cooper (2001). This could be the hypothesised cause of the large <75 DMR different between the West Midlands and Greater London (see summary Figure 8.1), because no further age split among the <75 age group in this thesis. The DMR difference for the 75+ age group is relatively smaller but the West Midlands still remains higher. Information provided by the '*Health Profile – West Midlands*' also mentions that the deprivation and statutory homelessness are all worse than the England average. Excluding the infant issue, deprivation and local service quality could potentially make the West Midlands' elderly people at a high mortality risk. Under the influence of the elevated aUHI effect, each 1°C increase in aUHII also results in more elderly deaths in outer London and in inner West Midlands. Because the aUHI describes the increased temperature of urban air compared with the surrounding rural air. The temperature could vary depending on the characteristics of land cover/use, such as buildings, water bodies and parks. The higher elderly deaths in inner West Midlands are thought to be caused by the nature of inner metropolitan area where as one of the

most heavily urbanised regions in England. By contrast to the relatively open space in rural surroundings, the stored heat in inner band is hard to spread over to the outer at night, and subsequently the urban heat affects the most vulnerable elderly people. Reversely, outer London's elderly people are much more vulnerable to the increased aUHII, mainly because the significant larger elderly population living in rural surroundings (Table 6.4), and also because the less vegetation coverage and more infrastructure in outer London. The daytime stored urban heat releases into the surroundings and plus the existing rural heat, and then exacerbate the aUHI impact on elderly deaths in outer London.

Chapter 8 Conclusions and further research

8.1 Research Findings: fulfilment of research gaps and hypotheses

This thesis has focused on an investigation into the impacts of temperature and the UHI on mortality for the urban and rural areas of the West Midlands and Greater London. This chapter summarises the research findings from Chapters 4-6, including the assessment of urban climates and spatial-temporal UHIs in relation to LWTs; the T-M relationships (long-term, 2001-2009), the 2003 heatwave episode analyses (short-term, 2003 summer), the relationship between aUHI and summer heat-related mortality, and the unification of the aUHI and DMR conditioned by the LWTs. Mortality data were stratified into independent age groups of <75 and 75+ respectively, to distinguish the differences caused by age and demonstrate the vulnerability of elderly people to heat/cold and the UHI effect. The following sections outline the fulfilment of research gaps and hypotheses (Section 8.1) which were previously addressed in Section 2.4 and Section 1.2, respectively. Finally, recommendations for future research opportunities are suggested.

According to the literature reviews in Chapter 2, the following research gaps have been identified for further research in this thesis. Hypotheses were addressed on the basis of a survey of current research knowledge.

Research gaps

1. ***In depth studies are needed to stratify the UHIs by the LWTs for the West Midlands and Greater London, along with a comparison between T_{air}-related aUHI and LST-related sUHI during cloudless anticyclonic nights.***

In Chapter 4, the urban climates of Birmingham and London were analysed using $T_{air/max}$ and $T_{air/min}$ and the calculated intensities of aUHI and sUHI. The temporal and spatial UHIs were separately examined in relation to the LWTs. These preliminary analyses highlighted peaks in temperature and aUHII in heatwave years, particularly in 2003. On this basis, a specific focus on the short-term assessment of the T-M relationships was adopted in Chapter 5.

Urban climates, in particular the temperature and the UHI effect, have been well documented. Air and surface temperatures in densely populated and built-up areas are generally higher than in the surrounding rural areas. The urban climate of Birmingham was assessed using 9-years (2001-2009) of data in the summer months. The urban climate of London was assessed using 9-years (2001-2009) of data in the summer months. The Met Office's Heat-Health Watch sets the heatwave threshold values for the West Midlands at a maximum daytime temperature of 30°C and a night-time minimum temperature of 15°C. For Greater London, the daytime maximum

temperature threshold for a heatwave is defined as 32°C and the night-time minimum temperature is 18°C. These thresholds were used to identify the extreme hot days. Due to the geographical location of Greater London located in southern England, the weather and climate is warmer overall than in more northerly regions. The number of extreme hot days was also higher in London. Extreme hot days in both regions occurred on 9 August 2003 and 19 July 2006. In this thesis, further case studies of variations in temperature and the UHI effect were performed for the 9 August 2003. On a typical heatwave day (9 August 2003), $T_{air/max}$ was 33.2°C at Edgbaston, 32°C at Shawbury, 36°C at LWC, and 34.1°C at Rothamsted. Hourly variations in aUHII over 24 hours demonstrated that the night-time aUHII (Edgbaston-Shawbury) for the West Midlands peaked at 6.3°C, and the night-time aUHII (LWC-Rothamsted) for Greater London peaked at 7.1°C. The spatial distribution of LST highlighted the distinct UHI patterns for Birmingham and London, with a peak in sUHII of 3.8°C and 8.7°C, respectively. The large difference in sUHII between the two regions on the same day could be caused by factors such as population and settlement. Greater London is a densely populated region, particularly in the central areas. By comparison, Birmingham is less populated and has less vulnerable elderly people living in the central area.

Considering the availability and consistency of MIDAS/MODIS data, the study period was defined as between 8 July 2002 and 31 July 2007. Comparison between the daytime and night-time aUHII indicated that the daytime aUHII for the West Midlands was very weak with some negative values and the night-time aUHII for the West Midlands was comparatively strong particularly during the summer months. Greater London's daytime aUHII was observable above 1°C. Daytime aUHI was present but

still too weak to be involved for comparing with night-time aUHII. Therefore, the daytime aUHI were neglected from the main analyses.

Associating the UHIs with LWTs, the importance of the 'anticyclonic' weather type was confirmed for both the West Midlands and Greater London. Anticyclonic conditions covered the largest proportion among the chosen 11 LWTs, and were associated with the strongest night-time aUHI. The LWC-specific spatial patterns of sUHI (at the 1 km spatial resolution) suggested a peak sUHII for Birmingham of 4.16°C and a peak sUHII for London of 7.34°C. In both cases, anticyclonic conditions were prevalent. During the selected cloudless anticyclonic nights (48 nights for the West Midlands, 39 nights for Greater London), T_{air} and LST for each local weather station were correlated. Under settled weather conditions, the correlation between T_{air} and LST was strong and statistically significant. Although temperatures were strongly correlated, the correlations between aUHII and sUHII were weaker. The SPSS outputs suggested that the aUHII-sUHII for the West Midlands had a slope of ~0.55, and the aUHII-sUHII for Greater London had a slope of ~0.67. A simple analytical model assuming a 'built-up' area fraction between the urban pixel and the rural pixel was created reflecting the physical basis behind the relationship. Indeed, the model was derived from two assumptions which are reasonably justifiable. Findings relating to the aUHII-sUHII relationship may lead to the development of methods to derive spatial patterns of aUHI from satellite images.

Partial results from Chapter 4 have been published in 'Progress in Physical Geography --Special Section on Applied Meteorology and Climatology' (Zhang et al., 2014). See Appendix 7 for more information.

2. ***The relationship between temperature and mortality using a relatively new, flexible and straightforward STATA's FP regression model, based upon the previous research of health effects of climate change in the West Midlands.***

This popular research topic on the T-M relationship has been widely investigated (reviews in Section 2.2). This thesis selected an efficient method, the FP regression model, to examine relationships for the West Midlands and Greater London (Chapter 5). The research focused on two important UK regions to provide representative results, which may be used to guide future research on other cities. Long-term T-M relationships displayed U-shaped curves, with decreasing mortality in cold-mild climates and rapidly increasing mortality in hot climates, particularly above the 'minimum mortality temperature' (T_{mm}, or 'threshold temperature'). It seems that the decreased winter mortality may outweigh the increased summer mortality in the West Midlands, whereas the increased summer mortality seems to be more significant than the decreased winter mortality in Greater London. During heatwaves, the heat-related mortality rate is expected to be higher in the inner band than in the outer band. In fact, only the results for Greater London show the typical correlated peaks in the $T_{air/max}$ and DMR, in particular, the 75+ age group shows the most intense short-term increased mortality caused by extreme high $T_{air/max}$. By contrast, the 2003 heatwave event had gentle effect on the West Midlands.

Following the examination of the long-term T-M relationships, the 2003 heatwave episode analyses over July and August in 2003 demonstrate the short-term intense increases in mortality as a result of the extreme T_{air}. London has experience an intense heatwave-related mortality risk particularly among the 75+ people, with

same-day peaks in $T_{air/max}$ of 36°C and the DMR of 42.2 (per 100,000) on 10 August 2003 in outer London, and up to 2-day lagged peaks in $T_{air/max}$ of 37.6°C (10 August) and the DMR of ~53/100,000 on 11-12 August.

The UKCP09 heatwave projections up to the 2080s demonstrate that Edgbaston is likely to experience an average of four heatwaves in June, nine in July and eight in August by the 2080s under the medium emission scenario. Under the high emission scenario, there is an average of five heatwaves in June, eleven in July and ten in August by the 2080s. These climate change projections will form the basis of the future projection for the mortality.

3. ***The relationship between aUHII and summer DMR for the West Midlands and Greater London, using bin-average analyses in each 0.5°C aUHII interval allowing a reduction in observation biases.***

It is well known that UHI has both beneficial and adverse impacts on human health. This thesis looked into the heat-related mortality over the summer months. For the purposes of comparison, Figure 8.1 shows the region-specific aUHII-DMR relationships after BA analyses for the outer and inner bands for the <75 and 75+ populations, respectively. There is consistently higher DMR in the West Midlands than in Greater London, due to its highest regional infant mortality rate, deprivation and access to local services. The most significant impact of the aUHI on mortality can be found among the 75+ very elderly people. The impact of increasing aUHI effect on 75+ rural people in Greater London is considerably stronger than the impact on <75

rural people. Age-specific impact of aUHI on mortality in the West Midlands is comparatively weaker than Greater London, and the increasing aUHI only has obviously strong impact on the 75+ urban people. Referring to Table 6.3, The 75+ people in the inner West Midlands are affected by the increasing UHIs, causing 33 excess summer deaths for each 1°C increase in aUHII. The impact of excess summer mortality caused by the UHIs over the study period of 2001-2009 is strongest for Greater London, associated with extra 77 and 24 excess summer deaths among the 75+ very elderly people in the outer and inner London, respectively. These findings suggest the higher aUHI-related mortality risk is related to aging. As a whole, 75+ elderly people in Greater London are more vulnerable to be affected by the increasing aUHI than the West Midlands. In fact, the impact of aUHI on mortality may not be as strong as the impact of temperature on mortality, but a gradually increasing correlation can still be observed. In this research, further attention was focussed on the health impacts of elevated urban heating, due to increasing urbanisation and urban climate modification.

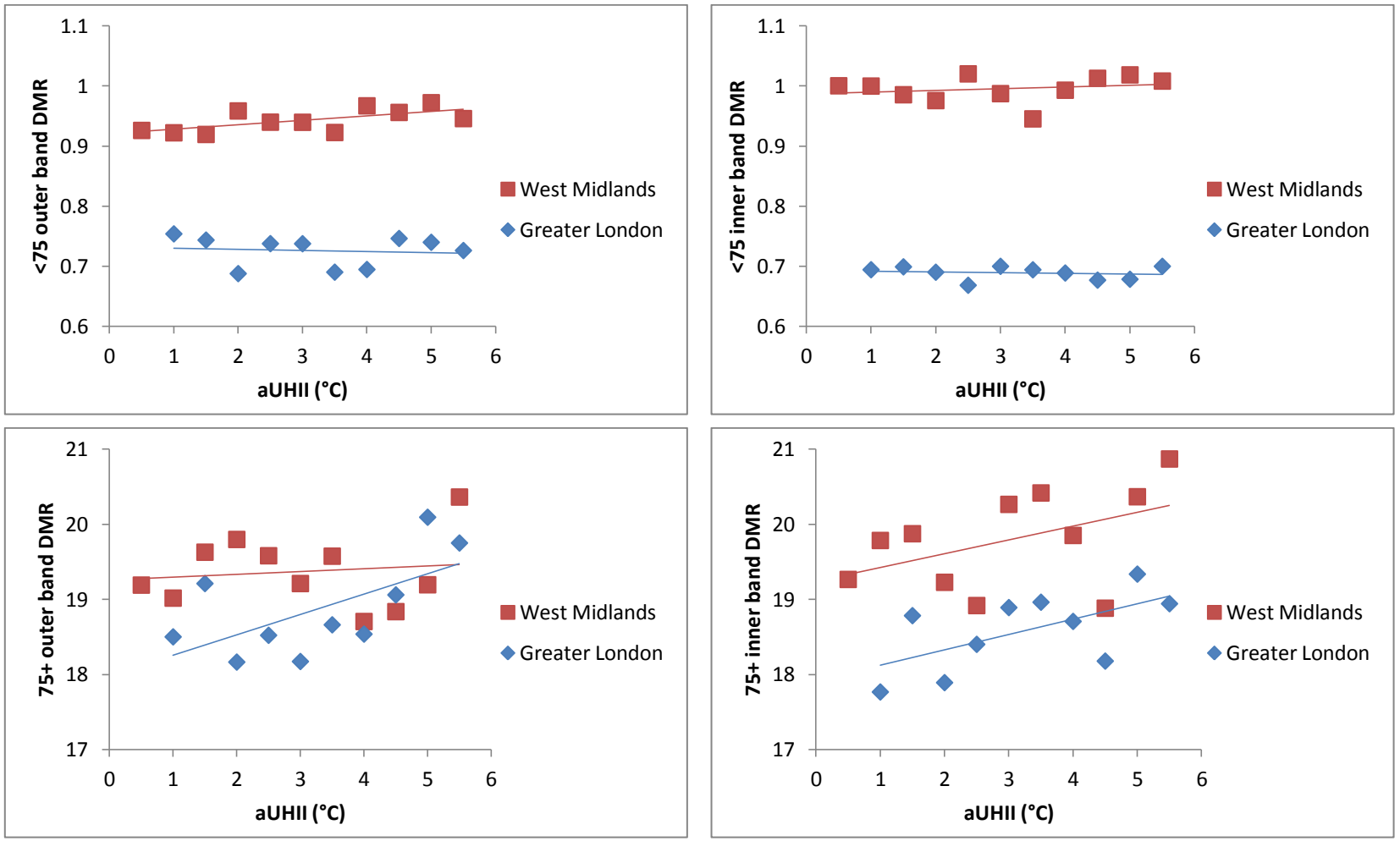

Figure 8.1: All-cause DMRs (per 100,000 population) and the aUHII, by age (<75, 75+), by region (West Midlands, Greater London), by band (inner band, outer band).

Hypotheses

1. ***Due to frequent spells of heatwaves and warmer winters, the heat effect on mortality is expected to outweigh the cold effect on mortality, although cold-related mortality accounts for more deaths than heat-related mortality* (Hajat et al., 2014).**

In Chapter 5, research findings suggested that both heat and cold stress have various impacts on mortality, depending upon the location and intensity of the heat (or cold). The significance of the impact of heatwaves on mortality is well known, particularly during extended hot periods. Indeed, a single hot day may not cause immediate increases in mortality. Although the cold burden remains higher than the heat burden in all periods (Figure 2.5), the heat-related mortality rate is projected to increase while the cold-related mortality rate is projected to decrease in future decades, and thus the effect of cold on mortality was not fully taken into consideration as the research focus of this thesis was on the urban heating. The heat effect on mortality is comparatively strong for Greater London, and the cold effect on mortality is slightly stronger for the West Midlands, although the heat effect can also be observed. During the 2003 typical heatwave months (July and August), London's short-term increase in mortality was pronounced, particularly during the August heatwave days.

2. ***Heatwaves lead to short-term increased mortality, and the UHI effect may exacerbate heatwaves and urban mortality risk. The impact of the aUHI on mortality in Greater London is expected to be stronger than that in the West Midlands. The elderly population is more vulnerable to heat stress and the UHI effect.***

Analysis of the 2003 heatwave episode confirmed that this event had a significant impact on mortality. During heatwave days, peaks in $T_{air/max}$ and DMR were positively correlated. During the most severe period (4-10 August) for the West Midlands, a total mortality of 1,058 was observed. Greater London experienced the most severe heatwave during 6-11 August, resulting in a total mortality of 1,292. Using the Met Office threshold temperatures ($T_{air/max}$ of 30°C and $T_{air/min}$ of 15°C for the West Midlands; $T_{air/max}$ of 32°C and $T_{air/min}$ of 18°C for Greater London), there were many more hot days exceeding the thresholds observed at the urban Edgbaston and LWC weather stations. The mortality risk was correspondingly elevated. The presence of the UHIs for the West Midlands and Greater London has been highlighted using T_{air} and LST in Chapter 4. In relation to the mortality, T_{air} and T_{air}-related aUHII were associated with DMR to assess their impacts. As expected, T_{air} has a direct impact on mortality, with elevated DMR at lower and higher temperatures.

However, the relationship between DMR and aUHII was not altogether expected. The impact of aUHII was found to be much weaker than T_{air} on mortality. A slightly increased regression trend was observed, suggesting that urban heating can affect all-cause

mortality to a certain extent. Due to London's strong aUHI, for example, on a typical heatwave day, the aUHII and sUHII peaked at 7.1°C and 8.7°C, respectively. The impact of UHI mortality had been hypothesised to be stronger. In fact, all-age DMRs dominated by the aUHII (Edgbaston-Shawbury) for the West Midlands were consistently larger than for Greater London. The 75+ elderly population has much higher DMRs than the <75 population, particularly for the inner band of the West Midlands, where DMR is almost doubled compared to the outer band.

3. **Under the influence of weather types, the strongest UHI is associated with anticyclonic type and the weakest UHI is associated with cyclonic type. The mortality rate conditioned by weather types may also follow these circumstances.**

As examined in Chapter 4, both in the West Midlands and Greater London, have the strongest mean UHIs in association with anticyclonic weather type, and weak mean UHIs in association with cyclonic weather types. However, the easterly type (for the West Midlands), and northerly and north-easterly types (for Greater London) are also associated with very low UHI values.

In addition, the work undertaken in Section 6.3.3 represents the first attempt to categorise the mortality data into the LWTs. Unlike the LWT-specific aUHIs (Figure 6.6), the results of LWT-specific DMR demonstrate almost evenly distribution, implying the

insignificant influence of the corresponding synoptic condition on mortality, which is more realistically affected by direct heat and cold stress, as well as other climate change consequences such as air pollution (respiratory diseases) etc. Despite the results do not agree with the hypothesis, this research attempt may still prove the curiousness the impact of the synoptic weather conditions on mortality.

8.2 Future research

As mentioned earlier, the choice of methodology of FP regression model may still have certain weakness, such as the poor or inappropriate end effects at the extreme predictor values (i.e. end effects). Further studies are needed to focus on the methodology improvement or consider alternative better splines or kernel methods to overcome such difficulties, despite the FP regression model worked well on predicting the T-M best fitted curves and identifying the T_{mm} thresholds. Confounding factors, such as air quality which has potential synergistic effect with temperature on mortality, and gender (male and female), and socioeconomic factors, may be considered to be adjusted in the regression model.

In this thesis, the 2003 heatwave event was the only focus among the UK's typical heatwaves including the 2006 heatwave and the more recent 2013 heatwave. Future studies could look into the LST map under various heatwave conditions to assess the vulnerability/hazard index and the heatwave health risk map. Based on the future

heatwave projections using UKCP09, the projection of future mortality up to the 2080s can also be considered.

Cause-specific mortality data (including all-cause, cardiovascular and respiratory diseases and other-cause) are currently available, and the attempted analyses conducted in Chapter 6 could be upgraded using cardiovascular and respiratory diseases as the main causes of illness and mortality during a heatwave. The impact of climate change (e.g. heat- and cold-related extreme weather events) on ambulance call-outs and response times have been studied by Thornes et al. (2014) and Wolf et al. (2013) could be a potential subject of future research. The research findings could be used as part of the Syndromic Surveillance System at the Health Protection Agency.

The key components in this thesis include the synoptic weather types, temperature, the UHI and mortality. They have been well linked with each other, except the association between weather types and mortality. A research idea assessing the synoptic weather patterns, air pollution and human mortality will be considered as a depth study.

In June 2011, a new weather station in Birmingham was installed at the University of Birmingham (Winterbourne 2). This new station is expected to provide more representative urban weather data and better information for future research into Birmingham's UHI and the effect of climate change on extreme weather events. Unfortunately, the Edgbaston weather station used in this thesis has now closed. Meteorological data obtained from the new weather station will need to be used in future analyses. The Birmingham Urban Climate Laboratory (BUCL) established in the University of Birmingham is a near real-time, high-density urban climate network

containing 25 weather stations and over 100 T_{air} sensors. The recent HiTemp project examines Birmingham's UHI and sees the world's densest T_{air}-sensor network. Further research will consider better weather station selection on the basis of the HiTemp/BUCL urban meteorological network.

In London, the most popular urban stations include the LWC (used in this thesis, installed on a rooftop at a height of 43 m, but closed in 2010), St. James' Park, Kew Gardens and Heathrow. Indeed, they are not ideal stations as defined by the UK Met Office, which indicates that stations should be at ground level, unshaded by trees and unaffected by other local effects. In reality, it is not possible to find a perfect weather station. The LWC, St James' Park and Kew Gardens are largely surrounded by trees, potentially altering the prevalent local weather conditions. Heathrow is indeed an airport and cannot be considered ideally as either an urban or rural station. Further research may need to focus attention on improving the coverage of weather stations in urban areas to improve the accuracy and representativeness of measurements. Since the UHI phenomenon describes the local-scale (regional) urban warming, the aUHII calculated from different pairs of urban-rural stations could produce different UHI effects. Wan et al. (2002) raised the issue of the impact of rural station selection on UHII estimation. More urban and rural weather stations will need to be considered in future research to compare the impact of station selection on UHI effects.

Appendices

Appendix 1: The urban-rural classification in England (Pateman, 2011)

Appendix 2: Data access agreement for non-disclosive microdata

Appendix 3: Age-specific population estimates and total mortality for the West Midlands and Greater London from 2001 to 2009.

West Midlands							
Population				**Total Mortality**			
Year	All-age	75 and over	Under 75	Year	All-age	75 and over	Under 75
2001	5280727	391992	4888735	2001	53989	34001	19988
2002	5293885	397481	4896404	2002	54352	34655	19697
2003	5309767	401136	4908631	2003	55670	35921	19749
2004	5323900	405388	4918512	2004	52666	33963	18703
2005	5347210	410397	4936813	2005	53163	34396	18767
2006	5362203	416583	4945620	2006	52224	33791	18433
2007	5378358	422806	4955552	2007	52203	34165	18038
2008	5408429	427783	4980646	2008	52053	34255	17798
2009	5431079	432232	4998847	2009	48122	32010	16112

Greater London							
Population				**Total Mortality**			
Year	All-age	75 and over	Under 75	Year	All-age	75 and over	Under 75
2001	7,322,403	426,530	6,895,873	2001	58154	35838	22316
2002	7,368,902	425,775	6,943,127	2002	57444	35552	21892
2003	7,379,687	424,109	6,955,578	2003	57730	36247	21483
2004	7,413,086	422,876	6,990,210	2004	53628	33369	20259
2005	7,484,931	424,934	7,059,997	2005	52983	33329	19654
2006	7,546,568	428,255	7,118,313	2006	51019	31762	19257
2007	7,602,241	431,215	7,171,026	2007	49946	31442	18504
2008	7,668,330	433,704	7,234,626	2008	49805	31663	18142
2009	7,753,555	436,893	7,316,662	2009	48002	30158	17844

Appendix 4: T_{air} and LST at the urban and rural stations and the calculated aUHII and sUHII for the West Midlands (48 nights) and Greater London (39 nights).

West Midlands (48 nights)							
Date	**Edgbaston (T_{air})**	**Edgbaston (LST)**	**Shawbury (T_{air})**	**Shawbury (LST)**	**sUHII**	**aUHII**	**aUHII (01:30 UTC)**
02/09/2002	9.2	7.43	4.3	1.57	5.86	4.9	5.95
24/09/2002	7.5	6.63	2.8	2.91	3.72	4.7	4.1
06/01/2003	-2	-2.59	-4.4	-4.15	1.56	2.4	2.7
15/02/2003	-2.8	-3.03	-6.8	-4.71	1.68	4	1.35
15/03/2003	0.6	0.41	-1.1	-3.57	3.98	1.7	1.8
22/03/2003	0.5	1.11	-0.7	-1.53	2.64	1.2	1.25
23/03/2003	1.1	0.57	-1	-2.13	2.7	2.1	2.4
09/04/2003	-0.4	-2.79	-2.5	-3.23	0.44	2.1	1.7
23/04/2003	6	3.95	1.1	2.01	1.94	4.9	3.75
15/05/2003	3.4	2.47	-0.5	-0.35	2.82	3.9	1.65
13/06/2003	9.5	9.63	7.2	6.77	2.86	2.3	1.95
25/06/2003	13.7	13.11	8.8	8.57	4.54	4.9	4.9
10/08/2003	18.7	20.15	16.3	16.37	3.78	2.4	5.45
15/08/2003	11.3	10.83	6.2	7.57	3.26	5.1	2.6
17/10/2003	5.2	4.81	0.2	0.43	4.38	5	1.5
08/12/2003	-1.7	-1.95	-3	-4.69	2.74	1.3	1.4
09/02/2004	-1.1	-2.11	-2.7	-3.21	1.1	1.6	2.1
02/03/2004	-1.6	-4.55	-7.1	-6.01	1.46	5.5	5.15
17/05/2004	12.4	11.81	10	8.13	3.68	2.4	4.35
23/05/2004	6.5	5.67	2.9	3.51	2.16	3.6	3.1

24/05/2004	9	7.81	2.6	3.23	4.58	6.4	4.75
25/05/2004	9.4	9.53	3.9	4.03	5.5	5.5	5
13/06/2004	11.8	11.77	6.6	6.81	4.96	5.2	3.6
05/09/2004	15.2	15.65	11	11.55	4.1	4.2	4.9
11/05/2005	2.7	1.93	-0.8	-1.05	2.98	3.5	1.8
28/06/2005	13.2	13.07	7.7	7.75	5.32	5.5	5.65
17/07/2005	13.2	14.01	9.5	10.05	3.96	3.7	3.7
03/09/2005	11.6	12.59	9.1	9.21	3.38	2.5	3.8
19/11/2005	-0.6	-1.21	-6.7	-4.23	3.02	6.1	4.8
21/11/2005	0.7	-0.39	-3.9	-2.19	1.8	4.6	4.75
22/01/2006	0.8	-1.33	-2.7	-2.77	1.44	3.5	5.9
05/04/2006	-0.6	-2.13	-3.7	-3.81	1.68	3.1	2.6
10/04/2006	-0.3	-0.95	-2.3	-1.65	0.7	2	0.65
10/05/2006	8.5	8.73	5.5	6.57	2.16	3	1.65
11/05/2006	9	8.09	7.2	6.75	1.34	1.8	0.25
14/07/2006	10.7	11.53	7.2	6.97	4.56	3.5	2.15
18/07/2006	18.5	16.65	12	13.15	3.5	6.5	6.15
24/07/2006	14.3	13.27	10.4	10.41	2.86	3.9	3.2
08/09/2006	8.5	8.71	4.5	5.67	3.04	4	3.65
09/09/2006	10.2	10.37	7.9	6.73	3.64	2.3	1.65
03/02/2007	0.8	0.41	-4.5	-3.47	3.88	5.3	3.85
04/02/2007	0.2	0.13	-5.3	-2.89	3.02	5.5	5.85
14/03/2007	5	2.57	-1.7	0.31	2.26	6.7	4.3
02/04/2007	4.1	4.05	1.1	2.27	1.78	3	2.25
05/04/2007	4.6	3.91	-0.7	0.85	3.06	5.3	4.3
07/04/2007	4.3	4.77	0	1.39	3.38	4.3	4.1
11/04/2007	8.5	5.93	2.4	2.67	3.26	6.1	6.8
22/05/2007	9.5	8.01	5.6	4.91	3.1	3.9	2.65

Greater London (39 nights)							
Date	**LWC (T_{air})**	**LWC (LST)**	**Rothamsted (T_{air})**	**Rothamsted (LST)**	**sUHII**	**aUHII**	**aUHII (01:30 UTC)**
28/09/2002	10.8	11.07	6.2	6.19	4.88	4.6	3.05
04/10/2002	10.9	11.75	5.5	5.67	6.08	5.4	4.7
15/02/2003	-0.2	-0.13	-3.1	-3.45	3.32	2.9	2.75
15/03/2003	3.9	2.71	1.5	-1.69	4.4	2.4	2.9
16/03/2003	4	4.07	0.6	-2.09	6.16	3.4	3.9
20/03/2003	5.9	5.87	-0.5	-1.17	7.04	6.4	6.9
22/03/2003	2.6	3.31	-0.4	-2.97	6.28	3	3.5
23/03/2003	3.6	4.35	-1.1	-2.35	6.7	4.7	5.25
31/03/2003	5.9	6.95	-0.2	0.71	6.24	6.1	4.7
08/04/2003	1.1	2.13	-3.1	-3.83	5.96	4.2	4.05
09/04/2003	1.2	1.03	-2.7	-3.85	4.88	3.9	4.35
23/04/2003	8.6	8.87	3.2	2.87	6	5.4	5
21/06/2003	12.8	14.45	6.4	6.85	7.6	6.4	5.35
03/08/2003	16.2	16.39	10.6	9.89	6.5	5.6	5.05
04/08/2003	17.4	17.13	13.1	13.45	3.68	4.3	4.75
07/08/2003	19.2	21.05	15.9	16.05	5	3.3	4.65
08/08/2003	20.4	20.45	15	14.13	6.32	5.4	4.6
10/08/2003	23.7	22.95	16	14.77	8.18	7.7	6.4
15/08/2003	14.3	16.19	9.1	8.25	7.94	5.2	5.85
04/09/2003	13.1	12.61	7.5	6.55	6.06	5.6	5.9
16/09/2003	15	12.97	8.4	5.09	7.88	6.6	6.95
24/09/2003	7.9	7.77	1.6	1.29	6.48	6.3	5.1
17/10/2003	7.3	7.57	3.9	3.75	3.82	3.4	2.65
08/12/2003	1.1	0.93	-2.8	-3.41	4.34	3.9	4.15
16/12/2003	1.7	0.21	-4	-4.79	5	5.7	4.5

09/02/2004	0.7	-0.09	-2.7	-3.95	3.86	3.4	2.6
01/03/2004	-0.4	0.69	-4	-4.49	5.18	3.6	2.5
02/03/2004	0.5	0.33	-5.1	-4.91	5.24	5.6	6.25
30/03/2004	5.6	5.69	3.8	2.07	3.62	1.8	2.15
17/05/2004	13.8	12.99	7.3	6.57	6.42	6.5	5.75
22/05/2004	6.4	6.43	2.6	0.67	5.76	3.8	2.1
23/05/2004	8	7.63	1.5	3.01	4.62	6.5	5.3
06/07/2004	13.2	13.05	6.4	5.91	7.14	6.8	7.15
28/07/2004	17.1	17.43	12.7	14.43	3	4.4	3.1
05/09/2004	17.7	17.43	13.5	14.37	3.06	4.2	4.3
26/10/2004	8.1	6.75	2.5	2.73	4.02	5.6	4.75
11/12/2004	4	2.91	-0.7	-3.49	6.4	4.7	5.7
14/07/2006	12.8	13.53	9.9	9.41	4.12	2.9	3.05
08/09/2006	10.6	12.27	8	6.75	5.52	2.6	3.65

Appendix 5: Exact timing of MODIS/Aqua image acquisition and MIDAS T_{air} measurement

Date	MODIS (GMT)	MODIS (BST)	MODIS (local time)	MIDAS (GMT)	MIDAS (BST)	MIDAS (local time)
02/09/2002	0148 h	0248 h	0248 h	0500 h	0600 h	0600 h
24/09/2002	0106 h	0206 h	0206 h	0600 h	0700 h	0700 h
06/01/2003	0154 h	-	0154 h	0400 h	-	0400 h
15/02/2003	0106 h	-	0106 h	0700 h	-	0700 h
15/03/2003	0130 h	-	0130 h	0500 h	-	0500 h
22/03/2003	0136 h	-	0136 h	0600 h	-	0600 h
23/03/2003	0218 h	-	0218 h	0600 h	-	0600 h
09/04/2003	0130 h	0230 h	0230 h	0500 h	0600 h	0600 h
23/04/2003	0000 h	0100 h	0100 h	0500 h	0600 h	0600 h
15/05/2003	0242 h	0342 h	0342 h	0400 h	0500 h	0500 h
13/06/2003	0206 h	0306 h	0306 h	0400 h	0500 h	0500 h
25/06/2003	0230 h	0330 h	0330 h	0300 h	0400 h	0400 h
10/08/2003	0106 h	0206 h	0206 h	2300 h	0000 h	0000 h
15/08/2003	0124 h	0224 h	0224 h	0600 h	0700 h	0700 h
17/10/2003	0224 h	0324 h	0324 h	0400 h	0500 h	0500 h
08/12/2003	0154 h	-	0154 h	0800 h	-	0800 h
09/02/2004	0112 h	-	0112 h	0500 h	-	0500 h
02/03/2004	0218 h	-	0218 h	0700 h	-	0700 h
17/05/2004	0242 h	0342 h	0342 h	2300 h	0000 h	0000 h
23/05/2004	0206 h	0306 h	0306 h	0400 h	0500 h	0500 h
24/05/2004	0106 h	0206 h	0206 h	0400 h	0500 h	0500 h
25/05/2004	0154 h	0254 h	0254 h	0400 h	0500 h	0500 h
13/06/2004	0224 h	0324 h	0324 h	0300 h	0400 h	0400 h
05/09/2004	0200 h	0300 h	0300 h	0200 h	0300 h	0300 h
11/05/2005	0106 h	0206 h	0206 h	0500 h	0600 h	0600 h

28/06/2005	0106 h	0206 h	0206 h	2300 h	0000 h	0000 h
17/07/2005	0000 h	0100 h	0100 h	0300 h	0400 h	0400 h
03/09/2005	0000 h	0100 h	0100 h	0600 h	0700 h	0700 h
19/11/2005	0106 h	-	0106 h	0700 h	-	0700 h
21/11/2005	0230 h	-	0230 h	2000 h	-	2000 h
22/01/2006	0106 h	-	0106 h	0900 h	-	0900 h
05/04/2006	0242 h	0342 h	0342 h	0400 h	0500 h	0500 h
10/04/2006	0118 h	0218 h	0218 h	0400 h	0500 h	0500 h
10/05/2006	0000 h	0100 h	0100 h	0400 h	0500 h	0500 h
11/05/2006	0218 h	0318 h	0318 h	0500 h	0600 h	0600 h
14/07/2006	0218 h	0318 h	0318 h	0400 h	0500 h	0500 h
18/07/2006	0154 h	0254 h	0254 h	0400 h	0500 h	0500 h
24/07/2006	0118 h	0218 h	0218 h	0400 h	0500 h	0500 h
08/09/2006	0130 h	0230 h	0230 h	0500 h	0600 h	0600 h
09/09/2006	0212 h	0312 h	0312 h	0500 h	0600 h	0600 h
03/02/2007	0242 h	-	0242 h	0500 h	-	0500 h
04/02/2007	0324 h	-	0324 h	0600 h	-	0600 h
14/03/2007	0112 h	-	0112 h	0700 h	-	0700 h
02/04/2007	0006 h	0106 h	0106 h	0500 h	0600 h	0600 h
05/04/2007	0212 h	0312 h	0312 h	0500 h	0600 h	0600 h
07/04/2007	0200 h	0300 h	0300 h	0600 h	0700 h	0700 h
11/04/2007	0136 h	0236 h	0236 h	0500 h	0600 h	0600 h
22/05/2007	0130 h	0230 h	0230 h	0200 h	0300 h	0300 h

Appendix 6: STATA outputs for T-M relationships

West Midlands (<75)

```
. fracpoly regress  outerbandDMR  ShawburyTmax, degree(2)
.........
-> gen double IShaw__1 = X^3-4.464507965 if e(sample)
-> gen double IShaw__2 = X^3*ln(X)-2.226537939 if e(sample)
   (where: X = (ShawburyTmax+2.899998426437378)/10)
```

Source	SS	df	MS
Model	7.44414833	2	3.72207416
Residual	140.891371	3282	.04292851
Total	148.335519	3284	.045169159

Number of obs = 3285
F(2, 3282) = 86.70
Prob > F = 0.0000
R-squared = 0.0502
Adj R-squared = 0.0496
Root MSE = .20719

outerbandDMR	Coef.	Std. Err.	t	P>|t|	[95% Conf.	Interval]
IShaw__1	-.0411194	.0039407	-10.43	0.000	-.0488458	-.033393
IShaw__2	.0334498	.0037217	8.99	0.000	.0261528	.0407468
_cons	.9883588	.0042292	233.70	0.000	.9800666	.996651

Deviance: -1022.47. Best powers of ShawburyTmax among 44 models fit: 3 3.

```
. fracpoly regress  outerbandDMR  ShawburyTmin, degree(2)
.........
-> gen double IShaw__1 = X^3-4.249561794 if e(sample)
-> gen double IShaw__2 = X^3*ln(X)-2.049444482 if e(sample)
   (where: X = (ShawburyTmin+10.09999847412109)/10)
```

Source	SS	df	MS
Model	5.88494507	2	2.94247254
Residual	142.450574	3282	.043403588
Total	148.335519	3284	.045169159

Number of obs = 3285
F(2, 3282) = 67.79
Prob > F = 0.0000
R-squared = 0.0397
Adj R-squared = 0.0391
Root MSE = .20834

outerbandDMR	Coef.	Std. Err.	t	P>|t|	[95% Conf.	Interval]
IShaw__1	-.039009	.0058175	-6.71	0.000	-.0504152	-.0276027
IShaw__2	.03209	.0061486	5.22	0.000	.0200346	.0441454
_cons	.9919784	.0046938	211.34	0.000	.9827753	1.001181

Deviance: -986.32. Best powers of ShawburyTmin among 44 models fit: 3 3.

```
. fracpoly regress  innerbandDMR  EdgbastonTmax, degree(2)
.........
-> gen double IEdgb__1 = X^3-6.329396402 if e(sample)
-> gen double IEdgb__2 = X^3*ln(X)-3.893011035 if e(sample)
   (where: X = (EdgbastonTmax+5.099998474121094)/10)
```

Source	SS	df	MS
Model	11.1642781	2	5.58213904
Residual	169.69896	3270	.051895706
Total	180.863238	3272	.055276051

Number of obs = 3273
F(2, 3270) = 107.56
Prob > F = 0.0000
R-squared = 0.0617
Adj R-squared = 0.0612
Root MSE = .22781

innerbandDMR	Coef.	Std. Err.	t	P>|t|	[95% Conf.	Interval]
IEdgb__1	-.04947	.003818	-12.96	0.000	-.0569558	-.0419842
IEdgb__2	.039287	.003312	11.86	0.000	.0327933	.0457807
_cons	1.024883	.0047242	216.94	0.000	1.01562	1.034146

Deviance: -397.86. Best powers of EdgbastonTmax among 44 models fit: 3 3.

```
. fracpoly regress  innerbandDMR  EdgbastonTmin, degree(2)
.........
-> gen double IEdgb__1 = X^3-2.138644783 if e(sample)
-> gen double IEdgb__2 = X^3*ln(X)-.5419128762 if e(sample)
   (where: X = (EdgbastonTmin+5.499998569488525)/10)
```

Source	SS	df	MS
Model	10.5227705	2	5.26138524
Residual	170.340467	3270	.052091886
Total	180.863238	3272	.055276051

Number of obs = 3273
F(2, 3270) = 101.00
Prob > F = 0.0000
R-squared = 0.0582
Adj R-squared = 0.0576
Root MSE = .22824

innerbandDMR	Coef.	Std. Err.	t	P>|t|	[95% Conf.	Interval]
IEdgb__1	-.0879288	.0074353	-11.83	0.000	-.1025071	-.0733505
IEdgb__2	.0955298	.0095144	10.04	0.000	.076875	.1141846
_cons	1.027615	.0050336	204.15	0.000	1.017745	1.037484

Deviance: -385.51. Best powers of EdgbastonTmin among 44 models fit: 3 3.

West Midlands (75+)

```
. fracpoly regress  outerbandDMR  ShawburyTmax, degree(2)
.........
-> gen double IShaw__1 = X^3-4.464507965 if e(sample)
-> gen double IShaw__2 = X^3*ln(X)-2.226537939 if e(sample)
   (where: X = (ShawburyTmax+2.899998426437378)/10)
```

Source	SS	df	MS		
Model	11868.4726	2	5934.23628	Number of obs =	3285
Residual	42246.7335	3282	12.8722527	F(2, 3282) =	461.01
				Prob > F =	0.0000
Total	54115.2061	3284	16.4784428	R-squared =	0.2193
				Adj R-squared =	0.2188
				Root MSE =	3.5878

outerbandDMR	Coef.	Std. Err.	t	P>|t|	[95% Conf.	Interval]
IShaw__1	-1.638016	.0682379	-24.00	0.000	-1.771809	-1.504223
IShaw__2	1.331272	.0644453	20.66	0.000	1.204915	1.457629
_cons	21.10407	.0732345	288.17	0.000	20.96048	21.24766

Deviance: 17712.84. Best powers of ShawburyTmax among 44 models fit: 3 3.

```
. fracpoly regress  outerbandDMR  ShawburyTmin, degree(2)
.........
-> gen double IShaw__1 = X^3-4.249561794 if e(sample)
-> gen double IShaw__2 = X^3*ln(X)-2.049444482 if e(sample)
   (where: X = (ShawburyTmin+10.09999847412109)/10)
```

Source	SS	df	MS		
Model	8143.58389	2	4071.79195	Number of obs =	3285
Residual	45971.6222	3282	14.0071975	F(2, 3282) =	290.69
				Prob > F =	0.0000
Total	54115.2061	3284	16.4784428	R-squared =	0.1505
				Adj R-squared =	0.1500
				Root MSE =	3.7426

outerbandDMR	Coef.	Std. Err.	t	P>|t|	[95% Conf.	Interval]
IShaw__1	-1.359447	.1045074	-13.01	0.000	-1.564353	-1.154541
IShaw__2	1.088262	.1104552	9.85	0.000	.8716938	1.30483
_cons	21.31132	.0843213	252.74	0.000	21.14599	21.47665

Deviance: 17990.42. Best powers of ShawburyTmin among 44 models fit: 3 3.

```
. fracpoly regress  innerbandDMR  EdgbastonTmax, degree(2)
.........
-> gen double IEdgb__1 = X^3-6.329396402 if e(sample)
-> gen double IEdgb__2 = X^3*ln(X)-3.893011035 if e(sample)
   (where: X = (EdgbastonTmax+5.099998474121094)/10)
```

Source	SS	df	MS		
Model	13322.3802	2	6661.19008	Number of obs =	3273
Residual	48474.3549	3270	14.8239617	F(2, 3270) =	449.35
				Prob > F =	0.0000
Total	61796.735	3272	18.8865327	R-squared =	0.2156
				Adj R-squared =	0.2151
				Root MSE =	3.8502

innerbandDMR	Coef.	Std. Err.	t	P>|t|	[95% Conf.	Interval]
IEdgb__1	-1.594673	.0645278	-24.71	0.000	-1.721192	-1.468154
IEdgb__2	1.236038	.0559759	22.08	0.000	1.126287	1.345789
_cons	21.438	.0798449	268.50	0.000	21.28144	21.59455

Deviance: 18110.18. Best powers of EdgbastonTmax among 44 models fit: 3 3.

```
. fracpoly regress  innerbandDMR  EdgbastonTmin,degree(2)
.........
-> gen double IEdgb__1 = X^3-2.138644783 if e(sample)
-> gen double IEdgb__2 = X^3*ln(X)-.5419128762 if e(sample)
   (where: X = (EdgbastonTmin+5.499998569488525)/10)
```

Source	SS	df	MS		
Model	11467.8222	2	5733.91109	Number of obs =	3273
Residual	50328.9128	3270	15.3911048	F(2, 3270) =	372.55
				Prob > F =	0.0000
Total	61796.735	3272	18.8865327	R-squared =	0.1856
				Adj R-squared =	0.1851
				Root MSE =	3.9231

innerbandDMR	Coef.	Std. Err.	t	P>|t|	[95% Conf.	Interval]
IEdgb__1	-2.619857	.1278052	-20.50	0.000	-2.870444	-2.369271
IEdgb__2	2.705853	.163543	16.55	0.000	2.385196	3.02651
_cons	21.60665	.0865221	249.72	0.000	21.43701	21.77629

Deviance: 18233.06. Best powers of EdgbastonTmin among 44 models fit: 3 3.

Greater London (<75)

```
. fracpoly regress  outerbandDMR  RothamstedTmax, degree(2)
.........
-> gen double IRoth__1 = X^3-4.484528662 if e(sample)
-> gen double IRoth__2 = X^3*ln(X)-2.243211161 if e(sample)
   (where: X = (RothamstedTmax+2.29999852180481)/10)
```

Source	SS	df	MS		
Model	4.38702627	2	2.19351313	Number of obs	3278
Residual	67.6193181	3275	.02064712	F(2, 3275)	106.24
				Prob > F	0.0000
Total	72.0063444	3277	.021973251	R-squared	0.0609
				Adj R-squared	0.0604
				Root MSE	.14369

outerbandDMR	Coef.	Std. Err.	t	P>|t|	[95% Conf.	Interval]
IRoth__1	-.0321663	.0023401	-13.75	0.000	-.0367546	-.0275781
IRoth__2	.0273112	.0021401	12.76	0.000	.0231151	.0315073
_cons	.7465152	.0029252	255.21	0.000	.7407798	.7522505

Deviance: -3419.67. Best powers of RothamstedTmax among 44 models fit: 3 3.

```
. fracpoly regress  outerbandDMR  RothamstedTmin, degree(2)
.........
-> gen double IRoth__1 = X^3-4.065509386 if e(sample)
-> gen double IRoth__2 = X^3*ln(X)-1.900678551 if e(sample)
   (where: X = (RothamstedTmin+9.099998474121094)/10)
```

Source	SS	df	MS		
Model	2.55728656	2	1.27864328	Number of obs	3279
Residual	69.493722	3276	.02121298	F(2, 3276)	60.28
				Prob > F	0.0000
Total	72.0510086	3278	.021980173	R-squared	0.0355
				Adj R-squared	0.0349
				Root MSE	.14565

outerbandDMR	Coef.	Std. Err.	t	P>|t|	[95% Conf.	Interval]
IRoth__1	-.0339806	.0041255	-8.24	0.000	-.0420695	-.0258918
IRoth__2	.0311637	.0044078	7.07	0.000	.0225213	.0398061
_cons	.7495246	.0033166	225.99	0.000	.7430218	.7560274

Deviance: -3332.06. Best powers of RothamstedTmin among 44 models fit: 3 3.

```
. fracpoly regress  innerbandDMR  LWCTmax, degree(2)
.........
-> gen double ILWCT__1 = X^2-2.509983305 if e(sample)
-> gen double ILWCT__2 = X^3-3.976548184 if e(sample)
   (where: X = LWCTmax/10)
```

Source	SS	df	MS		
Model	3.94208994	2	1.97104497	Number of obs	3280
Residual	106.714385	3277	.032564658	F(2, 3277)	60.53
				Prob > F	0.0000
Total	110.656475	3279	.033747019	R-squared	0.0356
				Adj R-squared	0.0350
				Root MSE	.18046

innerbandDMR	Coef.	Std. Err.	t	P>|t|	[95% Conf.	Interval]
ILWCT__1	-.0787495	.0076542	-10.29	0.000	-.093757	-.063742
ILWCT__2	.0244394	.0026126	9.35	0.000	.0193169	.0295618
_cons	.7113938	.0038518	184.69	0.000	.7038416	.718946

Deviance: -1927.22. Best powers of LWCTmax among 44 models fit: 2 3.

```
. fracpoly regress  innerbandDMR  LWCTmin, degree(2)
.........
-> gen double ILWCT__1 = X^3-1.74777892 if e(sample)
-> gen double ILWCT__2 = X^3*ln(X)-.3252883357 if e(sample)
   (where: X = (LWCTmin+2.29999852180481)/10)
```

Source	SS	df	MS		
Model	3.31214169	2	1.65607085	Number of obs	3282
Residual	107.431587	3279	.032763522	F(2, 3279)	50.55
				Prob > F	0.0000
Total	110.743729	3281	.033753041	R-squared	0.0299
				Adj R-squared	0.0293
				Root MSE	.18101

innerbandDMR	Coef.	Std. Err.	t	P>|t|	[95% Conf.	Interval]
ILWCT__1	-.0549085	.0058491	-9.39	0.000	-.0663768	-.0434403
ILWCT__2	.0656491	.0078493	8.36	0.000	.0502591	.0810391
_cons	.7168784	.0038957	184.02	0.000	.7092401	.7245167

Deviance: -1908.41. Best powers of LWCTmin among 44 models fit: 3 3.

Greater London (75+)

```
. fracpoly regress  outerbandDMR  RothamstedTmax, degree(2)
........
-> gen double IRoth__1 = X^3-4.484528662 if e(sample)
-> gen double IRoth__2 = X^3*ln(X)-2.243211161 if e(sample)
   (where: X = (RothamstedTmax+2.29999852180481)/10)
```

Source	SS	df	MS		
Model	14136.2569	2	7068.12845	Number of obs =	3278
Residual	36625.4891	3275	11.1833555	F(2, 3275) =	632.02
				Prob > F =	0.0000
				R-squared =	0.2785
				Adj R-squared =	0.2780
Total	50761.746	3277	15.49031	Root MSE =	3.3442

outerbandDMR	Coef.	Std. Err.	t	P>|t|	[95% Conf.	Interval]
IRoth__1	-1.749191	.0544621	-32.12	0.000	-1.855974	-1.642408
IRoth__2	1.453145	.0498075	29.18	0.000	1.355488	1.550802
_cons	20.50047	.0680778	301.13	0.000	20.36699	20.63395

Deviance: 17214.05. Best powers of RothamstedTmax among 44 models fit: 3 3.

```
. fracpoly regress  outerbandDMR  RothamstedTmin,degree(2)
........
-> gen double IRoth__1 = X^3-4.066590475 if e(sample)
-> gen double IRoth__2 = X^3*ln(X)-1.901544385 if e(sample)
   (where: X = (RothamstedTmin+9.099998474121094)/10)
```

Source	SS	df	MS		
Model	8285.42271	2	4142.71135	Number of obs =	3280
Residual	42542.8554	3277	12.9822568	F(2, 3277) =	319.11
				Prob > F =	0.0000
				R-squared =	0.1630
				Adj R-squared =	0.1625
Total	50828.2782	3279	15.5011522	Root MSE =	3.6031

outerbandDMR	Coef.	Std. Err.	t	P>|t|	[95% Conf.	Interval]
IRoth__1	-1.693311	.10205	-16.59	0.000	-1.893399	-1.493222
IRoth__2	1.481504	.1090368	13.59	0.000	1.267717	1.695291
_cons	20.72162	.0820412	252.58	0.000	20.56076	20.88247

Deviance: 17713.79. Best powers of RothamstedTmin among 44 models fit: 3 3.

```
. fracpoly regress  innerbandDMR  LWCTmax, degree(2)
........
-> gen double ILWCT__1 = X^3-3.976498992 if e(sample)
-> gen double ILWCT__2 = X^3*ln(X)-1.829722098 if e(sample)
   (where: X = LWCTmax/10)
```

Source	SS	df	MS		
Model	14441.0908	2	7220.54542	Number of obs =	3278
Residual	69437.8696	3275	21.2024029	F(2, 3275) =	340.55
				Prob > F =	0.0000
				R-squared =	0.1722
				Adj R-squared =	0.1717
Total	83878.9604	3277	25.596265	Root MSE =	4.6046

innerbandDMR	Coef.	Std. Err.	t	P>|t|	[95% Conf.	Interval]
ILWCT__1	-1.89464	.0761985	-24.86	0.000	-2.044042	-1.745239
ILWCT__2	1.638548	.0706563	23.19	0.000	1.500013	1.777083
_cons	19.94271	.0934056	213.51	0.000	19.75957	20.12585

Deviance: 19310.95. Best powers of LWCTmax among 44 models fit: 3 3.

```
. fracpoly regress  innerbandDMR  LWCTmin, degree(2)
........
-> gen double ILWCT__1 = X^3-1.747578697 if e(sample)
-> gen double ILWCT__2 = X^3*ln(X)-.3251843342 if e(sample)
   (where: X = (LWCTmin+2.29999852180481)/10)
```

Source	SS	df	MS		
Model	10865.1515	2	5432.57576	Number of obs =	3280
Residual	73037.2166	3277	22.2878293	F(2, 3277) =	243.75
				Prob > F =	0.0000
				R-squared =	0.1295
				Adj R-squared =	0.1290
Total	83902.3681	3279	25.5877914	Root MSE =	4.721

innerbandDMR	Coef.	Std. Err.	t	P>|t|	[95% Conf.	Interval]
ILWCT__1	-3.075356	.1526133	-20.15	0.000	-3.374584	-2.776129
ILWCT__2	3.619	.204806	17.67	0.000	3.217439	4.02056
_cons	20.01197	.1016719	196.83	0.000	19.81262	20.21131

Deviance: 19486.49. Best powers of LWCTmin among 44 models fit: 3 3.

Appendix 7: Published paper

Applied Meteorology and Climatology

Progress in Physical Geography
2014, Vol. 38(4) 431–447

DOI: 10.1177/0309133314538725
ppg.sagepub.com
SAGE

Birmingham's air and surface urban heat islands associated with Lamb weather types and cloudless anticyclonic conditions

Fang Zhang
University of Birmingham, UK
Xiaoming Cai
University of Birmingham, UK
John E. Thornes
University of Birmingham, UK

Abstract
This study investigates the characteristics of the air and surface urban heat islands (aUHI and sUHI) of Birmingham in relation to Lamb weather types (LWTs) over the period 2002–2007, with a particular focus on cloudless anticyclonic conditions. Ground-based MIDAS air temperatures within the urban canopy layer at the urban Edgbaston and rural Shawbury weather stations were used to derive the aUHI intensity (aUHII). Satellite-derived MODIS/Aqua land surface temperatures (LST) under cloudless conditions were used to derive the spatial patterns of the sUHI as well as the sUHI intensity (sUHII). Using Jenkinson's objective daily synoptic indices, a combined subset of 11 LWTs were examined for their association with the nocturnal aUHI. Over the study period, the most frequently occurring LWT, 'anticyclonic' (21.1%), gives a strongest mean/maximum nocturnal aUHII of 2.5°C/7°C (391 nights) and the largest proportion of nocturnal heat island events of 65.2%. The spatial patterns of nocturnal sUHI for each LWT were also assessed, and the results demonstrate Birmingham's urban warming of up to 4.16°C (48 clear nights) in the city centre under cloudless anticyclonic conditions. The scatter plot of nocturnal aUHII and sUHII for the 48 nights demonstrates a linear relationship. We also developed a simple analytical model that links the slope of the aUHII–sUHII relationship to the difference of 'built-up' area fraction between the urban pixel and the rural pixel in satellite imagery of land cover. This partially explains the physical basis behind the relationship. These findings of the aUHII–sUHII relationship may lead to the future development of a generic methodology of deriving the spatial patterns of aUHI from satellite measurements.

Keywords
air temperature, anticyclonic, Birmingham, Lamb weather types, land surface temperature, MODIS, urban heat island

1 Introduction

During the 20th century, the urban population of England increased from 77% to 89% (Hicks and Allen, 1999). With rapid urbanization and

Corresponding author:
Xiaoming Cai, School of Geography, Earth and Environmental Sciences, University of Birmingham, Edgbaston, Birmingham B15 2TT, UK.
Email: x.cai@bham.ac.uk

List of References

Akbari, Bell, R., Brazel, T., et al. (2008) "Urban Heat Island Basics". **Reducing Urban Heat Islands: Compendium of Strategies**. US Environmental Protection Agency 22.

Alcoforado, M. and Andrade, H. (2008) "Global Warming and the Urban Heat Island". In Marzluff, J.;Shulenberger, E.;Endlicher, W.;Alberti, M.;Bradley, G.;Ryan, C.;Simon, U. & ZumBrunnen, C. (Eds.) **Urban Ecology**. Springer US 249-262.

Almeida, S., Casimiro, E. and Calheiros, J. (2010) Effects of apparent temperature on daily mortality in Lisbon and Oporto, Portugal. **Environmental Health**, 9: (1): 12.

Analitis, A., Katsouyanni, K., Biggeri, A., et al. (2008) Effects of Cold Weather on Mortality: Results From 15 European Cities Within the PHEWE Project. **American Journal of Epidemiology**, 168: (12): 1397-1408.

APHO (2010a) **Health Profile 2010 - London** [online]. http://www.apho.org.uk/resource/view.aspx?RID=50215&REGION=50156&SPEAR= Association of Public Health Observatories, Public Health England [Accessed May 2014]

APHO (2010b) **Health Profile 2010 - West Midlands** [online]. http://www.apho.org.uk/resource/view.aspx?RID=50215&REGION=50154&SPEAR Association of Public Health Observatories, Public Health England [Accessed May 2014]

Aqua (2014) [online]. http://science.nasa.gov/missions/aqua/ NASA Science Missions [Accessed September 2014]

ARUP (2014) "Reducing urban heat risk: A study on urban heat risk mapping and visualisation".

ASC (2014) "ASC progress report 2014. Managing climate risks to well-being and the economy. ". **Chapter 5: Well-being and public health**. Committee on Climate Change.

Baccini, M., Biggeri, A., Accetta, G., et al. (2008) Heat effects on mortality in 15 European cities. **Epidemiology**, 19: (5): 711-719.

Baccini, M., Kosatsky, T., Analitis, A., et al. (2011) Impact of heat on mortality in 15 European cities: attributable deaths under different weather scenarios. **J Epidemiol Community Health**, 65: (1): 64-70.

BADC (2011) "Met Office Integrated Data Archive System (MIDAS) Land and Marine Surface Stations Data (1853-current)". In BADC (Ed.).

Basara, J.B., Basara, H.G., Illston, B.G., et al. (2010) The Impact of the Urban Heat Island during an Intense Heat Wave in Oklahoma City. **Advances in Meteorology**, 2010: 1-11.

Basu, Dominici, F. and Samet, J.M. (2005) Temperature and mortality among the elderly in the United States: a comparison of epidemiologic methods. **Epidemiology**, 16: (1): 58-66.

Basu and Samet, J.M. (2002) Relation between Elevated Ambient Temperature and Mortality: A Review of the Epidemiologic Evidence. **Epidemiologic Reviews**, 24: (2): 190-202.

Box, G.E.P., Jenkins, G.M. and Reinsel, G.C. (2008) **Time Series Analysis: Forecasting and Control, 4th Edition**. Wiley.

Brázdil, R. and Budíková, M. (1999) An urban bias in air temperature fluctuations at the Klementinum, Prague, The Czech Republic. **Atmospheric Environment**, 33: (24–25): 4211-4217.

Brown, G., Fearn, V. and Wells, C. (2010) Exploratory analysis of seasonal mortality in England and Wales, 1998 to 2007. **Health Stat Q**, (48): 58-80.

BUCCANEER Project (2011) [online]. http://www.birminghamclimate.com [Accessed September 2014]

BUCL (2011) **HiTemp project** [online]. http://www.birmingham.ac.uk/schools/gees/centres/bucl/hitemp/index.aspx [Accessed September 2014]

Burkart, K., Schneider, A., Breitner, S., et al. (2011) The effect of atmospheric thermal conditions and urban thermal pollution on all-cause and cardiovascular mortality in Bangladesh. **Environ Pollut**, 159: (8-9): 2035-2043.

Carson, C., Hajat, S., Armstrong, B., et al. (2006) Declining vulnerability to temperature-related mortality in London over the 20th century. **Am J Epidemiol**, 164: (1): 77-84.

Celik, G., Baykan, O.K., Kara, Y., et al. (2014) Predicting 10-day mortality in patients with strokes using neural networks and multivariate statistical methods. **J Stroke Cerebrovasc Dis**, 23: (6): 1506-1512.

Cifuentes, L., Borja-Aburto, V.H., Gouveia, N., et al. (2001) Assessing the health benefits of urban air pollution reductions associated with climate change mitigation (2000-2020): Santiago, São Paulo, México City, and New York City. **Environmental Health Perspectives**, 109: (Suppl 3): 419-425.

Clarke, J.F. (1972) Some effects of the urban structure on heat mortality. **Environmental Research**, 5: (1): 93-104.

Cooper, N. (2001) "Geographic Variations in Health". **Chapter 7 Analysis of infant mortality rates by risk factors and by cause of death in England and Wales**.

Curriero, F., Heiner, K., Samet, J., et al. (2002) Temperature and mortality in 11 cities of the eastern United States. **Am J Epidemiol**, 155: (1): 80-87.

Danks, D.M., Webb, D.W. and Allen, J. (1962) Heat Illness in Infants and Young Children. **British Medical Journal**, 2: (5300): 287-293.

Davis, R.E., Knappenberger, P.C., Michaels, P.J., et al. (2003) Changing heat-related mortality in the United States. **Environ Health Perspect***,* 111: (14): 1712-1718.

Dessai, S. (2002) **Heat stress and mortality in Lisbon part I. model construction and validation**.

Dessai, S. (2003) Heat stress and mortality in Lisbon Part II. An assessment of the potential impacts of climate change. **Int J Biometeorol***,* 48: (1): 37-44.

Doick, K. and Hutchings, T. (2013) "Air temperature regulation by urban trees and green infrastructure". London: Forestry Commission.

Dominici, F., McDermott, A., Zeger, S.L., et al. (2002) On the Use of Generalized Additive Models in Time-Series Studies of Air Pollution and Health. **American Journal of Epidemiology***,* 156: (3): 193-203.

Donaldson, G.C., Kovats, R.S., Keatinge, W.R., et al. (2001) "Heat-and-cold-related mortality and morbidity and climate change". **Health Effects of Climate Change in the UK***.* London, Department of Health.

Dousset, B., Gourmelon, F., Laaidi, K., et al. (2011) Satellite monitoring of summer heat waves in the Paris metropolitan area. **International Journal of Climatology***,* 31: (2): 313-323.

Doyon, B., Belanger, D. and Gosselin, P. (2008) The potential impact of climate change on annual and seasonal mortality for three cities in Quebec, Canada. **International Journal of Health Geographics***,* 7: (1): 23.

Ebi, K.L. and Mills, D. (2013) Winter mortality in a warming climate: a reassessment. **Wiley Interdisciplinary Reviews: Climate Change***,* 4: (3): 203-212.

El-Zein, A., Tewtel-Salem, M. and Nehme, G. (2004) A time-series analysis of mortality and air temperature in Greater Beirut. **Sci Total Environ***,* 330: (1-3): 71-80.

Ellis, F.P., Prince, H.P., Lovatt, G., et al. (1980) MORTALITY AND MORBIDITY IN BIRMINGHAM DURING THE 1976 HEATWAVE. **Quarterly Journal of Medicine***,* 49: (193): 1-8.

Fisher, P. (2009) "An Examination of the Association between Temperature and Mortality in the West Midlands from 1981 to 2007". University of Birmingham.

Fouillet, A., Rey, G., Wagner, V., et al. (2008) Has the impact of heat waves on mortality changed in France since the European heat wave of summer 2003? A study of the 2006 heat wave. **Int J Epidemiol***,* 37: (2): 309-317.

Frich, P., Alexander, L.V., Della-Marta, P., et al. (2002) Observed coherent changes in climatic extremes during the second half of the twentieth century. **Climate Research***,* 19: 193-212.

Fung, K.Y., Krewski, D., Chen, Y., et al. (2003) Comparison of time series and case-crossover analyses of air pollution and hospital admission data. **International Journal of Epidemiology***,* 32: (6): 1064-1070.

Gao, Lan, L., Qiao, D.J., et al. (2012) [A preliminary study on the effects of meteorological factors on intracerebral hemorrhage death using the BP neural network model]. **Zhonghua Liu Xing Bing Xue Za Zhi***,* 33: (9): 937-940.

Gao, Sun, Y., Liu, Q., et al. (2015) Impact of extreme high temperature on mortality and regional level definition of heat wave: a multi-city study in China. **Sci Total Environ***,* 505: 535-544.

García-herrera, R., Díaz, J., Trigo, R.M., et al. (2005) Extreme summer temperatures in iberia: health impacts and associated synoptic conditions. **Annales Geophysicae***,* 23: 239-251.

Garssen, J., Harmsen, C. and DeBeer, J. (2005) **The effect of the summer 2003 heat wave on mortality in the Netherlands** [online]. http://www.eurosurveillance.org/ViewArticle.aspx?ArticleId=557 Euro Surveill. 10(7): 557 [Accessed May 2014]

GLA (2006) "London's Urban Heat Island: A Summary for Decision Makers". London, UK, Mayor of London, Greater London Authority.

GLA (2014) "London Infrastructure Plan 2050".

Gosling, S.N., Lowe, J.A., McGregor, G.R., et al. (2009) Associations between elevated atmospheric temperature and human mortality: a critical review of the literature. **Climatic Change***,* 92: (3-4): 299-341.

Gosling, S.N., McGregor, G.R. and Paldy, A. (2007) Climate change and heat-related mortality in six cities part 1: model construction and validation. **Int J Biometeorol***,* 51: (6): 525-540.

Hajat, S., Armstrong, B., Baccini, M., et al. (2006) Impact of high temperatures on mortality: is there an added heat wave effect? **Epidemiology***,* 17: (6): 632-638.

Hajat, S. and Kosatky, T. (2010) Heat-related mortality: a review and exploration of heterogeneity. **J Epidemiol Community Health***,* 64: (9): 753-760.

Hajat, S., Kovats, R.S., Atkinson, R.W., et al. (2002) Impact of hot temperatures on death in London: a time series approach. **J Epidemiol Community Health***,* 56: (5): 367-372.

Hajat, S., O'Connor, M. and Kosatsky, T. (2010) Health effects of hot weather: from awareness of risk factors to effective health protection. **The Lancet***,* 375: (9717): 856-863.

Hajat, S., Vardoulakis, S., Heaviside, C., et al. (2014) Climate change effects on human health: projections of temperature-related mortality for the UK during the 2020s, 2050s and 2080s. **J Epidemiol Community Health**.

Hastie, T.J. and Tibshirani, R.J. (1990) **Generalized Additive Models**. New York: Chapman and Hall.

Hatzakis, A., Katsouyanni, K., Kalandidi, A., et al. (1986) Short-term effects of air pollution on mortality in Athens. **Int J Epidemiol***,* 15: (1): 73-81.

Hicks, J. and Allen, G. (1999) "A Century of Change: Trends in UK statistics since 1900". SOCIAL AND GENERAL STATISTICS SECTION. HOUSE OF COMMONS LIBRARY.

Holderness, T., Barr, S., Dawson, R., et al. (2013) An evaluation of thermal Earth observation for characterizing urban heatwave event dynamics using the urban heat island intensity metric. **International Journal of Remote Sensing***,* 34: (3): 864-884.

Howard, L. (1833) The Climate of London. **International association for urban climate**.

Huang, C., Barnett, A.G., Wang, X., et al. (2011) Projecting future heat-related mortality under climate change scenarios: a systematic review. **Environ Health Perspect***,* 119: (12): 1681-1690.

Hulme, M. and Barrow, E. (1997) "Climates of the British Isles: Present, Past and Future". Psychology Press ed., Nature pp.454.

Hung, T., Uchihama, D., Ochi, S., et al. (2006) Assessment with satellite data of the urban heat island effects in Asian mega cities. **International Journal of Applied Earth Observation and Geoinformation***,* 8: (1): 34-48.

Huynen, M.M., Martens, P., Schram, D., et al. (2001) The impact of heat waves and cold spells on mortality rates in the Dutch population. **Environmental Health Perspectives***,* 109: (5): 463-470.

IPCC (2007) "Climate change 2007 : impacts, adaptation and vulnerability : contribution of Working Group II to the Fourth Assessment Report of the Intergovernmental Panel on Climate Change / edited by Parry, M.L. et al". Cambridge, Cambridge University Press.

IPCC (2013) "Summary for Policymakers: The Physical Science Basis. Contribution of Working Group I to the IPCC Fifth Assessment Report.".

IPCC (2014) "Summary for Policymakers. Climate Change 2014: Impacts, Adaptation, and Vulnerability. Working Group II Contribution to the IPCC 5th Assessment Report.".

Jaimes, F., Farbiarz, J., Alvarez, D., et al. (2005) Comparison between logistic regression and neural networks to predict death in patients with suspected sepsis in the emergency room. **Crit Care***,* 9: (2): R150-R156.

Jbilou, J. and Adlouni, S.E. (2012) Generalized Additive Models in Environmental Health: A Literature Review. **INTECH**.

Jenkinson, A.F. and Collinson, B.P. (1977) **An initial climatology of gales over the North Sea**.

Johnson (1985) Urban modification of diurnal temperature cycles in birmingham, U.K. **Journal of Climatology***,* 5: (2): 221-225.

Johnson, Kovats, S., McGregor, G.R., et al. (2005) **The impact of the 2003 heat wave on daily mortality in England and Wales and the use of rapid weekly mortality**

estimates [online]. http://www.eurosurveillance.org/ViewArticle.aspx?ArticleId=558 Euro Surveill [Accessed May 2014]

Jones, P.D. and Lister, D.H. (2009) The urban heat island in Central London and urban-related warming trends in Central London since 1900. **Weather***,* 64: (12): 323-327.

Kahn, M.E. (2006) **Green Cities. Urban Growth and the Environment.** Washington. D.C.: Brookings Institution Press.

Kalkstein, L.S. (1991) A new approach to evaluate the impact of climate on human mortality. **Environ Health Perspect***,* 96: 145-150.

Kassomenos, P.A., Gryparis, A. and Katsouyanni, K. (2007) On the association between daily mortality and air mass types in Athens, Greece during winter and summer. **Int J Biometeorol***,* 51: (4): 315-322.

Katsouyanni, K., Trichopoulos, D., Zavitsanos, X., et al. (1988) THE 1987 ATHENS HEATWAVE. **The Lancet***,* 332: (8610): 573.

Keating, A. and Handmer, J. (2013) "Future potential losses from extremes under climate change: the case of Victoria, Australia". **VCCCAR Project: Framing Adaptation in the Victorian Context.** . RMIT University.

Keatinge, W.R., Donaldson, G.C., Cordioli, E., et al. (2000) Heat related mortality in warm and cold regions of Europe: observational study. **BMJ***,* 321: (7262): 670-673.

Koppe, C., Kovats, S., Jendritzky, G., et al. (2004) "Heat-waves: risks and responses". No. 2.World Health Organization Copenhagen.

Kosatsky, T. (2005) **The 2003 European heat waves** [online]. http://www.eurosurveillance.org/ViewArticle.aspx?ArticleId=552 Euro Surveill [Accessed May 2014]

Kovats, R.S. and Jendritzky, G. (2006) Heat-waves and human health. Climate Change and Adaptation Strategies for Human Health, B. Menne and K.L. Ebi, Eds. **Springer, Darmstadt, Germany***,* 63-69.

Kravchenko, J., Abernethy, A.P., Fawzy, M., et al. (2013) Minimization of Heatwave Morbidity and Mortality. **American Journal of Preventive Medicine***,* 44: (3): 274-282.

Kunst, A.E., Looman, C.W.N. and Mackenbach, J.P. (1993) Outdoor Air Temperature and Mortality in the Netherlands: A Time-Series Analysis. **American Journal of Epidemiology***,* 137: (3): 331-341.

Laaidi, K., Zeghnoun, A., Dousset, B., et al. (2012) The Impact of Heat Islands on Mortality in Paris during the August 2003 Heat Wave. **Environmental Health Perspectives***,* 120: (2): 254-259.

Lamb, H.H. (1972) **British Isles weather types and a register of the daily sequence of circulation patterns, 1861-1971**. London: H.M.S.O.

Lee, D.O. (1992) URBAN WARMING?— AN ANALYSIS OF RECENT TRENDS IN LONDON'S HEAT ISLAND. **Weather***,* 47: (2): 50-56.

Lerner, A.M. and Eakin, H. (2011) An obsolete dichotomy? Rethinking the rural-urban interface in terms of food security and production in the global south. **Geogr J**, 177: (4): 311-320.

Liu, L. and Zhang, Y.Z. (2011) Urban Heat Island Analysis Using the Landsat TM Data and ASTER Data: A Case Study in Hong Kong. **Remote Sensing**, 3: (7): 1535-1552.

Marra, G. and Radice, R. (2011) Do We Adequately Control for Unmeasured Confounders When Estimating the Short-term Effect of Air Pollution on Mortality? **Water, Air, & Soil Pollution**, 218: (1-4): 347-352.

McCullagh, P. and Nelder, J.A. (1989) **Generalized Linear Models, Second Edition** Chapman and Hall/CRC; 2 edition.

McFall, S. (2014) **London's less central areas will be next hot spots** [online]. http://www.scmp.com/property/international/article/1556127/londons-less-central-areas-will-be-next-hot-spots 23 July, 2014 [Accessed May 2015]

MetOffice (2011a) "Fact sheet No. 14 – Microclimates". National Meteorological Library and Archive.

MetOffice (2011b) **Weather stations** [online]. http://www.metoffice.gov.uk/learning/science/first-steps/observations/weather-stations 14 February 2011 [Accessed April 2014]

MetOffice (2014a) **Global surface temperature** [online]. http://www.metoffice.gov.uk/research/monitoring/climate/surface-temperature 6 October 2014 [Accessed May 2015]

MetOffice (2014b) **Heatwave** [online]. http://www.metoffice.gov.uk/learning/learn-about-the-weather/weather-phenomena/heatwave 5 August 2014 [Accessed May 2015]

Michelozzi, P., de'Donato, F., Bisanti, L., et al. (2005) **The impact of the summer 2003 heat waves on mortality in four Italian cities** [online]. http://www.eurosurveillance.org/ViewArticle.aspx?ArticleId=558 Euro Surveill, 10(7): 556 [Accessed May 2014]

Mildrexler, D.J., Zhao, M. and Running, S.W. (2011) A global comparison between station air temperatures and MODIS land surface temperatures reveals the cooling role of forests. **Journal of Geophysical Research: Biogeosciences**, 116: (G3): G03025.

Miller, B.G. (2010) "Report on estimation of mortality impacts of particulate air pollution in London". Research Consulting Services.

Mills, G. (2006) Progress toward sustainable settlements: a role for urban climatology. **Theoretical and Applied Climatology**, 84: (1-3): 69-76.

MODIS Overview (2014) [online]. https://lpdaac.usgs.gov/products/modis_products_table/modis_overview LP DAAC [Accessed August 2014]

Morris, C.J.G. and Simmonds, I. (2000) Associations between varying magnitudes of the urban heat island and the synoptic climatology in Melbourne, Australia. **International Journal of Climatology***,* 20: (15): 1931-1954.

O'Hare, G., Sweeney, J. and Wilby, R.L. (2005) **Weather, climate, and climate change : human perspectives / Greg O'Hare, John Sweeney and Rob Wilby**. Harlow: Prentice Hall.

Oke (1982) The energetic basis of the urban heat island. **Quarterly Journal of the Royal Meteorological Society***,* 108: (455): 1-24.

Oke (1987) **Boundary layer climates / T.R. Oke**. 2nd.London: Methuen.

Oke (1997) "Urban climates and global change". In Perry, A. & Thompson, R. (Eds.) **Applied Climatology: Principles and Practice**. London: Routledge, 273-287.

ONS (2011) **The 2011 Census for England and Wales** [online]. http://www.ons.gov.uk/ons/guide-method/census/2011/index.html Office for National Statistics [Accessed April 2014]

Pan, W.H., Li, L.A. and Tsai, M.J. (1995) Temperature extremes and mortality from coronary heart disease and cerebral infarction in elderly Chinese. **Lancet***,* 345: (8946): 353-355.

Pasquill, F. and Smith, F.B. (1983) **Atmospheric diffusion**. 3rd / F. Pasquill and F.B. Smith.Chichester: Ellis Horwood.

Pateman, T. (2011) Rural and urban areas: comparing lives using rural/urban classifications. **Reg Trends***,* 43: (1): 11-86.

Pattenden, S., Nikiforov, B. and Armstrong, B.G. (2003) Mortality and temperature in Sofia and London. **J Epidemiol Community Health***,* 57: (8): 628-633.

Peng, R., Bobb, J., Tebaldi, C., et al. (2011) Toward a quantitative estimate of future heat wave mortality under global climate change. **Environ Health Perspect***,* 119: (5): 701-706.

Peterson, T.C. and Owen, T.W. (2005) Urban Heat Island Assessment: Metadata Are Important. **Journal of Climate***,* 18: (14): 2637-2646.

Pirard, P., Vandentorren, S., Pascal, M., et al. (2005) **Summary of the mortality impact assessment of the 2003 heat wave in France** [online]. http://www.eurosurveillance.org/ViewArticle.aspx?Articleid=554 Euro Surveill [Accessed May 2014]

Qian, Z., He, Q., Lin, H.M., et al. (2008) High temperatures enhanced acute mortality effects of ambient particle pollution in the "oven" city of Wuhan, China. **Environ Health Perspect***,* 116: (9): 1172-1178.

Rizwan, A.M., Dennis, L.Y.C. and Liu, C. (2008) A review on the generation, determination and mitigation of Urban Heat Island. **Journal of Environmental Sciences***,* 20: (1): 120-128.

Roberts, J.J. (2011) **Getting Started with Marine Geospatial Ecology Tools** [online]. http://code.nicholas.duke.edu/projects/mget/export/HEAD/MGET/Trunk/PythonPackage/dist/TracOnlineDocumentation/Documentation/GettingStarted.html [Accessed

Roberts, J.J., Best, B.D., Dunn, D.C., et al. (2010) Marine Geospatial Ecology Tools: An integrated framework for ecological geoprocessing with ArcGIS, Python, R, MATLAB, and C++. **Environmental Modelling & Software***,* 25: (10): 1197-1207.

Robinson, P.J. (2001) On the Definition of a Heat Wave. **Journal of Applied Meteorology***,* 40: (4): 762-775.

Rooney, C., McMichael, A.J., Kovats, R.S., et al. (1998) Excess mortality in England and Wales, and in Greater London, during the 1995 heatwave. **J Epidemiol Community Health***,* 52: (8): 482-486.

Rosenfeld, A.H., Akbari, H., Romm, J.J., et al. (1998) Cool communities: strategies for heat island mitigation and smog reduction. **Energy and Buildings***,* 28: (1): 51-62.

Roth, M., Oke, T.R. and Emery, W.J. (1989) Satellite-derived urban heat islands from three coastal cities and the utilization of such data in urban climatology. **International Journal of Remote Sensing***,* 10: (11): 1699-1720.

Royston and Altman, D.G. (1994) Regression Using Fractional Polynomials of Continuous Covariates: Parsimonious Parametric Modelling. **Journal of the Royal Statistical Society. Series C (Applied Statistics)***,* 43: (3): 429-467.

Royston and Altman, D.G. (1995) **Using fractional polynomials to model curved regression relationships**. StataCorp LP.

Royston and Altman, D.G. (1997) Approximating statistical functions by using fractional polynomial regression. **Journal of the Royal Statistical Society: Series D (The Statistician)***,* 46: (3): 411-422.

Royston, Ambler, G. and Sauerbrei, W. (1999) The use of fractional polynomials to model continuous risk variables in epidemiology. **International Journal of Epidemiology***,* 28: (5): 964-974.

Schwarz, N., Schlink, U., Franck, U., et al. (2012) Relationship of land surface and air temperatures and its implications for quantifying urban heat island indicators—An application for the city of Leipzig (Germany). **Ecological Indicators***,* 18: (0): 693-704.

Scott, A., Gilbert, A. and Gelan, A. (2007) "The Urban-Rural Divide: Myth or Reality". In Carter, C. (Ed.), The Macaulay Land Use Research Institute.

Semenza, J.C., McCullough, J.E., Flanders, W.D., et al. (1999) Excess hospital admissions during the July 1995 heat wave in Chicago. **American Journal of Preventive Medicine***,* 16: (4): 269-277.

Simon, F., Lopez-Abente, G., Ballester, E., et al. (2005) **Mortality in Spain during the heat waves of summer 2003** [online]. http://www.eurosurveillance.org/ViewArticle.aspx?ArticleId=555 Euro Surveill [Accessed May 2014]

Smargiassi, A., Goldberg, M.S., Plante, C., et al. (2009) Variation of daily warm season mortality as a function of micro-urban heat islands. **J Epidemiol Community Health***,* 63: (8): 659-664.

Smoyer, K.E., Rainham, D.G. and Hewko, J.N. (2000) Heat-stress-related mortality in five cities in Southern Ontario: 1980-1996. **Int J Biometeorol***,* 44: (4): 190-197.

Stedman, J.R. (2004) The predicted number of air pollution related deaths in the UK during the August 2003 heatwave. **Atmospheric Environment***,* 38: (8): 1087-1090.

Tan, J., Zheng, Y., Tang, X., et al. (2010) The urban heat island and its impact on heat waves and human health in Shanghai. **Int J Biometeorol***,* 54: (1): 75-84.

Terra (2014) [online]. http://science.nasa.gov/missions/terra/ NASA Science Missions [Accessed September 2014]

TheEurowinterGroup (1997) Cold exposure and winter mortality from ischaemic heart disease, cerebrovascular disease, respiratory disease, and all causes in warm and cold regions of Europe. The Eurowinter Group. **Lancet***,* 349: (9062): 1341-1346.

Thornes, J.E., Fisher, P.A., Rayment-Bishop, T., et al. (2014) Ambulance call-outs and response times in Birmingham and the impact of extreme weather and climate change. **Emerg Med J***,* 31: (3): 220-228.

Tolman, H.L. (1998) Effects of observation errors in linear regression and bin-average analyses. **Quarterly Journal of the Royal Meteorological Society***,* 124: (547): 897-917.

Tomlinson, C.J., Chapman, L., Thornes, J.E., et al. (2011) Remote sensing land surface temperature for meteorology and climatology: a review. **Meteorological Applications***,* 18: (3): 296-306.

Tomlinson, C.J., Chapman, L., Thornes, J.E., et al. (2012a) Derivation of Birmingham's summer surface urban heat island from MODIS satellite images. **International Journal of Climatology***,* 32: (2): 214-224.

Tomlinson, C.J., Chapman, L., Thornes, J.E., et al. (2012b) Comparing night-time satellite land surface temperature from MODIS and ground measured air temperature across a conurbation. **Remote Sensing Letters***,* 3: (8): 657-666.

Toulemon, L. and Barbieri, M. (2008) The mortality impact of the August 2003 heat wave in France: investigating the 'harvesting' effect and other long-term consequences. **Popul Stud (Camb)***,* 62: (1): 39-53.

Trigo, R.M., Ramos, A.M., Nogueira, P.J., et al. (2009) Evaluating the impact of extreme temperature based indices in the 2003 heatwave excessive mortality in Portugal. **Environmental Science & Policy***,* 12: (7): 844-854.

Unwin, D.J. (1980) THE SYNOPTIC CLIMATOLOGY OF BIRMINGHAM'S URBAN HEAT ISLAND, 1965–74. **Weather***,* 35: (2): 43-50.

Vardoulakis, S., Dear, K., S., H., et al. (2014) Comparative assessment of the effects of climate change on heat- and cold-related mortality in the United Kingdom and Australia. **Environ Health Perspect***,* 122: 1285–1292.

Voogt, J.A. (2002) "Urban Heat Island". In Douglas, I. (Ed.) **Encyclopedia of Global Environmental Change: Causes and Consequences of Global Environmental Change***.* Wiley-Blackwell 660-666.

Wan and Dozier, J. (1996) A generalized split-window algorithm for retrieving land-surface temperature from space. **Ieee Transactions on Geoscience and Remote Sensing***,* 34: (4): 892-905.

Wan, Zhang, Y., Zhang, Q., et al. (2004) Quality assessment and validation of the MODIS global land surface temperature. **International Journal of Remote Sensing***,* 25: (1): 261-274.

Wang, W., Liang, S. and Meyers, T. (2008) Validating MODIS land surface temperature products using long-term nighttime ground measurements. **Remote Sensing of Environment***,* 112: (3): 623-635.

Watkiss, P., Horrocks, L., Pye, S., et al. (2009) "Impacts of climate change in human health in Europe. PESETA-Human health study". European Commission, Joint Research Centre, Institute for Prospective Technological Studies.

Weinberg, C. (1995) How bad is categorization? **Epidemiology***,* 6: (4): 345-347.

Whitman, S., Good, G., Donoghue, E.R., et al. (1997) Mortality in Chicago attributed to the July 1995 heat wave. **Am J Public Health***,* 87: (9): 1515-1518.

Wikipedia (2014) **Remote sensing satellite and data overview** [online]. http://en.wikipedia.org/wiki/Remote_sensing_satellite_and_data_overview 18 November 2014 [Accessed May 2015]

Wikipedia (2015) **Greater London** [online]. http://en.wikipedia.org/wiki/Greater_London 27 May 2015 [Accessed May 2015]

Wikitravel (2009) **Talk:London/Districts** [online]. http://wikitravel.org/en/Talk:London/Districts [Accessed September 2014]

Wilby (2003) Past and projected trends in London's urban heat island. **Weather***,* 58: (7): 251-260.

Wilby, Betts, R. and McCarthy, M. (2009) "UK Climate Projections science report: climate change projections - Annex 7: urban heat island effects". University of Loughborough & Met Office Hadley Centre.

Wilby, Jones, P.D. and Lister, D.H. (2011) Decadal variations in the nocturnal heat island of London. **Weather***,* 66: (3): 59-64.

Williams, S., Nitschke, M., Weinstein, P., et al. (2012) The impact of summer temperatures and heatwaves on mortality and morbidity in Perth, Australia 1994–2008. **Environment International***,* 40: (0): 33-38.

WMPHO (2010) "Health Effects of Climate Change in the West Midlands: Technical Report ". In May, E.;Fisher, P.;Baiardi, L. & Kemm, J. (Eds.), In association with: DEFRA, Health Protection Agency, WMPHO, UK Climate Projections, Environment Agency.

Wolf, T. and McGregor, G. (2013) The development of a heat wave vulnerability index for London, United Kingdom. **Weather and Climate Extremes***,* 1: 59-68.

Wolf, T., McGregor, G. and Analitis, A. (2013) Performance Assessment of a Heat Wave Vulnerability Index for Greater London, United Kingdom. **Weather, Climate, and Society***,* 6: (1): 32-46.

Wolfe, R.E., Nishihama, M., Fleig, A.J., et al. (2002) Achieving sub-pixel geolocation accuracy in support of MODIS land science. **Remote Sensing of Environment***,* 83: (1–2): 31-49.

Wong, K.V., Paddon, A. and Jimenez, A. (2013) Review of World Urban Heat Islands: Many Linked to Increased Mortality. **Journal of Energy Resources Technology-Transactions of the Asme***,* 135: (2).

Xoserve (2013) **Weather Station Closure Update** [online]. http://www.gasgovernance.co.uk/sites/default/files/Weather%20Station%20Closure_280113.pdf [Accessed April 2014]

Zhang, F., Cai, X. and Thornes, J.E. (2014) Birmingham's air and surface urban heat islands associated with Lamb weather types and cloudless anticyclonic conditions. **Progress in Physical Geography***,* 38: (4): 431-447.

Zupancic, T., Westmacott, C. and Bulthuis, M. (2015) "The impact of green space on heat and air pollution in urban communities: A meta-narrative systematic review". David Suzuki Foundation.